PAPEL DA PROTEÍNA PRION CELULAR E SEUS LIGANTES NO DESENVOLVIMENTO DO SISTEMA NERVOSO

TIAGO GÓSS DOS SANTOS

Tese de doutorado apresentada à Fundação Antônio Prudente para a obtenção do título de Doutor em Ciências

Área de concentração: Oncologia

Orientadora: Dra. Vilma Regina Martins

São Paulo

2009

FICHA CATALOGRÁFICA

Preparada pela Biblioteca da Fundação Antônio Prudente

Santos, Tiago Góss dos

Papel da proteína prion celular e seus ligantes no desenvolvimento do sistema nervoso / Tiago Góss dos Santos – São Paulo, 2009.

123p.

Tese (doutorado) Fundação Antônio Prudente.

Curso de Pós-Graduação em Ciências-Área de concentração: Oncologia.

Orientadora: Vilma Regina Martins

Descritores: 1. DOENCAS DE PRION. 2. SISTEMA NERVOSO/ cres./desenvolvimento. 3. CITOLOGIA. 4. SINALIZACAO DO CALCIO.

AGRADECIMENTOS

Às pessoas mais importantes da minha vida, meu pai Carlos, minha mãe Eunice e aos meus irmãos Beto e Bruna.

À Ana Lívia, que recentemente entrou em minha vida e nesse pouco tempo já me transformou em uma pessoa melhor.

Meus sinceros agradecimentos à minha orientadora Vilma Martins, pelo acolhimento, investimento e incentivo. Certamente me tornei um profissional melhor sob sua tutela.

À inestimável presença da minha amiga Marilene que além do exemplo de ser humano, representa um modelo de conduta profissional.

À Glaucia pela grande e inquestionável amizade, por toda a ajuda e aconselhamentos.

Ao meu brother Flavio, um sujeito formidável, por toda a ajuda, companheirismo e pelas dezenas de litros de cerveja ingeridos nesses 4 anos de convivência.

Ao Bruno, meu grande amigo e conterrâneo, parceiro de apê e psicólogo alcoólico de plantão! Muito obrigado.

Ao amigão Gabriel (não convém escrever seu apelido aqui), obrigado por toda ajuda, principalmente na minha chegada a São Paulo.

Á Camila, Nicolle, Evânia, Ana Paula, Michele, Cleiton, Iara, Eliane, Guilherme, Dominique, minha família paulistana.

Aos grandes amigos da Virologia e LMBG

Aos professores Luiz Fernando Lima Reis e Fernando Augusto Soares pela excelente condução de nossa pós-graduação. E agradeço também a Ana Maria Kuninari, Luciana Pitombeira e Suely Francisco pelo pronto atendimento.

Aos bioteristas Wanderlei Gonçalves, Eder Machado e Oraci Lima pela amizade e pelos serviços prestados.

Aos animais utilizados neste estudo.

À Fapesp pelo auxílio financeiro.

RESUMO

Santos TG. **Papel da proteína prion celular e seus ligantes no desenvolvimento do sistema nervoso**. São Paulo: 2009. [Tese de Doutorado-Fundação Antônio Prudente].

A proteína prion celular (PrP^C) é altamente expressa no sistema nervoso e sua modificação estrutural está relacionada as encefalopatias espongiformes transmissíveis. PrP^C associa-se com proteínas de matriz extracelular, como a laminina (Ln) e vitronectina (Vn) e também com a co-chaperonina *stress inducible protein 1* (STI1). Estes complexos estão envolvidos em diferentes processos relacionados ao desenvolvimento do sistema nervoso. No desenvolvimento embrionário de camundongo a distribuição de PrP^C, Vn e STI1 é espaço-temporalmente relacionada, iniciando-se a partir do oitavo dia embrionário para STI1 e Vn e no décimo para PrP^C. As três proteínas apresentam um padrão de expressão na medula espinhal em forma de gradiente, com maior expressão na região ventral do tubo neural e notocorda e diminuindo na porção dorsal, o que sugere o seu envolvimento na organização do sistema nervoso. A STI1 assim como o peptídeo da cadeia γ1 laminina (Ln-γ1), correspondente ao domínio de ligação de PrP^C, são capazes de promover axonogênese em neurônios de gânglios da raiz dorsal. Quando combinados, Ln-γ1 e STI1 apresentam um efeito sinérgico sobre a axonogênese através da mobilização intracelular de cálcio e pela ativação de Erk1/2. O aumento na concentração intracelular de cálcio pela ligação de STI1 a PrP^C é mediado pela abertura de canais presentes na membrana. Por outro lado, o complexo PrP^C-Ln-γ1 mobiliza cálcio a partir de estoques intracelulares. A interação PrP^C-STI1 também é importante na biologia de células tronco neurais. Precursores neurais (neuroesferas) derivados de animais deficientes para PrP^C apresentam comprometimento de auto-renovação quando comparados aqueles provenientes animais tipo-selvagem. A ligação de STI1 a PrP^C promove um aumento na proliferação de precursores neurais, desempenhado um papel chave nos mecanismos de auto-renovação destas. Portanto, PrP^C é capaz de se associar a diferentes ligantes desempenhando um papel relevante no desenvolvimento do sistema nervoso central e periférico.

SUMMARY

Santos TG. **[Role of prion protein and its ligands in nervous system development]**. São Paulo: 2009. [Tese de Doutorado-Fundação Antônio Prudente].

The cellular prion protein (PrP^C) is highly expressed in thenervous system and its structural modification is associated to transmissible espongiform encephalopathies. PrP^C associates with extracellular matrix proteins, such as laminin (Ln) and vitronectin (Vn) and also to the co-chaperonin stress inducible protein 1 (STI1). These PrP^C complexes are involved in to the development of the nervous system. During the mouse embryo development, PrP^C, Vn and STI1 distribution is spatio-temporally related. STI1 and Vn expression became evident at embrionary day 8 (E8), while PrP^C is initialy detected at E10. These three proteins present a gradient of expression in spinal cord, more abundant in the notochord and floor plate, suggesting that they can have a role in brain patterning. STI1 as well as the peptide from laminin γ1 chain (Ln-γ1), which corresponds to PrP^C binding site, are able to promote axonogenesis in dorsal root ganglia neurons. When combined, STI1 and Ln-γ1 shown a synergic effect upon axonogenesis through intracellular Ca^{2+} mobilization and Erk1/2 activation. The increment of intracellular Ca^{2+} promoted by STI1 binding to PrP^C is mediated by Ca^{2+} channels at the plasma membrane. On the other hand, the complex Ln-γ1-PrP^C mobilizes Ca^{2+} from intracellular stores. The interaction between PrP^C and STI1 is also important in neural stem cells biology. Neural precursors (neurospheres) derived from PrP^C-null mice present impairment of self-renewal compared to wild-type neuronal precursors. In addition, STI1 binding to PrP^C promotes the proliferation of neural precursors, performing a key role in the self-renewal of stem cells. Thus, PrP^C is able to associate with different ligands and presents a relevant role in the development of central and peripheric nervous system.

LISTA DE FIGURAS E QUADRO

Figura 1 Diferentes proteínas ligantes de PrP^C..... 15

Figura 2 Modelos para o mecanismo de neurodegeneração associados ao mal dobramento e agregação de proteínas..... 17

Figura 3 Formação do tubo neural……. 20

Figura 4 Desenho esquemático representando gânglios da raiz dorsal..... 40

Figura 5 Ln-γ1 e STI1 podem interagir com PrP^C, de maneira sinérgica, transduzindo sinais neurotróficos envolvidos com o crescimento axonal..... 108

Figura 6 Envolvimento de PrP^C e STI1 na auto-renovação e proliferação de precursores neurais..... 109

Quadro 1 As doenças de prion..... 2

Quadro 2 Atividade dos sinais de orientação axonal..... 43

LISTA DE ABREVIATURAS

5-HT 5-hidróxi-triptamina

AMPA α-amino-3-hidroxil-5-metil-4-isoxazol-propionato

AMPc Adenosina monofosfato cíclico

ATP Adenosina trifosfato

BDNF Fator de crescimento derivado de cérebro

BMP Proteína morfogenética de osso

BrdU Bromo-desóxiuridina.

BSE Encefalopatia espongiforme bovina

CAM Móléculas de adesão celular

CJD Doença de Creutzfeldt-Jakob

CSG Camada sub-granular do hipocampo

CTN Células tronco neurais

CWD Doença debilitante do cervo

EGF Fator de crescimento epidermal

ERK Proteína quinase regulada por fatores extracelulares

FFI Insônia familial fatal

FGF Fator de crescimento de fibroblasto

GDP Guanosina difosfato

GPI Glicosilfosfatidilinositol-trifosfato

GSS Doença de Gerstmann-Straussler-Scheinker

GMPc Guanosina monofosfato cíclico

Hop Heat shock-organizing protein, homólogo humano de STI1

Hsp Proteína de choque térmico

IP_3 Inositol-trifosfato

IP_3-R Receptor de IP_3

KDI Tripeptídeo Lisina-Aspartato-Isoleucina

Ln Laminina

LR/LRP Receptor de laminina/Precursor de receptor de laminina

MEC Matriz extracelular

mGluR	Receptor metabotrópico de glutamato
NCAM	Molécula de adesão neural
NGF	Fator de crescimento de nervo
NMDA	N-metil-D-aspartato
PKA	Proteína quinase dependente de AMPc
PKC	Proteína quinase dependente de cálcio/fosfolipídeo
PLC	Fosfolipase C
PrP^{C}	Proteína prion
PrP^{Sc}	Prion scrapie
SNC	Sistema nervoso central
SNP	Sistema nervoso periférico
STI1	Stress inducible protein 1
Vn	Vitronectina
ZSV	Zona subventricular
ZV	Zona ventricular

ÍNDICE

1 INTRODUÇÃO.....1

1.1 Prion e Encefalopatias Espongiforme Transmissíveis.....1

1.1.1 Descoberta de prion.....2

1.1.2 Proteína prion.....4

1.1.3 Função de PrP^C.....6

1.1.4 Biologia de PrP^C.....16

2 OBJETIVOS.....18

2.1 Objetivos Específicos.....18

3 RESULTADOS.....19

PARTE I.....19

PARTE II.....39

PARTE III.....74

4 CONCLUSÕES.....105

5 REFERÊNCIAS BIBLIOGRÁFICAS.....110

ANEXOS

Anexo 1 Interação entre PrP^C e Vitronectina estimula axonogênese em gânglios da raiz dorsal

Anexo 2 Interação entre a proteína prion celular e o peptídeo da cadeia γ1 de laminina ativa receptores metabotrópicos de glutamato do tipo 1

PREFÁCIO

O presente trabalho foi idealizado para avaliar o papel da proteína prion e sua interação com os ligantes laminina, STI1 e vitronectina em processos distintos do desenvolvimento embrionário de camundongo. A tese foi organizada da seguinte maneira: a introdução (item 1) e os objetivos (item 2) serão abordados em português, contemplando os conceitos inclusos nos manuscritos que estão publicados ou em processo de publicação na língua inglesa. O capítulo de resultados (item 3) está dividido em três partes, contendo os artigos científicos originais em sua forma integral. Em cada uma delas será apresentada uma introdução referente ao tema e uma breve discussão em português relatando as principais idéias e a minha participação nos respectivos trabalhos. A metodologia empregada nos trabalhos está descrita somente no item *material and methods* nos manuscritos. Após a apresentação dos resultados, a conclusão (item 4) reunirá um panorama do trabalho desenvolvido com suas conclusões e as perpectivas para os próximos estudos. O item 5 contém as referências bibliográficas citadas no item 1 por sua vez a literatura correspondente a pontos específicos de cada trabalho está contida nos respectivos artigos compilados no ítem 3. Finalmente, foi adicionado um anexo, onde estão apresentados dois artigos científicos que contaram com a minha contribuição.

1 INTRODUÇÃO

1.1 PRIONS E ENCEFALOPATIAS ESPONGIFORMES TRANSMISSÍVEIS

As doenças por prion são enfermidades neurodegenerativas fatais que afetam humanos e uma grande variedade de outros animais (AGUZZI 2005). Enquanto as doenças por prion podem apresentar certas características patológicas semelhantes às encontradas em outras encefalopatias progressivas, como a doença de Alzheimer e Parkinson, elas são únicas pelo fato de serem transmissíveis (AGUZZI e RAEBER 1998). A inoculação intracerebral de homogenatos de tecido cerebral de indivíduos afetados em um indivíduo sadio da mesma espécie recapitula a doença. Esta peculiaridade foi identificada na primeira metade do século passado em um caso de *scrapie* (Cuille e Chelle 1939, citado por AGUZZI 2006 p.1729), o protótipo de doença por prion que afeta o gado ovino (AGUZZI 2005). No início da década de 90 ocorreu uma epidemia alarmante da doença no gado bovino do Reino Unido (encefalopatia espogiforme bovina ou doença da vaca louca) constituiu na provável infecção em humanos, ocasionada pela ingestão de derivados de carne produzidos a partir de animais contaminados. Todas essas doenças são caracterizadas por demência progressiva, ataxia associada por degeneração espongiforme do cérebro e eventual deposição de material amilóide no SNC (SAKUDO e IKUTA 2009). As doenças de prions estão descritas no Quadro 1.

Quadro 1 - As doenças de prion.

Doença	*Hospedeiro*	*Mecanismo de Patogênese*
Kuru	Humanos	Infecção por rituais de canibalismo em tribos Fore da Nova Guiné.
CJD iatrogênica	Humanos	Infecção por enxertos de dura-mater, hormônio de crescimento, etc.
CJD variante	Humanos	Infecção por carne bovina contaminada por prions.
CJD familial	Humanos	Mutações germinativa no gene de PRNP.
GSS	Humanos	Mutação germinativa no gene de PRNP
FFI	Humanos	Mutação germinativa no gene de PRNP (D178N, M129).
CJD esporádica	Humanos	Mutação somática ou conversão espontânea.
sFI	Humanos	Mutação somática ou conversão espontânea.
Scrapie	Ovinos	Infecção em ovelhas geneticamente suceptíveis.
BSE	Bovinos	Infecção por ração contaminada por prions.
TME	Martas	Infecção por prions de ovelhas e bovinos.
CWD	Cervos	Desconhecido.
FSE	Gatos	Infecção por prions de ovelhas e bovinos.
EUE	Antílopes	Infecção por prions de ovelhas e bovinos.

Fonte: Adaptado de PRUSINER 2004.

Abreviações: BSE - encefalopatia espongiforme bovina; CJD - doença de Creutzfeldt-Jakob; CWD – doença debilitante do cervo; EUE – encefalopatia de ungulados exóticos; FFI - Insônia Familial Fatal; FSE - encefalopatia espongiforme felina; sFI - insônia fatal esporádica; GSS – síndrome de Gerstmann-Sträussler-Scheinker; TME – encefalopatia transmissível de martas.

1.1.1 Descoberta e desenvolvimento do conceito de prion

A doença denominada de *scrapie* tem sido motivo de preocupação desde o século XVIII (AGUZZI 2006; BROWN 2009). Na década de 20 foram descritos os primeiros possíveis casos possíveis de CJD por Creutzfeldt (1920) e Jakob (1921), citados por AGUZZI (2006, p.1729). Um dos primeiros indícios de que se tratava de uma doença transmissível foi acidentalmente descoberto em 1937 em rebanhos da Escócia. Na tentativa de se vacinar o gado ovino contra encefalomielite infecciosa, causada por um vírus (*louping ill virus*), os animais receberam uma inóculo combinado de homogenatos derivados de cérebro e baço, tratados com formalina. O que foi demonstrado subsequentemente foi que os animais dos quais os homegenatos

foram preparados estavam contaminados com *scrapie*, e após dois anos, muitos animais que receberam este material na vacinação desenvolveram a doença e pela primeira vez foi demonstrado que o agente causador da doença era resistente ao tratamento com formalina, ao contrário da maioria dos vírus que são prontamente inativados com tal tratamento (PRUSINER 2004).

Um avanço crucial para o entendimento da doença foi alcançado nos anos de 1930 pela transmissão experimental de *scrapie* em cabras (Cuille e Chelle 1939, citado por AGUZZI 2006 p.1729). Nas duas décadas seguintes, poucos avanços foram realizados até que Carleton Gajdusek demonstrou que o Kuru, doença responsável por uma alta mortalidade em Papua, Nova Guiné, era na verdade uma encefalopatia espongiforme transmissível e sua propagação seria atribuída aos hábitos canibais dos aborígenes (AGUZZI 2006). As primeiras tentativas de se transmitir o Kuru para primatas falharam pela mesma dificuldade encontrada para se transmitir o *scrapie* em ovinos: o tempo de incubação da doença. Por ser bastante elevado, isso desencorajava os cientistas da época (AGUZZI 2006). Porém, Gajdusek teve a paciência necessária pra comprovar a transmissão de Kuru a chimpanzés (GAJDUSEK et al. 1966; GAJDUSEK et al. 1967) e pouco tempo mais tarde também foi bem sucedido em demonstrar a transmissão da Doença de Creutzfeldt-Jakob (GIBBS, Jr. et al. 1968).

Inicialmente, imaginava-se que o agente patogênico responsável pela transmissibilidade da doença fosse um vírus de ação lenta (CHO 1976). Investigações posteriores levaram a conclusões contrárias a esta hipótese, suportando a proposta de *protein-only*, inicialmente comcebida por Griffith no final dos anos 60 (GRIFFITH 1967). O agente patogênico era substancialmente diferente de vírus e

outros agentes convencionais, foi demonstrado que o *scrapie* apresenta uma elevada resistência a tratamentos que destroem ácidos nucléicos como luz ultravioleta e radiação ionizante (ALPER et al. 1967). Posteriormente, foi demonstrado que a massa mínima de infectividade estaria na faixa de 200kDa, excluindo, portanto, qualquer agente conhecido até então (ALPER et al. 1966). A hipótese de um agente infeccioso composto unicamente por proteína foi reforçada e corroborada por uma série de elegantes trabalhos conduzidos principalmente pelo grupo de Stanley Prusiner ao longo da década de 80, que nomeou o agente infeccioso de prion a partir do inglês *proteinaceus infectious protein*.

A elucidadação da natureza química dos prions aconteceu após o isolamento do material infeccioso (BOLTON et al. 1982) a partir de cérebros infectados. O material purificado mostrou-se altamente insolúvel e com características típicas de agregados amilóides (PRUSINER et al. 1983). Posteriormente, agentes químicos que modificam atividade e estrutura de proteínas como proteases, detergentes, sais caotrópicos e fenol foram capazes de inativar a infecção promovida pelo material purificado. Estes dados fortaleceram o conceito de prion, demonstrando a composição exclusivamente protéica do agente infeccioso (PRUSINER 1982).

1.1.2 Proteína Prion

As partículas infecciosas purificadas a partir de cérebros de animais com *scrapie* foram utilizadas na produção de anticorpos que, inesperadamente, reconheceram uma proteína de 33-35kDa, encontrada tanto no cérebro de animais sadios quanto de animais infectados (MEYER et al. 1986; OESCH et al. 1985). Posteriormente, o sequenciamento dos resíduos da região amino-terminal da proteína

infecciosa possibilitou a geração de sondas degeneradas que permitiram a clonagem de um gene, a partir de bibliotecas de cDNA de hamsters normais e infectados (BASLER et al. 1986). Desta forma, foi demonstrando que, de fato, a partícula infecciosa é composta de uma proteína codificada por um gene do hospedeiro, denominada então Proteína Prion Celular (PrP^{C}) e para diferenciá-la de sua isoforma infecciosa o agente patogênico foi denominado de Prion Scrapie (PrP^{Sc}).

PrP^{C} e PrP^{Sc} possuem a mesma sequência de aminoácidos e diferem somente em sua estrutura secundária, a qual confere características físico-químicas distintas para as isoformas (TURK et al. 1988). Enquanto PrP^{C} é solúvel e susceptível a ação de proteases, PrP^{Sc} é bastante insolúvel e parcialmente resistente a proteólise (MEYER et al. 1986). Esta propriedade de PrP^{Sc} favorece a formação de agregados insolúveis que se depositam de maneira lenta e progressiva em diversas regiões do sistema nervoso, levando eventualmente a morte neuronal.

O gene *PRNP* que codifica a isoforma normal ou PrP^{C}, está localizado no braço curto do cromossomo 20 de humanos e no cromossomo 2 de camundongos e ratos (*Prnp*) (CHESEBRO et al. 1985; OESCH et al. 1985). A proteína apresenta aproximadamente 250 aminoácidos (27kDa), com dois resíduos na região amino-terminal que apresentam glicosilação e uma âncora de glicosil-fosfatidil-inositol (GPI) na região carboxi-terminal (PRUSINER 1998). PrP^{C} é abundantemente expressa no SNC e SNP, também encontrada no coração, fígado, tecido linfático, músculo e intestino (PRUSINER 1998). Sua expressão pode ser regulada por fatores de crescimento durante o desenvolvimento (MANSON et al., 1994) e pela estrutura da cromatina (CABRAL et al. 2002). Quanto a localização subcelular, PrP^{C} está preferencialmente localizada em domínios de membrana ricos em colesterol (*lipid*

rafts) de terminais pré-sinápticos (HERMS et al. 2000), axônios em crescimento (SALES et al., 2002) e também no citoplasma de alguns tipos neuronais (MIRONOV, Jr. et al. 2003).

1.1.3 Funções de PrP^C

a- Animais transgênicos: Desde o início dos anos 90, diversas contruções de animais deficientes para o gene *Prnp* (*Prnp*$^{0/0}$ e *Prnp*$^{-/-}$) foram geradas na tentativa de elucidar as funções de PrP^C *in vivo* (BUELER et al. 1992; MANSON et al. 1994). Os primeiros trabalhos com camundongos deficientes para *Prnp* não revelaram alterações de fenótipo aparente, levando a conclusão que a expressão de PrP^C não seria essencial para o desenvolvimento normal, ou de alguma forma a ausência de expressão da proteína seria compensada por outras moléculas (BUELER et al. 1992; MANSON et al. 1994).

Entretanto, estudos posteriores demonstraram alterações sutis em certas características destes animais, em especial modificações na neurotransmissão e plasticidade sináptica (COLLINGE et al. 1994; MAGLIO et al. 2004; PRESTORI et al. 2008), memória hipocampal (CRIADO et al. 2005) e ritmos circadianos (TOBLER et al. 1996; TOBLER et al. 1997). Interessantemente, animais deficientes para PrP^C apresentam maior sensibilidade a condições estressantes que levam a morte neuronal, especialmente devido a sua hiperexcitabilidade (MCLENNAN et al. 2004; RANGEL et al. 2007; SHYU et al. 2005; WALZ et al. 1999; WEISE et al. 2004; WEISE et al. 2006). Portanto, apesar de existirem mecanismos que compensem a ausência de PrP^C, eles não são suficientes para manter o limiar de

excitabilidade que pode estar envolvido na morte neuronal devida a ausência de PrP^C.

Adicionalmente, foram geradas diversas linhagens de camundongos deficientes para PrP^C re-expressando formas mutadas ou deleções em *Prnp*, nesses animais foi possível observar anormalidades fenotípicas, como nas deleções dos aminoacidos 32-121 (PrPΔ32-121) ou 32-134 (PrPΔ32-134) nas quais os animais passaram a apresentar ataxia severa e apoptose no cerebelo (SHMERLING et al. 1998). Posteriormente também foi observado que estes animais apresentavam alta taxa de desmielinização (leucodistrofia) e perda axonal na medula espinhal e substância branca do cerebelo (RADOVANOVIC et al. 2005). Interessantemente, a re-expressão de PrP^C sítio-específica previne a degeneração observada nestes animais, sendo observada a diminuição quase completa da leucodistrofia quando a expressão de PrP^C ocorre em oligodendrócitos, porém não altera a morte de neurônios granulares. Por outro lado, a re-expressão de PrP^C em neurônios previne parcialmente a degeneração de neurônios granulares, mas não tem efeito sobre a desmielinização (RADOVANOVIC et al. 2005). Estes dados sugerem que os dois aspectos da degeneração cerebelar (leucodistrofia e apoptose) são eventos independentes e que a expressão endógena de PrP^C em neurônios e glia é necessária para a completa reversão do fenótipo degenerativo.

Camundongos transgênicos expressando a forma truncada de PrP Δ94-134 também apresentam extensiva desmielização no SNC e SNP, acompanhada de ataxia, que progride de paraparesia espástica até paraplegia completa que é seguida de morte (BAUMANN et al. 2007). A letalidade observada nestes animais não foi associada à presença de agregados de PrP, alteração de glicosilação, a má-localização

subcelular de PrP^C ou a topologia inapropriada da membrana plasmática (BAUMANN et al. 2007).

Interessantemente, o fenótipo mais aparente foi observado em animais expressando uma deleção menor (PrPΔ105-125), estes animais desenvolviam uma severa enfermidade dentro de duas semanas após o nascimento, com diminuição do tamanho e peso corporal, imobilidade, comprometimento de reflexo de orientação, mioclonia e tremores, com progressão ao óbito em um mês. A avaliação histopatológica demonstrou uma severa atrofia cerebelar, com perda de neurônios granulares e gliose reativa (LI et al. 2007). Importante destacar que a degeneração observada nos animais expressando as formas truncadas PrPΔ32-121, PrPΔ32-134, PrPΔ94-134 ou PrPΔ105-125 é prevenida pela introdução de uma cópia do gene *Prnp* tipo-selvagem (BAUMANN et al. 2007; LI et al. 2007; SHMERLING et al. 1998).

Camundongos transgênicos expressando formas truncadas de PrP^C da região C-terminal também apresentam alterações de fenótipo. A expressão da forma truncada Δ177-200 ou Δ201-217, quando associada à deleção dos aminoácidos 23-88, que por sua vez é inócua individualmente, promove neurodegeneração e desordem de sinais cerebelares (MURAMOTO et al. 1997). Ambas as deleções levam ao acúmulo de PrP^C no citoplasma na forma de corpos de inclusão e à diminuição no número de axônios na substância branca observada nos mutantes PrPΔ177-200, enquanto os animais PrPΔ201-217 apresentavam extensiva perda celular na região CA1 do hipocampo (MURAMOTO et al. 1997).

Além da construção de camundongos com deleções de domínios funcionais de PrP^C, também foram gerados animais transgênicos que carregam mutações do

gene *PRNP* humano associado à doenças. O domínio de PrP^{C} humano compreendido entre os aminoácidos 95 a 135 (equivalente aos aminoacidos 94 a 134 no gene de camundongo) pode apresentar pelo menos 5 mutações pontuais: P102L, P105L, G114V, A117V e G131V (as letras correspondem ao aminoácido original seguido do códon e da letra do aminoácido mutado), todas associadas a GSS. Estas mutações estão dentro do domínio no qual a deleção causa degeneração no camundongo, como discutido acima. Adicionalmente, foi demonstrado que a infusão intracerebral de homogenato de cérebro de paciente com GSS com a mutação P102L induz encefalopatia espogiforme em animais (MASTERS et al. 1981), e animais que superexpressam um transgene com a mesma mutação apresentam neurodegeneração espontânea sem a detecção de PrP^{Sc} (TELLING et al. 1996).

A mutação A117V que leva àa formação da isoforma transmembrana de PrP^{C}, também causa neurodegeneração em animais transgênicos, mas não causa deposição de PrP^{Sc} e não tem capacidade de infectar outros roedores (HEGDE et al. 1998). Em contrapartida, a expressão de mutações ligadas a CJD T183A (DEARMOND et al. 1997) ou E199K (TELLING et al. 1996) não promovem nenhum sinal patológico em camundongo.

A deleção de domínios específicos de PrP^{C} em animais transgênicos ou a presença de mutações no gene *PRNP* em humanos com doença por prions pode estar relacionada com a alteração de recrutamento de proteínas ligantes de PrP^{C}, que formam um complexo multiprotéico (LINDEN et al. 2008; MARTINS et al. 2009), em particular aqueles ligantes que já foram caracterizados por apresentarem propriedades neurotróficas. Adicionalmente, a composição destes complexos pode variar de acordo com o tipo celular (neurônios e glia), o que explicaria em parte, a

grande variedade de fenótipos degenerativos observados em animais transgênicos e em pacientes com doenças por prions (MARTINS et al. 2009).

b- Interações moleculares com PrP^C: PrP^C possui domínios funcionais onde ocorre interações com diferentes ligantes que possivelmente compõem uma complexa rede de interações multi-protéicas (MARTINS et al. 2009), como ilustrado na Figura 6. As deleções localizadas dentro da região N-terminal, um domínio menos estruturado que permite uma maior acessibilidade a interações, permitem explorar a relevância da interação de PrP^C com diversas moléculas, tais como proteoglicanos de heparan sulfato (WARNER et al. 2002), vitronectina (HAJJ et al. 2007), receptor de lipoproteína tipo 1 (TAYLOR e HOOPER 2007) e *stress inducible protein 1* (STI1) (ZANATA et al. 2002). Em relação às deleções da região C-terminal, já foi demonstrado a interação com receptor de laminina (37LRP/67LR) (GAUCZYNSKI et al. 2001; HUNDT et al. 2001), laminina (GRANER et al. 2000), NCAM (SCHMITT-ULMS et al. 2001) e, recentemente, também foi descrita a interação de PrP^C com um canal de potássio (TREK) (AZZALIN et al. 2006). Uma das características que todos estes ligantes tem em comum, é a capacidade de exercer atividades tróficas, sugerindo que PrP^C também possa apresentar um papel modulatório dentro das atividades de cada ligante, como será discutido adiante.

Moléculas de adesão e MEC: PrP^C interage com *neural cell adhesion molecule* (NCAM) (SCHMITT-ULMS et al. 2001), levando a estabilização de NCAM nos *lipid rafts* e através da ativação de $p59^{fyn}$ promove neuritogênese (SANTUCCIONE et al. 2005). Componentes da matriz extracelular (MEC), incluindo receptores de superfície, também já foram caracterizados como ligantes de

PrP^C, demonstrando a importância dessa proteína na organização correta e funcional da MEC (LIMA et al. 2007). Primeiramente foi identificada a interação de PrP^C com o receptor de laminina 37LRP/67LR (RIEGER et al. 1997), envolvido em processos como direcionamento e motilidade de filopódios, modulação de expressão gênica e na facilitação da interação laminina-integrina (NELSON et al. 2008). Adicionalmente, PrP^C interage com glicosaminoglicanos (GONZALEZ-IGLESIAS et al. 2002), proteoglicanos (KESHET et al. 2000), heparina e heparan sulfato (WARNER et al. 2002), entretanto, nenhuma função biológica foi associada a estas interações.

Também foi identificada a interação específica e de alta afinidade entre PrP^C e laminina (GRANER et al. 2000), a mais importante proteína não-colagênica da MEC (PAULSSON et al. 1987). Já é amplamente conhecido o papel de laminina na promoção de crescimento neurítico, alterando a velocidade e direção de cones de crescimento através de sua interação com diversas isoformas de receptores integrinas, além de outros como receptor de laminina (LR/LRP) e receptor distroglicana (LUCKENBILL-EDDS 1997). Em relação a interção PrP^C/laminina, nosso grupo demonstrou que o complexo PrP^C-laminina medeia neuritogênese, tanto em células PC-12 quanto em culturas primárias de hipocampo de ratos e camundongos. Nosso grupo também mapeou os domínios de interação entre PrP^C (entre os aminoácidos 173-182) e laminina, que acontece n cadeia gama-1 (γ1), entre os aminoácidos 1575-1584 (COITINHO et al. 2006; GRANER et al. 2000). O complexo PrP^C/laminina também está envolvido na consolidação da memória de longa duração sendo que este processo requer a ativação de vias clássicas de sinalização (PKA/Erk1-2) (COITINHO et al. 2006).

Anteriormente à identificação da interação entre PrP^C e o domínio RNIAEIIKDI da cadeia γ1 de laminina, já existiam diversos trabalhos na literatura sobre os efeitos de γ1 no crescimento neurítico e outras atividades neurotróficas (LIESI et al. 1989). Ln-γ1 promove mielinização e regeneração de axônios no SNP (CHEN e STRICKLAND 2003) e central (GRIMPE et al. 2002). Também foi identificado que o tripeptídeo terminal da sequencia de Ln-γ1 (KDI) é o responsável pela atividade biológica desta região (LIESI et al. 2001). O domínio KDI apresenta importante atividade neuroprotetora em modelos de trauma agudo e de doenças neurológicas crônicas, prevenindo a morte neuronal induzida por ácido kaínico (WIKSTEN et al. 2004) ou e 6-hidróxi-dopamina (6-OHDO) que leva a morte neuronal crônica de maneira similar à observada na doença de Parkinson (VAANANEN et al. 2006). KDI também estimula regeneração espinhal, após transecção experimental (WIKSTEN et al. 2004).

Nosso grupo também caracterizou interação de PrP^C com outra molécula de MEC, a vitronectina e demonstramos que esta associação está envolvida na axonogênese de neurônios de gânglios da raiz dorsal (HAJJ et al. 2007), consistente com dados da literatura que apontam o envolvimento desta proteína na diferenciação e axonogênese de neurônios motores, através da interação com o morfógeno Sonic Hedgehog (PONS e MARTI 2000), em células ganglionares da retina (BROCCO e PANZETTA, 1999) e em células de neuroblastoma (ARCANGELI et al. 1993; LESKAWA et al. 1995).

STI1: Outra proteína que teve sua interação com PrP^C identificada por nosso grupo, foi a *stress inducible protein 1* (STI1) (ZANATA et al. 2002), uma co-

chaperonina que ao associar-se às Hsp70 e Hsp90, facilita o dobramento e a maturação correta de proteínas no citoplasma (NICOLET e CRAIG 1989). Diversos trabalhos têm nos levado a considerar STI1 como uma nova molécula neurotrófica (ARANTES et al. 2009; ERLICH et al. 2007; LIMA et al. 2007; LOPES et al. 2005). Apesar de não apresentar peptídeo sinal de endereçamento para secreção, já foi demonstrado que STI1 pode ser secretada por diversos tipos celulares, incluindo linhagens de células tumorais (ERLICH et al. 2007; EUSTACE e JAY 2004) e astrócitos (LIMA et al. 2007). Uma vez no espaço extracelular, STI1 pode se ligar ao seu receptor PrP^C induzindo sua internalização (CAETANO et al. 2008), modulando diferentes processos celulares. Os sítios de interação entre PrP^C e STI1 já foram mapeados e correspondem aos aminoácidos 106-126 de PrP^C e 230-245 de STI1 (ZANATA et al. 2002). A ligação de STI1 a PrP^C induz fosforilação de Erk1/2 promovendo neuritogênese e ativa PKA, que por sua vez, está envolvida na proteção contra morte neuronal (CHIARINI et al. 2002; LOPES et al. 2005). STI1 também apresenta papel importante na proliferação de astrócitos (ARANTES et al. 2009) e em linhagens de glioma (ERLICH et al. 2007). Nosso grupo também demonstrou que a associação entre PrP^C e STI1 é importante em eventos relacionados à plasticidade neuronal *in vivo*, a interação entre as duas proteínas induz a retenção de memória de curta duração (STM) e consolidação de memória de longa duração (LTM) (COITINHO et al. 2007).

Receptores de neurotransmissores: Trabalhos da literatura tem demonstrado que componentes do sistema glutamatérgico também podem interagir direta ou indiretamente com PrP^C modulando seus sinais. Entre os diversos fenótipos

apresentados pelas cepas de animais deficientes para PrP^C, muitos deles tem o neurotransmissor glutamato como seu principal mediador, incluindo aumento da suceptibilidade a isquemia (MCLENNAN et al. 2004; SAKURAI-YAMASHITA et al. 2005; SPUDICH et al. 2005; WEISE et al. 2004; WEISE et al. 2006), hipersensibilidade a convulsões (WALZ et al. 1999), morte neuronal (RANGEL et al. 2007) e comprometimento de aprendizagem espacial (COLLINGE et al. 1994; CRIADO et al. 2005), sugerindo que receptores e transportadores de glutamato podem ser importantes parceiros de PrP^C. De fato, um trabalho recente demonstrou a conexão direta entre PrP^C e o sistema glutamatérgico (KHOSRAVANI et al. 2008). Foi demonstrado que PrP^C exerce uma regulação negativa na atividade de receptores N-metil-D-aspartato (NMDA), o que explicaria a hipersensibilidade de neurônios deficientes de PrP^C. Este efeito parece ser específico para este receptor uma vez os receptores α-amino-3-hidroxil-5-metil-4-isoxazol-propionato (AMPA) apresentam atividade normal em animais deficientes pra PrP^C (KHOSRAVANI et al. 2008).

Também foi demonstrado a associação de PrP^C com receptores de serotonina (MOUILLET-RICHARD et al. 2005). Esta interação foi determinada em uma linhagem imortalizada de progenitores ectodermais 1C11 (KELLERMANN et al. 1996). PrP^C ativa receptores 5-HT2A levando a um aumento na atividade de Fosfolipase A2 quando estas células são induzidas a diferenciar em neurônios serotoninérgicos. Nestas condições PrP^C também inibe receptores 5- HT1B/D, aumentando a atividade de adenilato ciclase. Portanto, este resultados demonstram que PrP^C pode atuar como modulador da função serotoninérgica (MOUILLET-RICHARD et al. 2005).

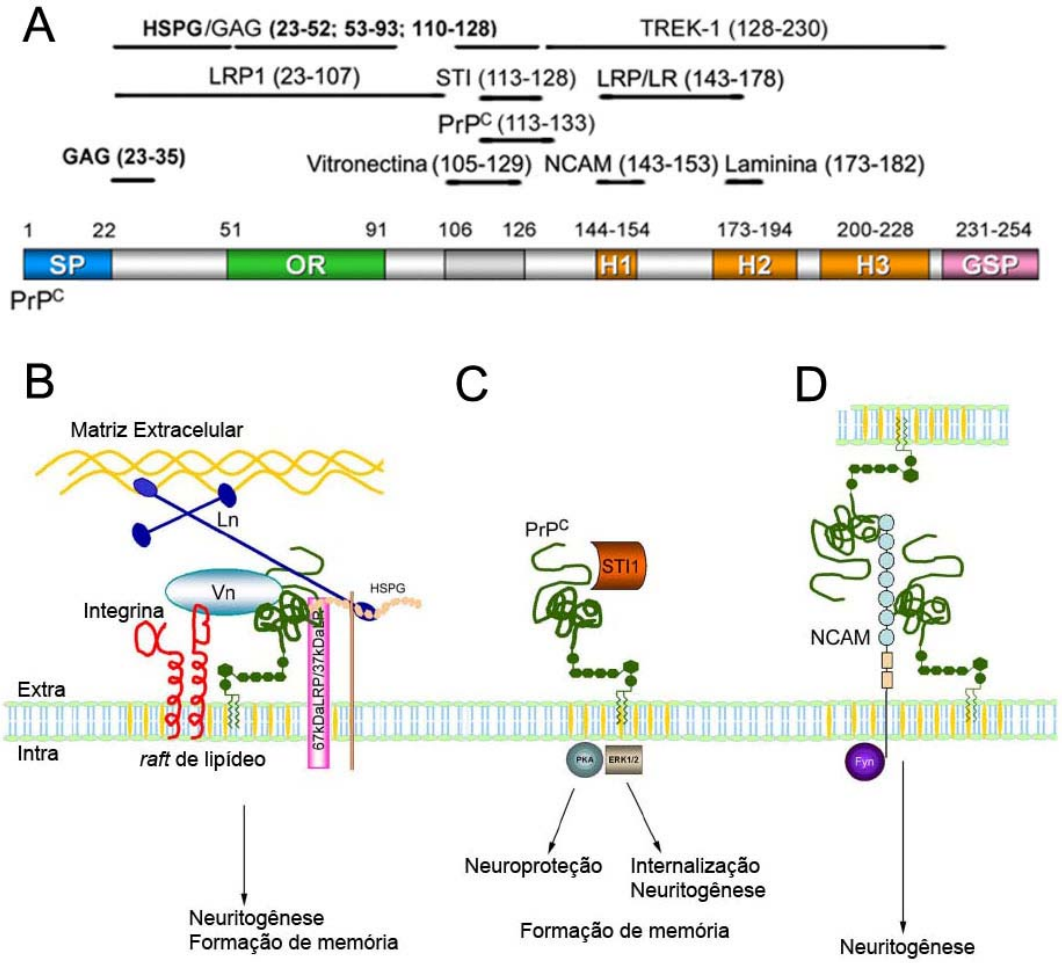

Fonte: Adaptado de MARTINS et al. 2009.

Figura 1 – Diferentes proteínas ligantes de PrP^C. **A**, representação esquemática de PrP^C com os sítios de ligação a diferentes moléculas. Os números entre parênteses indicam os resíduos dos sítios para cada ligante. SP, peptídeo sinal; OR, repetição de octapeptídeos; H1, H2 e H3, regiões de α-hélice; GPS, sequência para inserção da âncora de GPI. **B-D**, Ligantes de PrP^C envolvidos com atividade neurotrófica. **B**, PrP^C interage diretamente com proteínas da MEC, laminina (Ln) e vitronectina (Vn), com receptor de laminina (37LRP/67LR), possivelmente formando um complexo multiprotéico envolvido com neuritogênese e formação de memória. A interação de PrP^C com receptor de laminina é mediada por proteoglicanos de heparan sulfato (HSPG). Os receptores de MEC, integrinas também participam no complexo. **C**, PrP^C interage com STI1, mediando neuroproteção e neuritogênese através de vias de sinalização independentes (PKA e ERK1/2). **D**, NCAM interage com PrP^C através de contato *cis* ou *trans*, promovendo neuritogênese através da ativação de Fyn kinase.

1.1.4 Biologia de PrP^C

O estudo de funções de PrP^C é de grande interesse para o entendimento das bases patológicas das doenças por prions. Todas as evidências relatadas aqui suportam a idéia de que PrP^C está envolvida em um grande número de vias de sinalização relacionadas a fisiologia de células do sistema nervoso, contrabalançando a idéia inicial de que esta proteína não apresentava função relevante em situações normais, que passaria a ganhar função tóxica quando convertida à sua isoforma infecciosa. A Figura 7 ilustra as possibilidades que podem estar envolvidas na patologia das doenças priônicas. Inicialmente, acreditava-se somente a deposição de material amilóide era necessária para levar ao aparecimento da doença. Porém, com as frequêntes descobertas de funções fisiológicas de PrP^C, hoje admite-se que a perda de função desta proteína também está envolvida nas doenças por prions, juntamente com um componente neuroinflamatório (SOTO 2003).

Em especial às funções de PrP^C observadas nos mecanismos relacionados com a neuritogênese, é interessante ressaltar o papel desta proteína que ao associar-se com outras moléculas na superfície celular promove crescimento neurítico, evidenciando sua importância no estabelecimento correto das conexões neuronais, evento crucial para o funcionamento do sistema nervoso. Portanto, alterações na suas funções podem estar relacionadas não apenas com doenças por prions, mas também com outras desordens neurológicas. Desta forma, o entendimento das funções de PrP^C nos eventos que governam a formação de conexões neuronais é crucial para a elucidação da patoetiologia de várias desordens neurológicas, e também no desenvolvimento de terapias para estas patologias.

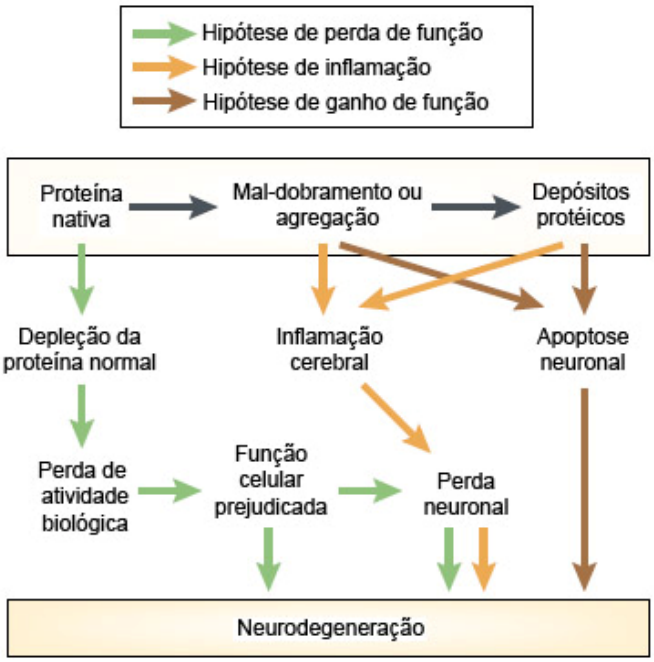

Fonte: Adaptado de SOTO 2003.

Figura 2 - Modelos para o mecanismo de neurodegeneração associada ao mal dobramento e agregação de proteínas. Três modelos são propostos, em todos eles o final do processo é o mesmo, porém os eventos que levam a morte neuronal são distintos. Enquanto que na perda de função a depleção da proteína nativa é o evento chave para a degeneração, no modelo de ganho de função, o mecanismo principal envolve a toxicidade causada pelo mal dobramento ou agregação de proteína. Na hipótese de inflamação, a morte neuronal é resultado indireto de reações inflamatórias crônicas promovidas por astrogliose e/ou ativação de microglia. Em algumas doenças, pode haver a combinação dos três mecanismos.

2 OBJETIVO

Este estudo tem por objetivo investigar a expressão e o papel da proteína prion e seus ligantes laminina, vitronectina e STI1 no desenvolvimento do sistema nervoso. Em particular, avaliar o papel funcional destes complexos na neuritogênese de neurônios de gânglio da raiz dorsal e na modulação da autorenovação de células tronco neurais.

2.1 OBJETIVOS ESPECÍFICOS

1 Determinar o padrão de expressão de PrP^{C}, STI1 e Vitronectina durante o desenvolvimento embrionário de camundongos;

2 Avaliar a interação entre PrP^{C} e seus ligantes (STI1, laminina e vitronectina) sobre a axonogênese em culturas de neurônios de gânglios da raiz dorsal de animais tipo-selvagem e deficientes para PrP^{C} e investigar as vias de sinalização envolvidas nestes processos;

3 Avaliar o papel da interação entre PrP^{C} e STI1 sobre a biologia de células tronco neurais derivadas de camundongos tipo-selvagem e deficientes para PrP^{C}.

3 RESULTADOS

Parte I

Expressão de PrP^C e seus ligantes STI1 e Vitronectina durante o desenvolvimento embrionário de camundongo.

A complexidade do sistema nervoso de vertebrados tem origem a partir de uma população de células da ectoderme dorsal do embrião. Através do processo de indução neural, estas células diferenciam-se e tornam-se distinguíveis das demais pela sua morfologia colunar, nesta etapa esta população de células passa a se chamar ectoderme neural. Subsequentemente, o processo de indução neural transforma esta população de células, que se extendem no sentido rostro caudal do embrião, na placa neural. As células formadoras da placa neural posteriormente organizam-se na forma de uma estrutura chamada tubo neural, o rudimento do sistema nervoso central (SNC), em um processo conhecido como neurulação. A porção medial da placa dará origem a região ventral do tudo neural, enquanto os limites laterais da placa darão origem a região dorsal, após terem suas extremidades unidas, como representado na Figura 1 (SANES et al. 2006).

A neurulação pode ser subdividida em numerosas etapas, cada uma com interações moleculares diferentes. Inicialmente a neurulação ocorre em duas fases chamadas de neurulação primária e secundária. A primeira fase usualmente compreende os processos de formação, dobramento e fechamento da placa neural tendo como produto final a formação do tubo neural. A neurulação secundária ocorre na região caudal (porção lombar e sacral) de aves e mamíferos, onde o tubo neural

desenvolve-se de maneira distinta da região rostral. Ao invés das células organizarem-se sob uma placa através de movimentos de rolagem como na neurulação primária, a secundária consiste na cavitação de um cordão epitelial sólido na cauda do embrião levando a formação de um lúmen que corresponde ao canal central do tubo neural (LADHER e SCHOENWOLF 2005).

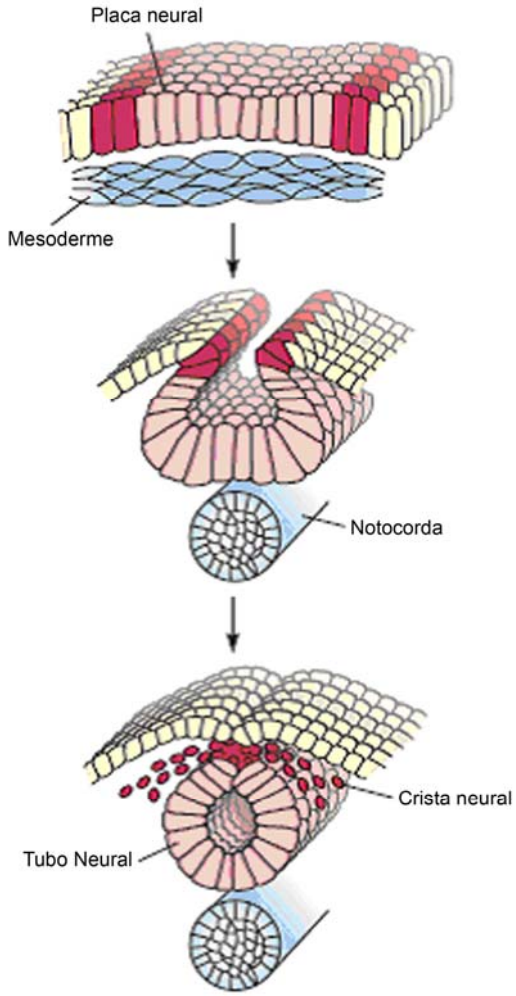

Fonte: Adaptado de SANES et al. 2006

Figura 3. Formação do tubo neural. A placa neural (vermelho claro) forma um tubo que se separa do resto da ectoderme. As células que involuem se condensam para formar a notocorda, logo abaixo do tubo neural. Ao mesmo tempo, as bordas da placa neural fundem-se para formar a porção dorsal do tubo neural, enquanto que um grupo de células destacam-se da região dorsal, constituindo as células da crista neural (vermelho escuro).

Assim que o tubo neural se fecha, o futuro sistema nervoso consistirá de uma única camada de células alinhadas ao lúmen do tubo. Este lúmen se desenvolverá formando o sistema ventricular do encéfalo, caracterizado pela presença de células tronco neurais (CTN) com rápida divisão celular que formarão a zona ventricular (ZV). As células proliferativas da ZV darão origem, direta e indiretamente, a todas as células do SNC (NOWAKOWSKI e HAYES 2005).

O desenvolvimento do tubo neural prossegue e passa pela formação de diferentes padrões de organização ao longo do eixo antero-posterior e dorso-ventral, iniciando uma série de eventos que finalmente darão origem ao complexo sistema nervoso de vertebrados (DARNELL 2005). Antes mesmo da porção posterior do tubo estar completamente formada, já é possível observar mudanças drásticas em seu arranjo na região anterior, onde identifica-se porções proeminentes como as três vesículas primárias, telencéfalo, mesencéfalo e rombencéfalo e ainda a medula espinhal (Figura 4), enquanto que no plano dorso-ventral nota-se a presença de neurônios sensoriais dorsais e neurônios motores ventrais (DARNELL 2005). Além disso, das margens laterais da neuroectoderme, os placodes sensoriais e a crista neural formam os nervos craniais e o sistema nervoso periférico.

Neste trabalho, a expressão de PrP^C, STI1 e Vn foi avaliada em diversas idades do desenvolvimento embrionário de camundongo. Foram utilizados embriões com 8, 10, 12, 14, 16 e 18 dias de idade, que foram processados para imunohistoquímica, imunofluorescência e *immunoblotting*. O padrão de distribuição das três proteínas é semelhante em função da localização e da idade. A expressão de STI1 e Vn torna-se evidente no sistema nervoso e coração, a partir de oito dias de idade embrionária (E8), enquanto PrP^C ainda não é detectada. Em E10, é possível

observar um gradiente de expressão das três proteínas na medula espinhal, mais abundante a partir da notocorda e placa ventral (*floor plate*) que diminui até a região dorsal. Este padrão de expressão é observado em proteínas envolvidas na organização de padrões dorso-ventral, como *wnt, bmp e shh* (SANES et al. 2006).

A mesma relação espaço-temporal pode ser observada em gânglios da raiz dorsal (GRD), onde em E10, a expressão de PrP^C, Vn e STI1 é mais abundante nos axônios e em neuritos do que nos corpos celulares. Em particular, PrP^C é altamente expressa em axônios em crescimento, como demonstrado pela colocalização com a proteína Tau. Em E14, as três proteínas estão presentes também no corpo celular, importante ressaltar que é neste período que são realizadas as culturas de neurônios periféricos (derivados de gânglio da raiz dorsal), presentes nas Partes II e IV desta tese. Em embriões E16, os GRD apresentam expressão abundante de STI1 e PrP^C nos corpos celulares, PrP^C também está presente nos neuritos em crescimento.

Em E16, STI1 e PrP^C estão altamente expressas no neocórtex. Enquanto STI1 apresenta um padrão mais amplo, a expressão de PrP^C é mais restrita a placa cortical, colocalizando com STI1. Entretanto, é possível observar algumas células marcadas para PrP^C na zona intermediária que podem ser neurônios recém-diferenciados que estão migrando da zona ventricular para a placa cortical.

Estes dados sugerem que PrP^C, STI1 e Vn possam atuar nos nos processos de motilidade celular que, por sua vez, está relacionada com eventos que vão desde a migração neuronal até o crescimento neurítico.

Em relação à expressão fora do sistema nervoso, é importante destacar a alta concentração de PrP^C, Vn e STI1 no tecido cardíaco que se inicia em E10 e mantém-se ao longo de toda a embriogênese. Rins e pulmão expressam baixas quantidades de

PrP^C até E14, enquanto que no fígado a expressão é praticamente indetectável. Nesta idade a expressão de STI1 é fraca nos rins e pulmão, mas presente no fígado. Por outro lado, a expressão de Vn é abundante nos rins e pulmão e, em especial, no fígado, um conhecido sítio de produção e secreção de Vn. A partir de E16, PrP^C e STI1 passam a ser detectadas no fígado e pulmão, o último apresenta uma expressão de PrP^C restrita ao tecido conectivo, enquanto STI1 é observada nos alvéolos em desenvolvimento. Em E18, PrP^C, STI1 e Vn passam a ser detectadas em praticamente todos os tecidos do embrião

Em suma, o padrão de expressão das três proteínas na medula espinhal, e sua localização em axônios em crescimento, sugerem que estas estão intimamente relacionadas com o desenvolvimento do sistema nervoso central e periférico, assim como de tecidos não-neurais. De fato, já foi demonstrado que Vn pode ser processada enzimaticamente na região ventral do tubo neural e notocorda, e atráves de sua interação com Shh, pode atuar na diferenciação de neurônios motores (PONS e MARTI 2000).

Neste trabalho, compartilho a autoria com a Dra. Glaucia Hajj, uma vez que realizei todos os ensaios de imunofluorescência. O artigo foi publicado no periódico *Journal of Comparative Neurology*.

The Journal of Comparative Neurology 000:000–000 (2009)
Research in Systems Neuroscience

Developmental Expression of Prion Protein and Its Ligands Stress-Inducible Protein 1 and Vitronectin

GLAUCIA N.M. HAJJ,[1] TIAGO G. SANTOS,[1,2] ZANITH S.P. COOK,[2] AND VILMA R. MARTINS[1]*
[1]Ludwig Institute for Cancer Research, São Paulo, Brazil 01323-903
[2]Centro Internacional de Pesquisa e Ensino, Hospital A.C. Camargo, São Paulo, Brazil 01509-900

ABSTRACT

Prion protein (PrP^C) is the normal isoform of PrP^{Sc}, a protein involved in neurodegenerative disorders. PrP^C participates in neuritogenesis, neuroprotection, and memory consolidation through its interaction with the secreted protein stress-inducible protein 1 (STI1) and the extracellular matrix protein vitronectin (Vn). Although PrP^C mRNA expression has been documented during embryogenesis, its protein expression patterns have largely not been evaluated. Furthermore, little is known about either Vn or STI protein expression. In this study, PrP^C, STI1, and Vn protein expression was explored throughout mouse embryonic life. We found that the distributions of the three proteins were spatiotemporally related. STI1 and Vn expression became evident at E8, earlier than PrP^C, in the nervous system and heart. At E10, we observed, in the spinal cord, a gradient of expression of the three proteins, more abundant in the notochord and floor plate, suggesting that they can have a role in axonal growth. As development proceeded, the three proteins were detected in other organs, suggesting that they may play a role in the development of nonneural tissues as well. Finally, although STI1 and Vn are PrP^C ligands, their expression was not altered in PrP^C-null mice. J. Comp. Neurol. 000:000–000, 2009. © 2009 Wiley-Liss, Inc.

Indexing terms: prion protein; vitronectin; STI1; protein expression; development

Prion protein (PrP^C) is the normal isoform of PrP^{Sc}, an infectious particle involved in neurodegenerative diseases referred to as *transmissible spongiform encephalopathies* (Prusiner, 1998). The physiological functions of PrP^C have been discussed extensively in recent years and include its participation in protection against oxidative stress, in programmed cell death, and in neural signaling and differentiation (Linden et al., 2008). The neuroprotection and neuritogenesis activities of PrP^C depend on its interaction with at least two partners, stress-inducible protein 1 (STI1; Chiarini et al., 2002; Lopes et al., 2005; Zanata et al., 2002) and vitronectin (Vn; Hajj et al., 2007).

Although the developmental expression of PrP^C has been addressed before, its protein expression pattern has not been properly addressed during embryonic development. Mouse PrP^C mRNA is highly expressed between E8.5 and E9 in the brain and neural tube, predominantly in the differentiating neuroepithelium. At E13.5, PrP^C mRNA is observed in both neural and nonneural tissues, whereas PrP^C protein was detected after birth (Miele et al., 2003). β-Galactosidase driven by the PrP^C promoter shows high expression at E12.5 in nervous tissue, which increases from neonatal to adult periods (Asante et al., 2002).

Vn is an abundant extracellular matrix protein present in most tissues (Seiffert, 1997). It is involved in several biological processes, such as cell adhesion, migration, and humoral defense mechanisms (Preissner, 1991). It binds glycosaminoglycans and collagen in the extracellular matrix and interacts with cell surface receptors (Ruoslahti and Pierschbacher, 1987; Suzuki et al., 1985), such as integrins $\alpha_V\beta_3$, $\alpha_V\beta_5$, and $\alpha_{IIb}\beta_3$ (Ding et al., 2003; Roberts et al., 2003). PrP^C has been shown to act as a Vn cell surface receptor (Hajj et al., 2007). Both proteins were found to interact in vitro, and, in developing dorsal root ganglia (DRG) explants, their engagement mediates axonal growth (Hajj et al., 2007). Additionally, Vn promotes survival and neuritogenesis of retinal neurons (Martinez-Morales et al., 1995). In the central nervous system, cerebellar granule cells, when migrating from the outer to the inner cell layer, switch their environment from a laminin (Ln)-rich to a Vn-rich extracellular matrix, which in turn promotes growth arrest and cell differentiation (Pons et al., 2001).

Additional Supporting Information may be found in the online version of this article.

The first two authors contributed equally to this work.

Grant sponsor: Fundação de Amparo à Pesquisa do Estado de São Paulo (FAPESP; to G.N.M.H., T.G.S., Z.C.); Grant number: 03-13189-2; Grant sponsor: Howard Hughes Medical Institute (to V.R.M.).

*Correspondence to: Dr. Vilma Regina Martins, Ludwig Institute for Cancer Research, Rua João Julião 245, 1st floor, São Paulo, Brazil 01323-903. E-mail: vmartins@ludwig.org.br

Received 25 November 2008; Revised 9 January 2009; Accepted 4 July 2009

DOI 10.1002/cne.22157

Published online in Wiley InterScience (www.interscience.wiley.com).

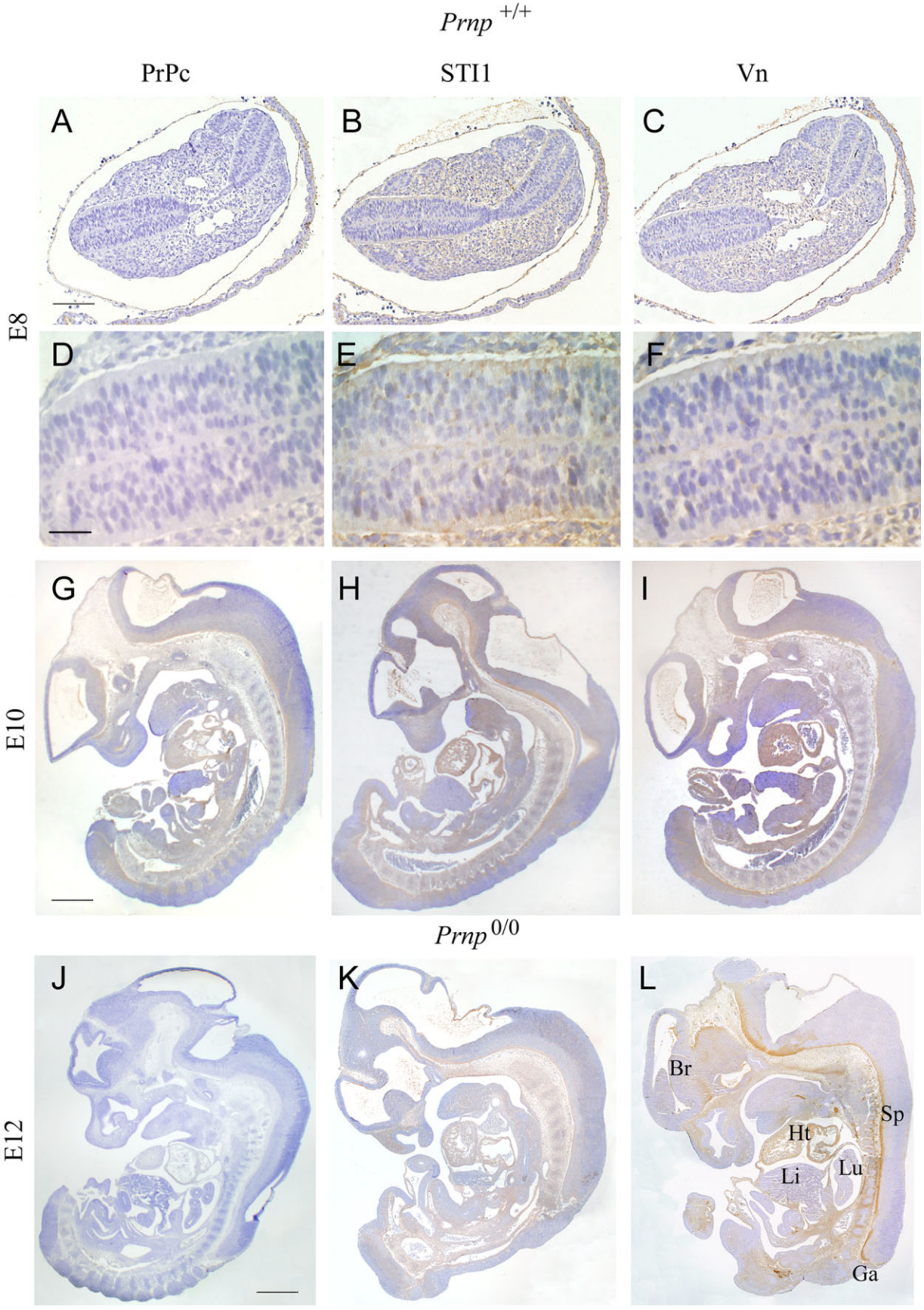

Figure 1

COLOR

The liver is the main Vn producer and as such expresses the highest amounts of Vn mRNA (Preissner, 1991), followed by the brain (Seiffert, 1997). In mouse and chicken embryos, Vn mRNA is detected in the liver and floor plate (Seiffert et al., 1995). In chicken embryos, Vn mRNA is also seen in the notochord (Pons and Marti, 2000). Patterning of the vertebrate neural tube depends on intercellular signals emanating from sources such as the notochord and floor plate. Vn, in association with sonic hedgehog (Shh), is responsible for the generation and differentiation of motor neurons (Martinez-Morales et al., 1997; Pons and Marti, 2000). Because Vn is a secreted protein, its distribution in tissues can be strikingly different from the observed mRNA expression, which specifically reveals the Vn producer cells. However, Vn protein distribution throughout embryogenesis has not been evaluated.

STI1, or its human homologue Hop (Hsp70/Hsp90-organizing protein), acta as a cochaperone molecule, associating with Hsp70 and Hsp90 (Smith et al., 1993). In addition to its activity as a stress-related protein, STI1 is involved in promoting neuritogenesis (Lopes et al., 2005) and neuroprotection in retinal and hippocampal neurons through its interaction with PrP^C (Chiarini et al., 2002; Zanata et al., 2002). STI1 is expressed predominantly in the cytoplasm, although a small fraction of STI1 can be detected in the nucleus (Lassle et al., 1997; Longshaw et al., 2004; Zanata et al., 2002) and at the cell surface (Zanata et al., 2002). Recent studies have also described a secreted form of STI1 (Eustace and Jay, 2004; Lima et al., 2007). Although a few studies of STI1 have been conducted, its distribution patterns during embryogenesis and in adult animals have never been documented.

Because previous studies have described specific roles for PrP^C, STI1, and Vn in different developmental events, it is important to examine the embryonic localization of these proteins. Here we investigate PrP^C, STI1, and Vn protein expression patterns throughout mouse embryonic life, from E8 to E18, and in PrP^C null (*Prnp*$^{0/0}$) mice.

MATERIALS AND METHODS

Animals

The wild-type (*Prnp*$^{+/+}$) mouse strain used here was generated by crossing F1 descendents from a 129/SV and C57BL/6J mating. PrP^C null (*Prnp*$^{0/0}$) mice were previously described (Bueler et al., 1992). One pregnant female was killed by cervical dislocation at 8, 10, 12, 16, or 18 days postcoitum. All embryos were removed and killed via hypothermia. All experiments were conducted strictly in accordance with the *Principles of laboratory animal care* (NIH publication 85-23, revised 1996). This study was approved by the Committee for Ethics in Use of Animals (CEUA) from Fundação Antonio Prudente/Hospital do Câncer (024-08), and all efforts were made to minimize the number of animals used and their suffering.

Antibodies

The anti-PrP^C antibody is a polyclonal raised in our laboratory by immunization of *Prnp*$^{0/0}$ mice with full-length recombinant mouse PrP^C. This serum is highly specific and recognizes three bands in Western blots from brain extracts of embryonic and adult mice, corresponding to the unglycosilated, monoglycosilated, and diglycosilated forms of PrP^C (Chiarini et al., 2002; Lee et al., 2001; Zanata et al., 2002). In immunofluorescence of cultured cells, it recognizes cell surface and a perinuclear region, compatible with the expected PrP^C localization (Chiarini et al., 2002; Lopes et al., 2005; Zanata et al., 2002).

The anti-STI1 antibody is a polyclonal custom made by Bethyl Inc. by immunizing rabbits with full-length recombinant mouse STI1. This purified IgG is highly specific and recognizes two bands of approximately 66 kDa in extracts from several organs from embryonic and adult mice (see Fig. 8). In immunofluorescence of cultured cells, the antibody presents a cytoplasmatic pattern, and in brain slices the antibody demonstrates a broad pattern of staining. When injected into the hippocampus, this antibody is able to block short- and long-term memory consolidation (Chiarini et al., 2002; Coitinho et al., 2007; Lopes et al., 2005; Zanata et al., 2002). To characterize this antibody further in immunofluorescence, we preadsorbed the anti-STI1 with recombinant STI1 for 30 minutes before addition into the tissues. Preadsorbed anti-STI1 did not demonstrate nonspecific reaction (Supp. Info. Fig. 1).

The anti-Vn is a polyclonal raised in our laboratory by immunizing rabbits with vitronectin purified from human plasma (Yatohgo et al., 1988). This antibody recognizes purified Vn as a band of approximately 75 kDa and another of approximately 60 kDa, which represent two cleavage forms of Vn (Hajj et al., 2007). In Western blots from mouse brain extracts, the anti-Vn also recognizes a 75- and a 60-kDa band. To characterize this antibody further in immunofluorescence, we preadsorbed the anti-Vn with purified Vn for 30 minutes before addition into the tissues. Preadsorbed anti-Vn did not demonstrate nonspecific reaction (Supp. Info. Fig. 1).

The anti-tau is a Dako polyclonal antiserum (catalog No. A0024) raised by immunizing rabbits with the recombinant C-terminal part (amino acids 243–441) of the human tau protein expressed in *Escherichia coli*. In Western blotting of lysates of Sf9 cells transfected with cDNA of human tau, the antibody labels tau independently of phosphorylation (Biernat et al., 2002). In immunohistochemistry of human brain, the staining of tau demonstrates neuronal loss in Alzheimer's disease patients (Pang et al., 2002). Dako anti-tau antibody also recognized tau in Western blots from human brain extracts and SH-SY5Y cells (Yu and Fraser, 2001). As demonstrated by immunohistochemistry and Western blotting of mouse brain, the antibody cross-reacts with the tau-equivalent protein in mouse (Taniguchi et al., 2005). In our

Figure 1.
Embryonic expression of PrP^C, STI1, and Vn proteins at E8, E10, and E12. Whole embryo coronal sections from E8 wild-type mice (**A–F**) were subjected to immunohistochemistry with anti-PrP^C (A,D), anti-STI1 (B,E), or anti-Vn (C,F) antibodies. STI1 and Vn expression can be observed, but no PrP^C expression was detected. D–F show a higher magnification of the neural tube. Whole embryo saggital sections from E10 wild-type mice (**G–I**) were subjected to immunohistochemistry with anti-PrP^C (G), anti-STI1 (H), or anti-Vn (I) antibodies. PrP^C expression was observed in the brain, spinal cord, and dorsal root ganglia. STI1 and Vn are broadly expressed. Whole embryo saggital sections from E12 *Prnp*$^{0/0}$ mice (**J–L**) were subjected to immunohistochemistry with anti-PrP^C (J), anti-STI1 (K), or anti-Vn (L) antibodies. The absence of PrP^C expression in *Prnp*$^{0/0}$ animals was observed, whereas STI1 and Vn presented the same pattern as the wild-type animals. Br, brain; Sp, spinal cord; Ht, heart; Li, liver; Lu, lung; Ga, dorsal root ganglia. Scale bars = 200 μm in A (applies to A–C); 40 μm in D (applies to D–F); 700 μm in G (applies to G–I) 1 mm in J (applies to J–L).

tapraid5/z3o-comp/z3o-comp/z3o03109/z3o6495d09g | sangreyj | S=7 | 7/31/09 | 17:24 | Art: 08-0488

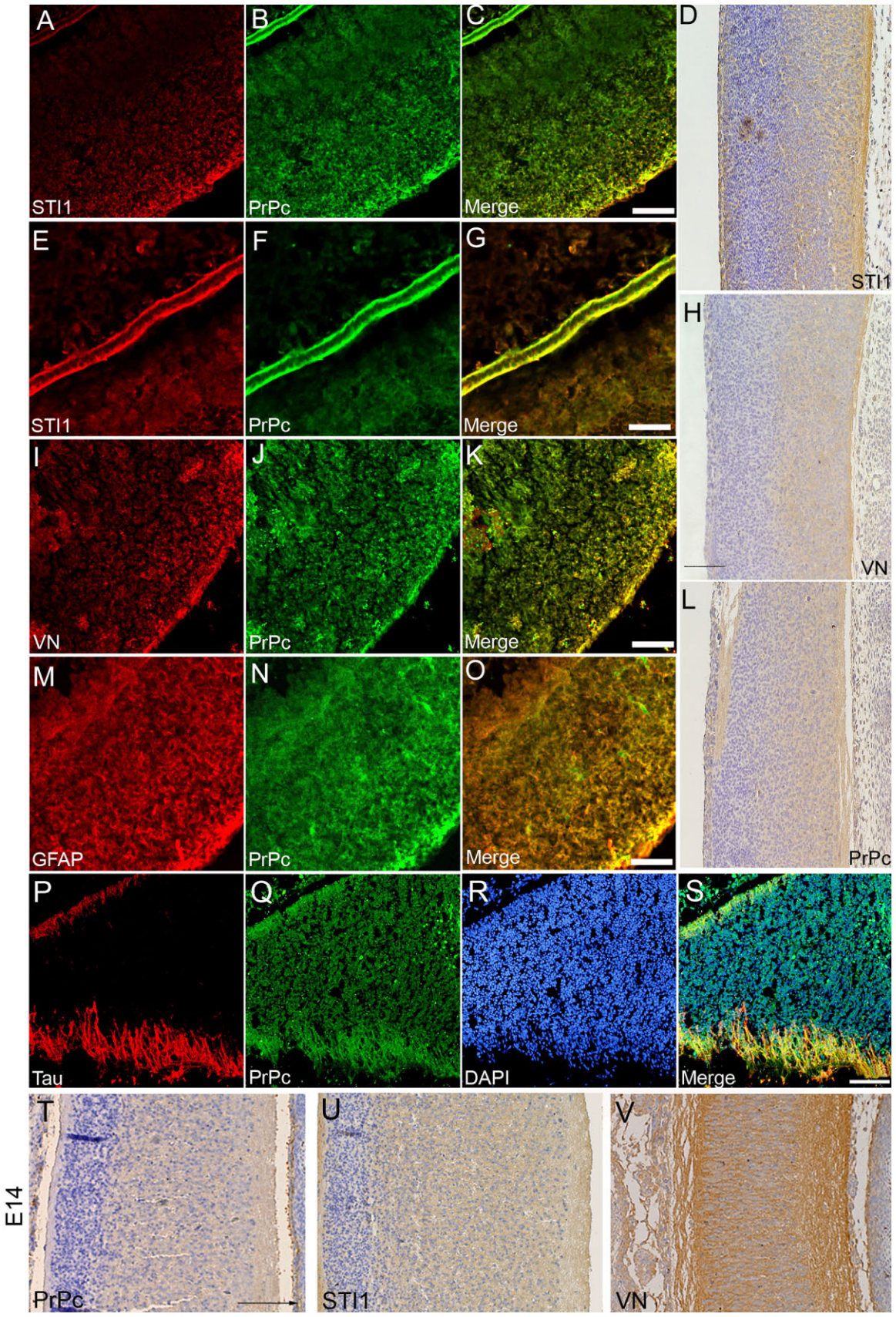

COLOR

Figure 2

experience, the antibody recognizes the growing nerves from mouse dorsal root ganglia (see Figs. 2P, 3M), which are mainly axons that grow from ganglia to innervate the peripheral regions of the body. In cultured mouse hippocampal neurons, this antibody specifically recognizes the largest neurite of the cell and does not colocalize with MAP-2 (data not shown). This labeling indicates that the anti-tau antibody is correctly recognizing axons, demonstrating the specificity of the antibody.

The anti-GFAP antibody is a rabbit polyclonal IgG from Dako (Carpinteria, CA; catalog No. Z0334), against GFAP isolated from cow spinal cord. GFAP shows 90–95% homology between species, and, as demonstrated by immunohistochemistry, the antibody cross-reacts with GFAP in cat, dog, mouse, rat, and sheep. In the rat hippocampal CAI region, the antibody recognized cells of astrocytic morphology that did not stain for other markers such as microglial nucleoside diphosphatase (Castellano et al., 1991). In cultured astrocytes, the antibody staining demonstrates a filamentous pattern, consistent with the GFAP presence in intermediate filaments. In Western blot from mouse brain extracts, it recognizes a band of approximately 55 kDa (Arantes et al., 2009).

Immunohistochemistry

After death, mouse embryos were formalin fixed and paraffin embedded. Sections (3–5 μm) were deparaffinized, rehydrated, and subjected to epitope retrieval (Martins et al., 1999). The endogenous peroxidase was blocked with 0.3 g/liter hydrogen peroxide. Sections were blocked in PBS plus 0.3% Triton X-100, 0.3% nonfat dried milk, 1% goat serum, then incubated overnight at 4°C with 1:1,000 anti-PrP^C, 1:250 anti-Vn, or 1:250 anti-STI1 in blocking buffer. Mouse nonimmune serum was used as negative control for anti-PrP^C; rabbit preimmune serum was used as negative control for anti-Vn; and rabbit nonimmune IgG was used as negative control for anti-STI1, antineurofilament, and anti-GFAP. Nonimmune goat IgG was used as negative control for anti-tau. The negative controls did not show any labeling. Reactions were followed by incubation for 60 minutes at room temperature with Dako EnVision Labeled Polymer peroxidase. Color was developed with 3,3′-diaminobenzidine tetrahydrochloride (DAB; Sigma, St. Louis, MO) and counterstained with hematoxylin. Slides were mounted with coverslips using Dako Faramount Aqueous Mounting Medium. Sections were visualized with an Olympus IMT2-NIC microscope, and images were acquired with Image Pro Plus (Media Cybernetics) and processed in Photoshop (Adobe Systems). Images were subjected to brightness/contrast adjustments.

Immunofluorescence

After death, embryos were immediately frozen in liquid nitrogen. Cryostat sections (3 mm) were fixed in ice-cold acetone for 30 minutes, air dried, and rehydrated in phosphate-buffered saline (PBS). Nonspecific binding was blocked by incubating sections in PBS containing 0.1% Triton X-100, 10% normal goat serum, and 50 μg/ml anti-mouse IgG at room temperature for 1 hour. Sections were then incubated overnight at 4°C with primary antibodies in PBS with 0.1% Triton X-100 and 1% goat serum (1:1,000 anti-PrP^C, 1:250 anti-Vn, 1:250 anti-STI1, 1:100 anti-tau, and 1:100 anti-GFAP). Mouse preimmune serum was used as negative control for anti-PrP^C; rabbit preimmune serum was used as negative control for anti-Vn; and rabbit irrelevant IgG was used as negative control for anti-STI1. The negative controls did not show any labeling. Reactions were followed by incubation for 60 minutes at room temperature with secondary antibodies coupled to Alexa 488, Alexa 546, or Alexa 405 (1:1,000 anti-mouse, 1:1,000 anti-rabbit, 1:1,000 anti-goat; Molecular Probes, Eugene, OR) and DAPI staining when necessary. Slides were mounted with coverslips using Fluorosave (Calbiochem, La Jolla, CA). Sections were imaged with a Bio-Rad (Hercules, CA) Radiance 2100 laser scanning confocal system running Laser Sharp 3.0 software, coupled with a Nikon microscope (TE2000-U). Images were processed in Photoshop (Adobe Systems).

Immunoblotting

Kidney, heart, cerebellum, hippocampus, cerebral cortex, and DRG from embryonic and postnatal mice were dissected and triturated in lysis buffer (50 mM Tris, 1 mM EDTA, 0.2% sodium deoxicolate, 0.5% Triton X-100) supplemented with a cocktail of protease inhibitors (Roche, Indianapolis, IN). Extracts were centrifuged for 10 minutes at 11,000*g*, and total protein in the supernatant was quantified. Protein extracts (50 μg) were resolved in 10% SDS-PAGE and transferred to a nitrocellulose membrane. Immunoblotting was performed with 1:1,000 anti-STI1 antibody and 1:300 antiactin antibodies, followed by incubation with peroxidase-coupled anti-rabbit IgG. The reaction was developed using enhanced chemiluminescence (ECL; Amersham, Arlington Heights, IL).

RESULTS

To verify the pattern of expression of PrP^C and its partners STI1 and Vn, immunohistochemistry and immunofluorescence were performed on sections from embryonic mice. At E8 and E10, wild-type whole embryo sections were analyzed (Fig. 1). F1
In these low-magnification photographs, STI1 and Vn expression can be observed as early as E8 throughout the entire embryo (Fig. 1B,C). The E8 neural tube (Fig. 1E,F) and mesoderm show labeling for both STI1 and Vn, but PrP^C appears only at E10 (Fig. 1A,D,G). At E10, PrP^C expression was observed in the brain, spinal cord, and DRG (Fig. 1G). Similarly to PrP^C, STI1 (Fig. 1H) and Vn (Fig. 1I) are broadly expressed but have higher levels of expression in the brain, spinal cord, and

Figure 2.
A–V: PrP^C, STI1, and Vn form a gradient of expression in the spinal cord. Immunoflourescence were performed on saggital sections from E10 wild-type embryos. Colocalization using anti-PrP^C (B,F,J, green), anti-STI1 (A,E, red), and anti-Vn (I, red) demonstrated that PrP^C colocalized with STI and Vn (C,G,K, merged). The notochord exhibited high expression of STI1 and PrP^C (E–G). Immunofluorescence with anti-PrP^C (N, green) and anti-GFAP (M, red) demonstrated that PrP^C is expressed in astrocytes (O, merged). Immunofluorescence with anti-PrP^C (Q, green), anti-tau (P, red), and DAPI (R, blue) demonstrated that PrP^C is concentrated on axons (S, merged). Immunohistochemistry was performed on saggital sections of E10 (D,H,L) and E14 (T–V) mouse embryos against PrP^C (L,T), STI1 (D,U), and Vn (H,V). The three proteins were expressed in a gradient at E10 but not at E14, with the highest levels of expression found in the ventral portion. All pictures show the spinal cord region of the embryo. A magenta-green copy of this figure is included as Supporting Information Figure 2. Scale bars = 80 μm in C (applies to A–C); 40 μm in G (applies to E–G); 40 μm in H (applies to D,H,L); 80 μm in K (applies to I–K); 115 μm in O (applies to M–O); 100 μm in S (applies to P–S); 40 μm in T (applies to T–V).

tapraid5/z3o-comp/z3o-comp/z3o03109/z3o6495d09g | sangreyj | S=7 | 7/31/09 | 17:24 | Art: 08-0488

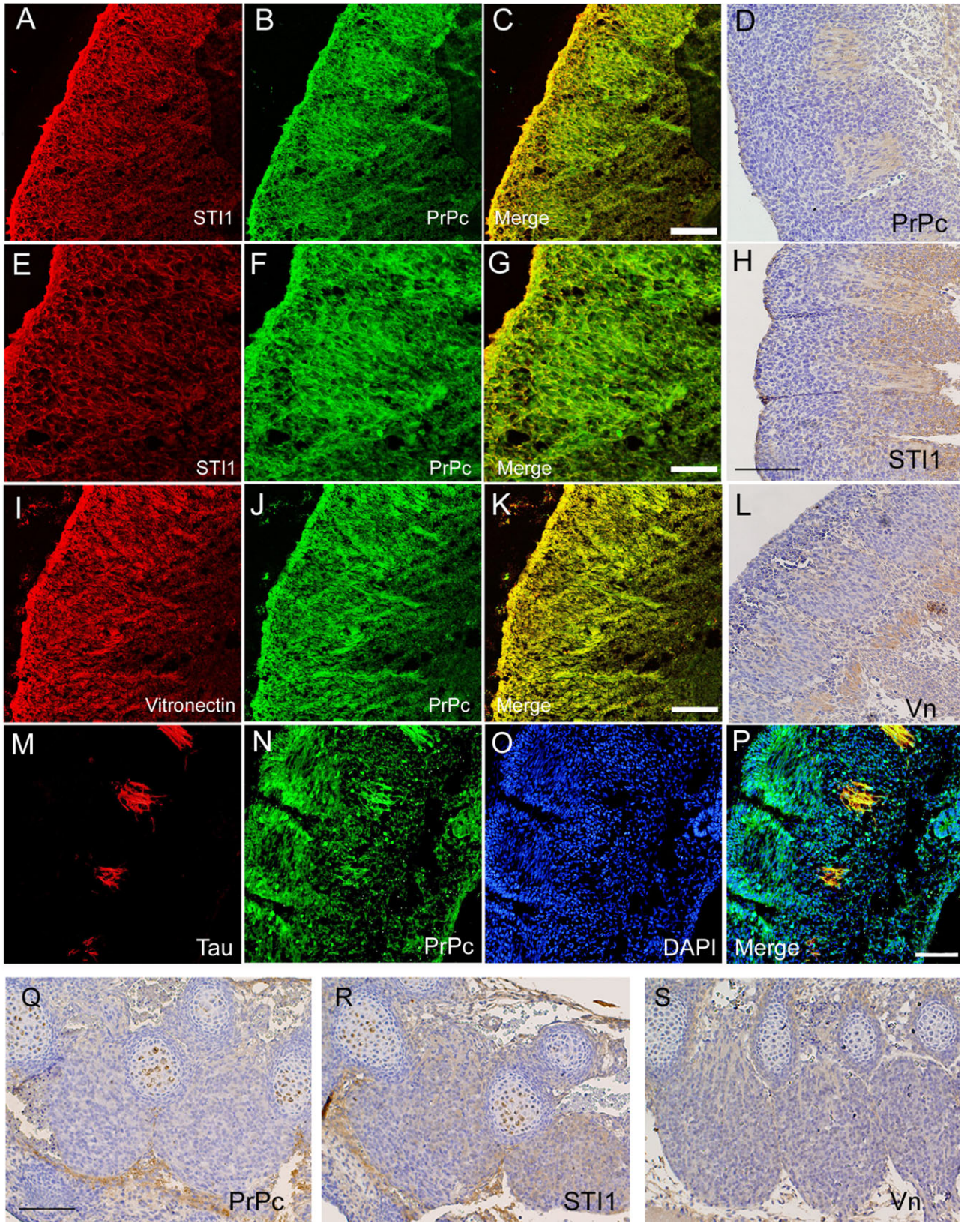

COLOR

Figure 3

heart (Fig. 1G–I). Immunohistochemistry confirmed the absence of PrP^C expression in *Prnp*$^{0/0}$ animals (Fig. 1J), whereas STI1 (Fig. 1K) and Vn (Fig. 1L) were expressed in the same patterns as observed in wild-type animals.

F2 In the wild-type spinal cord, PrP^C (Fig. 2B) and STI (Fig. 2A) partially colocalize (Fig. 2C). Remarkably, the notochord exhibited high expression of both STI1 (Fig. 2E) and PrP^C (Fig. 2F). Vn expression is also abundant (Fig. 2I), colocalized with PrP^C (Fig. 2J,K). In colocalization experiments with tau (Fig. 2P) and GFAP (Fig. 2M), we observed that PrP^C (Fig. 2Q,N) is expressed in both neurons and astrocytes (merged, Fig. 2O,S).

At E10, in the spinal cord, all three proteins were expressed in a gradient, with the highest levels of expression found in the ventral portion (Fig. 2D,H,L). E10 sections with immunolabeled PrP^C (Fig. 2Q), nuclei (Fig. 2R) and neuronal tau (Fig. 2P) showed PrP^C presence in axons in the ventral portion of the spinal cord. In contrast, the dorsal part of the spinal cord showed nuclear abundance. This demonstrates that the gradient observed was due to the enrichment of PrP^C in the axon zone of growing spinal cord (Fig. 2S). At E14, the gradient was abolished, and all three proteins were abundantly expressed in the spinal cord, Vn expression being the highest (Fig. 2T,U). The same pattern of expression for Vn and STI1 was observed in *Prnp*$^{0/0}$ embryos (data not shown).

F3 The same spatiotemporal relationship can be observed in the wild-type DRG, where, at E10, PrP^C (Fig. 3D), Vn (Fig. 3L) and STI1 (Fig. 3H) are more abundant in the axons and neurites than in the cell bodies. When double staining for tau (Fig. 3M) and PrP^C (Fig. 3N) was performed, we observed increased PrP^C expression in growing axons, as shown by tau colocalization (Fig. 3P). PrP^C, STI1, and Vn immunoreactivity patterns were highly colocalized (Fig. 3A–C,E–G,I–K). At E14, the three proteins could also be detected in the cell bodies (Fig. 3Q–S). The same pattern of expression for Vn and STI1 was observed in *Prnp*$^{0/0}$ embryos (data not shown).

F4 All three proteins were expressed in the wild-type heart beginning in early embryogenesis (Fig. 4). At E10 (Fig. 4A,D,G), the three proteins displayed high expression levels that were maintained through all embryogenesis. It is important to note that red blood cells, which are often present in the preparation, were not stained, demonstrating the specificity of the reaction and the absence of endogenous peroxidase in the preparation. Expression of the three proteins remained high in the heart at E14 (Fig. 4B,E,H) and E18 (Fig. 4C,F,I). Double-labeling experiments demonstrated PrP^C colocalization with Vn and STI1 in the heart. At E10, the three proteins were highly expressed and colocalized (Fig 4J–O). The same pattern of expression for Vn and STI1 was observed in *Prnp*$^{0/0}$ embryos (data not shown).

F5 In wild-type embryos, the kidneys (Fig. 5A) and lungs (Fig. 5D) expressed low levels of PrP^C at E14, and we observed almost undetectable levels of PrP^C expression in the liver (Fig. 5G). STI1 was barely expressed in kidney (Fig. 5B) and lung (Fig. 5E) but was present in the liver (Fig. 5H). On the other hand, Vn was abundantly expressed in kidney and lung (Fig. 5C,F). Vn expression was notably high in the liver (Fig. 5I), an organ known to produce and secrete this protein into the blood. Interestingly, Vn and STI1 were apparent in the connective tissue of the lung and kidney, but not in the forming bronchial tubes or glomeruli (Fig. 5B,C,E,F). The same pattern of expression for Vn and STI1 was observed in *Prnp*$^{0/0}$ embryos (data not shown).

F6 In wild-type embryos at E16, PrP^C and STI1 expressions were widespread (Fig. 6) and highly colocalized. In the neocortex, high expression of both proteins was observed, although STI1 had a more widespread expression pattern. Enhanced STI1 expression could be found in the cell bodies of the cortical plate of the neocortex (Fig. 6A). PrP^C expression was restricted to the cortical plate colocalized with STI1. However, we also observed some labeled cells in the intermediate zone that could be newly differentiated neurons migrating from the subventricular zone to the cortical plate (Fig. 6B). In DRG, STI1 expression was high and was mainly in the cell bodies (Fig. 6D). PrP^C immunoreactivity was also high in cell bodies but was observed in growing neurites as well (Fig. 6E). At this embryonic age, the heart, liver, and lung expressed both STI1 and PrP^C (Fig. 6G–O). In the lungs, PrP^C was restricted to the connective tissue, whereas STI1 could also be seen in the developing alveoli (Fig. 6M–O). The same pattern of expression for Vn and STI1 was observed in *Prnp*$^{0/0}$ embryos (data not shown).

F7 In E18 wild-type animals, PrP^C, STI1, and Vn were encountered in almost all tissues. PrP^C was detected at low levels in intestine (Fig. 7D). At E18, PrP^C was highly expressed in organs in which it had barely been detectable at E14, such as the lungs (Fig. 7A) and liver (Fig. 7M). For those tissues, we clearly observed cell membrane staining. Organs where PrP^C had been detected since early embryogenesis, such as spinal cord (Fig. 7J), heart (Fig. 7P), and DRG (Fig. 7S), showed increased expression at E18. We observed diffuse staining in spinal cord and heart, suggesting intracellular localization of the protein. For DRG, we observed nuclear localization only in large neurons, whereas nuclei of accompanying satellite cells were negative (Fig. 7S). It is important to note that skeletal muscle also expresses PrP^C at this stage (Fig. 7G), in a diffuse distribution, consistent with intracellular localization. Kidney PrP^C expression was present in the tubules but not in the glomeruli (data not shown). Endothelium was negative for PrP^C in our preparations (data not shown).

STI1 (Fig. 7B,E,H,K,N,Q,T) and Vn (Fig. 7C,F,I,L,O,R,U) were highly expressed in all organs evaluated at E18. STI1 localization was predominantly cytoplasmatic, consistent with its immunolocalization in cultured cells (Zanata et al., 2002). On the other hand, for the lungs (Fig. 7B) and DRG (Fig. 7T), we noticed some membrane localization. In kidney, STI1 was

Figure 3.
A–S: PrP^C, STI1, and Vn are expressed in DRG, especially in axons. Immunoflourescence was performed on saggital sections from E10 wild-type embryos. Immunofluorescence using anti-PrP^C (B,F,J, green), anti-STI1 (A,E, red), and anti-Vn (I, red) demonstrated that the three proteins are colocalized on this structure (C,G,K, merged). Colocalization of PrP^C (N, green) with Tau (M, red) and DAPI (O, blue) demonstrates that PrP^C is increased in axons (P, merged). Saggital sections of E10 (D,H,L) and E14 (Q–S) immunohistochemistry reactions were performed against PrP^C (D,Q), STI1 (H,R), and Vn (L,S). At E14, the three proteins could also be detected in the cell bodies. All pictures show the dorsal root ganglia region of the embryo. A magenta-green copy of this figure is included as Supporting Information Figure 3. Scale bars = 115μm in C (applies to A–C); 80 μm in G (applies to E–G); 120 μm in H (applies to D,H,L); 115 μm in K (applies to I–K); 100 μm in P (applies to M–P); 40 μm in Q (applies to Q–S).

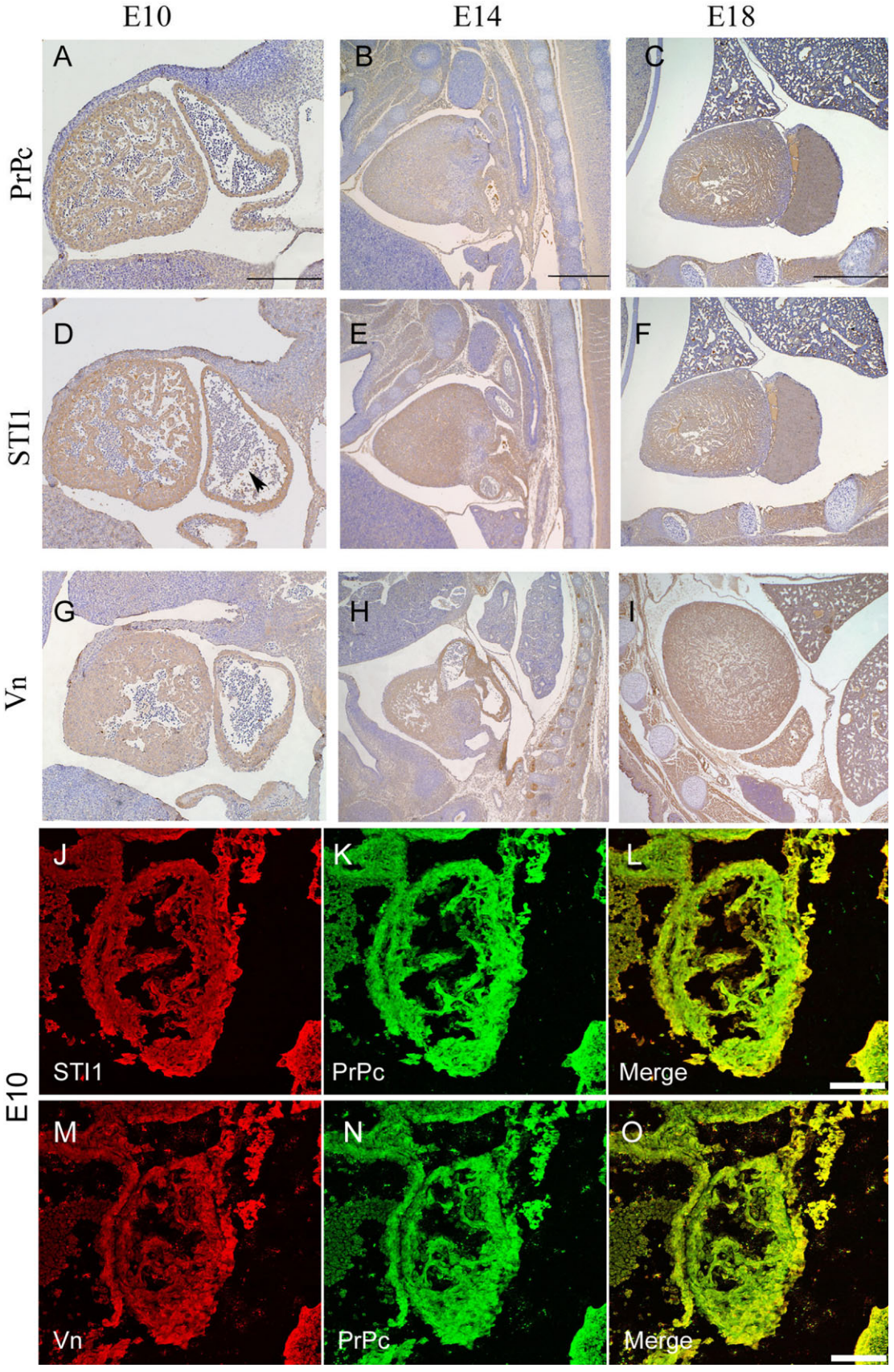

COLOR

Figure 4

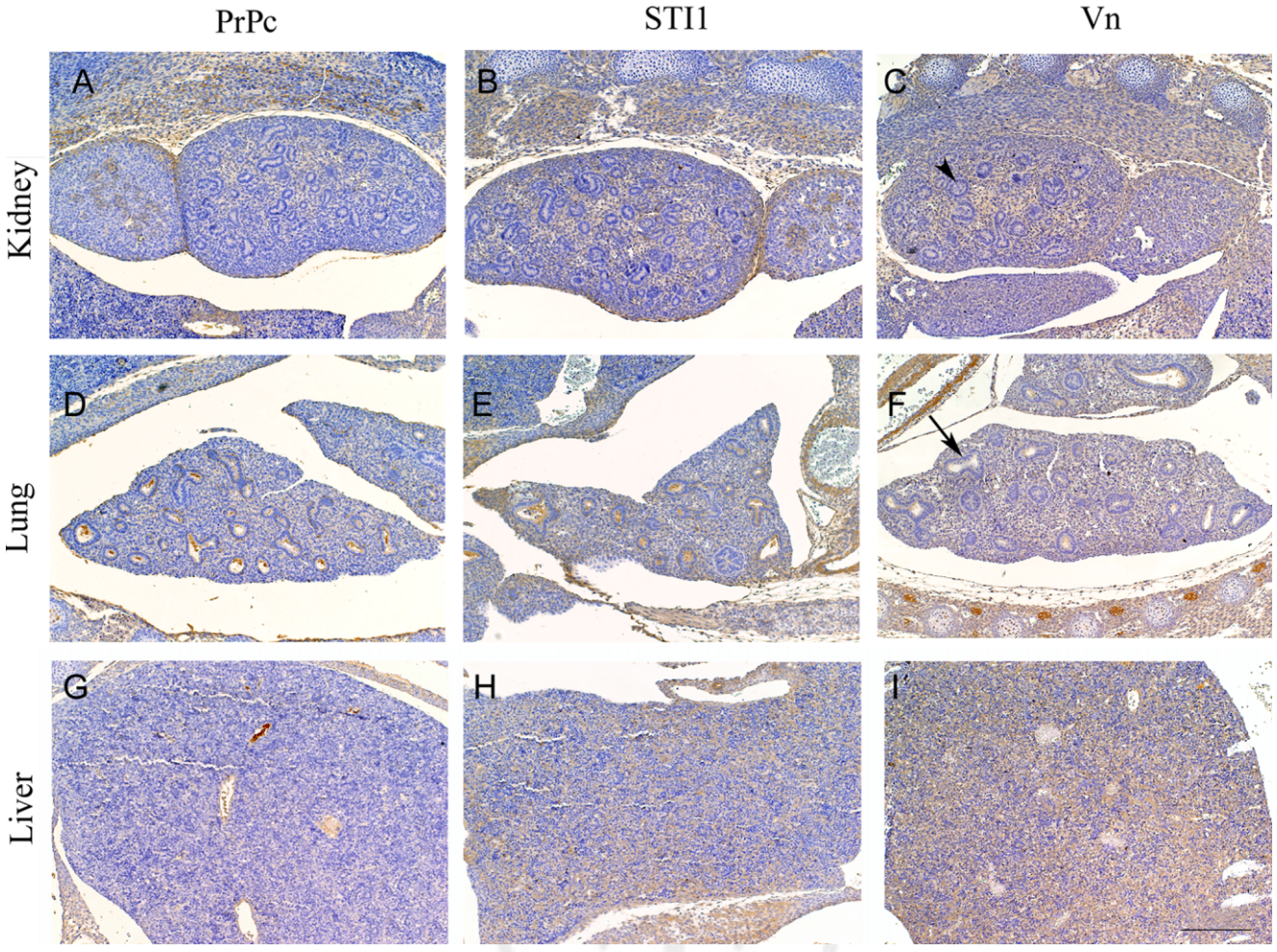

COLOR

Figure 5.
PrP^C, STI1, and Vn show low expression in the embryonic kidney, lung, and liver. Immunohistochemistry was performed on E14 sections with anti-PrP^C (**A,D,G**), anti-STI1 (**B,E,H**), or anti-Vn (**C,F,I**) antibodies. Figure shows higher magnifications of the kidney (A–C), lung (D–F), and liver (G–I) regions. Kidneys and lungs expressed low levels of PrP^C and STI1, whereas the liver had low amounts of PrP^C but had STI1 and Vn. Vn was abundantly expressed in kidney and lung. Arrowhead points to kidney glomeruli, and arrow points to the lung's forming bronchial tube. Scale bar = 80 μm.

expressed in an pattern identical to that of PrP^C, preferentially in tubules and not in the glomeruli (data not shown). The endothelium expressed high amounts of STI1 (data not shown), contrasting with the complete absence of PrP^C in this tissue.

Figure 4.
PrP^C, STI1, and Vn are expressed in the embryonic heart. Saggital sections of E10 (**A,D,B**), E14 (**B,E,H**), and E18 (**C,F,I**) mice were subjected to immunohistochemistry reactions with anti-PrP^C (A–C), anti-STI1 (D–F), or anti-Vn (G–I) antibodies. All three proteins displayed high expression levels that were maintained through embryogenesis. Double-labeling immunofluorescence of E10 saggital sections (**J–O**) using anti-PrP^C (K,N, green), anti-STI1 (J, red), and anti-Vn (M, red) demonstrated PrP^C colocalization with Vn and STI1 in the heart (L,O, merged). Figure shows higher magnifications of the heart region. Arrowhead indicates red blood cells. A magenta-green copy of this figure is included as Supporting Information Figure 4. Scale bars = 100 μm in A (applies to A,D,G); 200 μm in B (applies to B,E,H); 250 μm in C (applies to C,F,I); 115 μm in L (applies to J–L); 115 μm in O (applies to M–O).

Vn was expressed in a granular pattern, consistent with matrix deposition (Fig. 7C,F,I,L,O,R,U). We observed intracellular expression in some tissues, such as the heart (Fig. 7R), muscle (Fig. 7I), liver (Fig. 7O), and DRG (Fig. 7U), suggesting that these cells could be endocytosing or secreting Vn. The same pattern of expression for Vn and STI1 was observed in *Prnp*$^{0/0}$ embryos (data not shown).

Because very little is known about STI1 expression, we also performed semiquantitative Western blotting analyses of the protein at embryonic stages and perinatally in several organs. STI1 was found to be constitutively expressed in all organs (kidney, heart, cerebellum, hippocampus, cerebral cortex, and DRG) and throughout development beginning at E12. Protein loading was verified by probing the membranes with anti-β-tubulin antibody (Fig. 8). F8

The STI1 band appears as a doublet (Martins et al., 1997; Zanata et al., 2002; Fig. 8, arrowheads). With that in mind, it is particularly striking that, in kidney, hippocampus, cortex, and DRG, the higher molecular mass (66 kDa) form was more

tapraid5/z3o-comp/z3o-comp/z3o03109/z3o6495d09g | sangreyj | S=7 | 7/31/09 | 17:24 | Art: 08-0488

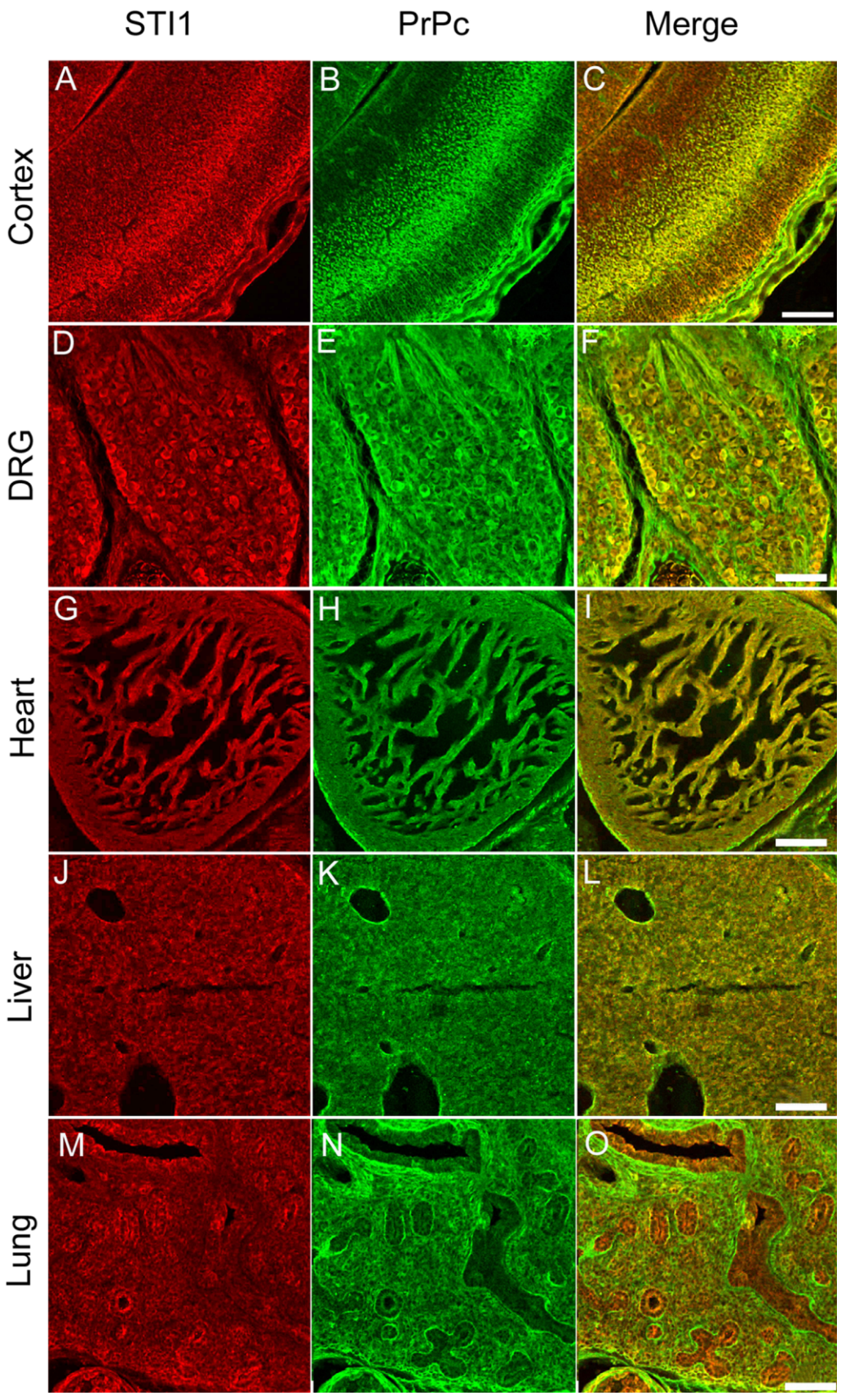

COLOR

Figure 6

abundant than the lower mass form (60 kDa), whereas, in heart and cerebellum, the lower molecular mass form was more predominant.

DISCUSSION

In this study, we evaluated the temporal expression pattern of STI1 and Vn and their colocalization with their ligand PrP^C. The present data demonstrate that PrP^C, STI1, and Vn are coexpressed in most of the tissues evaluated. STI1 and Vn could be detected at E8 and PrP^C at E10, first in the nervous system and later in other tissues.

For the E10 spinal cord, we observed a dorsoventral gradient of expression for PrP^C, STI1, and Vn, with enhanced expression in the floor plate. The areas of increased expression of the three molecules contained more axons than cell bodies. We also noticed PrP^C and STI1 expression in the notochord. This type of expression pattern is typical of morphogens such as Shh, a protein expressed in notochord and floor plate (Echelard et al., 1993) that is involved in dorsoventral patterning of the nervous system (Marti and Bovolenta, 2002). In fact, Vn expression has been demonstrated in the notochord and floor plate, where it interacts with Shh to promote motor neuron differentiation (Pons et al., 2001). This suggests that PrP^C, Vn, and STI1 could be involved in dorsoventral patterning of the nervous system or differentiation of neural populations in the spinal cord.

Because Vn is in the extracellular matrix and is also a blood-circulating protein, its reactivity could be a result of local synthesis and/or deposition. Therefore, care must be taken when evaluating its expression. We detected faint Vn reactivity in the nervous system beginning at E8 (Fig. 1C). At stage E8, liver development is just beginning. Therefore, it is unlikely that Vn reactivity is caused by deposition of liver-produced, circulating Vn. Vn deposition was observed in the ventral part of the spinal cord, liver, and heart in E10 embryos. Later in development, Vn was present in all organs studied, but we were not able to determine whether this deposition was due to local synthesis or to the already intense Vn production by the embryonic liver. As an extracellular matrix protein, the broad pattern of Vn expression is consistent with its functions in cell adhesion and migration (Schvartz et al., 1999). More specific roles for this protein could be observed in the patterning of the neural tube (Pons and Marti, 2000) and in the migration of precursor cells in the cerebellum (Pons et al., 2001). In DRG, it has also been demonstrated that Vn has a role in the elongation of axons through its binding to PrP^C (Hajj et al., 2007).

Figure 6.
PrP^C, STI1, and Vn are widely expressed in E16 mice. Immunofloures-cence was performed on saggital sections from E16 wild-type mice using anti-PrP^C (**B,E,H,K,N**, green) and anti-STI1 (**A,D,G,J,M**, red) antibodies. PrP^C and STI1 expression were widespread and highly colocalized (**C,F,I,L,O**, merged). In the neocortex, high expression of both proteins was observed (A–C). In dorsal root ganglia, PrP^C and STI1 were found in the cell bodies and PrP^C in growing neurites as well (D–F). The heart (G–I), liver (J–L), and lung (M–O) expressed both STI1 and PrP^C. A magenta-green copy of this figure is included as Supporting Information Figure 5. Scale bars = 100 μm in C (applies to A–C); 75 μm in F (applies to D–F); 155 μm in I (applies to G–I); 155 μm in L (applies to J–L); 40 μm in O (applies to M–O).

STI1 expression during development was described here for the first time. Its expression was observed in all organs studied beginning at E8 and increasing from E8 to E10, after which it was maintained at constant levels. STI1 is likely posttranslationally modified, which would account for a doublet observed in our immunoblotting assays. It is interesting to note that the predominant form of STI1 varies depending on the organ; this variation may reflect different functions of the protein. The role of STI1 as a cochaperone is consistent with its wide distribution. On the other hand, it has been recently described that STI1 can also be secreted (Lima et al., 2007) and has neurotrophic functions (Odunuga et al., 2004). It has been shown that STI1 provides neuroprotection and promotes neuritogenesis, both in the hippocampus and in the retina, through interaction with PrP^C (Chiarini et al., 2002; Lopes et al., 2005; Zanata et al., 2002).

PrP^C, STI1, and Vn immunoreactivity was pronounced in the heart starting at E10. These data strongly indicate that PrP^C interaction with STI1 and Vn outside of the nervous system may have important physiological roles in development, perhaps related to cell survival and differentiation. The presence of abnormal PrP^{Sc} deposition was previously demonstrated in the heart of a Creutzfeldt-Jakob patient with a severe dilated cardiomyopathy, whose etiology could not be established (Ashwath et al., 2005). Thus, we may speculate that loss-of-function might have important implications when PrP^C is converted to PrP^{Sc} in the heart (Bianchin et al., 2005).

PrP^C, STI1, and Vn expression in skeletal muscle beginning at E18 is also noteworthy. PrP^C is normally expressed in myoblasts and myotubes (Brown et al., 1998), and its expression has been shown to be increased in myositis and in neurogenic muscle atrophy (Kovacs et al., 2004). On the other hand, PrP^{Sc} has been detected in the muscle of patients with sporadic Creutzfeldt-Jakob disease and inclusion body myositis (Glatzel et al., 2003; Kovacs et al., 2004). As has been shown for heart and muscles, PrP^C may have pleiotrophic functions because of its association with STI1 and Vn in striated and skeletal muscles. Furthermore, pathological muscular symptoms in the presence of PrP^{Sc} may point to PrP^C loss-of-function.

At E16, PrP^C and STI1 can be found highly colocalized in the cortical plate of the neocortex. We further identified few labeled neurons in the intermediate zone, which seemed to be migrating to the cortical plate. During formation of the cerebral cortex, postmitotic neurons originate in the ventricular zone, migrate toward the marginal zone, and settle in the cortical plate in an inside-out manner. To organize this migratory process, multiple cellular events are required, including cell-to-cell recognition, adhesion, and detachment, guidance by extracellular factors, signaling cascades, and cell motility. The final location of each cortical neuron in the mature brain determines its morphology and patterns of synaptic connections (Garcia-Frigola et al., 2004). PrP^C and STI1 can be found in the cortical plate and in the intermediate zone, suggesting a role for PrP^C and STI1 in the patterning of neurons during formation of the cortex.

The constitutive expression of STI1 from E12 until adulthood was also confirmed by Western blot assays. Two forms of the protein can be detected, and their predominance varies between tissues. The presence of posttranslational modifica-

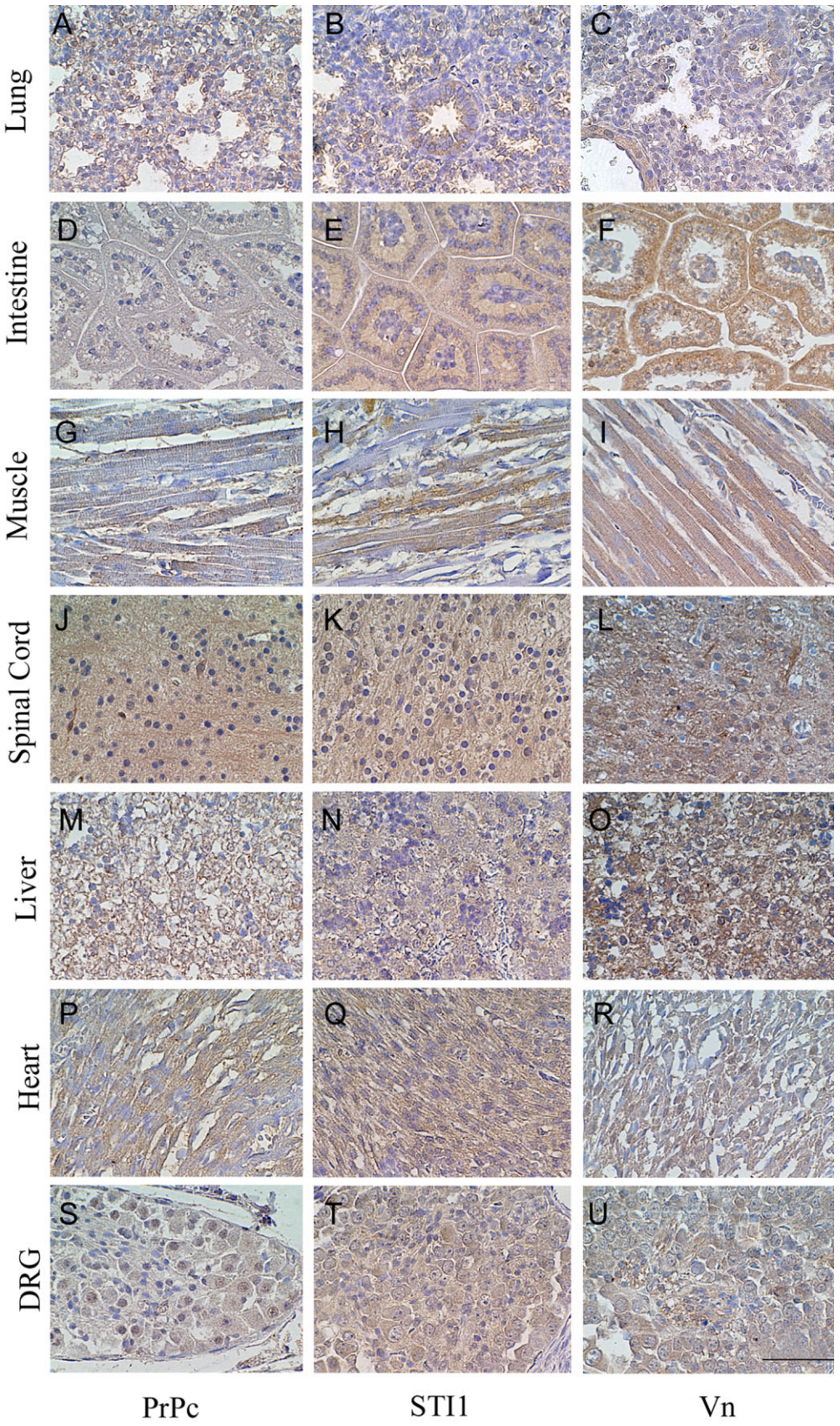

COLOR

Figure 7.
PrP^C, STI1, and Vn are widely expressed in E18 mice. Saggital sections of E18 mice were subjected to immunohistochemistry reactions with anti-PrP^C (**A,D,G,J,M,P,S**), anti-STI1 (**B,E,H,K,N,Q,T**), or anti-Vn (**C,F,I,L,O,R,U**). Figure shows high magnifications of the lung (A–C), intestine (D–F), skeletal muscle (G–I), spinal cord (J–L), liver (M–O), heart (P–R), and dorsal root ganglia (S–U). PrP^C, STI1 and Vn were encountered in almost all tissues. Scale bar = 20 μm.

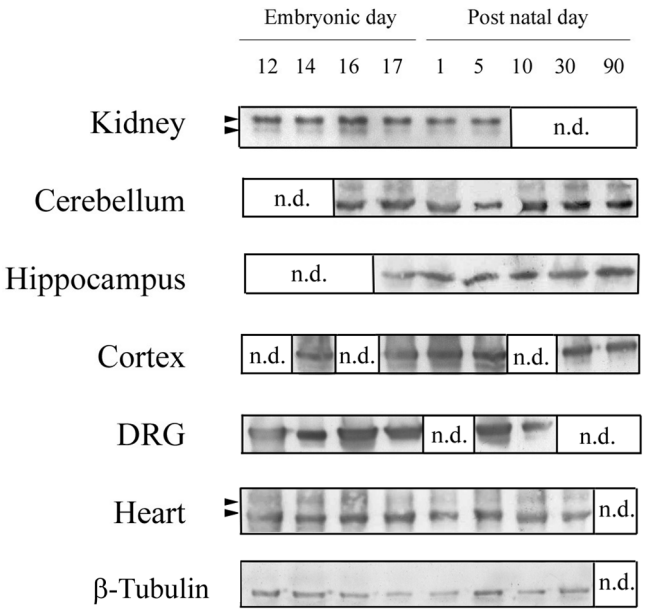

Figure 8.
STI1 is constitutively expressed from E10 until adulthood. Kidney, heart, cerebellum, hippocampus, cerebral cortex, and dorsal root ganglia (DRG) from mice at different embryonic and postnatal ages were dissected, and total protein extracts were subjected to SDS-PAGE. Immunoblotting assays were performed with anti-STI1 antibody. Membranes were reprobed with anti-β-tubulin as protein loading control. Arrowheads indicate the two forms of STI1. n.d., Not determined.

tions in STI1 and their contribution to protein function are presently under investigation.

Finally, we observed no differences in Vn or STI1 expression in PrP^C-null mice in labeling intensity or expression pattern, although these three proteins are all functionally related. We speculate that Vn and STI1 could interact with other cellular receptors in the absence of PrP^C, compensating for the loss of PrP^C and resulting in a normal phenotype in the null mice. This seems to be the case for Vn-PrP^C-dependent DRG axonal growth, which is compensated for, at least in part, by $\alpha v\beta 3$ integrin (Hajj et al., 2007). STI1 also has cell receptors other than PrP^C. We demonstrated that STI1 interacts with the cell surface and is internalized by a flotilin-dependent pathway in both wild-type and PrP^C-null cells (Caetano et al., 2008). Another possibility is that other PrP^C receptors at the cell surface, such as NCAM (Santuccione et al., 2005) or LRP/LR (Gauczynski et al., 2001), could interact with these proteins, maintaining their tissue architecture. Other proteins that could fulfill this role are ECM PrP^C interactors, such as glycosaminoglycans (Warner et al., 2002). Because Vn and STI1 can be secreted, it is possible that they interact with ECM components independently of PrP^C. Whether these interactions indeed happen remains to be established. More research is required to determine the relationship between PrP^C and its ligands, how its absence is compensated for, and whether its loss-of-function is related to prion diseases.

ACKNOWLEDGMENTS

We thank Carlos F. Nascimento and Miyuki Fukuda for technical assistance and Dr. Mariana M. Cajaíba for helpful discussions on the immunohistochemistry analysis.

LITERATURE CITED

Arantes C, Nomizo R, Lopes MH, Hajj GN, Lima FR, Martins VR. 2009. Prion protein and its ligand stress inducible protein 1 regulate astrocyte development. Glia (in press).

Asante EA, Gowland I, Linehan JM, Mahal SP, Collinge J. 2002. Expression pattern of a mini human PrP gene promoter in transgenic mice. Neurobiol Dis 10:1–7.

Ashwath ML, DeArmond SJ, Culclasure T. 2005. Prion-associated dilated cardiomyopathy. Arch Intern Med 165:338–340.

Basso AS, Frenkel D, Quintana FJ, Costa-Pinto FA, Petrovic-Stojkovic S, Puckett L, Monsonego A, Bar-Shir A, Engel Y, Gozin M, et al. 2008. Reversal of axonal loss and disability in a mouse model of progressive multiple sclerosis. J Clin Invest 118:1532–1543. AQ: 1

Beaulieu JM, Robertson J, Julien JP. 1999. Interactions between peripherin and neurofilaments in cultured cells: disruption of peripherin assembly by the NF-M and NF-H subunits. Biochem Cell Biol 77:41–45. AQ: 1

Bianchin MM, Walz R, Brentani RR, Martins VR. 2005. Dilated cardiomyopathy and Creutzfeldt-Jakob disease: evidence for a role of cellular prion protein in the heart? Arch Intern Med 165:1663–1664.

Biernat J, Wu YZ, Timm T, Zheng-Fischhofer Q, Mandelkow E, Meijer L, Mandelkow EM. 2002. Protein kinase MARK/PAR-1 is required for neurite outgrowth and establishment of neuronal polarity. Mol Biol Cell 13:4013–4028.

Brown DR, Schmidt B, Groschup MH, Kretzschmar HA. 1998. Prion protein expression in muscle cells and toxicity of a prion protein fragment. Eur J Cell Biol 75:29–37.

Bueler H, Fischer M, Lang Y, Bluethmann H, Lipp HP, DeArmond SJ, Prusiner SB, Aguet M, Weissmann C. 1992. Normal development and behaviour of mice lacking the neuronal cell-surface PrP protein. Nature 356:577–582.

Burkhalter A, Gonchar Y, Mellor RL, Nerbonne JM. 2006. Differential expression of I(A) channel subunits Kv4.2 and Kv4.3 in mouse visual cortical neurons and synapses. J Neurosci 26:12274–12282. AQ: 1

Caetano FA, Lopes MH, Hajj GN, Machado CF, Pinto AC, Magalhaes AC, Vieira MP, Americo TA, Massensini AR, Priola SA, et al. 2008. Endocytosis of prion protein is required for ERK1/2 signaling induced by stress-inducible protein 1. J Neurosci 28:6691–6702.

Castellano B, Gonzalez B, Jensen MB, Pedersen EB, Finsen BR, Zimmer J. 1991. A double staining technique for simultaneous demonstration of astrocytes and microglia in brain sections and astroglial cell cultures. J Histochem Cytochem 39:561–568.

Chiarini LB, Freitas AR, Zanata SM, Brentani RR, Martins VR, Linden R. 2002. Cellular prion protein transduces neuroprotective signals. EMBO J 21:3317–3326.

Coitinho AS, Lopes MH, Hajj GN, Rossato JI, Freitas AR, Castro CC, Cammarota M, Brentani RR, Izquierdo I, Martins VR. 2007. Short-term memory formation and long-term memory consolidation are enhanced by cellular prion association to stress-inducible protein 1. Neurobiol Dis 26:282–290.

Ding Q, Stewart J Jr, Olman MA, Klobe MR, Gladson CL. 2003. The pattern of enhancement of Src kinase activity on platelet-derived growth factor stimulation of glioblastoma cells is affected by the integrin engaged. J Biol Chem 278:39882–39891.

Echelard Y, Epstein DJ, St.-Jacques B, Shen L, Mohler J, McMahon JA, McMahon AP. 1993. Sonic hedgehog, a member of a family of putative signaling molecules, is implicated in the regulation of CNS polarity. Cell 75:1417–1430.

Eustace BK, Jay DG. 2004. Extracellular roles for the molecular chaperone, hsp90. Cell Cycle 3:1098–1100.

Garcia-Frigola C, Burgaya F, Calbet M, Lopez-Domenech G, Soriano E. 2004. A collection of cDNAs enriched in upper cortical layers of the embryonic mouse brain. Brain Res Mol Brain Res 122:133–150.

Gauczynski S, Peyrin JM, Haik S, Leucht C, Hundt C, Rieger R, Krasemann S, Deslys JP, Dormont D, Lasmezas CI, et al. 2001. The 37-kDa/67-kDa laminin receptor acts as the cell-surface receptor for the cellular prion protein. EMBO J 20:5863–5875.

Glatzel M, Abela E, Maissen M, Aguzzi A. 2003. Extraneural pathologic

prion protein in sporadic Creutzfeldt-Jakob disease. N Engl J Med 349:1812–1820.

Hajj GN, Lopes MH, Mercadante AF, Veiga SS, da Silveira RB, Santos TG, Ribeiro KC, Juliano MA, Jacchieri SG, Zanata SM, et al. 2007. Cellular prion protein interaction with vitronectin supports axonal growth and is compensated by integrins. J Cell Sci 120:1915–1926.

Kovacs GG, Lindeck-Pozza E, Chimelli L, Araujo AQ, Gabbai AA, Strobel T, Glatzel M, Aguzzi A, Budka H. 2004. Creutzfeldt-Jakob disease and inclusion body myositis: abundant disease-associated prion protein in muscle. Ann Neurol 55:121–125.

Lassle M, Blatch GL, Kundra V, Takatori T, Zetter BR. 1997. Stress-inducible, murine protein mSTI1. Characterization of binding domains for heat shock proteins and in vitro phosphorylation by different kinases. J Biol Chem 272:1876–1884.

Lee KS, Magalhaes AC, Zanata SM, Brentani RR, Martins VR, Prado MA. 2001. Internalization of mammalian fluorescent cellular prion protein and N-terminal deletion mutants in living cells. J Neurochem 79:79–87.

Lima FR, Arantes CP, Muras AG, Nomizo R, Brentani RR, Martins VR. 2007. Cellular prion protein expression in astrocytes modulates neuronal survival and differentiation. J Neurochem (in press).

Linden R, Martins VR, Prado MA, Cammarota M, Izquierdo I, Brentani RR. 2008. Physiology of the prion protein. Physiol Rev 88:673–728.

Longshaw VM, Chapple JP, Balda MS, Cheetham ME, Blatch GL. 2004. Nuclear translocation of the Hsp70/Hsp90 organizing protein mSTI1 is regulated by cell cycle kinases. J Cell Sci 117:701–710.

Lopes MH, Hajj GN, Muras AG, Mancini GL, Castro RM, Ribeiro KC, Brentani RR, Linden R, Martins VR. 2005. Interaction of cellular prion and stress-inducible protein 1 promotes neuritogenesis and neuroprotection by distinct signaling pathways. J Neurosci 25:11330–11339.

Marti E, Bovolenta P. 2002. Sonic hedgehog in CNS development: one signal, multiple outputs. Trends Neurosci 25:89–96.

Martinez-Morales JR, Marti E, Frade JM, Rodriguez-Tebar A. 1995. Developmentally regulated vitronectin influences cell differentiation, neuron survival and process outgrowth in the developing chicken retina. Neuroscience 68:245–253.

Martinez-Morales JR, Barbas JA, Marti E, Bovolenta P, Edgar D, Rodriguez-Tebar A. 1997. Vitronectin is expressed in the ventral region of the neural tube and promotes the differentiation of motor neurons. Development 124:5139–5147.

Martins VR, Graner E, Garcia-Abreu J, de Souza SJ, Mercadante AF, Veiga SS, Zanata SM, Neto VM, Brentani RR. 1997. Complementary hydropathy identifies a cellular prion protein receptor. Nat Med 3:1376–1382.

Martins AR, Dias MM, Vasconcelos TM, Caldo H, Costa MC, Chimelli L, Larson RE. 1999. Microwave-stimulated recovery of myosin-V immunoreactivity from formalin-fixed, paraffin-embedded human CNS. J Neurosci Methods 92:25–29.

Miele G, Alejo Blanco AR, Baybutt H, Horvat S, Manson J, Clinton M. 2003. Embryonic activation and developmental expression of the murine prion protein gene. Gene Expr 11:1–12.

Odunuga OO, Longshaw VM, Blatch GL. 2004. Hop: more than an Hsp70/Hsp90 adaptor protein. Bioessays 26:1058–1068.

Pang JT, Giunti P, Chamberlain S, An SF, Vitaliani R, Scaravilli T, Martinian L, Wood NW, Scaravilli F, Ansorge O. 2002. Neuronal intranuclear inclusions in SCA2: a genetic, morphological and immunohistochemical study of two cases. Brain 125:656–663.

Pons S, Marti E. 2000. Sonic hedgehog synergizes with the extracellular matrix protein vitronectin to induce spinal motor neuron differentiation. Development 127:333–342.

Pons S, Trejo JL, Martinez-Morales JR, Marti E. 2001. Vitronectin regulates sonic hedgehog activity during cerebellum development through CREB phosphorylation. Development 128:1481–1492.

Preissner KT. 1991. Structure and biological role of vitronectin. Annu Rev Cell Biol 7:275–310.

Prusiner SB. 1998. Prions. Proc Natl Acad Sci U S A 95:13363–13383.

Roberts MS, Woods AJ, Shaw PE, Norman JC. 2003. ERK1 associates with alpha(v)beta 3 integrin and regulates cell spreading on vitronectin. J Biol Chem 278:1975–1985.

Ruoslahti E, Pierschbacher MD. 1987. New perspectives in cell adhesion: RGD and integrins. Science 238:491–497.

Santuccione A, Sytnyk V, Leshchyns'ka I, Schachner M. 2005. Prion protein recruits its neuronal receptor NCAM to lipid rafts to activate p59fyn and to enhance neurite outgrowth. J Cell Biol 169:341–354.

Schvartz I, Seger D, Shaltiel S. 1999. Vitronectin. Int J Biochem Cell Biol 31:539–544.

Seiffert D. 1997. Constitutive and regulated expression of vitronectin. Histol Histopathol 12:787–797.

Seiffert D, Iruela-Arispe ML, Sage EH, Loskutoff DJ. 1995. Distribution of vitronectin mRNA during murine development. Dev Dyn 203:71–79.

Smith DF, Sullivan WP, Marion TN, Zaitsu K, Madden B, McCormick DJ, Toft DO. 1993. Identification of a 60-kilodalton stress-related protein, p60, which interacts with hsp90 and hsp70. Mol Cell Biol 13:869–876.

Suzuki S, Oldberg A, Hayman EG, Pierschbacher MD, Ruoslahti E. 1985. Complete amino acid sequence of human vitronectin deduced from cDNA. Similarity of cell attachment sites in vitronectin and fibronectin. EMBO J 4:2519–2524.

Taniguchi T, Doe N, Matsuyama S, Kitamura Y, Mori H, Saito N, Tanaka C. 2005. Transgenic mice expressing mutant (N279K) human tau show mutation dependent cognitive deficits without neurofibrillary tangle formation. FEBS Lett 579:5704–5712.

Warner RG, Hundt C, Weiss S, Turnbull JE. 2002. Identification of the heparan sulfate binding sites in the cellular prion protein. J Biol Chem 277:18421–18430.

Yatohgo T, Izumi M, Kashiwagi H, Hayashi M. 1988. Novel purification of vitronectin from human plasma by heparin affinity chromatography. Cell Struct Funct 13:281–292.

Yu WH, Fraser PE. 2001. S100beta interaction with tau is promoted by zinc and inhibited by hyperphosphorylation in Alzheimer's disease. J Neurosci 21:2240–2246.

Zanata SM, Lopes MH, Mercadante AF, Hajj GN, Chiarini LB, Nomizo R, Freitas AR, Cabral AL, Lee KS, Juliano MA, et al. 2002. Stress-inducible protein 1 is a cell surface ligand for cellular prion that triggers neuroprotection. EMBO J 21:3307–3316.

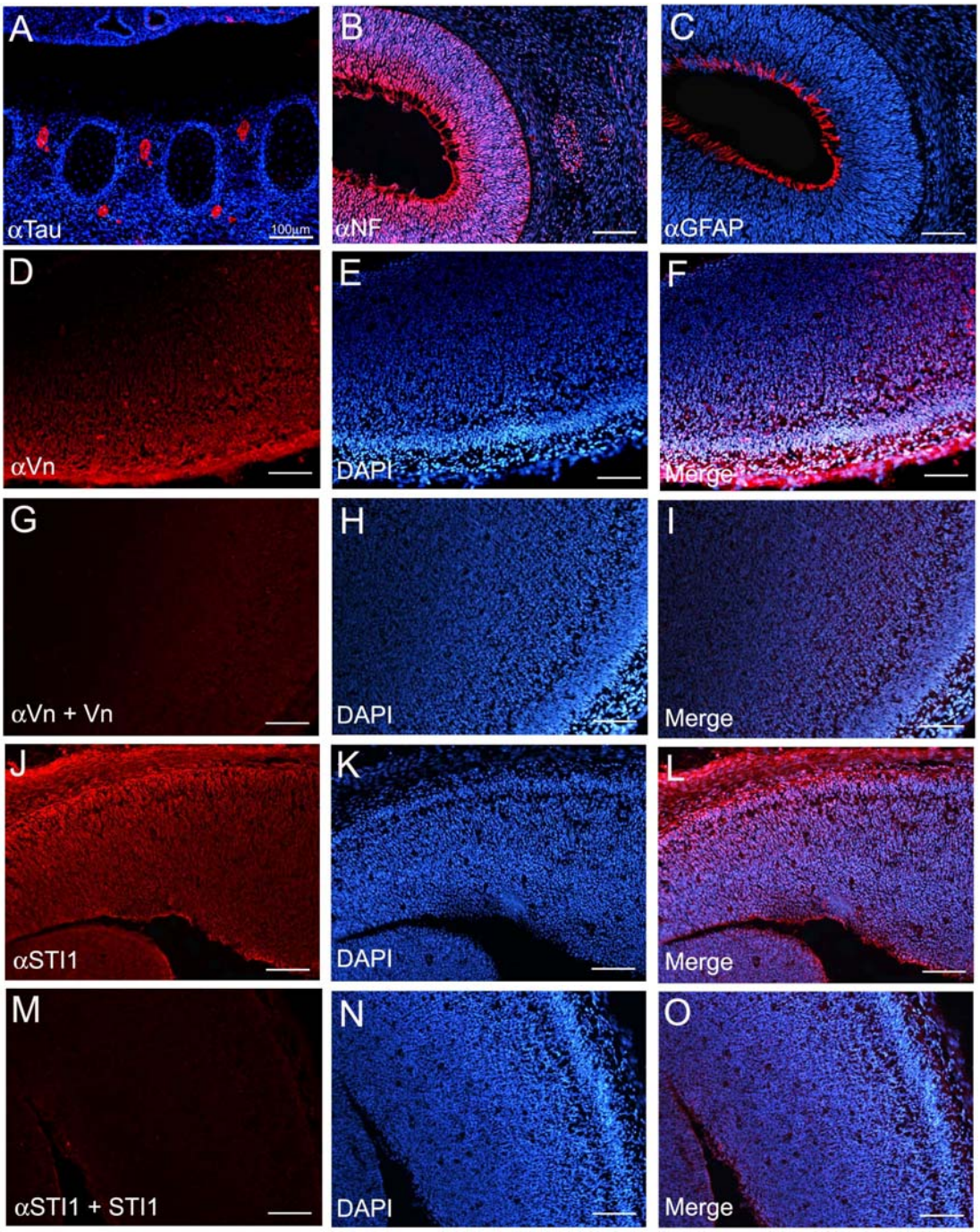

Suplementaty Figure 1 – Saggital sections from E14 wild-type mice were submitted to immunofluorescence to anti-Tau (A), anti-neurofilament (B), anti-GFAP (C), anti-Vn (D), anti-Vn pre-absorbed with purified plasma Vn (G), anti-STI1 (J) and anti-STI1 pre-absorbed with recombinant STI1 (M). Superimpose with DAPI (blue) are shown in merge (A, B, C, F, I, L, O). Pictures denote the following regions: dorsal root ganglia (A), retina (B, C) and brain (D-O). Scale bar, 100 µm.

PARTE II

Peptídeo da cadeia γ1 de laminina e STI1 atuam sinergicamente no crescimento axonal de gânglios da raiz dorsal pela interação com PrP^C.

1. Desenvolvimento do sistema nervoso periférico: gânglio da raiz dorsal.

A origem dos precursores neuronais de gânglios da raiz dorsal (GRD) está relacionada com a crista neural (CN, Figura 3), que corresponde a um grupo de células pluripotentes que participam da formação de ossos, tendões, tecidos conjuntivos, tecido adiposo, derme, glândulas, além do SNP. As células da CN são formadas na região dorsal do tubo neural, num gradiente rostro-caudal durante a neurulação. Adquirindo propriedades mesenquimais, as células da CN migram por rotas distintas de maneira tempo-específica até chegarem ao seu sítio final de diferenciação (LE DOUARIN et al. 1992).

Os precursores neuronais de GRD da CN migram e posicionam-se ventro-lateralmente na medula espinhal, onde no período gestacional de 13 dias no rato, já podem ser identificadas como um gânglio (LAWSON et al. 1974). Nos GRD lombares, a última divisão celular é observada entre os dias gestacionais 12-14 em rato e 10-13 no camundongo, após a saída do ciclo celular os precursores neuronais adquirem características maduras (LE DOUARIN et al. 1992).

Os GRD apresentam diversas funções dentro da organização do sistema nervoso periférico (SNP), onde cada segmento da medula espinhal apresenta uma raiz dorsal sensorial e uma raiz ventral motora (Figura 4) (PERL 1992). Durante o desenvolvimento, é possível observar diversas interações entre os processos que

partem dos GRD e os tecidos em formação da periferia. Quando um prolongamento de um neurônio imaturo não consegue estabelecer contato com um tecido alvo, é normal observar sua degeneração, que culmina com a morte do neurônio nascente. Em contrapartida, a ausência de neurônios de GRD pode levar ao bloqueio de certos aspectos da maturação de tecidos periféricos associados com terminais nervosos (DENNY-BROWN 1951). No adulto, a perda de aferências primárias de neurônios pode levar ao comprometimento de tecidos associados com seus terminais periféricos (GUTMANN 1976). Portanto, neurônios de GRD apresentam efeitos de suporte trófico para certas características dos tecidos que eles inervam (PERL 1992).

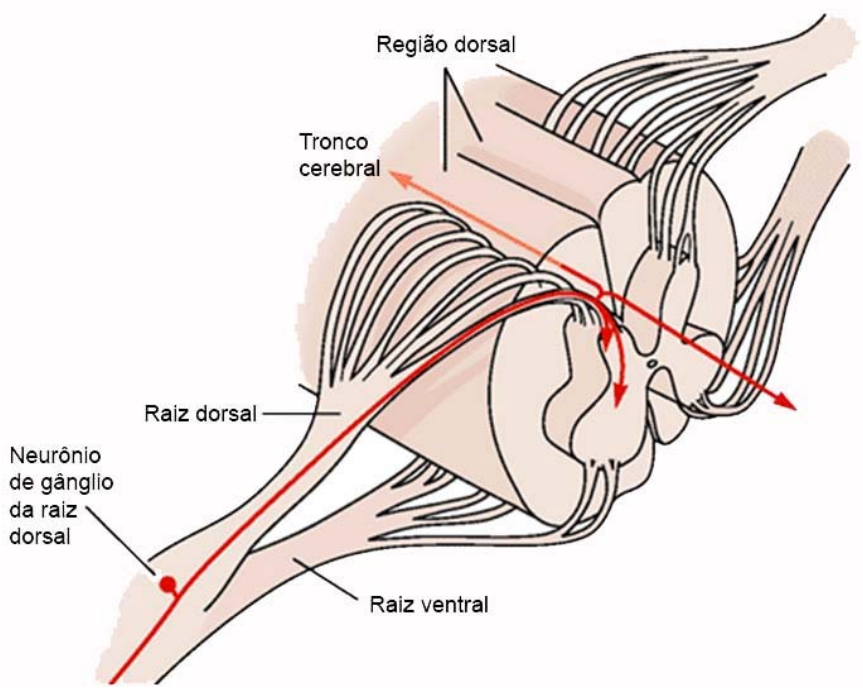

Fonte: Adaptado de KANDEL et al. (2000).
Figura 4 - Desenho esquemático representando gânglios da raiz dorsal.

2. Crescimento e orientação de axônios e dendritos:

O estabelecimento de conexões neuronais corretas é crucial para o funcionamento do sistema nervoso. O encéfalo humano, por exemplo, é constituído por dezenas de bilhões de neurônios, dos mais diferentes tipos, que se organizam uma rede altamente complexa, com número de conexões que podem alcançar a ordem de 10^{15} (KANDEL et al. 2000). O entendimento do funcionamento do cérebro passa pelo estudo de como essa rede neuronal é formada com tamanha precisão durante o desenvolvimento do sistema nervoso (CHIEN 2005).

Ao longo do desenvolvimento do sistema nervoso, uma etapa crucial corresponde ao crescimento direcionado de processos neurais a partir do corpo celular do neurônio, que ao final de sua maturação formarão os axônios e dendritos. Com morfologias bem distintas, neurônios em geral apresentam um único axônio, relativamente fino e longo, que não se ramifica extensivamente, exceto próximo aos terminais sinápticos. Em contrapartida, neurônios apresentam um grande número de dendritos, mais curtos e espessos, se ramificam de maneira elaborada e dão suporte a densidades pós-sinápticas e espinhas dendríticas (KANDEL et al. 2000).

Para conseguir conectar com seus alvos, neurônios extendem seus processos e na sua extremidade está localizada uma especialização subcelular denominda de cone de crescimento (PLACHEZ e RICHARDS 2005). Nos anos de 1880, Santiago Ramón y Cajal foi o pioneiro na descrição do cone de crescimento como uma estrutura móvel de axônios em extensão. Durante o desenvolvimento do sistema nervoso, os cones de crescimento percorrem caminhos específicos, reconhecem seus alvos e então formam conexões sinápticas elaborando terminais ramificados (CHIEN 2005). Na sua rota, o comportamento de cones de crescimento segue o caminho

apropriado através da interação com alvos intermediários. A rota a ser seguida é resultado de uma combinação de vários tipos de pistas de orientação (*guidande cues*), incluindo sinais atrativos e repulsivos (PLACHEZ e RICHARDS 2005). A forma na qual os cones de crescimento respondem a estas pistas não é fixa, ou seja, é um processo dinâmico que apresenta diversas mudanças durante a navegação de acordo com a informação posicional encontrada (SANES et al. 2006). A maneira pela qual um sinal quimioatratente ou quimiorepulsivo é transmitido pode variar desde o contato direto do cone de crescimento com uma célula que expressa o ligante, ou por moléculas secretadas que difundem por distâncias maiores chegando ao alcance do cone.

Um grande número de pistas e receptores já foram identificados (MUELLER 1999; TESSIER-LAVIGNE et al. 1988). Existem quatro famílias de moléculas envolvidas na orientação de cones de crescimento: netrinas, slits, semaforinas e efrinas com seus respectivos receptores. Entretanto, um grande número de moléculas fora destas famílias também já foram caracterizados como sendo pistas de orientação, incluindo morfógenos, esteróides, moléculas de adesão e componentes da matriz extracelular, como a família da laminina, tenascina, colágeno, fibronectina e proteoglicanos (PLACHEZ e RICHARDS 2005). A maioria destas famílias de moléculas é importante para a orientação axonal em todo o reino animal. Portanto, trata-se de um mecanismo celular de controle de motilidade celular bastante antigo que foi cooptado durante a evolução (CHIEN 2005). O Quadro 2 mostra as principais moléculas envolvidas no controle do crescimento de processos neuronais.

Quadro 2 - Atividade dos sinais de orientação axonal.

	Moléculas de Superfície	**Moléculas Secretadas**
Positivo	*Adesão*	*Permissivo*
	Caderinas	Laminina
	NCAM	Fibronectina
		Atrativo
		Netrinas
		Semaforinas
		BDNF
Negativo	*Repulsivo*	*Inibitório*
	Ephrinas	Proteoglicanos de condroitin sulfato
	Semaforinas	*Repulsivo*
	Nogo	Netrina
	MAG	Slit
		Semaforinas
Modulatório		Proteoglicanos de heparan sulfato
		Laminina
		Slit

Nota: Os sinais de orientação podem ser tanto de superfície celular quanto secretados, e podem apresentar atividade positiva, negativa ou modulatória. Um determinado sinal pode ter atividades múltiplas dependendo do contexto celular.

3. Mecanismos de transdução de sinal associados ao crescimento neurítico

Quando um sinal envolvido com orientação une-se a um receptor na membrana plasmática do cone de crescimento, a informação deve ser transmitida de alguma maneira para que ocorra o rearranjo do citoesqueleto. A informação posicional transduzida obedece as seguintes etapas: distribuição da informação pela célula, amplificação de pequenos sinais em grandes efeitos no citoesqueleto, que será modificado em função de um sinal atrativo ou repulsivo. A integração dos sinais

recebido pelo cone de crescimento definirá o resultado de crescimento, retração ou repulsão. A sinalização envolvida na orientação de cones de crescimento é extremamente complexa e tem sido cada vez mais estudada (CHIEN 2005), entretanto, alguns segundos mensageiros essenciais governam este evento. São eles:

a- Cálcio: O íon Ca^{2+} é conhecido por atuar em diversas vias de sinalização e, obviamente, desempenha um papel primordial nas vias que regulam o crescimento neurítico (BOLSOVER 2005; GOMEZ e ZHENG 2006; ZHENG e POO 2007). Curiosamente, o Ca^{2+} entá envolvido tanto na estimulação de crescimento de filopódios (LAU et al. 1999) quanto na inibição de crescimento axonal (GOMEZ e SPITZER 1999). Portanto, o Ca^{2+} pode apresentar efeitos opostos dependendo do tipo e do contexto celular, por exemplo, já foi demonstrado que gradiente de netrina-1 induz aumento na concentração de cálcio no cone de crescimento, mas o resultado de atração ou repulsão dependerá do padrão preciso deste aumento (HONG et al. 2000).

b- Nucleotídeos cíclicos: A Adenosina Monofosfato cíclico e Guanosina Monofosfato cíclico (AMPc e GMPc, respectivamente) apresentam uma variedade de efeitos no cone de crescimento, principalmente como moduladores de diferentes sinais de orientação (SONG e POO 1999). Netrina-1, fator de crescimento de nervos (NGF) e fator de crescimento derivado de cérebro (BDNF) , são moléculas que estão envolvidas na atração de cones de crescimento, e este efeito é revertido quando a sinalização por AMPc é inibida por um antagonista competitivo. Por outro lado, um sinal que normalmente está envolvido na repulsão de cones de crescimento como o MAG, promove a atração quando a via de AMPc é ativada. Muitos sinais também são mediados por GMPc: neurotrofina-3 (NT3) muda de um sinal atrativo para

repulsivo quando a sinalização por GMPc é inibida, enquanto que Sema3A promove a atração de cone de crescimento, ao invés de repulsão quando a via de GMPc é ativada. Estes dados mostram de maneira clara que um cone de crescimento responde diferentemente a sinais dependendo da concentração de nucleotídeos cíclicos, que por sua vez pode ser controlada por uma infinidade de sinais extracelulares (SONG e POO 1999).

c- GTPases Rho, Rac e cdc42: Muitas proteínas de vias de sinalização estão envolvidas na modulação do cone de crescimento, incluindo as quinases Abl ou Pak, que presumidamente contribuem na amplificação de sinal. Proteínas adaptadoras como a Dock e Ena, que conectam os receptores de membrana a seus componentes de sinalização, também participam neste evento. Porém, as GTPases pequenas pertencentes às família Rho, Rac e cdc42 são as melhores caracterizadas no que concerne a regulação do citoesqueleto em função de sinais de atração/repulsão (LUO 2000). Estas proteínas funcionam como interruptores moleculares, no estado ligado a GTP elas permanecem ativas. Sua atividade GTPásica intrínseca promove a hidrólise de GTP (guanosina trifosfato) a GDP (guanosina difosfato), tornando-as inativas. A substiuição do GDP por GTP promove sua ativação novamente. Este ciclo é regulado por proteínas ativadoras de GTPase (denominadas GAP, de *GTPase-activating protein*) e por proteínas trocadoras de nucleotídeos da guanina (GEF, de *guanine nucleotides exchange factors*). As Rho GTPases controlam as mudanças de citoesqueleto e a motilidade de filopódios (CHIEN 2005).

Neste trabalho, demonstramos que, semelhante ao observado com Vn (ANEXO I), STI1 e o peptídeo da cadeia γ1 deLn (Ln-γ1) também estão envolvidos

no crescimento axonal dependente de PrP^C em neurônios de GRD. Também observamos que utilizando diferentes combinações de doses de STI1 e Ln-γ1 também é possível observar um efeito sinérgico sobre a axonogênese.

Descrevemos algumas vias de sinalização pelas quais os ligantes de PrP^C podem exercer suas funções, como as vias dependentes de cálcio intracelular. Enquanto STI1, ao unir-se a PrP^C, promove a abertura de canais na membrana plasmática, Ln-γ1 leva a mobilização de cálcio de estoques intracelulares, como o retículo endoplasmático. As proteínas responsáveis por transduzir os sinais do complexo PrP^C/STI1 e PrP^C/Ln-γ1 ainda não foram identificadas. Entretanto, os dados do presente artigo sugerem que sejam proteínas transmembrana distintas, como por exemplo canais de Ca^{2+} para o complexo PrP^C/STI1 e receptores acoplados a proteína G para o complexo PrP^C/Ln-γ1. De fato, no artigo apresentado na Parte V desta tese será demostrado com maiores detalhes a descrição do complexo PrP^C/Ln-γ1 com receptores acoplados a proteína G.

Estes dados corroboram a visão de STI1 e Ln-γ1 como fatores neurotróficos que se associam a diferentes domínios de seu receptor PrP^C e são capazes de deflagar vias de sinalização distintas e processos envolvidos no desenvolvimento e plasticidade do sistema nervoso

Este trabalho foi conduzido por mim, incluindo o planejamento e execução dos experimentos, organização dos dados e a confecção do artigo que será submetido à publicação.

Laminin-γ1 chain and stress inducible protein 1 synergistically mediate PrP^C-dependent axonal growth via Ca^{2+} mobilization in dorsal root ganglia.

Tiago G. Santos[§,¶], ; Flavio H. Beraldo[§,‡]; Glaucia N. M. Hajj[§]; Marilene H. Lopes[§]; Vilma R. Martins[§]*.

§ – Ludwig Institute for Cancer Research, Hospital Alemão Oswaldo Cruz, São Paulo, Brazil.

¶ – Centro de Tratamento e Pesquisa, Hospital A.C. Camargo, São Paulo, Brazil.

‡ – Robarts Research Institute, Department of Physiology and Pharmacology. University Western Ontario, London, ON, Canada

* Corresponding author: Dr. Vilma R. Martins, Ludwig Institute for Cancer Research, São Paulo, 01323-903, Brazil e-mail:vmartins@ludwig.org.br

Running head

Laminin-γ1 and STI1 synergism in axonogenesis

Abbreviations

PrP^C, prion protein; STI1- Stress Inducible protein 1, Ln-laminin.

Abstract

Prions are infectious pathogens associated to neurodegenerative diseases generated by the structural conversion of the prion protein (PrP^C), a cell surface glycoprotein abundantly expressed in the nervous system. The cellular functions of PrP^C and loss-of-function in prion diseases are under intensive investigation. We have characterized that PrP^C mediates neuritogenesis and neuronal protection through laminin-γ1 chain peptide (Ln- γ1) or stress inducible protein 1 (STI1) interaction. Herein, we investigated the involvement of PrP^C in axonogenesis when engaged with Ln- γ1 or STI1 in dorsal root ganglia neurons, assessing the role of calcium signaling. The Ln-γ1, corresponding to PrP^C binding site, and STI1 were able to promote axonogenesis (axon sprouting and outgrowth) in wild-type neurons while no effect was observed in PrP^C-null neurons. Moreover, suboptimal combinations of Ln-γ1 and STI1 induced axonogenesis, suggesting a synergic effect of STI1 plus Ln-γ1. PrP^C binding to Ln-γ1 or STI1 causes an increase intracellular Ca^{2+} by distinct mechanisms, whereas STI1 promotes extracellular Ca^{2+} influx, Ln-γ1 recruits calcium from intracellular stores. These results suggest that PrP^C acts as a pivotal molecule in a multimolecular complex including laminin and STI1 which in turn mediate axonogenesis through distinct signaling pathways.

Introduction

Prion protein (PrP^C), existing mainly on cell surface protein anchored through a glycosylphosphatidylinositol, is a ubiquitous protein frequently associated to transmissible spongiform encephalopathies (TSE). The conversion of PrP^C to scrapie form PrP^{Sc} in the TSEs results in neuronal loss and progressive neurodegeneration (Moore et al., 2009). However, in the past decade many groups have shown physiological functions of PrP^C, supporting that depletion of this protein can contribute to TSE pathogenesis by a loss-of-function mechanism (Sakudo and Ikuta, 2009).

In the nervous system, many PrP^C roles have been characterized; many of them through interaction with cell surface molecules (Linden et al., 2008). PrP^C directly interacts with neural cell adhesion molecule (NCAM) (Schmitt-Ulms et al., 2001), leading to stabilization of NCAM in lipid rafts and activation of $p59^{fyn}$ to induce NCAM-dependent neuritogenesis (Santuccione et al., 2005). Components of extracellular matrix (ECM) and their cell surface receptors, have been shown to interact with PrP^C, revealing the importance of this protein in proper organization and function of ECM, which represents a well-known microenvironment involved in cell survival, migration and differentiation (Venstrom and Reichardt, 1993). Among those, it was described the interaction between PrP^C and 37-kDa/67-kDa Laminin Receptor Precursor (37LRP/67LR) (Rieger et al., 1997; Gauczynski et al., 2001). Association of 37LRP/67LR with ECM glycoprotein laminin (Ln) is involved in dynamic cellular processes, e.g, increased filopodia, directional motility, modulation of gene expression and facilitation of Ln-integrins interaction (Nelson et al., 2008). Additionally, PrP^C itself directly interacts with Ln, within Ln-γ1 chain (between

amino acids 1575-1584) and with vitronectin (between amino acids 307-320), inducing neuritogenesis in hippocampal neurons and axonogenesis in dorsal root ganglia, respectively (Graner et al., 2000; Hajj et al., 2007). PrP^C also binds to ECM glycosaminoglycans heparin and heparan sulfate, however further biological function need to be determined for those interactions (Warner et al., 2002). A recent report have shown that PrP^C could be a receptor for Aβ oligomers, small soluble aggregates of amyloid-β peptides involved in Alzheimer's disease (Hardy and Selkoe, 2002). The authors suggest that Aβ oligomers bind to PrP^C (within amino acid residues 95-110), inhibiting long-term potentiation, impairing synaptic function and neuronal plasticity (Lauren et al., 2009).

PrP^C has also been shown to interact with stress inducible protein 1 (STI1), a co-chaperone which associates to Hsp70 and Hsp90, facilitating protein folding and maturation (Nicolet and Craig, 1989). STI1 is secreted by astrocytes reaching the extracellular milieu (Lima et al., 2007) and its interaction with PrP^C promotes phosphorilation of Erk1/2, which is involved in neuritogenesis and also activates PKA promoting neuroprotection against cell death (Lopes et al., 2005).

The intracellular mechanisms involved in PrP^C-dependent signals are in constant investigation and the participation of intracellular calcium homeostasis emerge as one of the main second messenger responsible to mediate PrP^C function (Sorgato and Bertoli, 2009). The first link between prion protein and calcium dynamics was the evidence of reduction of bradykinin-induced intracellular calcium ($[Ca^{2+}]_i$) mobilization in neuronal cell lines infected with prions (Kristensson et al., 1993;Wong et al., 1996). Thereafter, it has been shown that PrP^C-null neurons present altered intracellular calcium homeostasis in cerebellar granule neurons

(Herms et al., 2000) and hippocampal CA1 neurons (Fuhrmann et al., 2006). Moreover, the hyperexcitability attributed to PrP^C-null mice (Collinge et al., 1994;Colling et al., 1996;Walz et al., 1999;Mallucci et al., 2002) may be due the absence of PrP^C negative modulation of NMDAR currents which could lead to higher excitability (Khosravani et al., 2008). Heterologous expression of PrP^C in CHO cells also alters intracellular calcium fluctuation in different cell compartments after activation of purinergic receptors (Brini et al., 2005).

The large number of PrP^C-interacting molecules led us to hypothesize that PrP^C is a key member of a multiprotein complex in plasma membrane that organizes signaling modules involved in cellular processes such as cell survival, differentiation and proliferation (Martins et al, 2002; Linden et al., 2008). In this context, we asked whether PrP^C-mediated axonogenesis could be triggered by combination of distinct PrP^C ligands such as Ln-γ1 chain peptide and STI1 in dorsal root ganglia neurons. The signaling pathways triggered by PrP^C interaction with these ligands was also addressed, particularly the role of Ca^{2+}-related pathways. Our data indicate that combination of suboptimal concentrations of Ln-γ1 with STI1 has a prominent effect axonogenesis. The binding of Ln-γ1 and STI1, alone or combined, triggered rapid intracellular calcium mobilization which is necessary for sprouting processes, axon growth and maintenance.

Experimental Procedures

Dorsal root ganglia (DRG) primary cultures and morphometric evaluation: primary DRG cultures were obtained from E12,5 wild type (*Prnp*$^{+/+}$) and PrP^C knockout (*Prnp*$^{0/0}$) mice embryos (Bueler et al., 1992). DRG were dissected in HBSS

(Gibco) and trypsinized (0.25%) for 20 min at 37ºC. Trypsin was inactivated with 10% FCS in Neurobasal medium, after washing with HBSS, cells were mechanically dissociated in Neurobasal medium. Cells (5 x 10^6 cells) were transferred to Poly-L-Lysine (5 μg/ml) pre-coated coverslips and cultured in Neurobasal medium supplemented with B-27 (Gibco), glutamine (2mM, Sigma), streptomycin (100 μg/ml) and penicillin (100U/ml) and 50 ng/ml Nerve Growth Factor (Sigma). Cells were treated with recombinant STI1, full-length Ln (purified from EHS tumors as described by Paulsson et al., 1987), synthetic Ln-γ1 peptide (Ln-γ1, Sequence RNIAEIIKDI, Neosystem) or scrambled Ln-γ1 peptide (SCR, Sequence IRADIEIKID, Neosystem). In axonogenesis assays, Ln, Ln-γ1 or SCR peptide were previously adsorbed on coverslips and cells were cultured onto these substrates. To allow proper adsorption, peptides were conjugated to bovine serum albumin (BSA). Cells were incubated at 37º C at humidified atmosphere 5% CO_2 for 2 or 6 hours and, then fixed with 4% paraformaldehyde for 20 min, after washing with PBS, cells were stained with hematoxylin. Images were acquired with Olympus IX70 inverted microscope coupled with DP30BW camera. Morphometric analyses were done using ImageJ software (National Institutes of Health, NIH, Bethesda, MD) with Neuron J. The morphometric parameters evaluated were: the percentage of cells with axons and axon length. Three to five fields (around 300 hundred cells) per treatment were analyzed.

Immunofluorescence: *Prnp*$^{+/+}$ and *Prnp*$^{0/0}$ cells were plated on glass coverslips, fixed with 4% paraformaldehyde and 0.12M sucrose in PBS. For permeabilization, the cells were incubated with 0.2% Triton X-100 in PBS for 5 min at room temperature. After rinsing with PBS, cells were blocked with PBS plus 20% horse

serum. Labeling with βIII-tubulin antibody (Tuj, Chemicon) was used to identify neurons. Anti-Tuj (1:100) was incubated in PBS plus 1% horse serum at room temperature for 1 hour. The reaction proceeded by incubation of secondary antibody, anti-mouse Alexa Fluor® 546 (1:1000, Molecular Probes), followed by nuclei staining with 4′,6-diamino-2-phenylindole (1:1000, DAPI). After washing, coverslips were mounted on slides using Fluorsave Reagent (Calbiochem). Immunolabeled cells were imaged with Bio-Rad (Hercules, CA) Radiance 2100 laser scanning confocal system running the software Laser Sharp 3.0, coupled to a Nikon (Melville, NY) Microscope (TE2000-U). Green HeNe (543 nm) and Blue Diode (405 nm) lasers were used to excite the fluorophores.

Signaling pathways evaluation: signaling pathways in DRG axonogenesis were addressed using specific pharmacological inhibitors of Mitogen Activated Protein Kinase, MAPK/Erk (U0126 50nM), cyclic AMP-dependent Protein Kinase, PKA (KT5720 60nM), Calcium/Phosphatidyl-inositol triphosphate-dependent Protein Kinase, PKC (chelerythrine chloride 100nM), Phosphoinositide 3-Kinase, PI3-K (LY294002 5 μM), Phospholipase C, PLC (U73122 1μM) and Inositol 1,4,5-Triphosphate Receptor, $InsP_3$-R (2-APB 250μM). All inhibitors were purchased from Calbiochem. After 30 min of inhibitors pre-incubation, the cells were plated in the presence of PrP^C ligands and cultured for 2 or 6 hours at 37ºC at humidified atmosphere 5% CO_2.

Fluorescence calcium measurements with Fluo-3 indicator: DRG neurons were plated on 50mm Glass botton microwell dishes (Mat-Tek Corporation, Ashland, MA) for 1 hour with Neurobasal medium + NGF. Cells were incubated with fluorescent calcium indicator Fluo-3-AM (10 μM, Calbiochem) for 30 min in the

presence of 2 mM $CaCl_2$ at 37ºC at humidified atmosphere 5% CO_2. After that, cells were washed 3x with HBSS and maintained in Krebs buffer (NaCl 118 mM, KCl 4.7 mM, $CaCl_2$ 2.5 mM, $MgSO_4$ 1.2 mM, KH_2PO_4 1.2 mM, $NaHCO_3$ 25 mM, glucose 5.55 mM, pH 7,4) with $CaCl_2$. The variation of cytoplasmatic fluorescence intensity after treatments was analyzed by confocal microscopy. Argon laser (488 nm) was used to excite Fluo-3 with emission filters 522-535. Images were acquired in 512 x 512 resolution in 250 seconds assays in cycles of 1 second. Drugs were added to the medium after 50 seconds of imaging and fluorescence intensity was quantified with WCIF ImageJ software performing initial and final fluorescence ratio (F1/F0). In some experiments, extracellular calcium was removed through washing with HBSS and incubating cells in a calcium-free Krebs buffer plus 2 mM EGTA.

Statistical analyses: results represent the mean ± standard error of at least three independent experiments. One-way ANOVA with Dunnet´s post hoc test was used to analyse axonogenesis and calcium experiments.

Results

Ln-γ1 and STI1 promote axonogenesis through PrP^C interaction.

To determine the effect of Ln-γ1 and STI1 in axonogenesis (sprouting processes) and axonal extension (axon growth and maintenance) of peripheral neurons, dorsal root ganglia (DRG) neurons were treated with STI1, Ln or Ln-γ1 (Ln peptide corresponding to PrP^C binding domain on γ1 chain). Figure 1A to D show representative pictures from *$Prnp^{+/+}$* neurons cultured in the presence of poly-L-lysine (1A), 0.5 μM STI1 (1B), 2μg/mL full-length Ln (1C) or 37μM Ln-γ1 (1D). The neurons were labeled with βIII-tubulin and nuclei stained with DAPI. The

morphology of neurons was altered when cultured in the presence of STI1, presenting increased number of cells with short axons after 6 h of incubation (Figure 1B). This effect was also observed with Ln-γ1 (Figure 1D). The effect of Ln was more evident, with neurons presenting longer axons in almost all cells in the field (Figure 1C).

The quantification of axonogenesis was performed in hematoxylin stained *Prnp*$^{+/+}$ and *Prnp*$^{0/0}$ cells (Figs 1E and 1F). STI1 and Ln-γ1 were able to increase the number of neurons with axons in a PrP^{C}-dependent manner after 6 h of incubation (Fig 1E), while full-length Ln promoted extensive increase in the number of cells with axons in both genotypes (Fig 1F). Cells cultured onto poly-L-lysin or on peptide containing a scrambled amino acid sequence of Ln-γ1 (SCR 37μM), had no effect upon axonogenesis either in wild-type or PrP^{C}-null cells. When the axon length was evaluated (Figure 1F), STI1 and Ln-γ1 had no effect (Figure 1B), being this parameter altered in both genotypes only by full-length Ln. This effect was expected, considering that laminin presents other surface receptors, including a number of integrins subunits, proteins directly associated with formation of cellular extensions (Belkin and Stepp, 2000). The scrambled peptide had no effect in cell morphology, indicating a specific effect of Ln-γ1 chain sequence in axonogenesis through PrP^{C} binding on cell surface.

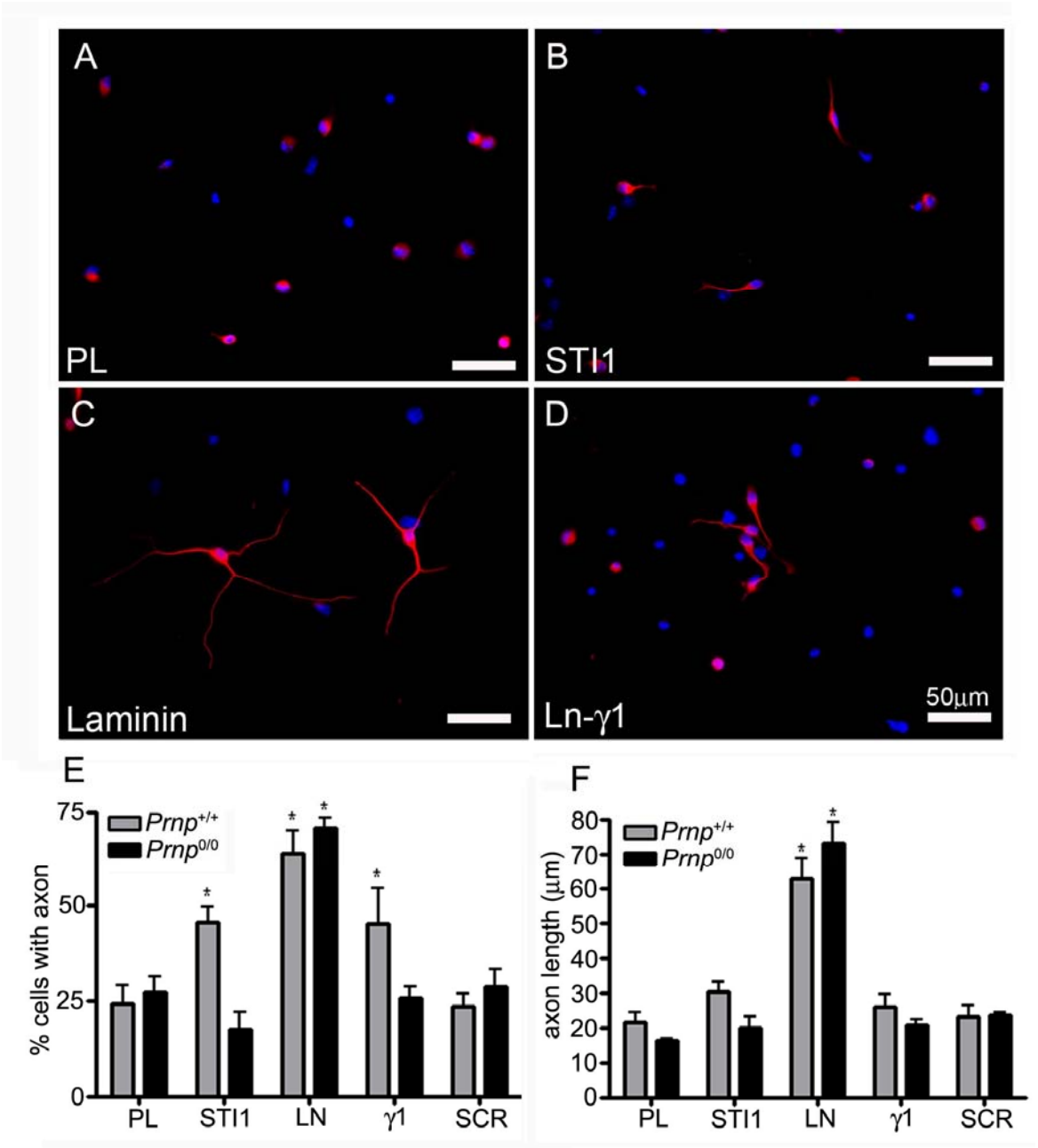

Figure 1. PrP^{C}/ligands interaction stimulates axonogenesis in DRG from E12.5 mouse embryos. *Prnp*$^{+/+}$ DRG neurons were cultured in the presence of Poly-L-Lysine (A), 0.5μM STI1 (B), 2μg/mL full-length Ln (C) and 37μM Ln-γ1 peptide (D) for 6 h, Cells were fixed and immunolabeled for βIII-Tubulin (red) plus DAPI (blue). *Prnp*$^{+/+}$ (gray bars) and *Prnp*$^{0/0}$ (black bars) neurons were cultured onto Poly-L-lysine (PL), 0.5μM STI1, 2 mg/mL full-length Ln (LN), 37μM synthetic Ln-γ1 or scrambled peptide (SCR) for 6 hours, fixed and stained with hematoxylin. The percentage of cells with axons and axon length were measured (E and F). Three to five fields (around 300 cells) per treatment were analyzed. Date presented as mean ± standard error of 4 independent experiments.* $p<0.01$ vs control (PL), after ANOVA followed of Dunnett´s test. Calibration bars, 50μm.

Ln-γ1 and STI1 cooperate to stimulate axonogenesis in Prnp$^{+/+}$ neurons.

To investigate whether PrP^{C} ligands can mutually cooperate during axonogenesis process, different suboptimal concentrations of Ln and STI1 were combined (Fig. 2). The suboptimal concentrations used were determined with a dose-response curve for each ligand (Suplementary Fig. 1). Considering the robustness of Ln response in axonogenesis after 6 h of treatment, Ln treatment plus STI1 was performed for 2 hours and compared to 2 h of poly-L-lysin incubation. *Prnp*$^{+/+}$ neurons cultured in the presence of poly-L-lysine (Fig. 2A), 0.2μg/mL Ln (Fig. 2B) or 0.2μg/mL Ln + 0.1μM STI1 (Fig. 2C) for 2 h and labeled with βIII-Tubulin and DAPI. The quantification of percentage of cells with axons (Fig. 2G) and axonal extension (Fig. 2H) was performed after 2 hs of Ln/STI1 association. Ln and STI1 at concentrations 10 and 20 fold lower than those necessary to induce neuritogenesis (see Fig. 1) had no effect upon axonogenesis (Figs 2G and 2Hectevely). However, when suboptimal concentrations of Ln and STI1 (0.25 and 0.1 μM) were incubated together, an increase in the number of cells with axons (Fig. 2G) and in the axonal length (Fig. 2H) was observed in *Prnp*$^{+/+}$ neurons while any effect was observed in PrP^{C}-null neurons (Figs. 2G and H).

Neurons were also cultured for 6 h in the presence of 0.1μM STI1 (Fig. 2D), 3.7μM Ln-γ1 (Fig. 2E) and 3.7μM Ln-γ1 + 0.1μM STI1 (Fig. 2F). Similarly to the results observed upon co-treatment with Ln plus STI1, suboptimal concentrations of Ln-γ1 combined with STI1 also stimulates axonogenesis (Fig. 2I) and axonal growth (Fig. 2J) in *Prnp*$^{+/+}$ neurons. In further experiments, the concentration of 0.1μM for STI1 in association of 3.7μM Ln-γ1 was used to study the events related to synergistic effect of these PrP^{C} ligands.

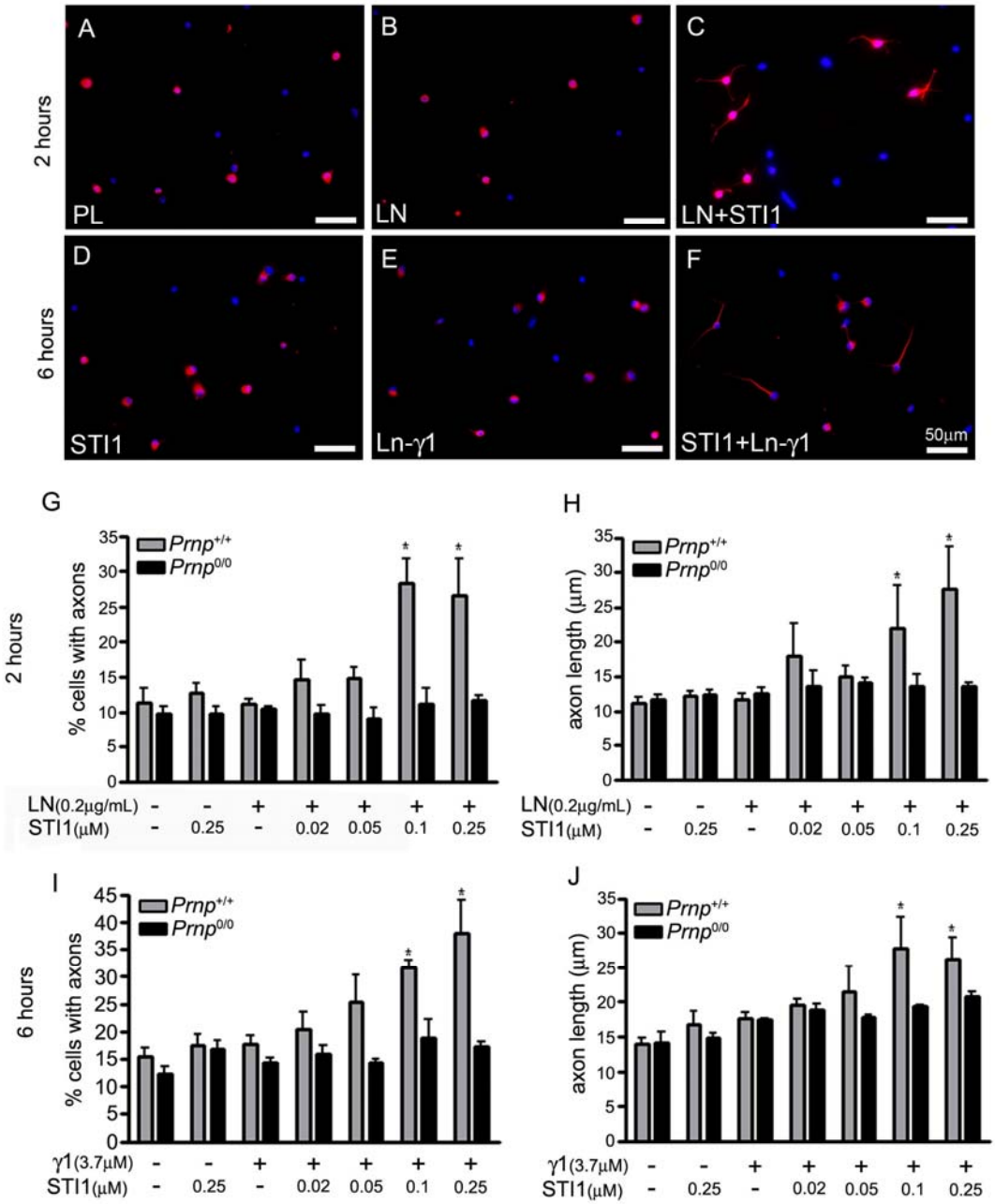

Figure 2. Association of suboptimal concentrations of Ln or Ln-γ1 peptide with STI1 supports axonogenesis in *Prnp*$^{+/+}$ neurons. *Prnp*$^{+/+}$ DRG neurons were cultured onto poly-L-lysine (A), 0.2μg/mL Ln (B) or 0.2μg/mL Ln + 0.1μM STI1 (C) for 2 h or in the presence of 0.1μM STI1 (D), 3.7μM Ln-γ1 (E) or 3.7μM Ln-γ1 + 0.1μM STI1 (F) for 6h. Cells were fixed and imunolabeled for βIII-Tubulin (red) plus DAPI (blue). Cell morphometric parameters (percentage of cells with axons and axon length) were evaluated after fixation ans stained with hematoxylin. Graphs represent *Prnp*$^{+/+}$ (gray bars) and *Prnp*$^{0/0}$ (black bars) neurons cultured for 2 (Figures 2G and H) or 6 hours (Figures 2I and J). Three to five fields (around 300 cells) per treatment were analyzed. Date presented as mean ± standard error of 4 independent experiments.* $p<0.01$ vs control (PL), after ANOVA followed of Dunnett´s test. Calibration bars, 50μm.

Ln-γ1 and STI1 trigger a wide range of signaling pathways.

We then asked which signaling pathways are involved in PrP^C-dependent axonogenesis. PLC (U73122) or $InsP_3R$ (2-APB) inhibitors blocked the axonogenesis promoted by STI1, Ln-γ1, Ln-γ1+STI1 or Ln (Figs 3A-D respectively). An ERK1/2 inhibitor (U0126) also blocked STI1, Ln-γ1 and Ln-γ1+STI1 effect (Figs 3A-3C), but did not alter Ln-promoted axonogenesis (Fig. 3D) while PKC inhibition by chelerythrine chloride (CH) impaired only the STI1-induced axonogenesis (Fig. 3A). PI3-K activity, impaired by the specific inhibitor Ly294002 (LY) seems to be involved only in Ln-induced axonal formation (Fig. 3D). Inhibition of PKA activity with KT5720 did not alter the axonogenesis induced by any PrP^C ligand (Figs3A-D) and inhibitors alone did not modify axonogenesis (Suplementary Fig. 2).

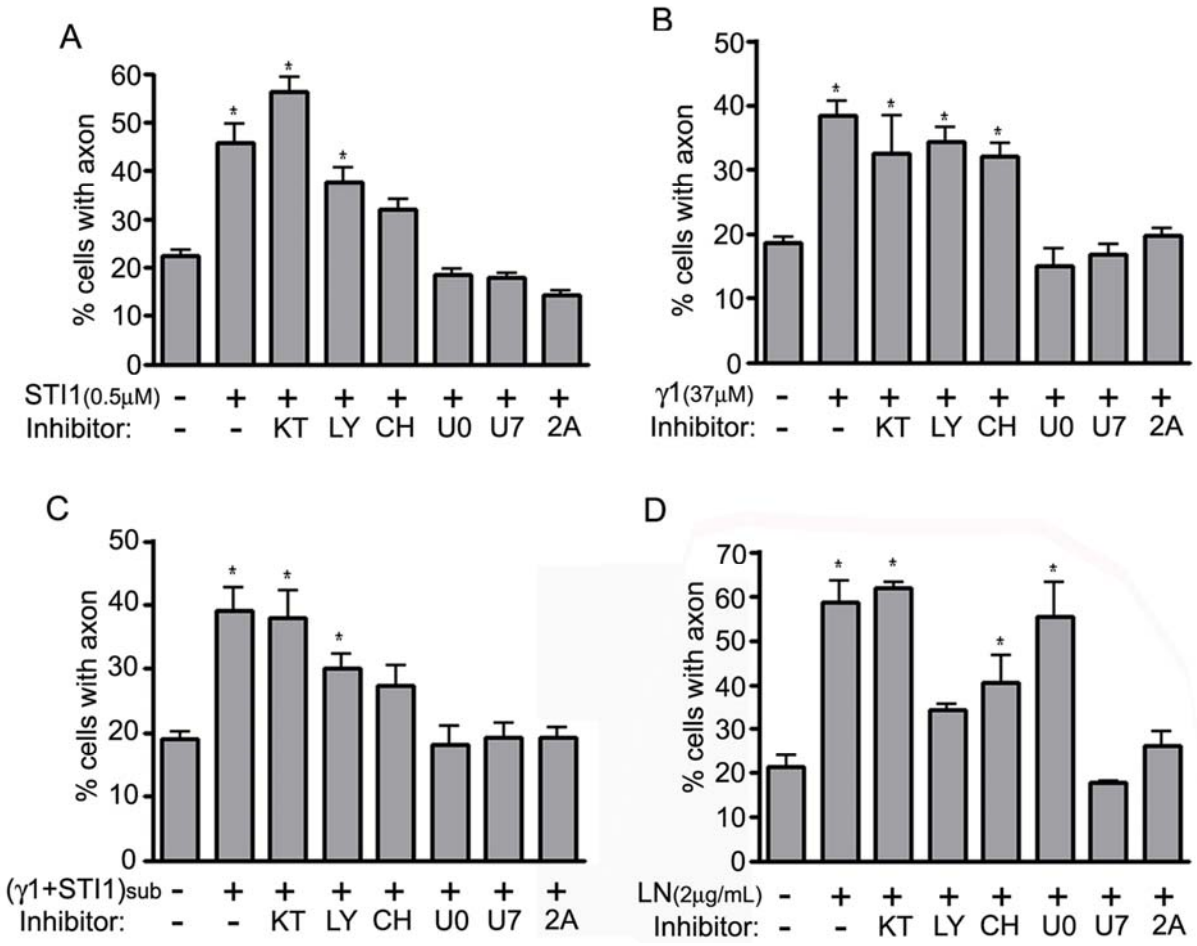

Figure 3. Different signaling pathways are required in ligand-induced PrP^C-dependent axonogenesis. *Prnp*$^{+/+}$ DRG neurons were pretreated for 30 min with specific inhibitor of PKA (KT5720, 60nM), PI3K (LY294002, 5mM), PKC (Chelerythrine chloride, 100nM), Erk (U0126, 50nM), PLC (U73122, 1μM) and $InsP_3$-R (2-APB, 250μM). Cells were plated onto poly-L-Lysine, plus 0.5μM STI1 (A), 37μM Ln-γ1 peptide (B), suboptimal (sub) concentrations 0.1μM STI1 + 3.7 Ln-γ1 peptide (C) or 2μg/mL full-length Ln (D) for 6 h. Cell morphometric parameters (percentage of cells with axons and axon length) were evaluated after fixation and stained with hematoxylin. Three to five fields (around 300 cells) per treatment were analyzed. Date presented as mean ± standard error of 3 independent experiments.* $p<0.01$ vs control (PL), after ANOVA followed of Dunnett´s test.

Ln-γ1 and STI1 promote $[Ca^{2+}]_i$ mobilization in $Prnp^{+/+}$ dorsal root ganglia neurons.

Since inhibition of calcium-dependent pathways (PKC, PLC and $InsP_3$-R) impaired PrP^C/ligand-induced axonogenesis, we evaluated whether calcium homeostasis and dynamics display a role in PrP^C-mediated signaling. DRG neurons were labeled with the fluorescent calcium indicator Fluo3-AM and fluorescence intensity was evaluated after neurons treatment with STI1, Ln-γ1 and Ln-γ1+STI1. STI1 (Fig. 4A) or Ln-γ1 (Fig. 4B) increased (2.5-3 fold) intracellular calcium fluorescence in *Prnp*$^{+/+}$ neurons (black line) while no effect was observed in *Prnp*$^{0/0}$ neurons (red line). The addition of THG (an endoplasmatic reticulum (ER) Ca^{2+}-ATPase inhibitor that promotes leakage of Ca^{2+} from ER to cytoplasm) to *Prnp*$^{0/0}$ neurons led to an increase in intracellular Ca^{2+}, ensuring that the lack of effect of STI1 on *Prnp*$^{0/0}$ neurons was not caused by impaired cell viability or impairement of intracellular Ca^{2+} stores (Figs. 4A,B). Subotimal concentrations of STI1 (Fig. 4C, $STI1_{sub}$, blue line) or Ln-γ1 (Ln-$\gamma1_{sub}$, green line) did not alter intracellular Ca^{2+} levels while their combination promoted a 2.0-fold increament in Ca^{2+} levels (Fig. 4C, black line). The relative Ca^{2+} levels for each treatment in 5 independet experimenst is demostrated in Fig. 4D

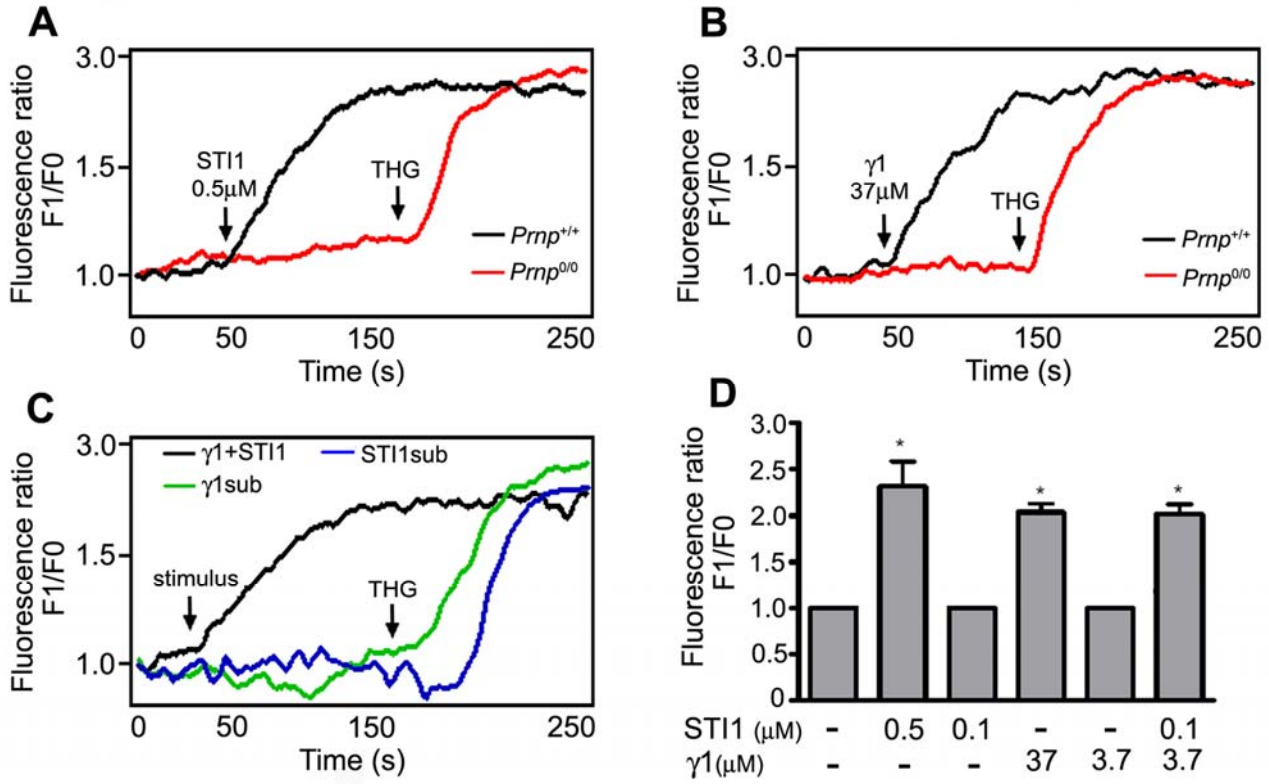

Figure 4. STI1 and Ln-γ1 promote PrP^{C}-dependent intracellular calcium increase. *Prnp*$^{+/+}$ and *Prnp*$^{0/0}$ DRG neurons were loaded with calcium indicator Fluo-3-AM (10μM), washed and the fluorescence was measured by confocal microscopy. Time course of cell fluorescence following application of 0.5μM STI1 (A) or 37μM Ln-γ1 peptide (B), to measure intracellular Ca^{2+} concentration in *Prnp*$^{+/+}$ neurons (black lines) and in *Prnp*$^{0/0}$ ones (red lines). (C) Time course of cell fluorescence following application of 0.1μM STI1 + 3.7μM Ln-γ1, in *Prnp*$^{+/+}$ neurons (black lines) and application of 0.1μM STI1 or 3.7μM Ln-g1 peptide (blue and green lines, respectively). Cells were viable as demonstrated by release of Ca^{2+} from intracellular stocks by thapsigargin (THG 2μM) treatment. In 4A to C, each trace represents one individual cell. (D) Quantification of fluorescence ratio from 30-40 cells after treatment with 0.5μM STI1, 0.1μM STI1, 37μM Ln-γ1, 3.7μM Ln-γ1 or Ln-γ1+STI1$_{SUB}$. Date presented as mean ± standard error of 5 independent experiments. * $p<0.01$ vs control, after ANOVA followed of Dunnett´s test.

Ln-γ1-induced $[Ca^{2+}]_i$ increase requires intracellular calcium stores while STI1 promotes extracellular calcium influx.

In attempt to elucidate the mechanisms by which PrP^C ligands modulate intracellular calcium levels, we evaluated which Ca^{2+} source (extra or intracellular stores) is recruited upon PrP^C/ligands association. The increase in intracellular Ca^{2+} levels promoted upon DRG neurons treatment with STI1 (Fig. 5A, blue line) was completely impaired when extracellular Ca^{2+} was removed (Fig. 5A, black line). Thus, suggesting that PrP^C binding to STI1 promotes activation of Ca^{2+} channels in the plasma membrane. On the other hand, Ca^{2+} withdrawal (Fig. 5B, black line) did not affect Ln-γ1 effect upon the increament of intracellular Ca^{2+} concentration (Fig. 5B, blue line) while the inhibition of PLC (U73) completely abrogates Ca^{2+} signaling. Thus, suggesting Ln-γ1 binding to PrP^C activates signaling pathways that modulates PKC activity and increases intracellular Ca^{2+} levels. When extracellular Ca^{2+} was depleted and cells were stimulated using a combination of subotimal concentrations of Ln-γ1+STI1 there was an increase Ca^{2+} concentration, however in lower levels (Fig. 5C, black line) than those observed in the presence of extracellular Ca^{2+} (Fig. 5C, blue line). Indicating that intracellular Ca^{2+} stores and Ca^{2+} influx contributes to global Ca^{2+} signaling mediated by the combined treatment of Ln-γ1 plus STI1. This result is consistent with the type of Ca^{2+} mobilization mediated by Ln-γ1 or STI1 binding to PrP^C. The relative levels of Ca^{2+} increase by PrP^C ligands in the absence of extracellular Ca^{2+} is shown in Fig. 5D.

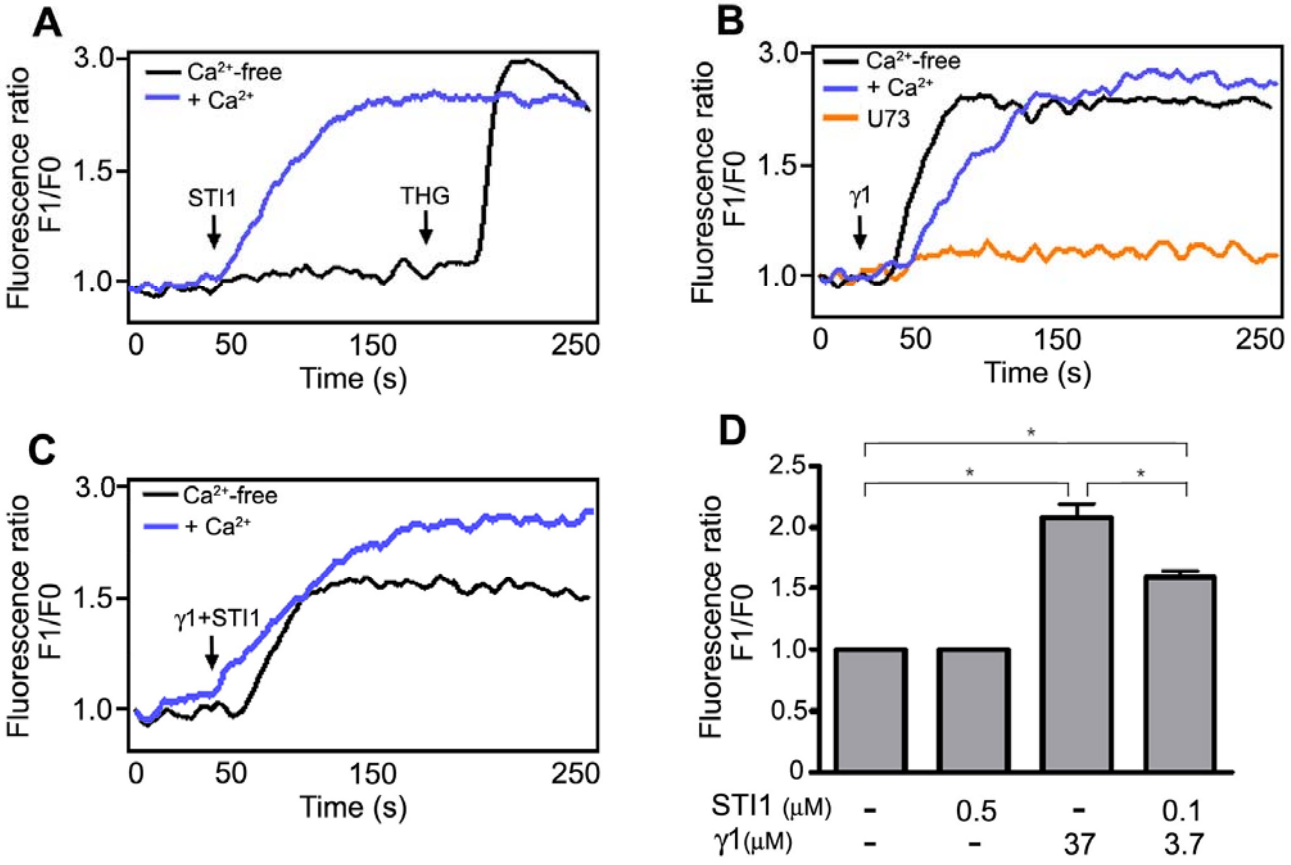

Figure 5. Role of extracellular calcium on STI1, Ln-γ1 and (Ln-γ1+STI1)$_{SUB}$ effect. *Prnp*$^{+/+}$ DRG neurons were loaded with calcium indicator Fluo-3-AM (10μM), washed and the fluorescence was measured by confocal microscopy. Neurons were treated in calcium-free Krebbs buffer plus 2mM EGTA. (A) Time course of cell fluorescence following application of 0.5μM STI1 (black line) or Ca^{2+}-Krebbs buffer (blue line). (B) Time course of cell fluorescence following application of 37μM Ln-γ1 in absence (black line) or presence of extracellular calcium (blue line) and with PLC inhibitor U73122 (orange line). (C) (Ln-γ1+STI1)$_{SUB}$ treatment was partially shorter in absence of extracellular calcium (black line) than observed in Ca^{2+}-Krebbs buffer (blue line). In 5A to C, each trace represents one individual cell. (D) Quantification of fluorescence ratio from 30-40 cells after treatment with 0.5μM STI1, 37μM Ln-γ1 or (Ln-γ1+STI1)$_{SUB}$ in a calcium-free medium. Date presented as mean ± standard error of 5 individual experiments. * $p<0.01$ vs control, after ANOVA followed of Dunnett´s test.

Discussion

This work demonstrated that Ln-γ1 and STI1 induce axonogenesis in a PrP^C-dependent manner in dorsal root ganglia neurons, similar to observed in hippocampal neurons (Graner et al., 2000; Lopes et al., 2005). However, particularly in peripheral neurons there is a synergistic effect on axonogenesis when these molecules were combined in suboptimal concentrations. The interaction of Ln-γ1 and STI1 with PrP^C triggers different mechanisms of Ca^{2+} mobilization. STI1 induces the opening of plasma membrane Ca^{2+} channels while Ln-γ1 peptide increases intracellular Ca^{2+} through activation of inositol triphosphate receptor ($InsP_3$-R) in ER.

Since the characterization of STI1 as a PrP^C ligand (Martins et al., 1997; Zanata et al., 2002), some reports support STI1 as a soluble neurotrophic factor (Chiarini et al, 2002; Lopes et al., 2005; Lima et al., 2007; Arantes et al., 2009). STI1 expression is abundant and ubiquitous since early stages of nervous system development and presents similar spatio-temporal expression pattern to its receptor PrP^C (Hajj et al., 2009). It has been described that STI1 could be secreted by many cell types, including tumor cell lines (Eustace and Jay, 2004; Erlich et al., 2007) and astrocytes (Lima et al., 2007), enabling STI1 to reach extracellular milieu, although it lacks signal peptides which drives its secretion. When present on extracellular environment, STI1 could interact with PrP^C and trigger neurotrophic signals involved in neuritogenesis and neuronal survival in hippocampal neurons, through activation of Erk1/2 and PKA, respectively (Lopes et al., 2005) and astrocyte development (Arantes et al., 2009). Additionally, in vivo experiments shown that STI1 interaction with PrP^C enhance short- and long-term memory formation (Coitinho et al., 2007).

One of the elusive aspects of PrP^C function is how the signal is transduced through plasma membrane, since PrP^C is a GPI-anchored protein that lacks a transmembrane domain (Taylor and Hooper, 2006). At least 2 important transmembrane proteins with well-established neurotrophic activities were identified as PrP^C ligand, neural cell adhesion molecule (NCAM) and 37-kDa/67-kDa Ln Receptor Precursor (37LRP/67LR). NCAM plays important roles in brain development and in the adult brain, including pivotal functions in neurite outgrowth and axonal regeneration (Ditlevsen et al., 2008). Interestingly, NCAM homophilic binding (NCAM-NCAM) is able to induce neuronal differentiation (Soroka et al., 2002) and neurite outgrowth through intracellular Ca^{2+} mobilization (Ronn et al., 2002).

PrP^C is a heterophilic binding partner of NCAM (Schmitt-Ulms et al., 2001), leading to activation of $p59^{fyn}$ and promoting NCAM-dependent neurite outgrowth (Santuccione et al., 2005). An important downstream component of NCAM-mediated signaling is PLC, which in turn is also a pathway induced by PrP^C interaction with Ln-γ1 and STI1. PLC activity is also necessary for axonogenesis and Ln-γ1 induced Ca^{2+} mobilization. These effects seem to be mediated by $InsP_3$, which leads to ER calcium channel opening (Bird et al., 2008).

Another transmembrane PrP^C partner is 37LRP/67LR, a cell surface receptor for Ln, which is involved in cell adhesion to the basement membrane and signal transduction (Nelson et al., 2008). 37LRP/67LR binds on PrP^C between amino acids 144-179 (Hundt et al., 2001), partially covering Ln binding site (173-183) (Coitinho et al., 2006). However, heparan sulfate proteoglycans facilitate binding of 37LRP/67LR in an alternative site, located inside the domain 53-93 of PrP^C molecule

(Warner et al., 2002). These multiple interactions permit alternative protein complexes that could be involved in neurotrophic activities.

In agreement with those reports showing the role of PrP^C promoting cell adhesion and processes extension, recent data have shown that PrP^C accumulates in focal adhesions and promotes cell spreading and filopodia formation when overexpressed while PrP^C-knockdown increased the number of lamellipodia veils (Shrock et al. 2009). Additionally, the deletion of PrP^C orthologues *PrP1* and *PrP2* in zebrafish embryos revealed a loss-of-function phenotype. Antisense morpholino microinjection of *PrP1* leads to embryonic cell adhesion impairment and gastrulation arrest (Malaga-Trillo et al., 2009). *PrP2* knockdown affects latter stages of neuronal development possibly affecting proliferation and differentiation of developing neurons (Malaga-Trillo et al., 2009). The alterations related to *PrP1* are caused by deficient cell movements, which rely on E-cadherin–based adhesion. Additional experiments with fish, *Drosophila* and N2a cell line demonstrated that both the adhesion and triggered signaling are conserved across evolution. Thus, these data largely supports that PrP^C could play a major role of in cell-cell communication (Malaga-Trillo 2009).

Our previous work mapped different binding domains on PrP^C molecule for STI1 and Ln-γ1. While STI1 binds within 113-128 amino acid residues (Zanata et al., 2002), Ln-γ1 interacts within 163-182 region of PrP^C (Coitinho et al., 2006). Hence, when added together, Ln-γ1 and STI1 could bind to different PrP^C regions and cooperate in cellular signalling to reach optimal effects. The combined treatment with Ln and STI1 causes a robust and synergic effect upon axonogenesis in a short period of incubation (2 hours). Since the stimulation of integrin activity by Ln is

sufficient to promote short term axonogenesis (Kuhn et al., 1995), we speculate that, once in the presence of STI1, Ln could also binds to PrP^C, leading to a potentiaton of axonogenesis in response to activity of two receptors types (integrins and PrP^C).

Our data present evidence that STI1 and Ln-γ1 could synergistically operate to transduce neurotrophic activity through PrP^C interaction. Synergisms between molecules involved in neurotrophic activities are numerous in literature (Krieglstein, 2004). Neurotrophic factors from neurotrophins family (*e.g.* nerve growth factor, NGF), glial cell-line derived neurotrophic factor family ligands (e.g. GDNF) or neuropoietic cytokines (e.g. ciliary neurotrophic factor, CNTF) are known to have synergistic effects in neuronal differentiation, survival, synaptic function and axonal outgrowth/regeneration (Chao, 2003). Furthermore, there are reports showing the cooperativity between Ln and nerve growth factor (NGF) in increasing Ln/integrin-induced neurite outgrowth in sensory neurons (Tucker et al., 2005) and PC12 cells (Achyuta et al., 2009). Nevertheless, although all those factors present specific receptors, PrP^C could be used as a receptor for at least two different ligands

This work contributes to improve the understanding of intracellular mechanisms which PrP^C could play a role. We showed that STI1 and Ln-γ1, after binding to PrP^C, recruit distinct pathways that leads to $[Ca^{2+}]_i$ rising which is essential to axonal growth (Berridge et al., 2000). In conclusion, the data presented here describes the participation of PrP^C in the peripheral nerve development through the engagement with STI1 and Ln-γ1. Moreover, the evidence of cooperation of two PrP^C ligands signals to support axonogenesis demonstrates the ability of PrP^C in recruiting partners to plasma membrane microdomains. This recruitment might exerts scaffolding role required for a number of downstream signaling pathways

unraveling the neurotrophic properties of PrP^C which may provide new cellular substrates to study molecular basis of brain development and prion diseases.

Acknowledgements: This work was supported by Fundação de Amparo à Pesquisa do Estado de São Paulo (FAPESP 03-13189-2). V.R.M. is an International Research Scholar of the Howard Hughes Medical Institute. Fellowships from FAPESP to T.G.S, F.H.B, G.N.M.H. and M.H.L.

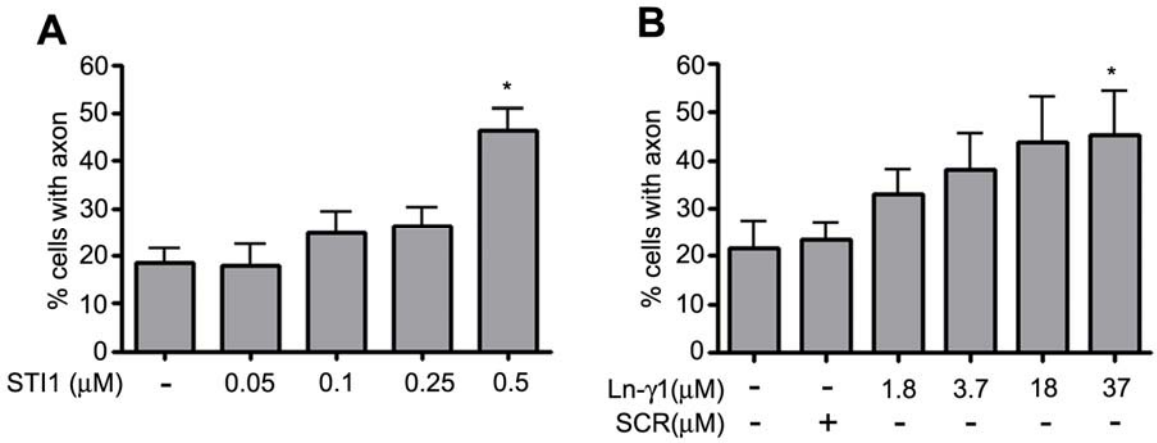

Suplementary Figure 1. STI1 and Ln-γ stimulates axonogenesis in *Prnp*$^{+/+}$ DRG neurons in a dose-dependent manner. Neurons were cultured in the presence of Poly-L-Lysine or increasing concentration of STI1 (A) or Ln-γ1 (B) for 6 hours, fixed and stained with hematoxylin. STI1: from 0.05 to 0.5 μM. Ln-γ1: from 1.8 to 37 μM. The percentage of cells with axons was measured. Three to five fields (around 300 cells) per treatment were analyzed. Date presented as mean ± standard error of 3 independent experiments.* $p<0.01$ vs control (PL), after ANOVA followed of Dunnett´s test.

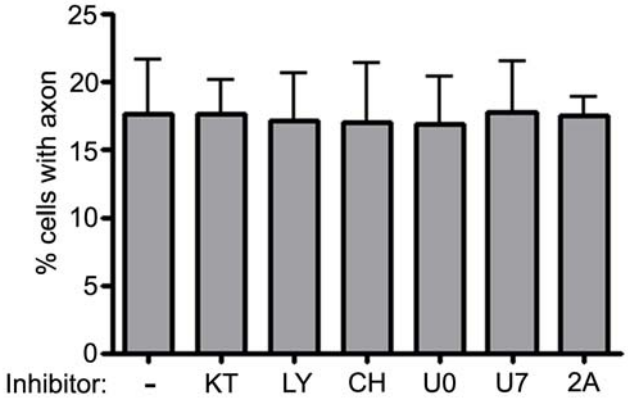

Suplementary Figure 2. Different signaling inhibitors did not alter axonogenesis. *Prnp*$^{+/+}$ DRG neurons were treated with specific inhibitor of PKA (KT5720, 60nM), PI3K (LY294002, 5mM), PKC (Chelerythrine chloride, 100nM), Erk (U0126, 50nM), PLC (U73122, 1μM) and $InsP_3$-R (2-APB, 250μM) for 6 hours, fixed and stained with hematoxylin. The percentage of cells with axons was evaluated. Three to five fields (around 300 cells) per treatment were analyzed. Date presented as mean ± standard error of 3 independent experiments.

References

Achyuta,A.K., Cieri,R., Unger,K., and Murthy,S.K. (2009). Synergistic effect of immobilized laminin and nerve growth factor on PC12 neurite outgrowth. Biotechnol. Prog. 25, 227-234.

Arantes,C., Nomizo,R., Lopes,M.H., Hajj,G.N., Lima,F.R., and Martins,V.R. (2009). Prion protein and its ligand stress inducible protein 1 regulate astrocyte development. Glia.

Belkin,A.M. and Stepp,M.A. (2000). Integrins as receptors for laminins. Microsc. Res. Tech. 51, 280-301.

Berridge,M.J., Lipp,P., and Bootman,M.D. (2000). The versatility and universality of calcium signalling. Nat. Rev. Mol. Cell Biol. 1, 11-21.

Bird,G.S., DeHaven,W.I., Smyth,J.T., and Putney,J.W., Jr. (2008). Methods for studying store-operated calcium entry. Methods 46, 204-212.

Brini,M., Miuzzo,M., Pierobon,N., Negro,A., and Sorgato,M.C. (2005). The prion protein and its paralogue Doppel affect calcium signaling in Chinese hamster ovary cells. Mol. Biol. Cell 16, 2799-2808.

Bueler,H., Fischer,M., Lang,Y., Bluethmann,H., Lipp,H.P., DeArmond,S.J., Prusiner,S.B., Aguet,M., and Weissmann,C. (1992). Normal development and behaviour of mice lacking the neuronal cell-surface PrP protein. Nature 356, 577-582.

Chao,M.V. (2003). Neurotrophins and their receptors: a convergence point for many signalling pathways. Nat. Rev. Neurosci. 4, 299-309.

Chen,Z.L. and Strickland,S. (2003). Laminin gamma1 is critical for Schwann cell differentiation, axon myelination, and regeneration in the peripheral nerve. J. Cell Biol. 163, 889-899.

Coitinho,A.S. et al. (2006). The interaction between prion protein and laminin modulates memory consolidation. Eur. J. Neurosci. 24, 3255-3264.

Coitinho,A.S., Lopes,M.H., Hajj,G.N., Rossato,J.I., Freitas,A.R., Castro,C.C., Cammarota,M., Brentani,R.R., Izquierdo,I., and Martins,V.R. (2007). Short-term memory formation and long-term memory consolidation are enhanced by cellular prion association to stress-inducible protein 1. Neurobiol. Dis. 26, 282-290.

Colling,S.B., Collinge,J., and Jefferys,J.G. (1996). Hippocampal slices from prion protein null mice: disrupted Ca(2+)-activated K+ currents. Neurosci. Lett. 209, 49-52.

Collinge,J., Whittington,M.A., Sidle,K.C., Smith,C.J., Palmer,M.S., Clarke,A.R., and Jefferys,J.G. (1994). Prion protein is necessary for normal synaptic function. Nature 370, 295-297.

Ditlevsen,D.K., Povlsen,G.K., Berezin,V., and Bock,E. (2008). NCAM-induced intracellular signaling revisited. J. Neurosci. Res. 86, 727-743.

Erlich,R.B., Kahn,S.A., Lima,F.R., Muras,A.G., Martins,R.A., Linden,R., Chiarini,L.B., Martins,V.R., and Moura,N., V (2007). STI1 promotes glioma proliferation through MAPK and PI3K pathways. Glia 55, 1690-1698.

Eustace,B.K. and Jay,D.G. (2004). Extracellular roles for the molecular chaperone, hsp90. Cell Cycle 3, 1098-1100.

Fuhrmann,M., Bittner,T., Mitteregger,G., Haider,N., Moosmang,S., Kretzschmar,H., and Herms,J. (2006). Loss of the cellular prion protein affects the Ca2+ homeostasis in hippocampal CA1 neurons. J. Neurochem. 98, 1876-1885.

Gauczynski,S. et al. (2001). The 37-kDa/67-kDa laminin receptor acts as the cell-surface receptor for the cellular prion protein. EMBO J. 20, 5863-5875.

Graner,E. et al. (2000). Cellular prion protein binds laminin and mediates neuritogenesis. Brain Res. Mol. Brain Res. 76, 85-92.

Grimpe,B., Dong,S., Doller,C., Temple,K., Malouf,A.T., and Silver,J. (2002). The critical role of basement membrane-independent laminin gamma 1 chain during axon regeneration in the CNS. J. Neurosci. 22, 3144-3160.

Hajj,G.N. et al. (2007). Cellular prion protein interaction with vitronectin supports axonal growth and is compensated by integrins. J. Cell Sci. 120, 1915-1926.

Hardy,J. and Selkoe,D.J. (2002). The amyloid hypothesis of Alzheimer's disease: progress and problems on the road to therapeutics. Science 297, 353-356.

Herms,J.W., Korte,S., Gall,S., Schneider,I., Dunker,S., and Kretzschmar,H.A. (2000). Altered intracellular calcium homeostasis in cerebellar granule cells of prion protein-deficient mice. J. Neurochem. 75, 1487-1492.

Hundt,C. et al. (2001). Identification of interaction domains of the prion protein with its 37-kDa/67-kDa laminin receptor. EMBO J. 20, 5876-5886.

Khosravani,H. et al. (2008). Prion protein attenuates excitotoxicity by inhibiting NMDA receptors. J. Gen. Physiol 131, i5.

Krieglstein,K. (2004). Factors promoting survival of mesencephalic dopaminergic neurons. Cell Tissue Res. 318, 73-80.

Kristensson,K., Feuerstein,B., Taraboulos,A., Hyun,W.C., Prusiner,S.B., and DeArmond,S.J. (1993). Scrapie prions alter receptor-mediated calcium responses in cultured cells. Neurology 43, 2335-2341.

Kuhn,T.B., Schmidt,M.F., and Kater,S.B. (1995). Laminin and fibronectin guideposts signal sustained but opposite effects to passing growth cones. Neuron 14, 275-285.

Lauren,J., Gimbel,D.A., Nygaard,H.B., Gilbert,J.W., and Strittmatter,S.M. (2009). Cellular prion protein mediates impairment of synaptic plasticity by amyloid-beta oligomers. Nature 457, 1128-1132.

Liesi,P., Laatikainen,T., and Wright,J.M. (2001). Biologically active sequence (KDI) mediates the neurite outgrowth function of the gamma-1 chain of laminin-1. J. Neurosci. Res. 66, 1047-1053.

Liesi,P., Narvanen,A., Soos,J., Sariola,H., and Snounou,G. (1989). Identification of a neurite outgrowth-promoting domain of laminin using synthetic peptides. FEBS Lett. 244, 141-148.

Lima,F.R., Arantes,C.P., Muras,A.G., Nomizo,R., Brentani,R.R., and Martins,V.R. (2007). Cellular prion protein expression in astrocytes modulates neuronal survival and differentiation. J. Neurochem. 103, 2164-2176.

Linden,R., Martins,V.R., Prado,M.A., Cammarota,M., Izquierdo,I., and Brentani,R.R. (2008). Physiology of the prion protein. Physiol Rev. 88, 673-728.

Lopes,M.H., Hajj,G.N., Muras,A.G., Mancini,G.L., Castro,R.M., Ribeiro,K.C., Brentani,R.R., Linden,R., and Martins,V.R. (2005). Interaction of cellular prion and stress-inducible protein 1 promotes neuritogenesis and neuroprotection by distinct signaling pathways. J. Neurosci. 25, 11330-11339.

Malaga-Trillo E, Solis GP, Schrock Y, Geiss C, Luncz L, Thomanetz V, Stuermer CA (2009) Regulation of embryonic cell adhesion by the prion protein. PLoS Biol 7:e55.

Mallucci,G.R., Ratte,S., Asante,E.A., Linehan,J., Gowland,I., Jefferys,J.G., and Collinge,J. (2002). Post-natal knockout of prion protein alters hippocampal CA1 properties, but does not result in neurodegeneration. EMBO J. 21, 202-210.

Martins,V.R., Graner,E., Garcia-Abreu,J., de Souza,S.J., Mercadante,A.F., Veiga,S.S., Zanata,S.M., Neto,V.M., and Brentani,R.R. (1997). Complementary hydropathy identifies a cellular prion protein receptor. Nat. Med. 3, 1376-1382.

Moore,R.A., Taubner,L.M., and Priola,S.A. (2009). Prion protein misfolding and disease. Curr. Opin. Struct. Biol. 19, 14-22.

Nelson,J., McFerran,N.V., Pivato,G., Chambers,E., Doherty,C., Steele,D., and Timson,D.J. (2008). The 67 kDa laminin receptor: structure, function and role in disease. Biosci. Rep. 28, 33-48.

Nicolet,C.M. and Craig,E.A. (1989). Isolation and characterization of STI1, a stress-inducible gene from Saccharomyces cerevisiae. Mol. Cell Biol. 9, 3638-3646.

Paulsson,M., Aumailley,M., Deutzmann,R., Timpl,R., Beck,K., and Engel,J. (1987). Laminin-nidogen complex. Extraction with chelating agents and structural characterization. Eur. J. Biochem. 166, 11-19.

Putney,J.W., Jr., Broad,L.M., Braun,F.J., Lievremont,J.P., and Bird,G.S. (2001). Mechanisms of capacitative calcium entry. J. Cell Sci. 114, 2223-2229.

Rieger,R., Edenhofer,F., Lasmezas,C.I., and Weiss,S. (1997). The human 37-kDa laminin receptor precursor interacts with the prion protein in eukaryotic cells. Nat. Med. 3, 1383-1388.

Ronn,L.C., Dissing,S., Holm,A., Berezin,V., and Bock,E. (2002). Increased intracellular calcium is required for neurite outgrowth induced by a synthetic peptide ligand of NCAM. FEBS Lett. 518, 60-66.

Sakudo,A. and Ikuta,K. (2009). Fundamentals of prion diseases and their involvement in the loss of function of cellular prion protein. Protein Pept. Lett. 16, 217-229.

Santuccione,A., Sytnyk,V., Leshchyns'ka,I., and Schachner,M. (2005). Prion protein recruits its neuronal receptor NCAM to lipid rafts to activate p59fyn and to enhance neurite outgrowth. J. Cell Biol. 169, 341-354.

Schmitt-Ulms,G. et al. (2001). Binding of neural cell adhesion molecules (N-CAMs) to the cellular prion protein. J. Mol. Biol. 314, 1209-1225.

Schrock Y, Solis GP, Stuermer CA (2009) Regulation of focal adhesion formation and filopodia extension by the cellular prion protein (PrPC). FEBS Lett 583:389-393.

Sorgato,M.C. and Bertoli,A. (2009). From cell protection to death: may Ca2+ signals explain the chameleonic attributes of the mammalian prion protein? Biochem. Biophys. Res. Commun. 379, 171-174.

Soroka,V., Kiryushko,D., Novitskaya,V., Ronn,L.C., Poulsen,F.M., Holm,A., Bock,E., and Berezin,V. (2002). Induction of neuronal differentiation by a peptide corresponding to the homophilic binding site of the second Ig module of the neural cell adhesion molecule. J. Biol. Chem. 277, 24676-24683.

Taylor,D.R. and Hooper,N.M. (2006). The prion protein and lipid rafts. Mol. Membr. Biol. 23, 89-99.

Thastrup,O., Cullen,P.J., Drobak,B.K., Hanley,M.R., and Dawson,A.P. (1990). Thapsigargin, a tumor promoter, discharges intracellular Ca2+ stores by specific inhibition of the endoplasmic reticulum Ca2(+)-ATPase. Proc. Natl. Acad. Sci. U. S. A 87, 2466-2470.

Tucker,B.A., Rahimtula,M., and Mearow,K.M. (2005). Integrin activation and neurotrophin signaling cooperate to enhance neurite outgrowth in sensory neurons. J. Comp Neurol. 486, 267-280.

Vaananen,A.J., Rauhala,P., Tuominen,R.K., and Liesi,P. (2006). KDI tripeptide of gamma1 laminin protects rat dopaminergic neurons from 6-OHDA induced toxicity. J. Neurosci. Res. 84, 655-665.

Venstrom,K.A. and Reichardt,L.F. (1993). Extracellular matrix. 2: Role of extracellular matrix molecules and their receptors in the nervous system. FASEB J. 7, 996-1003.

Walz,R., Amaral,O.B., Rockenbach,I.C., Roesler,R., Izquierdo,I., Cavalheiro,E.A., Martins,V.R., and Brentani,R.R. (1999). Increased sensitivity to seizures in mice lacking cellular prion protein. Epilepsia 40, 1679-1682.

Warner,R.G., Hundt,C., Weiss,S., and Turnbull,J.E. (2002). Identification of the heparan sulfate binding sites in the cellular prion protein. J. Biol. Chem. 277, 18421-18430.

Wiksten,M., Vaananen,A., Liebkind,R., Rauhala,P., and Liesi,P. (2004a). Soluble KDI domain of gamma1 laminin protects adult hippocampus from excitotoxicity of kainic acid. J. Neurosci. Res. 78, 411-419.

Wiksten,M., Vaananen,A.J., Liebkind,R., and Liesi,P. (2004b). Regeneration of adult rat spinal cord is promoted by the soluble KDI domain of gamma1 laminin. J. Neurosci. Res. 78, 403-410.

Wong,K., Qiu,Y., Hyun,W., Nixon,R., VanCleff,J., Sanchez-Salazar,J., Prusiner,S.B., and DeArmond,S.J. (1996). Decreased receptor-mediated calcium response in prion-infected cells correlates with decreased membrane fluidity and IP3 release. Neurology 47, 741-750.

Zanata,S.M. et al. (2002). Stress-inducible protein 1 is a cell surface ligand for cellular prion that triggers neuroprotection. EMBO J. 21, 3307-3316.

PARTE III

Interação PrP^C e STI1 estimula a auto-renovação de células tronco neurais.

1. Isolamento e cultivo de Células Tronco Neurais derivadas do SNC em desenvolvimento

Células precursoras multipotentes capazes de gerar neurônios, astrócitos e oligodendrócitos têm sido isoladas a partir de diferentes etapas do desenvolvimento embrionário/fetal e de cérebros adultos. A utilização de CTN é uma das ferramentas para se identificar os determinantes moleculares que promovem a diferenciação em neurônios ou glia. Consequentemente, a identificação destes determinantes tem implicações biotecnológicas importantes, uma vez que estas células podem ser utilizadas para o desenvolvimento de terapias de reposição celular em doenças neurodegenerativas (MARTINO e PLUCHINO 2006). Diferentes estratégias para isolar células multipotentes neurais de outros tipos celulares encontrados no encéfalo têm sido utilizadas. Uma delas é o enriquecimento da população destas células através da exposição contínua a agentes mitogênicos, como os fatores de crescimento EGF (fator de crescimento epidermal) e bFGF (fator de crescimento de fibroblasto básico) (REYNOLDS e RIETZE 2005). Nestas condições, as células responsivas ao estímulo mitogênico proliferam-se e organizam-se em agregados de células em suspensão chamadas neuroesferas. Quando dissociadas e replaqueadas em densidade clonal, as células dão origem a novas esferas. A cada passagem, as células das neuroesferas podem se diferenciar em neurônios, astrócitos e oligodendrócitos, confirmando que as células formadoras de neuroesferas representam células tronco

neurais. A utilização de neuroesferas é uma das principais ferramentas experimentais para o estudo de fatores que influenciam a determinação dos diferentes fenótipos neurais (CALDWELL et al. 2001). As neuroesferas são heterogêneas em relação ao seu diâmetro e na composição celular, contendo populações de CTN e células já diferenciadas embebidas em um complexo de matriz extracelular (CAMPOS et al. 2004).

2. Neurogênese no encéfalo adulto

A neurogênese no encéfalo adulto é bastante conservada na evolução, sendo observada desde crustáceos até vertebrados superiores, incluindo aves, roedores e primatas (LLEDO et al. 2006). A maioria dos estudos realizados em condições fisiológicas indica que níveis elevados de neurogênese ocorrem exclusivamente no giro denteado do hipocampo (ERIKSSON et al. 1998) e no bulbo olfatório (SANAI et al. 2004) de humanos. Nessas regiões, a inclusão de novos neurônios representa uma maneira adicional de modificação da circuitaria cerebral, além das mudanças moleculares, sinápticas ou morfológicas, usualmente observadas em eventos de plasticidade sináptica. Os neurônios recém gerados derivam de astrócitos que mantém características de células tronco neurais multipotentes (CTN), que proliferam, migram e diferenciam-se nos fenótipos neuronais específicos, células da glia (astrócitos e oligodendrócitos) e neurônios (MING e SONG 2005). Um aspecto curioso é que apesar das CTN estarem presentes em diversas regiões do encéfalo, a neurogênese permanece bastante restrita à camada subgranular (CSG) do giro denteado e na zona subventricular (ZSV), camada adjacente às paredes dos ventrículos laterais. A CSG e a ZSV dão origem primariamente às celulas granulares

denteadas e a interneurônios do bulbo olfatório, respectivamente (ALVAREZ-BUYLLA et al. 2002; GAGE 2000). Muitos trabalhos têm evidenciado que os novos neurônios conseguem integrar-se de maneira funcional no circuito pré-existente, embora a verdadeira relevância da neurogênese no encéfalo adulto permaneça desconhecida (SCHINDER e GAGE 2004).

A restrição da neurogênese a certas regiões do encéfalo adulto sugere que a maioria das estruturas cerebrais não necessita de novos neurônios em situações fisiológicas (SCHINDER e GAGE 2004). Isto implica em pelo menos duas possibilidades, a primeira seria que o encéfalo perderia a maior parte de sua capacidade neurogênica e o que resta no adulto é remascente do período de desenvolvimento, não apresentando significado fisiológico. A segunda possibilidade é de que a neurogênese é necessária para uma série de funções específicas que estão concentradas primariamente no hipocampo e no bulbo olfatório. De fato, os dados da literatura têm mostrado que a segunda possibilidade parece ser a verdadeira, sugerindo que a neurogênese apresenta um papel importante no processamento olfatório e em certas formas de aprendizagem e memória do encéfalo adulto (SCHINDER e GAGE 2004). Estes achados têm implicações importantes no estudo da fisiologia cerebral, uma vez que a neurogênese adulta não parece ser meramente estática e/ou restaurativa e, sim uma resposta adaptativa aos desafios impostos pelo ambiente (LLEDO et al. 2006).

3. PrP^C em células tronco neurais

O fato de PrP^C estar envolvido em diversos processos fisiológicos desde o desenvolvimento do sistema nervoso até o encéfalo adulto, sugere-se que PrP^C

também possa ter papel relevante na biologia de células tronco neurais. De fato, foi demonstrado que as células proliferativas na zona subventricular não expressam PrP^C, sendo que a expressão desta proteína está restrita aos neurônios ou precursores neuronais adjacentes a região proliferativa. Além disso, animais que superexpressam PrP^C apresentam maior número de células $BrdU^+$ na ZSV e no giro denteado comparado com animais deficientes para PrP^C, sugerindo que quanto maior a expressão de PrP^C maior o número de células em proliferação nas regiões neurogênicas. Adicionalmente, em CTN derivadas de telencéfalo, a expressão de PrP^C aumenta a diferenciação neuronal *in vitro* (STEELE et al. 2006). Portanto, PrP^C apresenta um importante papel na modulação da diferenciação neuronal durante o desenvolvimento e também na proliferação de CTN presentes no encéfalo adulto.

Neste trabalho avaliamos o papel da interação PrP^C-STI1 na biologia de células tronco neurais. Para determinar as funções biológicas desta interação, foram utilizadas neuroesferas derivadas do telencéfalo de animais E14. Considerando os trabalhos prévios da literatura que demonstraram que PrP^C apresenta importante função em eventos que governam a neurogênese pós-natal e durante o desenvolvimento, e ainda as evidências que apontam para STI1 ser considerada um novo fator neurotrófico, é importante verificar se as funções atribuídas a PrP^C podem ser moduladas pela sua ligação a STI1. De fato, demonstramos que STI1 é secretada pelas células da neuroesfera e a ligação a PrP^C está envolvida na modulação da auto-renovação de células tronco neurais. Diversas evidências suportam esta conclusão: a- células deficientes para PrP^C tem capacidade reduzida de gerar neuroesferas quando comparadas com células tipo-selvagem; b- o bloqueio da interação STI1-PrP^C com anticorpos prejudica a formação de neuroesferas, demonstrando que a associação

entre as duas proteínas é necessária para a auto-renovação; c- quando adicionada ao meio de cultivo, STI1 recombinante através de sua associação a PrP^C, potencializa a formação de neuroesferas de maneira dependente de concentração. O mecanismo pelo qual o complexo STI1-PrP^C medeia a auto-renovação depende da proliferação celular, sem interferir na sobrevivência e diferenciação celulares.

Este trabalho foi resultado da minha colaboração com a Dra. Marilene Lopes, de maneira conjunta elaboramos os protocolos e estabelecemos em nosso laboratório o cultivo de células tronco neurais para investigarmos o papel de PrP^C neste tipo celular.

Neural stem cell self-renewal is enhanced by stress inducible protein 1 engagment to prion protein.

Santos, T.G.[1,2]; Silva, I. R.[1]; Costa-Silva, B[1,2]; Lepique, A. P.[1]; Martins, V. R.[1] and Lopes, M.H[1*].

[1]Ludwig Institute for Cancer Research, São Paulo, Brazil;

[2]Centro de Tratamento e Pesquisa, Hospital A. C. Camargo, São Paulo, Brazil.

*Corresponding author: Dr. Marilene Hohmuth Lopes, Ludwig Institute for Cancer Research, Sao Paulo, Rua João Julião, 245 1st floor, Zip Code: 01323-903 Paraíso, São Paulo, Brazil.

Phone: 55 11 3388 3220

Fax: 55 11 3141-1325

E-mail:mhohmuth@ludwig.org.br

Running title: STI1-PrP^C in neural stem cell biology

Abbreviations: PrP^C- cellular prion protein, STI1-stress inducible protein 1, NSP-neurosphere, self-renewal, neural stem cell.

Keywords: PrP^C/STI1/NSP/self-renewal/neural stem cell/proliferation.

Abstract

The engagement of prion protein (PrP^C) with stress inducible protein 1 (STI1) plays pivotal roles in the developing and mature nervous system, modulating neural survival, neuritogenesis and memory formation. However, the role of PrP^C-STI1 in cell fate related-mechanisms is unknown. To address this issue, neurosphere (NSP) cultures, from fetal telencephalon of wild-type (*Prnp*$^{+/+}$) and PrP^C-null (*Prnp*$^{0/0}$) mice were studied. The expression of STI1, GFAP as well as nestin was uniform and presented similar levels in NSP derived from wild-type and PrP^C-null mice. Conversely, *Prnp*$^{0/0}$ NSP presented higher βIII-tubulin expression than wild-type NSP. The formation of NSP was significantly impaired in cultures derived from *Prnp*$^{0/0}$ embryos when compared to their wild-type counterparts, suggesting the participation of PrP^C in self-renewal. STI1 is secreted by NSP from both genotypes but increases proliferation only in NSP that express PrP^C. In contrast, the survival and differentiation of NSP was not affected by STI1. These data suggest that STI1-PrP^C interaction could play an essential role in the self-renewal of neural progenitor cells. These molecules may represent a novel therapeutic target for the treatment of neurodegenerative illness.

Introduction

The mammalian prion protein (PrP^C), a ubiquitous cell surface glycoprotein, has been intensively studied for its role in transmissible spongiform encephalopathies (TSEs) (Moore et al., 2009). Understanding the pathogenesis of TSEs requires the identification of functional properties of PrP^C. In the central nervous system, the

PrP^C expression starts at embryonic day 10 (E10) and later in other tissues. On the other hand, data from other goups demostrated that PrP^C expression started at E7.5 in several tissues including the developing head, brain and neural tube (Tremblay et al., 2007). Interestingly, in spinal cord, PrP^C expression presents a gradient expression in a dorsal-ventral fashion, suggesting that PrP^C could be involved in nervous system patterning or differentiation of neural populations within this tissue (Hajj et al., 2009).

Our group has focused in the investigation of PrP^C-interacting proteins to understand cellular signaling triggered and biological function(s) associated with PrP^C. We have characterized that the co-chaperone STI1 (Stress Inducible Protein 1) is a high-affinity partner for PrP^C (kd = 1.4 x 10^{-7} M). The binding domains were mapped in PrP^C at residues 113-128 and amino acids 230-245 within STI1 molecule (Zanata et al., 2002). STI1 expression is abundant and ubiquitous since early stages of nervous system development and present similar spatial-temporal expression pattern to PrP^C (Hajj et al., 2009). The interaction of STI1 with PrP^C induces neuronal survival and differentiationin in retina and hippocampal neurons through PKA and ERK1/2 pathays respectively (Zanata et al., 2002; Chiarini et al., 2002; Coitinho et al., 2007). Furthermore, we have demostrated that PrP^C-STI1 interaction enhances short- and long-term memory formation (Coitinho et al., 2007). STI1 is secreted by astrocytes and besides its neurotrophic properties it also presents autocrine activity upon proliferation, survival and differentiation of the former cells (Lima et al., 2007; Arantes et al., 2009).

The role of PrP^C in neural development and in adult neurogenesis has been investigated. PrP^C increases proliferation rate in subventricular zone and the dentate

gyrus in adult mice (Steele et al., 2006). Interestingly, PrP^C expression in the proliferating regions of the adult brain was found restricted to post-mitotic neurons, suggesting an indirect effect upon the proliferation of the underlying mitotic precursors. A model *in vitro* of human neurogenesis using GFAP-positive progenitor cells, showed that after the induction of neural differentiation, neuronal cells express higher levels of PrP^C when compared to glial cells, indicating a putative role for PrP^C in neuronal-cell fate (Witusik et al., 2007).

The function of STI1 in neural stem cell biology remains unclear. Strikingly, the main partners of STI1, the chaperones HSP70 e HSP90, have been associate to key cellular mechanisms of neural stem/progenitor cells. HSP70 mediates neuroprotection and increases survival of neuronal precursor cells after focal cerebral ischemia in mice (Doeppner et al., 2009). In addition, HSP90 may be involved in regulation of hypoxia-driven proliferation of embryonic neural stem/progenitor cells (Xiong et al., 2009).

Remarkably, the human homologous of STI1, referred as Hop (Hsp70/Hsp90 organizing protein), has been shown to facilite the phosphorylation and nuclear translocation of Stat3 (Signal transducer and activator of transcription) in mouse embryonic stem cells, implying a role for the Hsp70/Hsp90 chaperone heterocomplex machinery in pluripotency signaling (Longshaw et al., 2009).

Multipotent precursors capable to generate neurons, astrocytes and oligodendrocytes have been isolated through several strategies from different stages of developing and adult central nervous system. The enrichment of this population is accomplished by continuous exposure to mitogenic agents, such as epidermal growth factor (EGF) and basic fibroblast growth factor (bFGF). In these conditions, mitotic

responsive cells proliferate and form cell clusters called neurospheres (NSP) (Reynolds and Rietze, 2005; Campos, 2004). NSP are heterogeneous in size and cell composition, containing multipotent stem cells, progenitors and differentiated cells embedded in extracellular matrix (Campos et al., 2004).

Thus, given the abundant expression of PrP^C in the developing mammalian CNS ans its role in adult neurogenesis and the neurotrophic properties of its partner STI1, we decided to evaluate the participation of PrP^C-STI1 in cell fate related-mechanisms. Here, we reported that STI1 is secreted by neurospheres and its interaction with PrP^C influences self-renewal and proliferation of neural stem cells. These data indicates that PrP^C-STI1 interaction can modulates the biology of progenitor cells and may represent a novel therapeutic target for the treatment of neuronal disorders where neurons are lost and the repopulation of specific regions is necessary.

Material and Methods

Proteins and antibodies: mouse recombinant STI1 (His6-STI1) will be purified as described previously (Zanata et al., 2002). Epidermal Growth Factor (EGF) and Fibroblast Growth Factor-basic (b-FGF) were purchased from Sigma (St. Louis, MO). Synthetic STI1 peptides (pep-STI1 230-ELGNDAYKKKDFDKAL-245 and pep-NH_2 61-GCKTCDLKDDWGKGYS-76) were synthesized by Genescript (Piscataway, NJ). Monoclonal PrP^C antibody (6H4) was purchased from Prionics (Schilieren-Zurich, Switzerland), polyclonal antibodies against STI1 (anti-STI1) and PrP^C (anti-PrP^C) were previously characterized (Chiarini et al., 2002; Zanata et al., 2002) and anti-GAPDH antibody was purchase from Ambion (Austin, TX). Neural

markers anti-nestin, anti-GFAP and βIII-tubulin were from BD (San Jose, CA). Anti-mouse Alexa-568 and anti-rabbit Alexa-488 were from Invitrogen (Carlsbad, CA).

Animals: the Principles of laboratory animal care (NIH publication 85-23, 1996) were strictly followed in all experiments. PrP^{C}-null mice, $Prnp^{0/0}$, were provided by Dr Charles Weissmann (Scripps Florida, FL) (Bueler et al., 1992) and the correspondent wild-type mice, ZchI $Prnp^{+/+}$, was generated by crossing F1 descendants from 129/SV and C57BL/6J matings.

Neurosphere primary culture: NSP primary cultures were obtained from wild-type and $Prnp^{0/0}$ mice (Bueler et al., 1992) embryonic brains (E14). The telencephalon was aseptically dissected in Hank´s Balanced Salt Solution (HBSS) (Invitrogen) and treated with trypsin (0,06%) in HBSS for 20 min at 37ºC. The tripsin was washout with HBSS, and the cells were mechanically dissociated in DMEM-F12 medium containing B-27 supplement, Glutamine (2mM), penicillin (100IU) and streptomycin (100ug/ml) (all from Invitrogen). The cells were cultured in flasks in the presence of 20ng/ml of EGF and bFGF and incubated for 16 h at 37ºC and 5% CO2. After 7 days *in vitro* (DIV 7), the primary NSP were dissociated and used in all assays. For NSP cloning assay 200 cells/well were plated on 96 wells plate and incubated for additional 7 days at 37ºC and 5% CO2. Every 2 days the cells were treated with recombinant STI1. NSP were imaged by phase contrast microscope and the number and diameter of NSP were measured using Image J software (National Institute of Health) and Neuron J plug in. Data are presented as mean ± standard deviation from at least three independent experiments.

Immunofluorescence: whole NSP from wild-type and PrP^{C}-null mice were harvested, fixed with 4% paraformaldehyde, immediately frozen in Tissue Tek and

sectioned (10μm). Sections were hydrated with PBS and blocked with PBS (20mM Tris, 150mM NaCl) containing 0.2% Triton-X100, 20% normal goat serum at room temperature for 1 hour. NSP sections were then incubated at room temperature for 16 hours with anti-PrP^C mouse serum (1:250), anti-STI1 rabbit serum (1:100), anti-βIII-Tubulin (Tuj), anti-GFAP or anti-nestin in TBS 0.1% Triton-X100 with 1% normal goat serum. After washing, anti-mouse Alexa-568 1:3,000 or anti-rabbit Alexa-488 1:3,000 were added on slices and incubated in the same buffer for 1 hour at room temperature followed by DAPI staining. After additional washes, the slides were mounted with Fluorsave (Calbiochem, La Jolla, CA). Immunolabeled cells were imaged with a Bio-Rad Radiance 2100 laser scanning confocal system (Hercules, CA) running the software Laser Sharp 3.0 coupled to a Nikon microsocope (TE2000-U). Argon (488nm) and Green HeNe (543nm) lasers were used to excite the fluorophores. Image processing was done with Photoshop (Adobe Systems) and Image J software (National Institute of Health).

Immunoblotting analysis: Protein extracts or conditioned medium (CM) from wild-type (*Prnp*$^{+/+}$) and PrP^C-null mice (*Prnp* $^{0/0}$) NSP were analyzed. Protein extracts were prepared in Laemmli buffer and CM was previously centrifuged (10,000 x g) filtered (20μm filter) and 50 X concentrated (Minicon, Millipore). Samples were subject to 10% SDS-PAGE followed by immunoblotting with polyclonal antibody anti-STI1 (1:10,000) or anti-PrP^C (1:100). Protein loading control was performed with anti-actin polyclonal antibody (1:200, Sigma). Rabbit or mouse non-immune purified IgG was used as immunoblotting negative control. GAPDH antibody was used as cell lysis control in NSP CM.

Flow cytometry: In non-permeabilized conditions a total of 10^5 NSP primary cells were dissociated into single cells and and incubated with anti-PrP^C (1:100) antobody diluted in PBS 5% BSA for 30 minutes at 4°C. After three washes, cells were incubated with anti-mouse Alexa-568 (1:3,000) for additional 30 min at 4°C. In fixed and permeabilized cells conditions 10^5 NSP primary cells were dissociated into single cells and washed twice with PBS. The fixation and permeabilization was carried out using (BD Cytofix/Cytoperm™ Plus) according manufacture's instructions. Briefly, cells were ressuspended in 250µl of Fixation/Permeabilization solution by vortexing and incubated for 20 min at 4°C followed by two waches with 1× BD Perm/Wash™ buffer. The double staining was performed incubating combinations of primary antibodies (anti-nestin, anti-GFAP or βIII-tubulin) diluted in PBS 5% BSA for 30 minutes on ice and washed three times with Fixation/Permeabilization solution. After washing, secondary antibodies anti-mouse Alexa-568 or Alexa-488 (1:3,000) and anti-rabbit Alexa-568 or Alexa-488 (1:3,000) were incubated for 30 min at 4°C. The cells were kept on ice and the cell suspension was passed through a 40 µm cell strainer (Falcon) before sorting. FACS analysis was performed using a FACSCALIBUR (Becton Dickinson) connected to a Macintosh running CellQuest Software. Cells were analysed using forward scatter, side scatter and fluorescence using an Argon Laser (480nm excitation, 520nm emission).

Enzyme-linked Immunosorbent Assay*:* A 96-well Greiner MICROLON® 600 high binding plate (Greiner, Frickenhausen, Germany) was coated overnight at 4°C with 50 µl of each pair of fractions in PBS, pH 7.4. The wells were washed three times with wash buffer (0.3% Triton X-100 in PBS) and blocked with 100 µl of blocking buffer (5% milk in PBS) for 2h at 37°C. After washing, 50 µl of anti-STI1 in PBS

(7 μg/ml) was added to the wells and incubated for 2h at 37°C, the solution was removed and wells were washed and incubated with 50 μl of anti-rabbit-HRP in PBS (1:2,000) 1 hour at 37°C. The wells were washed and 50 μl of orthophenilenediamine solution (0.33 mg/ml in 0.5 M citrate buffer, pH 5.2, and 0.4% hydrogen peroxide) were added to each well. After 5 minutes at room temperature the reaction was stopped by 50 μl of 4 M sulfuric acid and mesured at 490 nm using a Bio-Rad Benchmark Micro plate Reader.

Cell death assay: Dissociated *Prnp*$^{+/+}$ NSP primary cells (4x10^{5}cells) were grown onto poly-L-lysine coated coverslips, and incubated with STI1, staurosporin or control buffer (TBS) for 24 h at 37ºC and 5% CO_2. The cell cultures were fixed with 4% paraformaldehyde plus 0.12M sucrose in phosphate buffer saline pH 7.4 for 20 min. Cells were incubated at room temperature for 1h with anti-caspase-3 cleaved (1:100).followed by anti-rabbit Alexa 488 (1:3,000) and DAPI staining. Immunolabeled cells were imaged by fluorescence microscope and the percentage of caspase 3 positive cells was quantified. At least three independent experiments were performed and 3 microscopic fields were counted in each group.

Proliferation assay: NSP cells cultured and treated as described above (cloning assay) were pulsed with 0.4 μCi [^{3}H] thimidine/well for 16 h at 37ºC and 5% CO_2. NSP were imaged with a contrast phase microscope for further counting. The medium was removed, cells were washed with PBS and lysed with 1% SDS for 15 min at RT. Cell lysates were transferred to scintillation vials and [^{3}H] thimidine incorporation was measured. The NSP number was counted and the ratio between number of formed sphere/cpm was plotted. Data are presented as mean ± standard deviation from at least three independent experiments.

Statistical analysis: The results represent the mean ± standard deviation of at least three independent experiments. One-way ANOVA with a Tukey post hoc test was used for NSP cloning assay, cell death and proliferation experiments.

Results

Expression and co-localization of STI1 and PrPc in neurosphere

In the present work, we have evaluated the role(s) of PrP^C-interaction on neural stem cells clonally derived from neurospheres (NSP), a valuable in vitro tool for investigation of mechanisms involved in neural stem cells maintenance and differentiation (Leone et al., 2005). Therefore, NSP cultures were obtained from wild-type and PrP^C-null developing forebrain (E14). Cells were maintened for several passages in the presence of EGF and bFGF, without apparent loss of either self-renewal, or multipotenciality, as assessed by their continuous capacity to differentiate in astrocytes, oligodendrocyte and neurons as a result of differentiation induction (data not shown).

To determine whether fetal neural stem cells express STI1 and PrP^C we examined the presence of both molecules in the whole NSP culture at second passage. When viewed through confocal fluorescence microscopy, sections from whole *Prnp*$^{+/+}$ NSP showed strong and homogenious immunoreactivity for both PrP^C (Fig. 1A) and STI1 (Fig. 1B) while no signal was observed in controls using non-immune total serum or IgG (data not shown). STI1 also showed high levels of expression in *Prnp*$^{0/0}$ mouse NSP (Fig.1F), while PrP^C was not detected (Fig. 1E),

demonstrating the specificity of the PrP^C staining. The distribution of both PrP^C and STI1 in *Prnp*$^{+/+}$ NSP is relatively uniform, and immunolabeling is colocalized (Fig.1D), suggesting that both proteins can interact in progenitor cells.

STI1 and PrP^C levels were examined in NSP homogenates from *Prnp*$^{+/+}$ and *Prnp*$^{0/0}$ mice using SDS-PAGE followed by immunoblotting. STI1 levels are similar in both NSP genotypes (Fig. 1I), indicating that NSP STI1 expression is independent of PrP^C expression. The expression of PrP^C at the plasma membrane of primary NSP cells was also confirmed using flow cytometry analysis (Fig. 1J).

Since the soluble form of STI1 presents neurotrophic properties (Arantes et al., 2009; Lima et al., 2007), we evaluated whether NSP cultures are also able to secrete STI1 to extracellular microenvironment. Secreted STI1 could be detected in high ammounts in conditioned medium from *Prnp*$^{0/0}$ and *Prnp*$^{+/+}$ NSP cultures by ELISA and immunoblotting (Figs. 1K and 1L). The faint detection of GAPDH in CM (Fig. 1L) indicates the ocurrence of a small amount of cell lysis which probaly has a minor contribution to the STI1 detected in the CM.

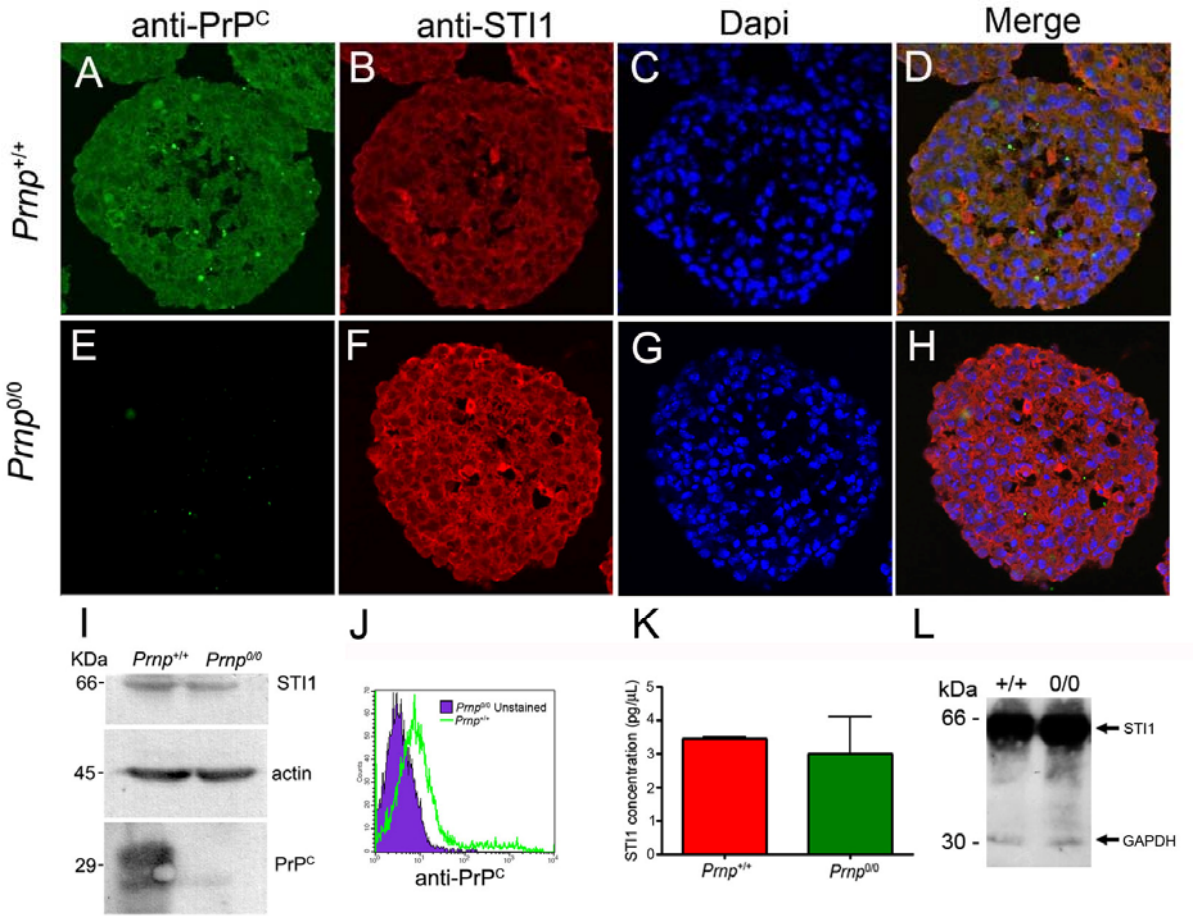

Figure 1: STI1 and PrP^C expression in NSP from *Prnp*$^{+/+}$ and *Prnp*$^{0/0}$ mice. NSP derived from *Prnp*$^{+/+}$ (**A** to **D**) and *Prnp*$^{0/0}$ (**E-H**) mice were cultured in low-density cell suspension in the presence of EGF and bFGF. NSPs were fixed, frozen and sectioned (10µm). The immunofluorescence was performed to detect PrP^C (green) and STI1 (red), the nuclei were stained with DAPI (blue), 200x magnification. **I**, immunodetection of PrP^C and STI1 and actin (loading control) in protein extracts from NSPs. **J**, histogram of *Prnp*$^{+/+}$ (green curve) or *Prnp*$^{0/0}$ (purple curve) NSP cells immunolabeled with anti-PrP^C antibody. **K**, STI1 quantification in conditioned medium of NSP *Prnp*$^{+/+}$ and *Prnp*$^{0/0}$ by ELISA. **L**, STI1 detection in conditioned medium from NSP *Prnp*$^{+/+}$ and *Prnp*$^{0/0}$ *by* immunoblotting with anti-STI1. Immunobloting with anti-GAPDH was used as control for cell lysis.

PrP^C modulates neurosphere formation

In order to address whether PrP^C is involved in neural stem cell maintenance, self-renewal was tested in *$Prnp^{+/+}$* and *$Prnp^{0/0}$* neural stem cells. Primary NSP were dissociated and plated in cloning density in the presence of EGF and bFGF. After 7 days *in vitro* (DIV7) the number of PrP^C-null cells derived NSP is decreased when compared with NSP that express PrP^C (Fig. 2A-C). In additon, the bulk of NSP population presented similar size (50-130μm diameter) in both genotypes (Fig. 2D), indicating that ablation of PrP^C reduces the number of NSP, but does not influence sphere diameter.

STI1-PrPC interaction enhances self-renewal

Considering that STI1 secretion can act as an autocrine factor, through binding to its receptor PrP^C, we asked if the depletion of soluble STI1 with specific antibodies (Arantes et al., 2009; Lopes et al., 2005; Lima et al., 2007) could impair the NSP formation. In a cloning assay, the treatment of *$Prnp^{+/+}$* with anti-STI1 (Fig. 3A) or anti-PrP^C (Fig. 3B) antibodies decreases the formation of spheres while no effect was observed in *$Prnp^{0/0}$* cells (Fig. 3A,B). Pre-immune IgG from rabbit or mouse was used as control.

STI1 treatment induces a dose-dependent increament in the number of *$Prnp^{+/+}$* NSP formation but not in *$Prnp^{0/0}$* NSP (Fig. 3C), indicating that PrP^C is required for STI1 activity. Remarkable, contrary to what has been described before for neurons (Zanata, Lopes) but in agremment to results observed in astrocytes (Arantes et aal., 2009), the STI1 peptide (pep-STI1) which represents the PrP^C binding site is unable to mimick the effect os the entire STI1 molecule (Figure 3C).

Hence, these data indicate that PrP^C-STI1 engagement is important to modulate NSP formation and other STI1domains besides the PrP^C binding site may regulate this activity.

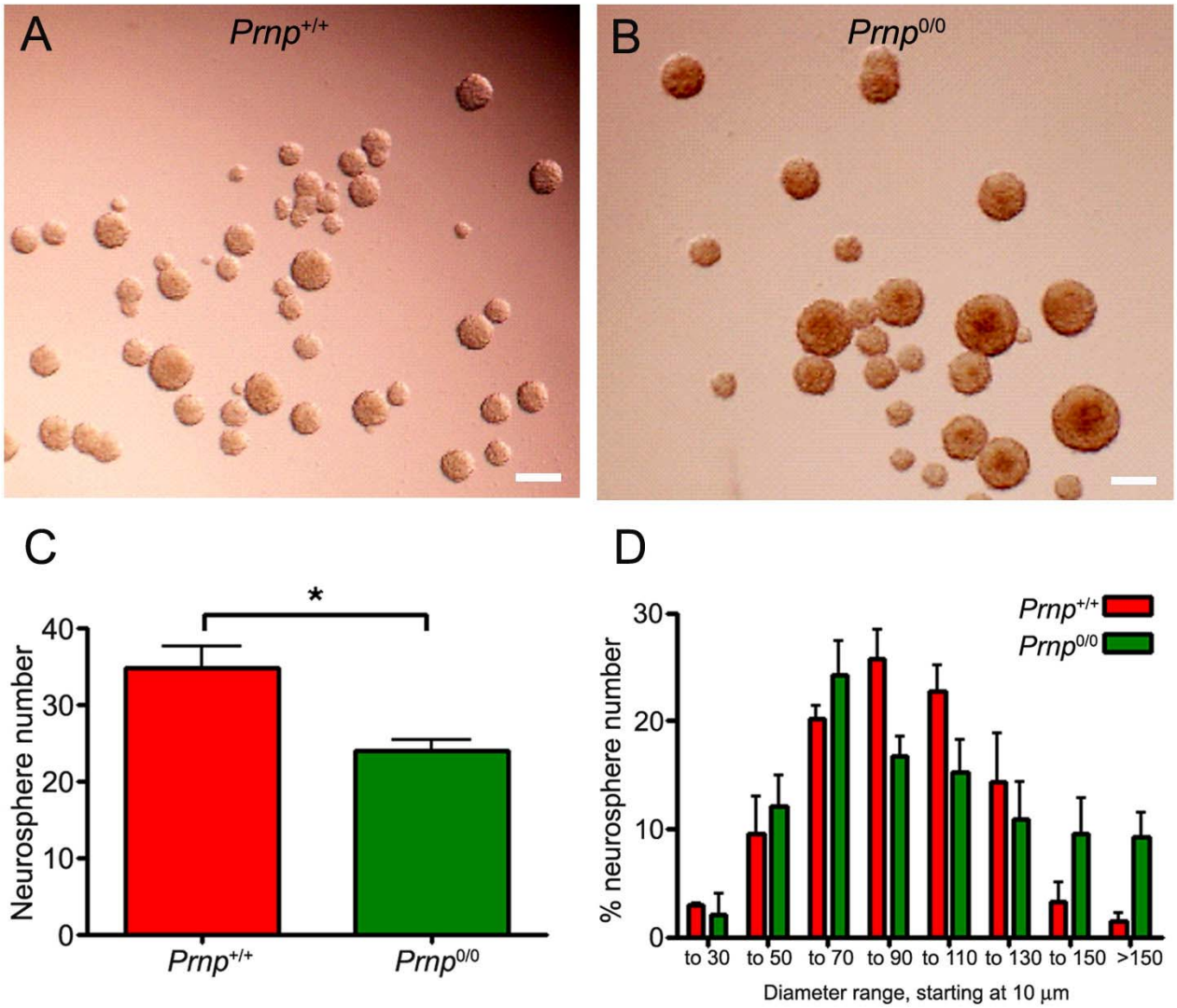

Figure 2: PrP^C ablation impairs NSP formation. Dissociated primary NSP cells *Prnp*$^{+/+}$ and *Prnp*$^{0/0}$ were cultured in low-density for 7 days in the presence of EGF and bFGF. Representative images of NSP cultures *Prnp*$^{+/+}$ (**A**) and *Prnp*$^{0/0}$ (**B**). The NSP number (**C**) and diameter (**D**) were measured using software ImageJ. Values represent the mean and standard deviation of at least three independent experiments. **p<0.001 *p<0.002 (ANOVA). Calibration bars, 200µm.

.

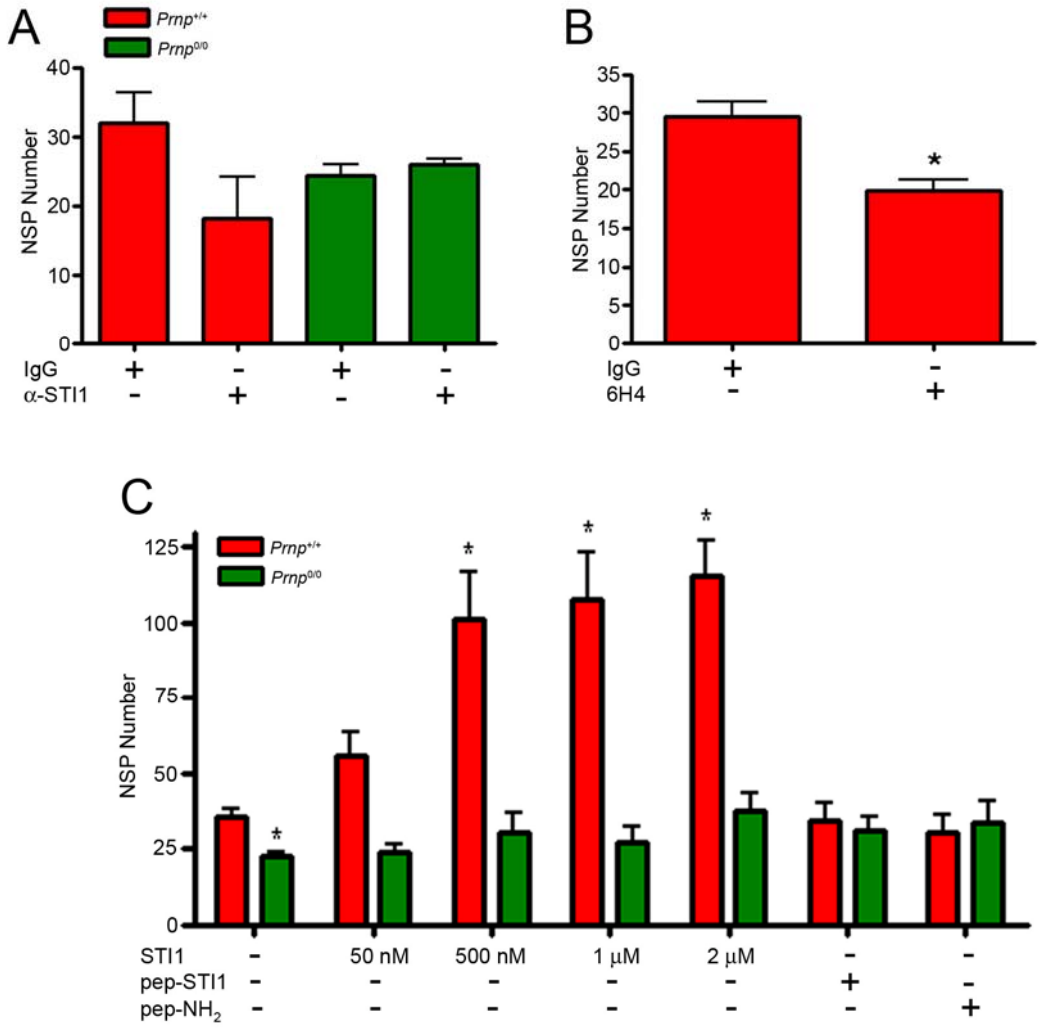

Figure 3: STI1 increases NSP formation in a PrP^C–dependent manner. Dissociated *Prnp*$^{+/+}$ and *Prnp*$^{0/0}$ cells were cultured for 7 days in the presence of EGF and bFGF and treated every 48h cells with antibodies, protein or peptides. Cells were treated with 6 µg/ml of antibodies against STI1 (**A**) or PrP^C (**B**) or increasing concentrations of recombinant STI1 (0.05 to 2 µM) or 8 µM of the STI1 peptide which represents the PrP^C binding site (pep-STI1) or a peptde from the N-terminal domain of STI1 (**C**). Values represent the mean and standard deviation of at least three independent experiments. *$p<0.05$, ANOVA followed by Tukey´s Multiple Comparison Test. Calibration bars, 200µm.

Neurosphere-increased number is not mediated by neuroprotective effects of STI1

Considering the key effect of STI1 in neurosphere formation, we next search for the mechanism which this protein could be modulating in association with PrP^C. Since our previous studies reported a neuroprotective effect promoted by STI1 (Chiarini et al., 2002; Zanata et al., 2002; Lopes et al., 2005), we evaluate whether STI1 effect under NSP formation caused by its protective activity. To address this issue, the presence of cleaved caspase-3 in dissociated *Prnp*$^{+/+}$ cells treated with STI1 was evaluated. It is well known that after primary NSP dissociation most of the cells die under selective culture medium (Reynolds and Rietze, 2005). Thus, immediately after plated, the *Prnp*$^{+/+}$ cells were treated with STI1 for 24 h, fixed and immunostained with anti-cleaved caspase-3. Representative images of untreated (Fig. 4A) and STI1-treated cells (Fig. 4B) immunolabeled with cleaved caspase-3 (green) and DAPI (blue) are showed. STI1 had no effect on the activity of caspase-3 was, even at the highest STI1 concentration (Fig. 4C). As positive control the cells were treated with staurosporine (*Streptomyces staurospores*), a non-selective protein kinase inhibitor (Ruegg and Burgess, 1989), that is often used as a general inducer of apoptosis (Nicotera and Orrenius, 1998). These data indicates that STI1 is unable to decrease cell apoptosis by modulating capase-3 activity.

STI1 increases neurosphere proliferation: self-renewal evidence

Trying to elucidate the mechanism by which STI1 promotes the enhancement of self-renewal of neural stem cells, we addressed whether cell proliferation would be affected by STI1. NSP from cloning assays, treated with STI1 every 48 h for 7 days, were pulsed with [^{3}H]-Thymidine for 12 hours. STI1 significantly increases

[^{3}H]-Thymidine incorporation in *Prnp*$^{+/+}$ NSP (Fig. 5) at the same concentrations (0.5 to 2μM) necessary to enhance NSP number. In contrast, STI1 had no effect in *Prnp*$^{0/0}$ cells (Fig. 5). Thus, these results strongly suggest that STI1 stimulates NSP increasing formation by increasing cell proliferation.

PrP^C-null NSP express higher βIII-Tubulin than wild-type NSP.

In order to examine whether PrP^C expression modulates the ratio of undifferentiated/differentiated cell lineages, NSPs derived from wild-type and PrP^C-null mice were immunophenotyped by flow cytometry using cell markers of undifferentiated cells (nestin), astrocytes-committed cells (GFAP) and new-born neurons (βIII-tubulin). After NSP dissociation, fixation and permeabilization, cells were double-stained with anti-βIII-tub/anti-GFAP or anti- βIII-tub/anti-nestin. *Prnp*$^{+/+}$ (Figs 6A,B) or *Prnp*$^{0/0}$ (Figs. 6C,D) NSP cells express neuronal, glial or undifferentiated markers. A significant higher percentage of cells expressing βIII-tubulin was observed in PrP^C-null cells compared to wild-type NSP (Fig. 6E), suggesting that in PrP^C expression mantains NSP in a less differentiated state.

Immunofluorescence assays with *Prnp*$^{+/+}$ (Figs 6F, H anf J) and *Prnp*$^{0/0}$ (Figs. 6G, I, and K) NSP sections were also performed to evaluate βIII-tubulin (Figs 6F and G), GFAP (Figs. 6H and I) and nestin (Figs 6J and K) expression *in situ*. Consistent to what has been demostrated by flow cytometry assays, NSP express the three neural markers. Interestingly, nestin expression presents a non-homogeneous pattern with higher labeling cells on NSP periphery (Figs 6 J and K).

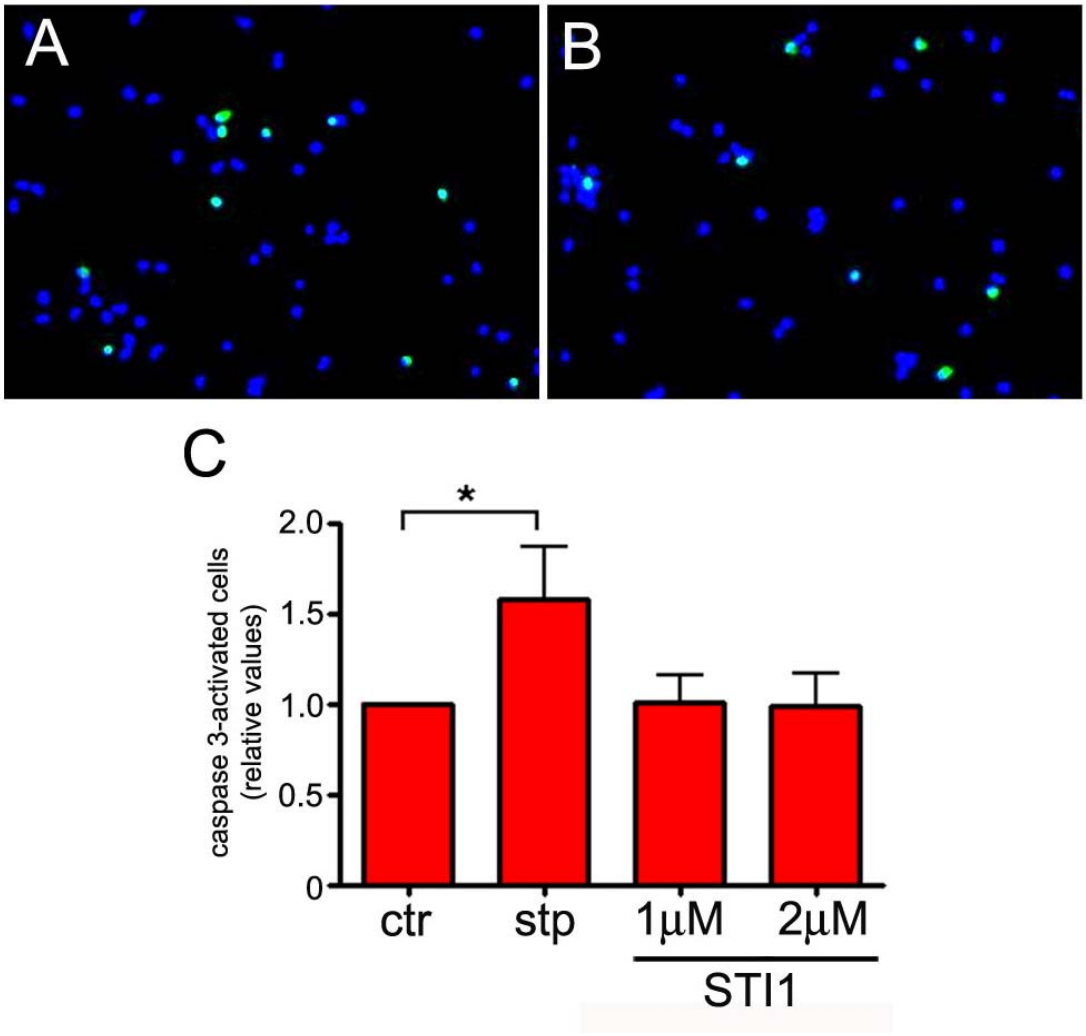

Figure 4. STI1 in unable to modulate caspase-3 activation in NSP cultures. NSP *Prnp*$^{+/+}$ were dissociated and plated onto poly-L-lysine coated coverslips for 24 h in the presence of STI1. Staurosporine (stp) was used as positive control of cell death. Cell death was assessed by immunostained with anti-caspase 3 activated. Representative images of NSP cells untreated (A) and treated with 1μM STI1 (B). Nuclei stained with DAPI (blue) and caspase 3-activated (green), 200x magnification. Values represent the mean and standard deviation (vertical bars) of at least three independent experiments. * Statistical significance when compared to control: $p < 0.05$ ANOVA followed by Tukey´s Multiple Comparison Test

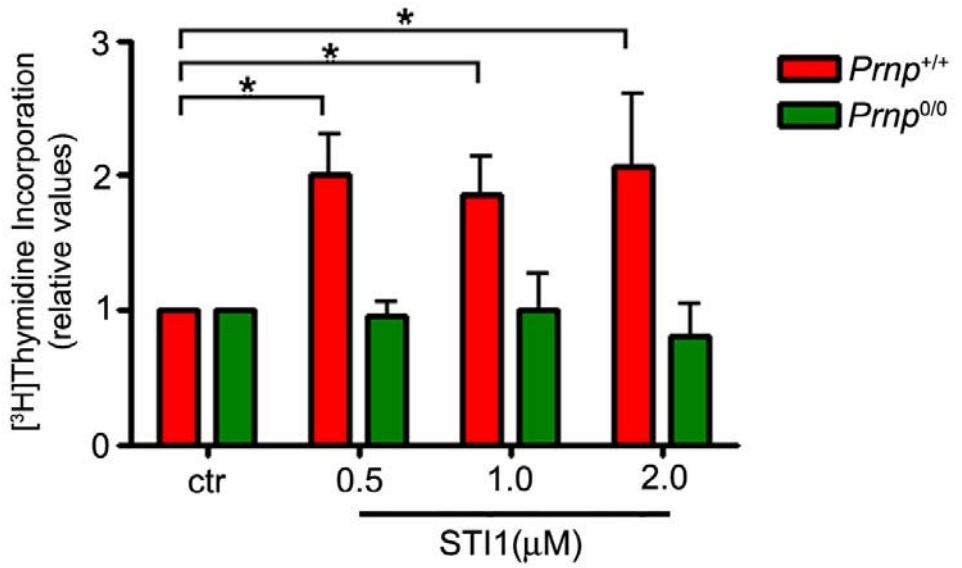

Figure 5. STI1 promotes the proliferation of NSP cells. Dissociated primary NSP cells *Prnp*$^{+/+}$ and *Prnp*$^{0/0}$ were cultured in low-density for 7 days in the presence of EGF and FGF-b. After the quantification of NSP, [^{3}H]Thymidine (1μCi/ml) and STI1 were added to the medium for additional 16 h. NSP were collected and radioactivity was measured. The values represent the ratio between labeling (CPM, counts per min) vs. NSP number. The graph shows relative values and standard deviation (vertical bars) of at least three independent experiments. * Statistical significance when compared to control: $p< 0.05$, ANOVA followed by Tukey´s Multiple Comparison Test.

Next, we evaluated whether STI1 modulates cell differentiation by, assessing the expression of neural markers (GFAP, nestin and βIII-tubulin) by flow cytometry. As shown in Figure 7, no significant difference was found in the pattern of neural markers βIII-tubulin (Fig. 7A), GFAP (Fig. 7B) and nestin (Fig. 7C) in either *Prnp*$^{+/+}$ or *Prnp*$^{0/0}$ NSP after STI1 treatment.

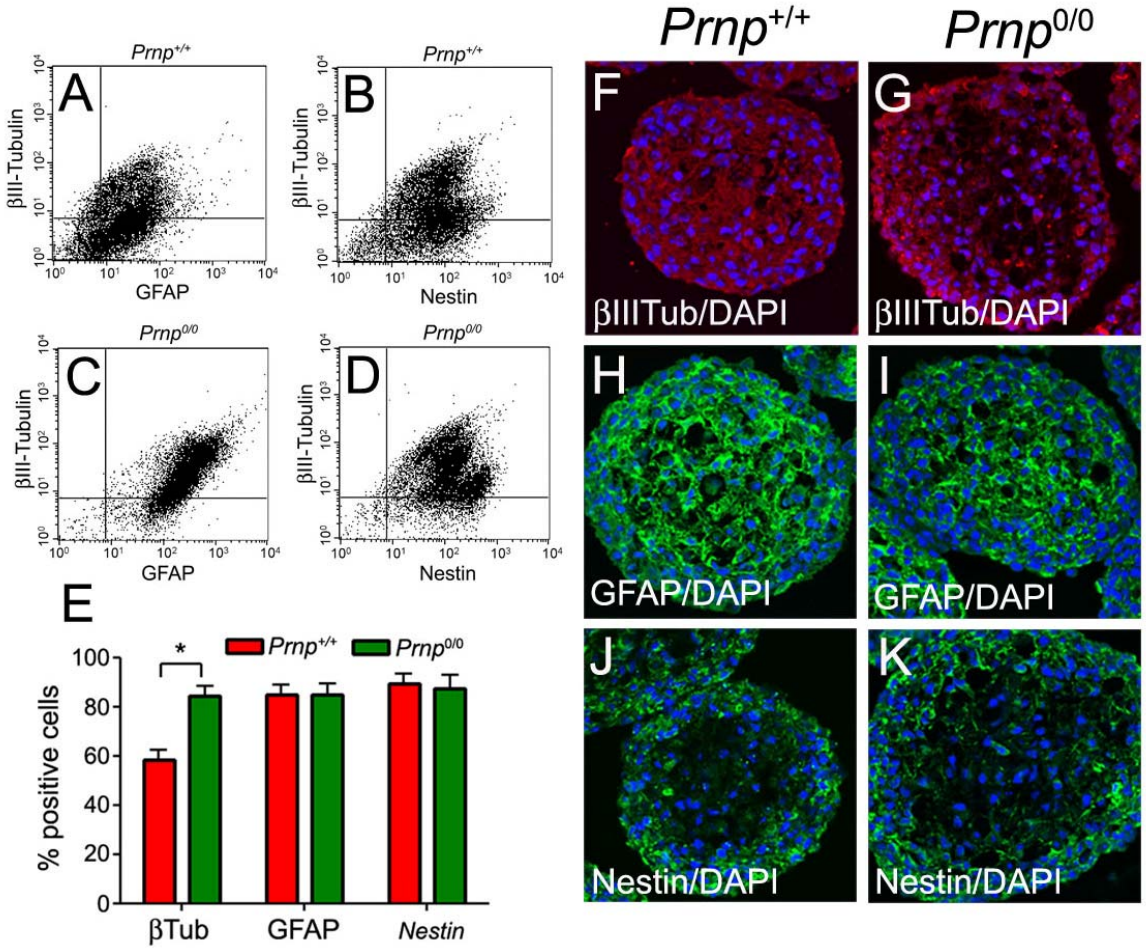

Figure 6: βIII-Tubulin positive cells are increased in PrP^{C}-null neurosheres. Cell cytometry of dissociated cells from *Prnp*$^{+/+}$ and *Prnp*$^{0/0}$ NSP. Cells suspensions were fixed and double-stained for βIII-Tubulin and GFAP (**A** and **C**) or for βIII-Tubulin and nestin (**B** and **D**. The percentage of positive cells for the three markers in NSP from wild-type (red bars) or PrPC-null (green bars) mice, Values represent the mean ± standard deviation of at least three independent experiments, *p<0.01, ANOVA followed by Tukey´s Multiple Comparison Test. *Prnp*$^{+/+}$ **(F, H** and **J)** and *Prnp*$^{0/0}$ **(G, I** and **K)** NSP were cultured in low-density cell suspension in the presence of EGF e FGFb. NSPs were fixed, frozen and sectioned (10μm). The immunofluorescence was performed to detect βIII-Tubulin (**F** and **G**, red), GFAP (**H** and **I**, green) and nestin (**J** and **K,** green). Superimpose with DAPI (blue) are shown in merge (**F - K**), 200x magnification.

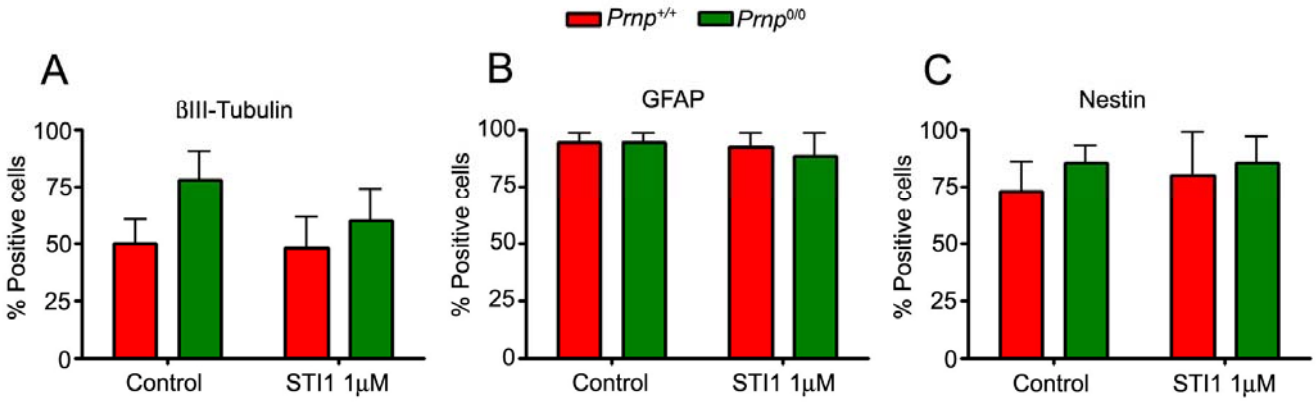

Figure 7. Differentiation of NSP is not altered by STI1 treatment. Dissociated primary NSP cells *Prnp*$^{+/+}$ and *Prnp*$^{0/0}$ were cultured in low-density for 7 days in the presence of EGF and bFGF and treated with 1μM STI1 every 48h. NSPs were harvested and dissociated. Cells from *Prnp*$^{+/+}$ and *Prnp*$^{0/0}$ were fixed and stained for βIII-Tubulin (**A**), GFAP (**B**) or nestin (**D**). The percentage of positive cells for the three markers was evaluated in wild-type (red bars) or PrP^{C}-null cells (green bars). There was no statistically difference between groups.

Discussion

In this study, we evaluated the neurotrophic activities of STI1/PrP^{C} interaction in neural stem cell self-renewal. The expression of both proteins is abundant and homogeneously distributed in primary neural stem cell cultures. Remarkably, large amounts of soluble STI1 are released to extracellular microenvironment from those cells. PrP^{C} ablation impairs neurosphere generation, suggesting that PrP^{C} plays a role in self-renewal. Furthermore, PrP^{C} could act as STI1 receptor, and the interaction of these proteins might trigger signals involved in proliferation of neural stem cells. These data strength the hypothesis that STI1 can act as a neurotrophic molecule through its major cell surface receptor, PrP^{C}.

PrP^{C} is involved in neurotrophic signal transduction via interaction with a number of partners (Linden et al., 2008; Martins et al., 2009). At least two important

transmembrane proteins with well-established neurotrophic activities were identified as PrP^C ligand, neural cell adhesion molecule (NCAM) (Schmitt-Ulms et al., 2001) and 37-kDa/67-kDa Laminin Receptor Precursor (37LRP/67LR) (Gauczynski et al., 2001; Rieger et al., 1997). NCAM plays important roles in developing and adult brain, including pivotal functions in neuronal differentiation and neurite outgrowth (Ditlevsen et al., 2008). PrP^C directly interacts with NCAM, leading to NCAM stabilization in lipid rafts and activation of $p59^{fyn}$ to induce NCAM-dependent neuritogenesis (Santuccione et al., 2005). On the other hand, PrP^C can indirectly modulate 37LRP/67LR-dependent neurotrophic activities, including cell adhesion and signal transduction (Nelson et al., 2008; Hundt et al., 2001).

PrP^C is also able to associate to extracellular matrix proteins (ECM), such as laminin and vitronectin, modulating neurite outgrowth in hippocampal neurons and axonogenesis in peripheral neurons, which may be relevant for its neurotrophic activity (Graner et al., 2000;Hajj et al., 2007). Interestingly, integrins, the major ECM receptors, regulate fundamental processes in neural stem cells, such as progenitor proliferation and survival, contributing to their maintenance (Leone et al., 2005; Campos et al., 2004).

One of the most extensively studied PrP^C partner is STI1 (Martins et al., 1997; Zanata et al., 2002). STI1 is secreted by astrocytes and modulates PrP^C-dependent neurotrophic effects (Arantes et al., 2009; Chiarini et al., 2002; Lima et al., 2007; Lopes et al., 2005; Zanata et al., 2002). In neurons, STI1 transduces neuroprotective signals through PKA activation and also promotes ERK1/2 phosphorylation which is involved in neuritogenesis (Lopes et al., 2005). STI1 induces PrP^C internalization which is necessary for ERK1/2 phosphorilation but not

for PKA activation (Caetano et al., 2008).Moreover, STI1 modulates differentiation and protection against cell death when engaged to PrP^C in astrocytes (Arantes et al., 2009). In vivo experiments demonstrated that antibodies against STI1 or anti-PrP^C, when injected directly into the hippocampus, impair memory formation and consolidation. Remarkably, the STI1 peptide that represents the PrP^C binding site improves memory formation and consolidation (Coitinho et al., 2007). Together these results point STI1 as a putative neurotrophin molecule whose binding to PrP^C modulates crucial mechanisms of neural plasticity.

STI1 and PrP^C are expressed in a variety of neurons and glial cells during brain development, suggesting potential roles for these proteins in neural stem cell-fate during brain development. Few reports have described functional roles of PrP^C and STI1 in stem cell biology. In fact, it has been reported that PrP^C-overexpression regulate neural precursor proliferation in developing and post-natal CNS (Steele et al., 2006). Recently, Hop (Hsp70/Hsp90 organizing protein), the human STI1 homologous, has been implicated in pluripotency signaling of mouse embryonic stem cells (Longshaw et al., 2009). Interestingly, the major ligands of STI1, the chaperones Hsp70 e Hsp90, have been associate with the maintenance of neural stem/progenitor cells. Hsp70 mediated neuroprotection and increased survival of neuronal precursor cells after focal cerebral ischemia in mice (Doeppner et al., 2009) and Hsp90 might be implicated in regulation of hypoxia-driven proliferation of embryonic neural stem/progenitor cells (Xiong et al., 2009).

Our data provide evidence that PrP^C-STI1 interaction is important for neural stem cell self-renewal. The major observations that support our conclusions: first, PrP^C and STI1 are homogenously expressed and colocalize, indicating their

association and functioning in NSP derived stem cells. Second, STI1 can be secreted by NSP sustaining its characterization as an autocrine neurotrophic factor. Third, PrP^C-null cells generate relatively few NSP than wild-type cells, suggesting that PrP^C is required for neural stem cell self-renewal. Fourth, antibody-blocking of STI1-PrP^C interaction impairs NSP formation, demonstrating that endogenous STI1-PrP^C engagement is needed for stem cell self-renewal properties. Fifth, when added to culture medium, recombinant STI1 potentiates self-renewal through its binding to PrP^C in a dose dependent-manner. Finally, the mechanism involved in STI1-PrP^C-mediated self-renewal depends on cell proliferation without affect on cell survival or differentiation. Together these results indicate an important role for STI1-PrP^C in the regulation of neural stem cell maintenance.

In conclusion, we were able to address the role of PrP^C-STI1 interaction in stem and neural progenitor cell biology. Therefore, it is conceivable that PrP^C-STI1 interaction-dependent regulation of neural progenitor/stem self-renewal and proliferation might also operate *in vivo* during normal development or following injury to the CNS, including prion diseases.

References

Arantes C, Nomizo R, Lopes MH, Hajj GN, Lima FR, Martins VR (2009) Prion protein and its ligand stress inducible protein 1 regulate astrocyte development. Glia.

Bueler H, Fischer M, Lang Y, Bluethmann H, Lipp HP, DeArmond SJ, Prusiner SB, Aguet M, Weissmann C (1992) Normal development and behaviour of mice lacking the neuronal cell-surface PrP protein. Nature 356:577-582.

Caetano FA, Lopes MH, Hajj GN, Machado CF, Pinto AC, Magalhaes AC, Vieira MP, Americo TA, Massensini AR, Priola SA, Vorberg I, Gomez MV, Linden R, Prado VF, Martins VR, Prado MA (2008) Endocytosis of prion protein is required for ERK1/2 signaling induced by stress-inducible protein 1. J Neurosci 28:6691-6702.

Campos LS (2004) Neurospheres: insights into neural stem cell biology. J Neurosci Res 78:761-769.

Campos LS, Leone DP, Relvas JB, Brakebusch C, Fassler R, Suter U, ffrench-Constant C (2004) Beta1 integrins activate a MAPK signalling pathway in neural stem cells that contributes to their maintenance. Development 131:3433-3444.

Chiarini LB, Freitas AR, Zanata SM, Brentani RR, Martins VR, Linden R (2002) Cellular prion protein transduces neuroprotective signals. EMBO J 21:3317-3326.

Coitinho AS, Lopes MH, Hajj GN, Rossato JI, Freitas AR, Castro CC, Cammarota M, Brentani RR, Izquierdo I, Martins VR (2007) Short-term memory formation and long-term memory consolidation are enhanced by cellular prion association to stress-inducible protein 1. Neurobiol Dis 26:282-290.

Ditlevsen DK, Povlsen GK, Berezin V, Bock E (2008) NCAM-induced intracellular signaling revisited. J Neurosci Res 86:727-743.

Doeppner TR, Nagel F, Dietz GP, Weise J, Tonges L, Schwarting S, Bahr M (2009) TAT-Hsp70-mediated neuroprotection and increased survival of neuronal precursor cells after focal cerebral ischemia in mice. J Cereb Blood Flow Metab 29:1187-1196.

Gauczynski S, Peyrin JM, Haik S, Leucht C, Hundt C, Rieger R, Krasemann S, Deslys JP, Dormont D, Lasmezas CI, Weiss S (2001) The 37-kDa/67-kDa laminin receptor acts as the cell-surface receptor for the cellular prion protein. EMBO J 20:5863-5875.

Graner E, Mercadante AF, Zanata SM, Forlenza OV, Cabral AL, Veiga SS, Juliano MA, Roesler R, Walz R, Minetti A, Izquierdo I, Martins VR, Brentani RR (2000) Cellular prion protein binds laminin and mediates neuritogenesis. Brain Res Mol Brain Res 76:85-92.

Hajj GN, Lopes MH, Mercadante AF, Veiga SS, da Silveira RB, Santos TG, Ribeiro KC, Juliano MA, Jacchieri SG, Zanata SM, Martins VR (2007) Cellular prion protein interaction with vitronectin supports axonal growth and is compensated by integrins. J Cell Sci 120:1915-1926.

Hajj GN, Santos TG, Cook ZSP, Martins VR (2009) Developmental expression of prion protein and its ligands stress inducible protein 1 and vitronectin.

Hundt C, Peyrin JM, Haik S, Gauczynski S, Leucht C, Rieger R, Riley ML, Deslys JP, Dormont D, Lasmezas CI, Weiss S (2001) Identification of interaction domains of the prion protein with its 37-kDa/67-kDa laminin receptor. EMBO J 20:5876-5886.

Leone DP, Relvas JB, Campos LS, Hemmi S, Brakebusch C, Fassler R, ffrench-Constant C, Suter U (2005) Regulation of neural progenitor proliferation and survival by beta1 integrins. J Cell Sci 118:2589-2599.

Lima FR, Arantes CP, Muras AG, Nomizo R, Brentani RR, Martins VR (2007) Cellular prion protein expression in astrocytes modulates neuronal survival and differentiation. J Neurochem 103:2164-2176.

Linden R, Martins VR, Prado MA, Cammarota M, Izquierdo I, Brentani RR (2008) Physiology of the prion protein. Physiol Rev 88:673-728.

Longshaw VM, Baxter M, Prewitz M, Blatch GL (2009) Knockdown of the co-chaperone Hop promotes extranuclear accumulation of Stat3 in mouse embryonic stem cells. Eur J Cell Biol 88:153-166.

Lopes MH, Hajj GN, Muras AG, Mancini GL, Castro RM, Ribeiro KC, Brentani RR, Linden R, Martins VR (2005) Interaction of cellular prion and stress-inducible

protein 1 promotes neuritogenesis and neuroprotection by distinct signaling pathways. J Neurosci 25:11330-11339.

Martins VR, Beraldo FH, Hajj GN, Lopes MH, Lee KS, Prado MA, Linden R (2009) Prion protein: orchestrating neurotrophic activities.

Martins VR, Graner E, Garcia-Abreu J, de Souza SJ, Mercadante AF, Veiga SS, Zanata SM, Neto VM, Brentani RR (1997) Complementary hydropathy identifies a cellular prion protein receptor. Nat Med 3:1376-1382.

Moore RA, Taubner LM, Priola SA (2009) Prion protein misfolding and disease. Curr Opin Struct Biol 19:14-22.

Nelson J, McFerran NV, Pivato G, Chambers E, Doherty C, Steele D, Timson DJ (2008) The 67 kDa laminin receptor: structure, function and role in disease. Biosci Rep 28:33-48.

Nicotera P, Orrenius S (1998) The role of calcium in apoptosis. Cell Calcium 23:173-180.

Reynolds BA, Rietze RL (2005) Neural stem cells and neurospheres--re-evaluating the relationship. Nat Methods 2:333-336.

Rieger R, Edenhofer F, Lasmezas CI, Weiss S (1997) The human 37-kDa laminin receptor precursor interacts with the prion protein in eukaryotic cells. Nat Med 3:1383-1388.

Ruegg UT, Burgess GM (1989) Staurosporine, K-252 and UCN-01: potent but nonspecific inhibitors of protein kinases. Trends Pharmacol Sci 10:218-220.

Santuccione A, Sytnyk V, Leshchyns'ka I, Schachner M (2005) Prion protein recruits its neuronal receptor NCAM to lipid rafts to activate p59fyn and to enhance neurite outgrowth. J Cell Biol 169:341-354.

Schmitt-Ulms G, Legname G, Baldwin MA, Ball HL, Bradon N, Bosque PJ, Crossin KL, Edelman GM, DeArmond SJ, Cohen FE, Prusiner SB (2001) Binding of neural cell adhesion molecules (N-CAMs) to the cellular prion protein. J Mol Biol 314:1209-1225.

Steele AD, Emsley JG, Ozdinler PH, Lindquist S, Macklis JD (2006) Prion protein (PrPc) positively regulates neural precursor proliferation during developmental and adult mammalian neurogenesis. Proc Natl Acad Sci U S A 103:3416-3421.

Tremblay P, Bouzamondo-Bernstein E, Heinrich C, Prusiner SB, DeArmond SJ (2007) Developmental expression of PrP in the post-implantation embryo. Brain Res 1139:60-67.

Witusik M, Gresner SM, Hulas-Bigoszewska K, Krynska B, Azizi SA, Liberski PP, Brown P, Rieske P (2007) Neuronal and astrocytic cells, obtained after differentiation of human neural GFAP-positive progenitors, present heterogeneous expression of PrPc. Brain Res 1186:65-73.

Xiong L, Zhao T, Huang X, Liu ZH, Zhao H, Li MM, Wu LY, Shu HB, Zhu LL, Fan M (2009) Heat shock protein 90 is involved in regulation of hypoxia-driven proliferation of embryonic neural stem/progenitor cells. Cell Stress Chaperones 14:183-192.

Zanata SM, Lopes MH, Mercadante AF, Hajj GN, Chiarini LB, Nomizo R, Freitas AR, Cabral AL, Lee KS, Juliano MA, de OE, Jachieri SG, Burlingame A, Huang L, Linden R, Brentani RR, Martins VR (2002) Stress-inducible protein 1 is a cell surface ligand for cellular prion that triggers neuroprotection. EMBO J 21:3307-3316.

4 CONCLUSÕES

Neste projeto foram realizadas diferentes abordagens para estudar a função da proteína prion celular e seus ligantes: STI1, laminina e vitronectina no desenvolvimento do sistema nervoso.

Expressão de PrP^C, STI1 e Vitronectina x Desenvolvimento:

Apesar da expressão de mRNA de PrP^C ao longo do desenvolvimento do sistema nervoso de mamíferos e aves já ter sido caracterizada (PRUSINER 2004), pouco se conhecia sobre o padrão de expressão proteíca. O mesmo ocorre para a vitronectina, onde já havia sido descrita sua expressão em diversos tecidos, porém por ser uma molécula secretada, o padrão de expressão gênica nem sempre corresponde com o sítio de detecção da proteína. Em relação a STI1, poucos trabalhos foram conduzidos no sentido de observar sua expressão protéica no sistema nervoso de vertebrados e considerando as evidências que apontam para STI1 como uma nova neurotrofina, é necessário demonstrar quais são os sítios de expressão desta proteína.

Desta maneira, descrevemos os padrões de expressão protéica de PrP^C, STI1 e Vn ao longo do desenvolvolvimento de camundongo, observando que as três proteínas apresentam um perfil similar de expressão espaço-temporal. E ainda, o padrão de expressão em forma de gradiente na medula espinhal, sugere um papel destas proteínas no desenvolvimento do sistema nervoso periférico.

PrP^C x Neuritogênese

A formação de prolongamentos neuronais é um dos eventos cruciais no desenvolvimento do encéfalo e é regulado por uma série de moléculas neurotróficas, dentre as quais PrP^C tem sido considerada como um importante componente.

Como demonstrado neste estudo, o acop lamento de PrP^C com as proteínas de matriz extracelular laminina (cadeia γ1) e vitronectina, juntamente com STI1 estimula a neuritogênese em neurônios do sistema nervoso central e periférico. Interessantemente, constatamos o efeito sinérgico entre Ln-γ1 e STI1 sobre a neuritogênese dependente de PrP^C. Este fenômeno é observado entre diferentes grupos de moléculas neurotróficas (Choi), que apresentam a capacidade de operar de maneira conjunta, porém, é importante ressaltar que PrP^C pode ser utilizado como receptor por, pelo menos, duas moléculas tróficas, neste caso STI1 e Ln-γ1.

PrP^C x Sinalização

Entre as diversas funções atribuídas a PrP^C, destacam-se àquelas que envolvem a modulação de vias de sinalização controladas por diversas outras proteínas na membrana plasmática. Devido a sua capacidade de recrutar diferentes ligantes, organizando módulos de sinalização envolvidos com diversos eventos celulares (Martins et al. 2009).

Já foi caracterizada que a sinalização de PrP^C pode ser mediada pela sua interação com moléculas transmembrana, como NCAM, integrinas, receptores acoplados a proteína G e canais iônicos de membrana. Nossos resultados sugerem

que as vias responsáveis pela mobilização de cálcio promovidas por STI1 são diferentes daquelas envolvidas na resposta a Ln-γ1. Provavelmente isto é resultado da interação de PrP^C com diferentes receptores da membrana plasmática. A identidade destas moléculas ainda é desconhecida e nosso grupo tem buscado por diferentes estratégias caracterizar novos parceiros de PrP^C. De fato, identificamos que em neurônios hipocampais a interação entre PrP^C e Ln-γ1 ativa receptores metabotrópicos de glutamato do tipo I (mGluRI) . A ativação deste receptores promove a mobilização intracelular de cálcio, que por sua vez está envolvida com a neuritogênese neste tipo celular (ANEXO II). A Figura 5 apresenta um esquema que ilustra o efeito cooperativo entre Ln-γ1 e STI1 sobre a axonogênese de gânglios da raiz dorsal.

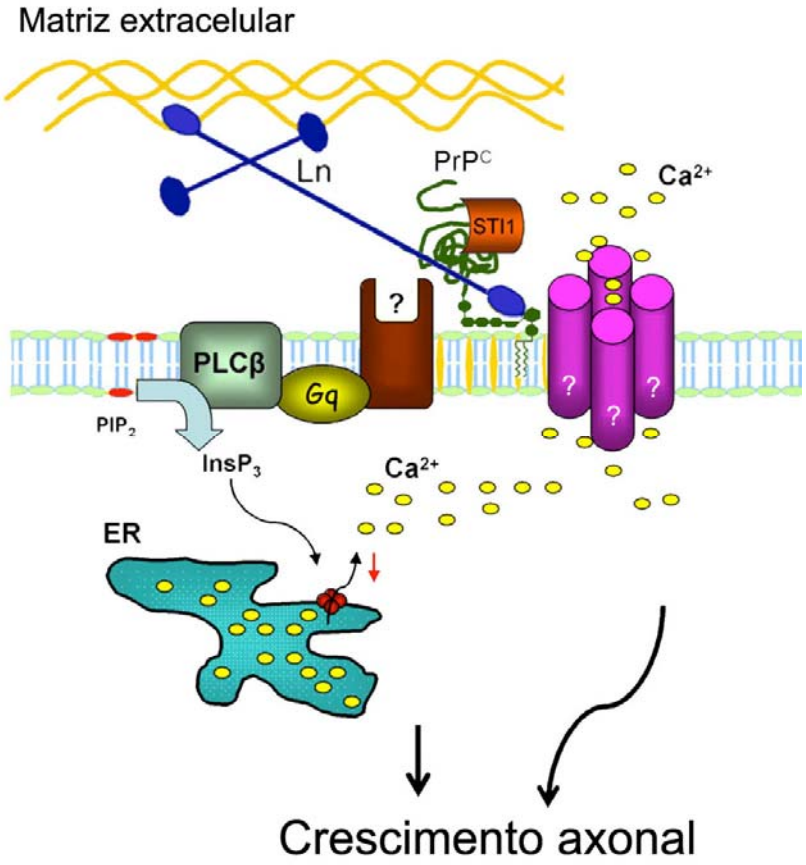

Figura 5. Ln-γ1 e STI1 podem interagir com PrP^C, de maneira sinérgica, transduzindo sinais neurotróficos envolvidos com o crescimento axonal. As proteínas responsáveis em transduzir os sinais de PrP^C (representados em marrom e roxo) ainda precisam ser identificadas.

PrP^C x Células Tronco Neurais

Uma das perspectivas para o estudo das funções de PrP^C em situações fisiológicas e patológicas é seu envolvimento com células tronco neurais. Demonstramos que a interação PrP^C-STI1 é importante para a auto-renovação e proliferação de células tronco neurais derivadas de tecido fetal. Ainda é necessário caracterizar melhor o mecanismo de ação de STI1.

Nosso próximo passo é investigar o papel da associação entre PrP^C e STI1 em células tronco residentes do encéfalo adulto. Também pretendemos avaliar o

envolvimento desta neurogênese nos processos de plasticidade sináptica nas quais PrP^C esté envolvido. Resultados preliminares do grupo demonstram que STI1 também aumenta o número de neuroesferas derivadas da ZSV de animais tipo-selvagem.

Entender a função de PrP^C nos eventos que governam a neurogênese adulta também pode contribuir para o entendimento de como a conversão de PrP^C pode levar ao aparecimento de doenças tão debilitantes quanto as causadas por prions.

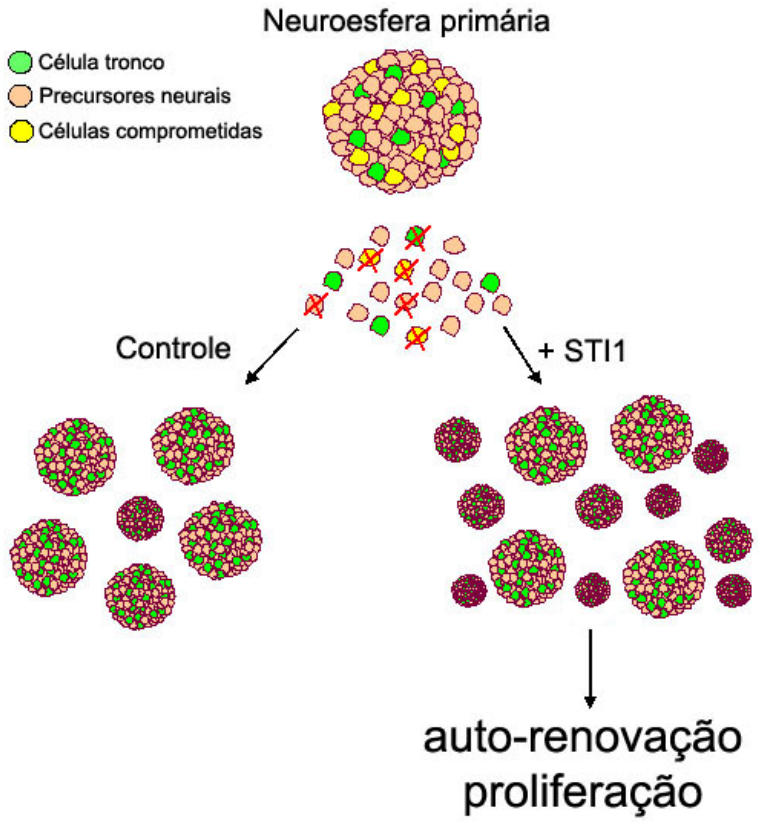

Figura 6. Envolvimento de PrP^C e STI1 na auto-renovação e proliferação de precursores neurais. Células precursoras derivadas de animais deficientes para PrP^C apresentam menor capacidade de formação de neuroesferas enquanto que STI1 estimula a formação e proliferação de precursores derivados de animais tipo-selvagem.

5. REFERÊNCIAS BIBLIOGRÁFICAS

Aguzzi, A. The Pathogenesis and Mechanisms of Prion Diseases. In: Beal, MF, Lang A.E., e Ludolph, A. **Neurodegenerative Diseases: neurobiology, pathogenesis and therapeutics**. Cambridge: Cambridge University Press; 2005. p.523-47.

Aguzzi A. Prion diseases of humans and farm animals: epidemiology, genetics, and pathogenesis. **J Neurochem** 2006; 97:1726-39.

Aguzzi A, Raeber AJ. Transgenic models of neurodegeneration. Neurodegeneration: of (transgenic) mice and men. **Brain Pathol** 1998; 8:695-7.

Alper T, Cramp WA, Haig DA, Clarke MC. Does the agent of scrapie replicate without nucleic acid? **Nature** 1967; 214:764-6.

Alper T, Haig DA, Clarke MC. The exceptionally small size of the scrapie agent. **Biochem Biophys Res Commun** 1966; 22:278-84.

Alvarez-Buylla A, Seri B, Doetsch F. Identification of neural stem cells in the adult vertebrate brain. **Brain Res Bull** 2002; 57:751-8.

Arantes C, Nomizo R, Lopes MH, et al. Prion protein and its ligand stress inducible protein 1 regulate astrocyte development. **Glia** 2009; 57:1439-49.

Arcangeli A, Becchetti A, Mannini A, et al. Integrin-mediated neurite outgrowth in neuroblastoma cells depends on the activation of potassium channels. **J Cell Biol** 1993; 122:1131-43.

Azzalin A, Ferrara V, Arias A, et al. Interaction between the cellular prion (PrPC) and the 2P domain K+ channel TREK-1 protein. **Biochem Biophys Res Commun** 2006; 346:108-15.

Basler K, Oesch B, Scott M, et al. Scrapie and cellular PrP isoforms are encoded by the same chromosomal gene. **Cell** 1986; 46:417-28.

Baumann F, Tolnay M, Brabeck C, et al. Lethal recessive myelin toxicity of prion protein lacking its central domain. **EMBO J** 2007; 26:538-47.

Bolsover SR. Calcium signalling in growth cone migration. **Cell Calcium** 2005; 37:395-402.

Bolton DC, McKinley MP, Prusiner SB. Identification of a protein that purifies with the scrapie prion. **Science** 1982; 218:1309-11.

Brocco MA e Panzetta P. Survival and process regrowth of purified chick retinal ganglion cells cultured in a growth factor lacking medium at low density. Modulation by extracellular matrix proteins. **Brain Res Dev Brain Res** 1999; 118:23-32.

Brose K, Bland KS, Wang KH, et al. Slit proteins bind Robo receptors and have an evolutionarily conserved role in repulsive axon guidance. **Cell** 1999; 96:795-806.

Brown P. Reflections on a half-century in the field of transmissible spongiform encephalopathy. **Folia Neuropathol** 2009; 47:95-103.
Bueler H, Fischer M, Lang Y, et al. Normal development and behaviour of mice lacking the neuronal cell-surface PrP protein. **Nature** 1992; 356:577-82.

Cabral AL, Lee KS, Martins VR. Regulation of the cellular prion protein gene expression depends on chromatin conformation. **J Biol Chem**. 2002; 277:5675-82.

Caetano FA, Lopes MH, Hajj GN, et al. Endocytosis of prion protein is required for ERK1/2 signaling induced by stress-inducible protein 1. **J Neurosci** 2008; 28:6691-702.

Caldwell MA, He X, Wilkie N, et al. Growth factors regulate the survival and fate of cells derived from human neurospheres. **Nat Biotechnol** 2001; 19:475-9.

Campos LS, Leone DP, Relvas JB, et al. Beta1 integrins activate a MAPK signalling pathway in neural stem cells that contributes to their maintenance. **Development** 2004; 131:3433-44.

Chen ZL e Strickland S. Laminin gamma1 is critical for Schwann cell differentiation, axon myelination, and regeneration in the peripheral nerve. **J Cell Biol** 2003; 163:889-99.

Chesebro B, Race R, Wehrly K, et al. Identification of scrapie prion protein-specific mRNA in scrapie-infected and uninfected brain. **Nature** 1985; 315:331-3.

Chiarini LB, Freitas AR, Zanata SM, Brentani RR, Martins VR, Linden R. Cellular prion protein transduces neuroprotective signals. **EMBO J** 2002; 21:3317-26.

Chien, C. Guidance of axons and dendrites. In: Rao MS, Jacobson M, editors **Developmental neurobiology**. 4 ed. New York: Kluwer Academic/Plenum Publishers; 2005. p.241-67.

Cho HJ. Is the scrapie agent a virus? **Nature** 1976; 262:411-2.

Coitinho AS, Freitas AR, Lopes MH, et al. The interaction between prion protein and laminin modulates memory consolidation. **Eur J Neurosci**. 2006; 24:3255-64.

Coitinho AS, Lopes MH, Hajj GN, et al. Short-term memory formation and long-term memory consolidation are enhanced by cellular prion association to stress-inducible protein 1. **Neurobiol Dis** 2007; 26:282-90.

Collinge J, Whittington MA, Sidle KC, et al. Prion protein is necessary for normal synaptic function. **Nature** 1994; 370:295-7.

Condic ML, Snow DM, Letourneau PC. Embryonic neurons adapt to the inhibitory proteoglycan aggrecan by increasing integrin expression. **J Neurosci** 1999; 19:10036-43.

Criado JR, Sanchez-Alavez M, Conti B, et al. Mice devoid of prion protein have cognitive deficits that are rescued by reconstitution of PrP in neurons. **Neurobiol Dis** 2005; 19:255-65.

Darnell DK. Anteroposterior and dorsoventral patterning. In: Rao MS, Jacobson M, editors. **Developmental neurobiology**. 4 ed. New York: Kluwer Academic/Plenum Pu; 2005. p.41-65.

DeArmond SJ, Sanchez H, Yehiely F, et al. Selective neuronal targeting in prion disease. **Neuron** 1997; 19:1337-48.

Denny-Brown D. The influence of tension and innervation on the regeneration of skeletal muscle. **J Neuropathol Exp Neurol** 1951; 10:94-6.

Diefenbach TJ, Guthrie PB, Kater SB. Stimulus history alters behavioral responses of neuronal growth cones. **J Neurosci** 2000; 20:1484-94.

Eriksson PS, Perfilieva E, Bjork-Eriksson T, et al. Neurogenesis in the adult human hippocampus. **Nat Med** 1998; 4:1313-7.

Erlich RB, Kahn SA, Lima FR, et al. STI1 promotes glioma proliferation through MAPK and PI3K pathways. **Glia** 2007; 55:1690-8.

Eustace BK e Jay DG. Extracellular roles for the molecular chaperone, hsp90. **Cell Cycle** 2004; 3:1098-100.

Gage FH. Mammalian neural stem cells. **Science** 2000; 287:1433-8.

Gajdusek DC, Gibbs CJ, Alpers M. Experimental transmission of a Kuru-like syndrome to chimpanzees. **Nature** 1966; 209:794-6.

Gajdusek DC, Gibbs CJ, Jr., Alpers M. Transmission and passage of experimenal "kuru" to chimpanzees. **Science** 1967; 155:212-4.

Gauczynski S, Peyrin JM, Haik S, et al. The 37-kDa/67-kDa laminin receptor acts as the cell-surface receptor for the cellular prion protein. **EMBO J** 2001; 20:5863-75.

Gibbs CJ Jr, Gajdusek DC, Asher DM, et al. Creutzfeldt-Jakob disease (spongiform encephalopathy): transmission to the chimpanzee. **Science** 1968; 161:388-9.

Gomez TM, Spitzer NC. In vivo regulation of axon extension and pathfinding by growth-cone calcium transients. **Nature** 1999; 397:350-355.

Gomez TM, Zheng JQ. The molecular basis for calcium-dependent axon pathfinding. **Nat Rev Neurosci** 2006; 7:115-25.

Gonzalez-Iglesias R, Pajares MA, Ocal C, Espinosa JC, Oesch B, Gasset M. Prion protein interaction with glycosaminoglycan occurs with the formation of oligomeric complexes stabilized by Cu(II) bridges. **J Mol Biol** 2002; 319:527-40.

Graner E, Mercadante AF, Zanata SM, et al. Cellular prion protein binds laminin and mediates neuritogenesis. **Brain Res Mol Brain Res** 2000; 76:85-92.

Griffith JS. Self-replication and scrapie. **Nature** 1967; 215:1043-4.

Grimpe B, Dong S, Doller C, et al.Temple K, Malouf AT, Silver J. The critical role of basement membrane-independent laminin gamma 1 chain during axon regeneration in the CNS. **J Neurosci** 2002; 22:3144-60.

Gutmann E. Neurotrophic relations. **Annu. Rev. Physiol** 1976; 38:177-216.

Hajj GN, Lopes MH, Mercadante AF, et al. Cellular prion protein interaction with vitronectin supports axonal growth and is compensated by integrins. **J Cell Sci** 2007; 120:1915-26.

Hegde RS, Mastrianni JA, Scott MR, et al. A transmembrane form of the prion protein in neurodegenerative disease. **Science** 1998; 279:827-34.

Herms JW, Korte S, Gall S, Schneider I, Dunker S, Kretzschmar HA. Altered intracellular calcium homeostasis in cerebellar granule cells of prion protein-deficient mice. **J Neurochem** 2000; 75:1487-92.

Hong K, Nishiyama M, Henley J, Tessier-Lavigne M, Poo M. Calcium signalling in the guidance of nerve growth by netrin-1. **Nature** 2000; 403:93-98.

Hopker VH, Shewan D, Tessier-Lavigne M, Poo M, Holt C. Growth-cone attraction to netrin-1 is converted to repulsion by laminin-1. **Nature** 1999; 401:69-73.

Hundt C, Peyrin JM, Haik S, et al. Identification of interaction domains of the prion protein with its 37-kDa/67-kDa laminin receptor. **EMBO J** 2001; 20:5876-86.

Kandel, ER Schwartz JH, Jessel TM. **Principles of neural sciences**. 4 ed. New York: McGraw-Hill; 2000.

Kellermann O, Loric S, Maroteaux L, Launay JM. Sequential onset of three 5-HT receptors during the 5-hydroxytryptaminergic differentiation of the murine 1C11 cell line. **Br J Pharmacol** 1996; 118:1161-70.

Keshet GI, Bar-Peled O, Yaffe D, Nudel U, Gabizon R. The cellular prion protein colocalizes with the dystroglycan complex in the brain. **J Neurochem** 2000; 75:1889-97.

Khosravani H, Zhang Y, Tsutsui S, et al. Prion protein attenuates excitotoxicity by inhibiting NMDA receptors. **J Gen Physiol** 2008; 131:i5-

Khosravani H, Zhang Y, Zamponi GW. Cellular prion protein null mice display normal AMPA receptor mediated long term depression. **Prion** 2008; 2:48-50.

Ladher R, Schoenwolf GC. Making a neural tube: neural induction and neurulation. In: Rao MS, Jacobson M, editors. **Developmental neurobiology**. 4 ed. New York: Kluwer Academic/Plenum Pu; 2005. p.1-20.

Lau PM, Zucker RS, Bentley D. Induction of filopodia by direct local elevation of intracellular calcium ion concentration. **J Cell Biol** 1999; 145:1265-75.

Lawson SN, Caddy KW, Biscoe TJ. Development of rat dorsal root ganglion neurones. Studies of cell birthdays and changes in mean cell diameter. **Cell Tissue Res** 1974; 153:399-413.

Le Douarin, NM, Kalchein, C, e Teillet, M. The cellular and molecular basis of early sensory ganglion development. In: Scott SA. **Sensory neurons: diversity, development and plasticity**. New York; Oxford University Press; 1992. p.143-69.

Leskawa KC, Maddox T, Webster KA. Effects of ethanol on neuroblastoma cells in culture: role of gangliosides in neuritogenesis and substrate adhesion. **J Neurosci Res** 1995; 42:377-84.

Li A, Christensen HM, Stewart LR, Roth KA, Chiesa R, Harris DA. Neonatal lethality in transgenic mice expressing prion protein with a deletion of residues 105-125. **EMBO J** 2007; 26:548-58.

Liesi P, Laatikainen T, Wright JM. Biologically active sequence (KDI) mediates the neurite outgrowth function of the gamma-1 chain of laminin-1. **J Neurosci Res** 2001; 66:1047-53.

Liesi P, Narvanen A, Soos J, Sariola H, Snounou G. Identification of a neurite outgrowth-promoting domain of laminin using synthetic peptides. **FEBS Lett** 1989; 244:141-148.

Lima FR, Arantes CP, Muras AG, Nomizo R, Brentani RR, Martins VR. Cellular prion protein expression in astrocytes modulates neuronal survival and differentiation. **J Neurochem** 2007; 103:2164-76.

Linden R, Martins VR, Prado MA, Cammarota M, Izquierdo I, Brentani RR. Physiology of the prion protein. **Physiol Rev** 2008; 88:673-728.

Lledo PM, Alonso M, Grubb MS. Adult neurogenesis and functional plasticity in neuronal circuits. **Nat Rev Neurosci** 2006; 7:179-93.

Lopes MH, Hajj GN, Muras AG, et al. Interaction of cellular prion and stress-inducible protein 1 promotes neuritogenesis and neuroprotection by distinct signaling pathways. **J Neurosci** 2005; 25:11330-9.

Luckenbill-Edds L. Laminin and the mechanism of neuronal outgrowth. **Brain Res Brain Res Rev** 1997; 23:1-27.

Luo L. Rho GTPases in neuronal morphogenesis. **Nat Rev Neurosci** 2000; 1:173-80.

Maglio LE, Perez MF, Martins VR, Brentani RR, Ramirez OA. Hippocampal synaptic plasticity in mice devoid of cellular prion protein. **Brain Res Mol Brain Res** 2004; 131:58-64.

Manson JC, Clarke AR, Hooper ML, Aitchison L, McConnell I, Hope J. 129/Ola mice carrying a null mutation in PrP that abolishes mRNA production are developmentally normal. **Mol Neurobiol** 1994; 8:121-7.

Martino G e Pluchino S. The therapeutic potential of neural stem cells. **Nat Rev Neurosci** 2006; 7:395-406.

Martins VR, Beraldo FH, Hajj GN, et al. Prion protein: orchestrating neurotrophic activities. **Curr Issues Mol Biol** 2009; 18:63-86.

Masters CL, Gajdusek DC, Gibbs CJ, Jr. Creutzfeldt-Jakob disease virus isolations from the Gerstmann-Straussler syndrome with an analysis of the various forms of amyloid plaque deposition in the virus-induced spongiform encephalopathies. **Brain** 1981; 104:559-88.

McLennan NF, Brennan PM, McNeill A, et al. Prion protein accumulation and neuroprotection in hypoxic brain damage. **Am J Pathol** 2004; 165:227-35.

Meyer RK, McKinley MP, Bowman KA, Braunfeld MB, Barry RA, Prusiner SB. Separation and properties of cellular and scrapie prion proteins. **Proc Natl Acad Sci U. S. A** 1986; 83:2310-4.

Ming GL e Song H. Adult neurogenesis in the mammalian central nervous system. **Annu Rev Neurosci** 2005; 28:223-50.

Mironov A Jr, Latawiec D, Wille H, et al. Cytosolic prion protein in neurons. **J Neurosci** 2003; 23:7183-7193.

Mouillet-Richard S, Pietri M, Schneider B, et al. Modulation of serotonergic receptor signaling and cross-talk by prion protein. **J Biol Chem** 2005; 280:4592-601.

Mueller BK. Growth cone guidance: first steps towards a deeper understanding. **Annu Rev Neurosci** 1999; 22:351-88.

Muramoto T, DeArmond SJ, Scott M, Telling GC, Cohen FE, Prusiner SB. Heritable disorder resembling neuronal storage disease in mice expressing prion protein with deletion of an alpha-helix. **Nat Med** 1997; 3:750-5.

Nelson J, McFerran NV, Pivato G, et al. The 67 kDa laminin receptor: structure, function and role in disease. **Biosci Rep** 2008; 28:33-48.

Nguyen-Ba-Charvet KT, Brose K, Marillat V, Sotelo C, Tessier-Lavigne M, Chedotal A. Sensory axon response to substrate-bound Slit2 is modulated by laminin and cyclic GMP. **Mol. Cell Neurosci**. 2001; 17:1048-1058.

Nicolet CM, Craig EA. Isolation and characterization of STI1, a stress-inducible gene from Saccharomyces cerevisiae. **Mol Cell Biol** 1989; 9:3638-46.

Nowakowski RS, Hayes NL. Cell proliferation in the developing mammalian brain. In: Rao MS, Jacobson M, editors. **Developmental neurobiology**. 4 ed. New York: Kluwer Academic/Plenum Pu; 2005. p. 21-39.

Oesch B, Westaway D, Walchli M, et al. A cellular gene encodes scrapie PrP 27-30 protein. **Cell** 1985; 40:735-46.

Paulsson M, Aumailley M, Deutzmann R, Timpl R, Beck K, Engel J. Laminin-nidogen complex: extraction with chelating agents and structural characterization. **Eur J Biochem** 1987; 166:11-9.

Perl ER. Function of dorsal root ganglion neurons: an overview. In: Scott SA, editor. **Sensory neurons: diversity, development and plasticity**. New York; Oxford University Press; 1992. p.3-26.

Plachez C, Richards LJ. Mechanisms of axon guidance in the developing nervous system. **Curr Top Dev Biol** 2005; 69:267-346.

Pons S, Marti E. Sonic hedgehog synergizes with the extracellular matrix protein vitronectin to induce spinal motor neuron differentiation. **Development** 2000; 127:333-42.

Prestori F, Rossi P, Bearzatto B, et al. Altered neuron excitability and synaptic plasticity in the cerebellar granular layer of juvenile prion protein knock-out mice with impaired motor control. **J Neurosci** 2008; 28:7091-103.

Prusiner SB. Novel proteinaceous infectious particles cause scrapie. **Science** 1982; 216:136-44.

Prusiner SB. Prions. **Proc Natl Acad Sci** U. S. A 1998; 95:13363-83.

Prusiner SB. **Prion biology and diseases**. 2 ed. Cold Spring Harbor: Cold Spring Harbor Laboratory Press; 2004.

Prusiner SB, McKinley MP, Bowman KA, et al. Scrapie prions aggregate to form amyloid-like birefringent rods. **Cell** 1983; 35:349-58.

Radovanovic I, Braun N, Giger OT, et al. Truncated prion protein and Doppel are myelinotoxic in the absence of oligodendrocytic PrPC. **J Neurosci** 2005; 25:4879-888.

Rangel A, Burgaya F, Gavin R, Soriano E, Aguzzi A, Del Rio JA. Enhanced susceptibility of Prnp-deficient mice to kainate-induced seizures, neuronal apoptosis, and death: Role of AMPA/kainate receptors. **J Neurosci Res** 2007; 85:2741-55.

Reynolds BA, Rietze RL. Neural stem cells and neurospheres--re-evaluating the relationship. **Nat Methods** 2005; 2:333-6.

Rieger R, Edenhofer F, Lasmezas CI, Weiss S. The human 37-kDa laminin receptor precursor interacts with the prion protein in eukaryotic cells. **Nat Med** 1997; 3:1383-8.

Sakudo A, Ikuta K. Fundamentals of prion diseases and their involvement in the loss of function of cellular prion protein. **Protein Pept Lett** 2009; 16:217-29.

Sakurai-Yamashita Y, Sakaguchi S, Yoshikawa D, et al. Female-specific neuroprotection against transient brain ischemia observed in mice devoid of prion protein is abolished by ectopic expression of prion protein-like protein. **Neuroscience** 2005; 136:281-7.

Sales N, Hassig R, Rodolfo K, et al. Developmental expression of the cellular prion protein in elongating axons. **Eur J Neurosci** 2002; 15:1163-77.

Sanai N, Tramontin AD, Quinones-Hinojosa A, et al. Unique astrocyte ribbon in adult human brain contains neural stem cells but lacks chain migration. **Nature** 2004; 427:740-4.

Sanes DH Reh TA, Harris WA. **Development of the nervous system**. 2 ed. New York: Academic Press; 2006.

Santuccione A, Sytnyk V, Leshchyns'ka I, Schachner M. Prion protein recruits its neuronal receptor NCAM to lipid rafts to activate p59fyn and to enhance neurite outgrowth. **J Cell Biol** 2005; 169:341-54.

Schinder AF, Gage FH. A hypothesis about the role of adult neurogenesis in hippocampal function. **Physiology** 2004; 19:253-61.

Schmitt-Ulms G, Legname G, Baldwin MA, et al. Binding of neural cell adhesion molecules (N-CAMs) to the cellular prion protein. **J Mol Biol** 2001; 314:1209-25.

Shmerling D, Hegyi I, Fischer M, et al. Expression of amino-terminally truncated PrP in the mouse leading to ataxia and specific cerebellar lesions. **Cell** 1998; 93:203-14.

Shyu WC, Lin SZ, Chiang MF, et al. Overexpression of PrPC by adenovirus-mediated gene targeting reduces ischemic injury in a stroke rat model. **J Neurosci** 2005; 25:8967-77.

Song HJ e Poo MM. Signal transduction underlying growth cone guidance by diffusible factors. **Curr Opin Neurobiol** 1999; 9:355-63.

Soto C. Unfolding the role of protein misfolding in neurodegenerative diseases. **Nat Rev Neurosci** 2003; 4:49-60.

Spudich A, Frigg R, Kilic E, et al. Aggravation of ischemic brain injury by prion protein deficiency: role of ERK-1/-2 and STAT-1. **Neurobiol Dis** 2005; 20:442-9.

Steele AD, Emsley JG, Ozdinler PH, Lindquist S, Macklis JD. Prion protein (PrPc) positively regulates neural precursor proliferation during developmental and adult mammalian neurogenesis. **Proc Natl Acad Sci. U. S. A** 2006; 103:3416-21.

Taylor DR, Hooper NM. The low-density lipoprotein receptor-related protein 1 (LRP1) mediates the endocytosis of the cellular prion protein. **Biochem J** 2007; 402:17-23.

Telling GC, Haga T, Torchia M, Tremblay P, DeArmond SJ, Prusiner SB. Interactions between wild-type and mutant prion proteins modulate neurodegeneration in transgenic mice. **Genes Dev** 1996; 10:1736-50.

Tessier-Lavigne M, Placzek M, Lumsden AG, Dodd J, Jessell TM. Chemotropic guidance of developing axons in the mammalian central nervous system. **Nature** 1988; 336:775-8.

Tobler I, Deboer T, Fischer M. Sleep and sleep regulation in normal and prion protein-deficient mice. **J Neurosci** 1997; 17:1869-79.

Tobler I, Gaus SE, Deboer T, et al. Altered circadian activity rhythms and sleep in mice devoid of prion protein. **Nature** 1996; 380:639-42.

Turk E, Teplow DB, Hood LE, Prusiner SB. Purification and properties of the cellular and scrapie hamster prion proteins. **Eur J Biochem** 1988; 176:21-30.

Vaananen AJ, Rauhala P, Tuominen RK, Liesi P. KDI tripeptide of gamma1 laminin protects rat dopaminergic neurons from 6-OHDA induced toxicity. **J Neurosci Res** 2006; 84:655-65.

Venstrom KA e Reichardt LF. Extracellular matrix. 2: Role of extracellular matrix molecules and their receptors in the nervous system. **FASEB J** 1993; 7:996-1003.

Walz R, Amaral OB, Rockenbach IC, et al. Increased sensitivity to seizures in mice lacking cellular prion protein. **Epilepsia** 1999; 40:1679-82.

Warner RG, Hundt C, Weiss S, Turnbull JE. Identification of the heparan sulfate binding sites in the cellular prion protein. **J Biol Chem** 2002; 277:18421-30.

Weise J, Crome O, Sandau R, Schulz-Schaeffer W, Bahr M, Zerr I. Upregulation of cellular prion protein (PrPc) after focal cerebral ischemia and influence of lesion severity. **Neurosci Lett** 2004; 372:146-50.

Weise J, Sandau R, Schwarting S, et al. Deletion of cellular prion protein results in reduced Akt activation, enhanced postischemic caspase-3 activation, and exacerbation of ischemic brain injury. **Stroke** 2006; 37:1296-1300.

Wiksten M, Vaananen A, Liebkind R, Rauhala P, Liesi P. Soluble KDI domain of gamma1 laminin protects adult hippocampus from excitotoxicity of kainic acid. **J Neurosci Res** 2004; 78:411-9.

Wiksten M, Vaananen AJ, Liebkind R, Liesi P. Regeneration of adult rat spinal cord is promoted by the soluble KDI domain of gamma1 laminin. **J. Neurosci. Res.** 2004; 78:403-410.

Zanata SM, Lopes MH, Mercadante AF, et al. Stress-inducible protein 1 is a cell surface ligand for cellular prion that triggers neuroprotection. **EMBO J** 2002; 21:3307-16.

Zheng JQ, Poo MM. Calcium signaling in neuronal motility. **Annu Rev Cell Dev.Biol** 2007; 23:375-404.

Anexo 1 - Interação entre PrP^C e Vitronectina estimula axonogênese em gânglios da raiz dorsal.

Neste trabalho, demonstramos que PrP^C interage com a proteína de matriz extracelular Vitronectina (Vn) mas não com fibronectina e colágeno. O sítio de interação entre PrP^C e Vn foi mapeado através de ensaios de *binding* com peptídeos sintéticos, e compreende a região entre os aminoácidos 105 a 119 da molécula de PrP^C e entre os aminoácidos 307 a 320 de Vn. A co-localização entre as duas proteínas foi determinada por imunofluorência em cortes de embrião E12,5 com uma marcação específica em gânglios da raiz dorsal (GRD). A adição de Vn a culturas de explantes de GRD estimula a extensão axonal em neurônios. Este efeito é mimetizado por um peptídeo sintético corresponde ao sítio de interação de Vn a PrP^C (pep Vn 307-320) e é abolido por anticorpos contra PrP^C. Adicionalmente, demonstramos que em GRD derivados de animais deficientes para PrP^C existe uma superestimulação da atividade de integrina $\alpha_v\beta_3$, que é sugerida como um mecanismo compensatório para a ausência de expressão de PrP^C.

Neste trabalho, minha contribuição aconteceu nos ensaios de axonogênese nos animais Npu *Prnp*$^{-/-}$ (Figuras 6i e 7c) e nos ensaios de ligação de vitronectina marcada com AlexaFluor-568 a PrP^C, em neurônios dissociados de gânglio da raiz dorsal e na linhagem SN-56 (Figura 5a).

Cellular prion protein interaction with vitronectin supports axonal growth and is compensated by integrins

Glaucia N. M. Hajj[1,2], Marilene H. Lopes[1,3], Adriana F. Mercadante[4], Silvio S. Veiga[5], Rafael B. da Silveira[5], Tiago G. Santos[1,3], Karina C. B. Ribeiro[3], Maria A. Juliano[6], Saul G. Jacchieri[3], Silvio M. Zanata[4] and Vilma R. Martins[1,*]

[1]Ludwig Institute for Cancer Research, Hospital Alemão Oswaldo Cruz, São Paulo, Brazil
[2]Departamento de Bioquímica, Instituto de Química, Universidade de São Paulo, São Paulo, Brazil
[3]Centro de Tratamento e Pesquisa Hospital do Câncer, São Paulo, Brazil
[4]Departamento de Patologia Básica, Universidade Federal do Paraná, Curitiba, Brazil
[5]Departamento de Biologia Celular, Universidade Federal do Paraná, Curitiba, Brazil
[6]INFAR, Universidade Federal de São Paulo, São Paulo, Brazil
*Author for correspondence (e-mail: vmartins@ludwig.org.br)

Accepted 11 April 2007
Journal of Cell Science 120, 1915-1926 Published by The Company of Biologists 2007
doi:10.1242/jcs.03459

Summary

The physiological functions of the cellular prion protein, PrP^C, as a cell surface pleiotropic receptor are under debate. We report that PrP^C interacts with vitronectin but not with fibronectin or collagen. The binding sites mediating this PrP^C-vitronectin interaction were mapped to residues 105-119 of PrP^C and the residues 307-320 of vitronectin. The two proteins were co-localized in embryonic dorsal root ganglia from wild-type mice. Vitronectin addition to cultured dorsal root ganglia induced axonal growth, which could be mimicked by vitronectin peptide 307-320 and abrogated by anti-PrP^C antibodies. Full-length vitronectin, but not the vitronectin peptide 307-320, induced axonal growth of dorsal root neurons from two strains of PrP^C-null mice. Functional assays demonstrated that relative to wild-type cells, PrP^C-null dorsal root neurons were more responsive to the Arg-Gly-Asp peptide (an integrin-binding site), and exhibited greater $\alpha v\beta 3$ activity. Our findings indicate that PrP^C plays an important role in axonal growth, and this function may be rescued in PrP^C-knockout animals by integrin compensatory mechanisms.

Supplementary material available online at
http://jcs.biologists.org/cgi/content/full/120/11/1915/DC1

Key words: Dorsal root ganglia, Extracellular matrix, Cellular prion protein, Vitronectin, Axon growth, Integrins

Introduction

Cellular prion protein (PrP^C) is a cell-surface, glycosyl-phosphatidylinositol-anchored protein associated with several physiological functions. PrP^C is conserved among species and is expressed in most tissues, especially in the central nervous system and lymphoid tissues (Oesch et al., 1985). It has the ability to bind copper (Brown et al., 1997), to protect against oxidative stress (Brown and Besinger, 1998) and has been shown to influence cell signaling mechanisms, neuronal survival and differentiation (Chen, S. et al., 2003; Chiarini et al., 2002; Lopes et al., 2005; Mouillet-Richard et al., 2000). PrP^C has also been shown to bind the laminin receptor (Gauczynski et al., 2001; Hundt et al., 2001), to promote neuritogenesis through its interaction with NCAM (Santuccione et al., 2005; Schmitt-Ulms et al., 2001) and to induce neurite maintenance and neuronal differentiation through binding to the extracellular matrix (ECM) protein laminin (Ln) (Graner et al., 2000a; Graner et al., 2000b).

ECM proteins are known to regulate neuronal differentiation and axonal regeneration (Turney and Bridgman, 2005; Easley et al., 2006; Tom et al., 2004). Vitronectin (Vn) is expressed during development on embryonic day 10 (E10) in mice, mainly in the central nervous system (Seiffert et al., 1995), and has been shown to support proliferation and differentiation of cultured neurons (Martinez-Morales et al., 1995). In dorsal root ganglia (DRG) neurons, Vn-mediated axonal growth can be inhibited by anti-Vn antibody (Isahara and Yamamoto, 1995). Vn can also induce motor neuron differentiation, and anti-Vn antibodies reduce the number of motor neurons generated in chicken embryos (Martinez-Morales et al., 1997; Pons and Marti, 2000).

The classical ECM receptors, integrins, can bind several molecules and have been associated with ECM biological functions. The integrin recognition sequence Arg-Gly-Asp (RGD) is present in numerous ECM proteins including collagen, Vn and Fibronectin (Fn). RGD peptide is biologically active and able to substitute for ECM proteins in a variety of situations (Hynes, 2002; Pierschbacher and Ruoslahti, 1984).

Given that PrP^C binds Ln, we hypothesized that PrP^C might act as a broad ECM ligand and tested whether PrP^C binds the ECM proteins Vn, Fn and type IV collagen. We also sought to characterize the cellular events associated with any such binding. We assessed the role of PrP^C-ECM interaction in DRG

axon outgrowth using primary cultures obtained from two different PrP^C-null mouse strains (ZrchI and Npu) and their respective wild-type controls. The role of integrins in wild-type and PrP^C-null DRG axonal growth was also addressed and integrin activity was evaluated using specific antibodies and in functional assays using RGD peptide.

Results

PrP^C-vitronectin interaction

The first evidence of the PrP^C-Vn interaction was obtained with an overlay experiment (Fig. 1a), in which we applied equal mass aliquots of Vn, Ln, Fn, type IV collagen or bovine serum albumin (BSA) onto a nitrocellulose membrane, which was then incubated with ^{125}I-His_6-PrP^C. The overlay showed that PrP^C binds Ln, as previously demonstrated (Graner et al., 2000a), and also interacts with Vn (note that 10 μg of Ln represents 10 times fewer moles than the other proteins, owing to its higher molecular mass of ~900 kDa). Conversely, PrP^C did not associate with Fn or type IV collagen. Binding assays demonstrated that His_6-PrP^C binding to Vn is dose dependent and saturable (Fig. 1b), with a K_d of 12 nM. His_6-PrP^C refolded in the presence of copper (Zanata et al., 2002b) presented a similar binding to Vn (data not shown). It is important to note that the Vn used here was highly pure (see supplementary material Fig. S1a), and recombinant PrP^C analyzed by circular dichroism spectra showed an α-helix structure (Cordeiro et al., 2004a; Cordeiro et al., 2004b).

PrP^C interaction with ^{125}I-Vn could be blocked dose-dependently by competition with increasing concentrations of unlabeled Vn, as well as by other PrP^C ligands, such as stress-inducible protein 1 (STI1) (Zanata et al., 2002b) and Ln (Graner et al., 2000a; Graner et al., 2000b), but not by BSA (Fig. 1c). Thus, only specific PrP^C ligands can disrupt its binding interactions. The peptide representing the specific PrP^C binding site in the STI1 molecule (STI1 peptide) (Chiarini et al., 2002; Zanata et al., 2002b), but not that from Ln (Ln γ-1 peptide) (Graner et al., 2000a), competed for the PrP^C-Vn interaction (Fig. 1d). These data suggest that STI1 and Vn share a binding site in the PrP^C molecule, whereas Ln must interact with another PrP^C domain. Other Vn ligands such as type I collagen, type IV collagen and heparin were also tested for their ability to compete with the PrP^C-Vn interaction (supplementary material Fig. S2b). Although they do not bind Vn in the same domain as PrP^C (supplementary material Fig. S2a), they are able to disturb the PrP^C-Vn interaction, probably by steric hindrance.

Characterization of the PrP^C and Vn interacting domains

Of the twenty peptides from mouse PrP^C covering the whole protein sequence used to compete for PrP^C-Vn binding, two of them, corresponding to PrP^C residues 103-122 and 113-132,

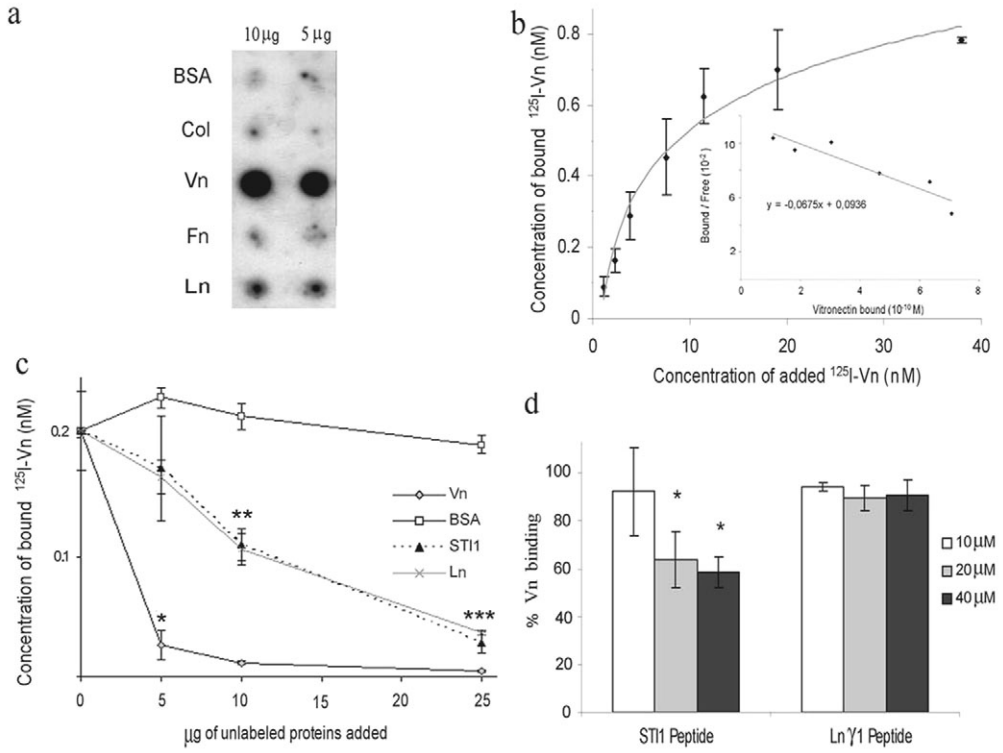

Fig. 1. Vn binds PrP^C in vitro and other PrP^C ligands can compete for this interaction. (a) Autoradiogram of overlay assay. Indicated amounts of Ln, Fn, Vn, type IV collagen (Col) and BSA were adsorbed onto a membrane and allowed to bind to ^{125}I-His_6-PrP^C. (b) PrP^C-coated wells were incubated with ^{125}I-Vn at the indicated concentrations. Wells were washed and radioactivity was measured. Scatchard plot is shown as an inset. The data represent mean ± s.d. (c) Competition assay in which ^{125}I-Vn was incubated over PrP^C-coated wells in the presence of increasing concentrations of unlabeled Vn, STI1, Ln or BSA. Bound ^{125}I-Vn differed from addition of 5 μg unlabeled Vn (*P<0.001), addition of 10 μg unlabeled Vn or Ln (**P<0.001), or addition of 25 μg unlabeled Vn, Ln or STI1 (***P<0.001) according to Tukey's Test. (d) Competition assay in which ^{125}I-Vn was incubated over PrP^C-coated wells in the presence of increasing concentrations of unlabeled STI1 peptide or Ln γ-1 peptide. The percentage of Vn binding was reduced in the presence of 20 or 40 μM STI1 peptide (*P<0.02, Student's t-test).

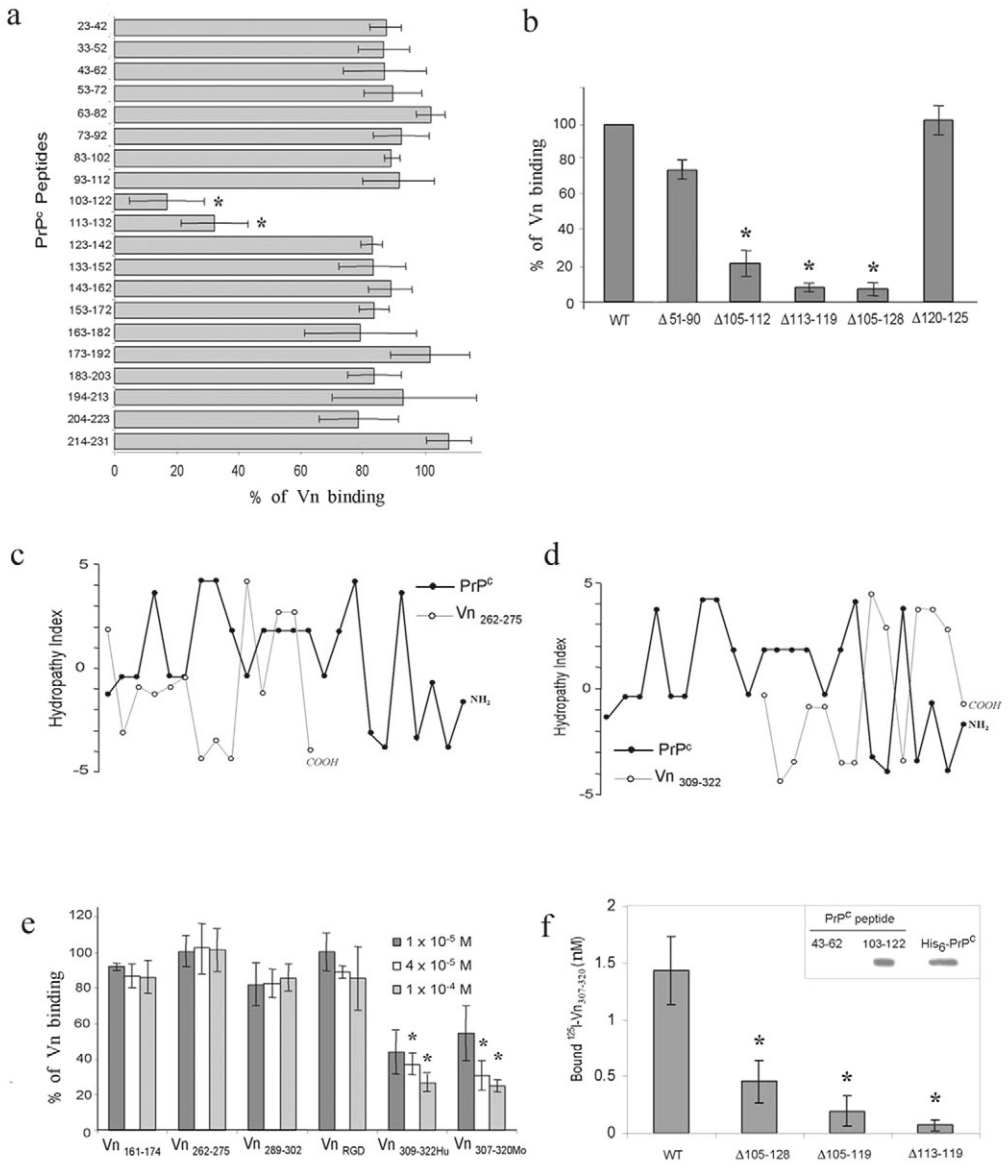

Fig. 2. Mapping the binding sites within Vn and PrP^C. (a) ^{125}I-Vn was incubated over PrP^C coated wells in the presence of PrP^C peptides. Binding to PrP^C was set as 100% and binding in the presence of peptides was expressed as a percentage thereof. PrP^C peptides 103-122 and 113-132 interfered with binding to Vn (*P<0.01, Student's t-test). (b) ^{125}I-Vn binding to deletion mutant proteins Δ105-112, Δ113-119, or Δ105-128 His$_6$-PrP^C was markedly reduced relative to binding to wild-type PrP^C, which was set as 100% (*P<0.01, Student's t-test). Δ51-90 and Δ120-125 His$_6$-PrP^C proteins exhibited ^{125}I-Vn binding that did not differ significantly from the wild-type protein. (c,d) The hydropathy plots compare the mouse PrP^C amino acid sequence from a.a. 104 to 127 and human Vn peptides with complementary hydropathy pattern: (c) Vn$_{262-275}$ and (d) Vn$_{309-322}$. (e) ^{125}I-Vn was incubated in PrP^C-coated wells in the presence or absence of the indicated concentrations of Vn peptides and radioactivity levels were determined. ^{125}I-Vn binding was disrupted in the presence of Vn$_{309-322Hu}$ and Vn$_{307-320Mo}$ (*P<0.01 vs binding to PrP^C alone, Student's t-test) at the two higher concentrations tested. (f) Binding of peptide Vn$_{307-320Mo}$ to immobilized PrP^C. Wells were coated with wild-type, Δ105-119, Δ113-119 or Δ105-128 His$_6$-PrP^C proteins and incubated with 1 μM ^{125}I-Vn$_{307-320Mo}$. ^{125}I-Vn$_{307-320Mo}$ binding to immobilized PrP^C was reduced in Δ105-128, Δ105-119 or Δ113-119 His$_6$-PrP^C proteins relative to wild-type PrP^C controls (*P<0.001, Tukey's test). Inset shows an overlay assay, where His$_6$-PrP^C or PrP^c peptides 43-62 and 103-122 spotted into a membrane were incubated with biotin labeled Vn$_{307-320Mo}$ followed by streptavidin-HRP.

effectively blocked (by ~80%) PrP^C-Vn binding (Fig. 2a). This implies that the amino acid sequence shared by both peptides may represent the putative binding site for Vn in the PrP^C molecule. The binding and competition assays were always performed with a freshly prepared peptide solution to avoid possible neurotoxic aggregates (Chiarini et al., 2002; Ettaiche et al., 2000). The lack of PrP^C-Vn interaction blockade by peptide 93-112, which can also form aggregates owing to the partial presence of the hydrophobic domain, provides further evidence that the interaction blockade was not the result of peptide aggregation.

Binding assays performed using four PrP^C molecules presenting small deletions on the putative Vn binding site, revealed that the PrP^C deletion mutants Δ105-112, Δ113-119,

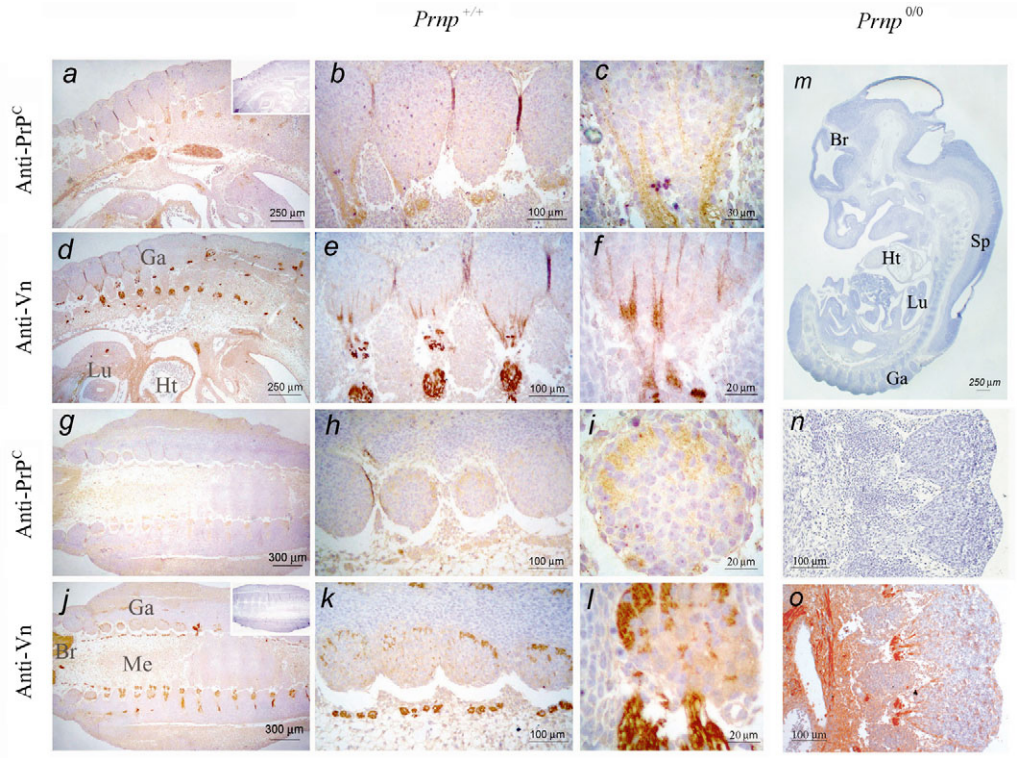

Fig. 3. PrP^{C} and Vn expression in mouse embryos. E12.5 *Prnp*$^{+/+}$ sagittal (a-f) or coronal (g-l) sections reacted with anti-PrP^{C} mouse serum (a,b,c,g,h,i), rabbit serum anti-Vn (d,e,f,j,k,l) or non-immune mouse or rabbit serum (insets in panels a and j, respectively). E12.5 ZrchI *Prnp*$^{0/0}$ mouse sagittal sections reacted with anti-PrP^{C} mouse serum (m and n) or anti-Vn serum (panel o). Br, brain; Ht, heart; Lu, lung; Sp, spinal cord; Ga, dorsal root ganglia.

and Δ105-128 did not bind Vn, whereas mutants Δ51-90 and Δ120-125 exhibited binding capacity similar to that of the wild-type molecule (Fig. 2b). These data corroborate that the region comprising a.a. 105-119 of PrP^{C} includes the binding site for Vn. As this domain is inserted into the N-terminal random coil of the PrP^{C} molecule (Riek et al., 1996), these deletions are not expected to disturb PrP^{C} secondary or tertiary structure. Since all the experiments herein were conducted with *E. coli* recombinant His$_{6}$-PrP^{C}, we were unable to evaluate possible roles of PrP^{C} sugar residues in this interaction. However, as the binding site was mapped to a region lying outside the glycosylation site, it is unlikely that sugar residues on PrP^{C} are essential for its interaction with Vn.

In accordance with the complementary hydropathy theory (Brentani, 1988), which states that peptides presenting opposite hydropathy profiles can bind one another, we used HYDROLOG software to search for Vn sequences whose hydropathy profile was more than 70% complementary to the PrP^{C} 105-119 peptide. Two human Vn domains presented this profile, one from residues 262-275 (Fig. 2c) and another from residues 309-322 (Fig. 2d). We performed competition assays using both peptides and, as controls, two peptides randomly chosen from within the Vn sequence (Vn$_{161\text{-}174}$ and Vn$_{289\text{-}302}$) along with a peptide containing the RGD sequence (Vn$_{RGD}$) (Ruoslahti and Pierschbacher, 1987). The peptides Vn$_{309\text{-}322Hu}$ (human Vn) and Vn$_{307\text{-}320Mo}$ (the equivalent peptide for mouse Vn) competed for PrP^{C}-Vn interaction, thus identifying this domain as the putative binding site for PrP^{C} (Fig. 2e).

We also performed binding assays using the ^{125}I-Vn$_{307\text{-}320Mo}$ peptide and wild-type His$_{6}$-PrP^{C} or PrP^{C} deletion mutants Δ105-128, Δ105-119 and Δ113-119. Vn$_{307\text{-}320Mo}$ peptide readily bound wild-type PrP^{C}, whereas very low binding was observed with all of the deletion mutants (Fig. 2f). Using overlay assays we demonstrated that peptide Vn$_{307\text{-}320Mo}$ directly binds the PrP^{C} peptide corresponding to a.a. 103-122, but not to a.a. 43-62 (Fig. 2f inset). These data are consistent with the presence of an interaction between the PrP^{C} domain 105-119 and the Vn domain 307-320 (mouse Vn).

Supplementary material Fig. S2a shows a schematic representation of PrP^{C} and Vn, along with their main ligands and respective binding sites (Lee et al., 2003; Schvartz et al., 1999). Although there is moderate sequence diversity in Vn across species, the PrP^{C} binding domain is generally well-conserved (see supplementary material Fig. S3a). Chicken Vn, which has the greatest divergence relative to human Vn, bound PrP^{C} in the same manner as human Vn (see supplementary material Fig. S3b). Furthermore, peptides from the PrP^{C}-binding domain derived from chicken and mouse Vn sequences were also able to inhibit the PrP^{C} interaction with human Vn (see supplementary material Fig. S3c), suggesting that the PrP^{C}-Vn interaction is evolutionarily conserved.

PrP^{C} and Vn expression in DRG from embryonic mice

Since Vn and PrP^{C} have been detected early in development (Miele et al., 2003; Seiffert et al., 1995), we performed immunohistochemistry assays in E12.5 mice embryos.

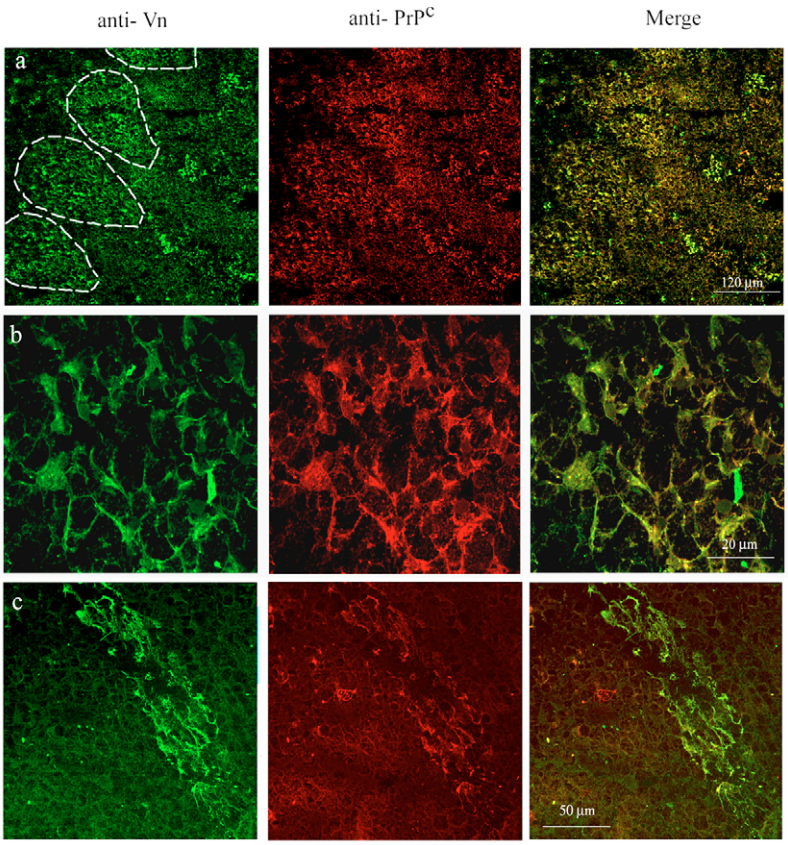

Fig. 4. PrP^C and Vn colocalize in embryonic DRG. Confocal microscopy images of E12.5 mouse sagittal sections reacted with anti-Vn rabbit serum (green) and anti-PrP^C mouse serum (red). Superimposed red and green images are shown in the merge column. The top row of images (a) shows three ganglia in a low magnification (as indicated by the dotted lines); the middle row of images (b) shows a single ganglion in a higher magnification; and the bottom row (c) shows a growing nerve region.

Immunohistochemistry assays were performed in ZrchI *Prnp*$^{+/+}$ (Fig. 3a-l) and ZrchI *Prnp*$^{0/0}$ (Fig. 3m-o) E12.5 mice embryos using anti-PrP^C (Fig. 3a-c,g-i,m,n) and anti-Vn antibodies (Fig. 3d-f,j-l,o) in sagittal sections (Fig. 3a-f,m-o) and coronal sections (Fig. 3g-l). The antibodies used have been extensively tested in western blotting assays, and show specificity for PrP^C (Zanata et al., 2002b) or Vn (data not shown). Control experiments with mouse or rabbit serum produced no immunolabeling (Fig. 3 insets in a and j, respectively).

In accordance with previous data (Miele et al., 2003), we observed strong PrP^C immunoreactivity in the developing brain, spinal cord (Fig. 3g) and DRG (Fig. 3a,g). In DRG, although axons and forming axonal fibers were heavily labeled, nuclei were not labeled and neuronal bodies showed only weak labeling (Fig. 3b,c,h,i). PrP^C expression could be detected only at E10, in the nervous system and in the heart (data not shown). As development proceeds, those organs still show high levels of immunoreactivity. Immunolabeling in other organs such as kidney, lungs and muscles could only be seen later (E18) in development (data not shown). Sections from Prnp$^{0/0}$ mouse embryos did not bind the anti-PrP^C antibody, proving the specificity of the immunohistochemistry reaction (Fig. 3m,n).

Vn immunolabeling was more intense than PrP^C, but presented a similar pattern in brain, spinal cord (Fig. 3j) and DRG (Fig. 3d,j). In the DRGs, expression was predominantly observed in growing axons and nerves (Fig. 3e,f,k,l). Vn starts to be expressed at E8, through the whole embryo. Similarly to PrP^C, at E10 it presents high expression in the heart and nervous system. As development proceeds, those organs still present high levels of immunoreactivity, whereas immunolabeling can also be seen in other organs such as kidney, lung and muscles. Expression in the liver is very abundant (data not shown), since this organ secretes Vn to the blood. In PrP^C-null mice, the pattern of Vn expression in DRG (Fig. 3o) as well as in other tissues (data not shown) was the same as that in wild-type mice. Immunofluorescent confocal images confirmed that PrP^C and Vn strongly co-localized in DRG cells (Fig. 4a,b) and in growing nerves (Fig. 4c).

Vn binds PrP^C in vivo

To verify whether Vn could bind PrP^C in the cell surface, we labeled Vn with Alexa Fluor 568 (see supplementary material Fig. S1b). Dissociated DRG cells were treated with Alexa 568-Vn and subjected to PrP^C fluorescent immunocytochemistry (Fig. 5a upper panel). We observed the co-localization of Vn and PrP^C at the cell surface. Images of live SN-56 cells (Blusztajn et al., 1992; Hammond et al., 1990) transfected with green fluorescent protein (GFP)-PrP^C and treated with Alexa 568-Vn showed co-localization of PrP^C with Vn at the cell surface (Fig. 5a bottom panel).

SDS-PAGE of GFP-PrP^C-transfected HEK293 cell proteins eluted from a pull-down assay using purified Vn covalently coupled to CNBr-Sepharose followed by immunoblotting, revealed a band of ~60 kDa [the expected molecular mass for GFP-PrP^C (Lee et al., 2001)] when anti-GFP (lane 3) or anti-PrP^C antibodies (lane 6) were applied (Fig. 5b). When the same procedure was conducted with extracts from non-transfected cells (lanes 1 and 4) or with those from cells transfected with GFP alone (lanes 2 and 5) no binding to the Vn-Sepharose was observed. These results indicate that PrP^C, but not GFP alone, binds to Vn. The levels of endogenous PrP^C in HEK293 cells were too low for their association with Vn to be detected.

PrP^C-Vn interaction mediates DRG axonal growth

We investigated the possible role in axonal growth of the interaction between PrP^C and Vn, which are expressed in elongating DRG and medulla axons and are implicated in neuronal differentiation (Graner et al., 2000a; Graner et al., 2000b; Martinez-Morales et al., 1995; Martinez-Morales et al., 1997; Pons et al., 2001; Sales et al., 2002). Cultured DRG explants from E12.5 mice expressing PrP^C (ZrchI *Prnp*$^{+/+}$) (Fig. 6a inset) in the presence of Vn for 36 hours produced axonal growth (Fig. 6a). Vn peptide, Vn$_{307\text{-}320\text{Mo}}$, corresponding to the PrP^C-binding site of the mouse Vn molecule elicited the same effect as that triggered by the whole molecule (Fig. 6b), whereas Vn peptide Vn$_{161\text{-}174}$ (Fig. 6d) had

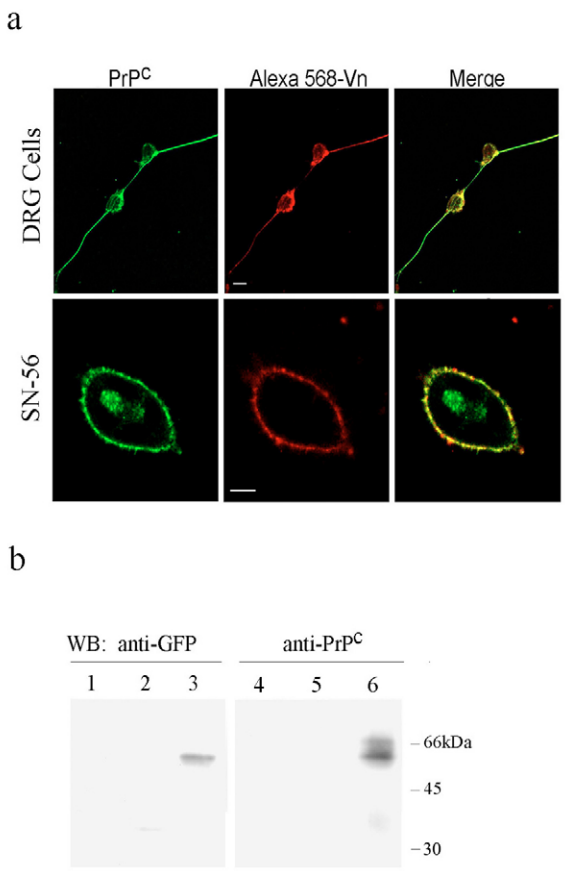

Fig. 5. Vn binds PrP^C in vivo. (a) Confocal images of dissociated DRG cells treated with Alexa 568-Vn (red) and immunolabeled with anti-PrP^C (green) are shown in the top row. Confocal images of SN56 cells transfected with GFP-PrP^C (green) and treated with Alexa 568-Vn (red) are shown in the bottom row. (b) Pull down assay from cell extracts incubated with Vn-Sepharose. Western blots of Vn-Sepharose-bound proteins from untransfected (lanes 1 and 4), GFP transfected (lanes 2 and 5) or GFP-PrP^C transfected (lanes 3 and 6) HEK293 cells. Blots immunolabeled with anti-GFP (lanes 1 to 3) or anti-PrP^C (lanes 4 to 6) antibodies revealed that PrP^C, but not GFP alone, binds to Vn.

no effect, even at concentrations 20-fold higher than peptide $Vn_{307\text{-}320Mo}$.

ZrchI *Prnp*$^{0/0}$ mouse (Bueler et al., 1992) DRG neurons cultured on Vn presented neurite growth rates (Fig. 6g) similar to that of wild-type DRG neurons (Fig. 6a). Nevertheless, in opposition to what has been demonstrated for wild-type DRG, Vn peptide $Vn_{307\text{-}320Mo}$ (Fig. 6f), which mimics the PrP^C binding site, was unable to induce axon growth in *Prnp*$^{0/0}$ DRG neurons. Vn peptide $Vn_{161\text{-}174}$ also had no effect on *Prnp*$^{0/0}$ DRG neurons (Fig. 6e). Treatment of Vn-stimulated DRG with rabbit anti-PrP^C antibody blocked axonal growth in cultures from wild-type animals but not in those from PrP^C-null mice (Fig. 6h). Data representing the average axon length from each treatment are summarized in Fig. 6h.

To rule out the possibility of spurious results because of genetic background, we conducted our key experiments in both ZrchI (Bueler et al., 1992) and Npu (Manson et al., 1994) PrP^C-null mice. DRG from Npu *Prnp*$^{-/-}$ mice and their wild-type controls plated for 24 hours in the presence of Vn presented similar axonal growth (Fig. 6i). On the other hand, when plated with $Vn_{307\text{-}320Mo}$, only Npu *Prnp*$^{+/+}$ DRG grew axons and no effect was observed with either knockout or wild-type cells when an irrelevant Vn peptide ($Vn_{161\text{-}174}$) was used (Fig. 6i). Inclusion of an antibody against PrP^C peptide 106-126 (Chiarini et al., 2002) (Fig. 6i) completely blocked axonal growth in cultures from wild-type animals, whereas non-immune purified IgG had no effect (Fig. 6i). We also carried out dissociated DRG cell cultures in the presence of Vn to measure the percentage of cells with neurites, and observed that the positive responsiveness to Vn was the same for ZrchI *Prnp*$^{+/+}$ and *Prnp*$^{0/0}$ neurons (Fig. 6j).

The experiments using anti-PrP^C antibodies or the $Vn_{307\text{-}320}$ peptide demonstrated that axonal growth can be supported specifically by the PrP^C-Vn interaction. Nonetheless, the whole Vn molecule induces the same axonal outgrowth pattern in wild-type and PrP^C-null neurons. The similarity between the effect of Vn in wild-type and PrP^C-null DRG suggests that there may be another Vn receptor that can compensate for the PrP^C deficiency.

In fact, flow cytometry analysis shows that Alexa 568-Vn is able to bind equally to the surface of PrP^C-null and wild-type cells (see supplementary material Fig. S4a). Indicating that in the absence of PrP^C other Vn receptors are present at the cell surface.

Integrin participation in Vn-induced axonal growth is enhanced in the absence of PrP^C

The obvious targets for the putative compensatory mechanism suggested by the above data are integrins, the classical Vn receptors that interact with this molecule through the Vn-RGD peptide. We performed functional assays using the RGD peptide, which has an advantage over antibodies in that it can simultaneously trigger or halt several integrin dimers (Isahara and Yamamoto, 1995; Monier-Gavelle and Duband, 1997). The RGD peptide can be used for inhibition or stimulation of the neuritogenesis depending on its presentation. In solution, the RGD peptide does not support cell adhesion and thus can be used to perform competition assays (Pierschbacher and Ruoslahti, 1987). Conversely, when coupled to BSA, the peptide adheres to the coverslip and supports cell adhesion (Danilov and Juliano, 1989).

As shown in Fig. 7a, the Vn_{RGD} peptide at a concentration of 8 μM inhibited Vn-stimulated axonal growth of ZrchI *Prnp*$^{0/0}$ DRG neurons. The impairment reached poly-L-lysine growth levels (about 50% of that observed in Vn). Vn-stimulated axonal growth in *Prnp*$^{+/+}$ neurons was impaired only when the Vn_{RGD} peptide reached a concentration of 12 μM. Additionally, we measured the axonal growth induced by Vn_{RGD}-BSA and observed that ZrchI *Prnp*$^{0/0}$ DRG are more responsive than *Prnp*$^{+/+}$ DRG (Fig. 7b). *Prnp*$^{0/0}$ DRG neurons extended axons in 0.5 nmol of adsorbed peptide, whereas *Prnp*$^{+/+}$ DRG neurons did not exhibit any axonal growth, even in the presence of a 20-fold higher concentration of the peptide. Thus, *Prnp*$^{0/0}$ DRG cells were more responsive than the *Prnp*$^{+/+}$ cells to the RGD peptide. To further confirm these results, we plated Npu *Prnp*$^{-/-}$ and *Prnp*$^{+/+}$ DRG over adsorbed RGD-BSA. We observed that Npu *Prnp*$^{-/-}$ DRG neurons were also more responsive to RGD-BSA than Npu *Prnp*$^{+/+}$ DRG neurons (Fig. 7c). Thus, we can be confident that the above

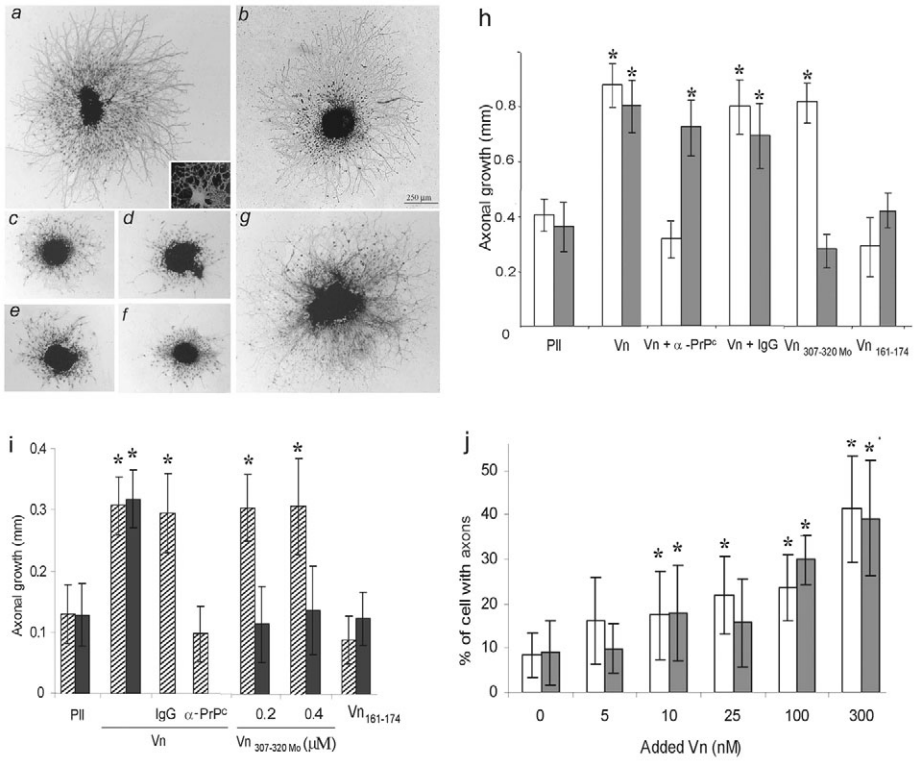

Fig. 6. PrP^{C}-Vn interaction supports axonal growth in DRG from E12.5 mouse embryos. ZrchI *Prnp*$^{+/+}$ (a-d) and ZrchI *Prnp*$^{0/0}$ (e-g) DRG were cultured on poly-L-lysine-coated coverslips (c), 200 nM Vn (a and g), 0.4 μM peptide Vn$_{307-320Mo}$ (b and f), 0.4 μM peptide Vn$_{161-174}$ (d and e) and Vn plus anti-recombinant PrP^{C} antibody 13 μg/ml or Vn plus irrelevant IgG 13 μg/ml (h). Inset dark-field image in a shows a DRG subjected to anti-PrP^{C} immunohistochemistry. (h) Comparison of mean axonal growth per DRG from ZrchI *Prnp*$^{+/+}$ (white bars) and *Prnp*$^{0/0}$ mice (grey bars) for the conditions described above. *P<0.001 vs Pll control, Tukey's Test. (i) Comparison of mean axonal growth per DRG of at least 12 ganglia from Npu *Prnp*$^{+/+}$ (striped bars) and *Prnp*$^{-/-}$ mice (black bars) for each of the following conditions: Pll, 200 nM Vn, 0.2 or 0.4 μM Vn$_{307-320Mo}$, 0.4 μM Vn$_{161-174}$, Vn plus irrelevant IgG or 0.6 μg/ml anti-PrP^{C} peptide 106-126. *P<0.001 vs Pll control, Tukey's Test. (j) The percentage of cells from ZrchI *Prnp*$^{+/+}$ (white bars) and ZrchI *Prnp*$^{0/0}$ (grey bars) dissociated DRG neurons that grow axons increased with increasing concentrations of Vn; *P<0.001 vs Pll control, Tukey's test.

findings were not due to any spurious effect present only in ZrchI animals. These data demonstrate that PrP^{C}-ablated DRG neurons have a greater dependence upon integrins for axonal outgrowth than do their respective wild-type cells.

To test whether the activation state of Vn-binding integrins was altered, we measured the level of active αvβ3 integrin in adhering ZrchI *Prnp*$^{0/0}$ DRG cells through an immunofluorescence assay with the ligand-mimetic antibody WOW-1 (Pampori et al., 1999). ZrchI *Prnp*$^{0/0}$ DRG neurons showed a 30% higher level of αvβ3 activation than *Prnp*$^{+/+}$ DRG neurons (Fig. 7d). We tested whether Npu *Prnp*$^{-/-}$ neurons presented a similar increase in integrin activity using the commercially available anti-ligand-induced binding sites (LIBS) antibody AP5 (Faccio et al., 2002). Dissociated Npu *Prnp*$^{-/-}$ DRG neurons showed greater β_3 activity than *Prnp*$^{+/+}$ cells (Fig. 7e). Accordingly, ZrchI *Prnp*$^{0/0}$ primary mouse embryonic fibroblasts (PMEFs) also showed 30% more integrin αv subunit expression than wild-type PMEFs (see supplementary material Fig. S4b). Together, these findings indicate that a higher integrin activity, particularly that from αvβ3 integrin, is present in DRG after ablation of PrP^{C}.

Discussion

In the past few years, many PrP^{C}-binding proteins have been identified. Among these the ECM protein Ln (Graner et al., 2000a; Graner et al., 2000b) and glycosaminoglycans (Gonzalez-Iglesias et al., 2002) have been of particular interest. These previous findings suggested that PrP^{C} might act as a wide-range cell surface receptor, capable of binding numerous ECM proteins. However, the present findings indicate that PrP^{C} interaction with ECM proteins is not a broad-spectrum phenomenon, but rather that PrP^{C} specifically binds Vn with high affinity, and does not readily bind Fn or type IV collagen.

We proposed that PrP^{C} participates in a multi-protein complex, the biological effects of which would be dependent both on the affinity and accessibility of each member of the complex (Martins and Brentani, 2002). The present competition experiments demonstrated that PrP^{C}-Vn interaction in vitro has a higher affinity, K_d 10^{-8} M, than that between PrP^{C} and STI1, K_d 10^{-7} M (Zanata et al., 2002b). Furthermore, the Vn binding domain in PrP^{C} in residues 105-119 (Fig. 2a) overlaps with the STI1-binding domain (Zanata et al., 2002b), indicating that PrP^{C} interactions with Vn or STI1 are mutually exclusive, with the first being more favorable and conditioning the latter to local protein availability and levels. The ability of PrP^{C}-STI1 to provide neuroprotection against programmed cell death (Chiarini et al., 2002) and neuritogenesis in hippocampal neurons (Lopes et al., 2005), whereas PrP^{C}-Vn engagement promotes axonal growth in DRG, provide prime examples of how cell fate can be directly influenced by the molecular environment of the cell.

PrP^{C} domain 105-128, which contains the Vn and STI1 binding sites, is highly conserved across species (Gabriel et al., 1992), and is indeed identical in mice and humans. This domain also includes proteolytic sites (Jimenez-Huete et al., 1998) and hereditary prion disease-associated mutations (Mastrianni and Roos, 2000), indicating that this region and probably its interaction with Vn and STI1 have an important role in vivo. For example, it was recently reported that this domain is linked to the toxicity of PrP^{C} accumulated in the cytosol through binding to Bcl-2 (Rambold et al., 2006).

Although PrP^{C}-Ln and PrP^{C}-Vn interactions present a similar K_d, (Graner et al., 2000a), we demonstrated that lower concentrations of Vn than Ln are needed to disrupt the PrP^{C}-Vn interaction. Since the Ln-binding site is located in residues 173-183 of PrP^{C} (Coitinho et al., 2006), the Ln γ1 peptide (the

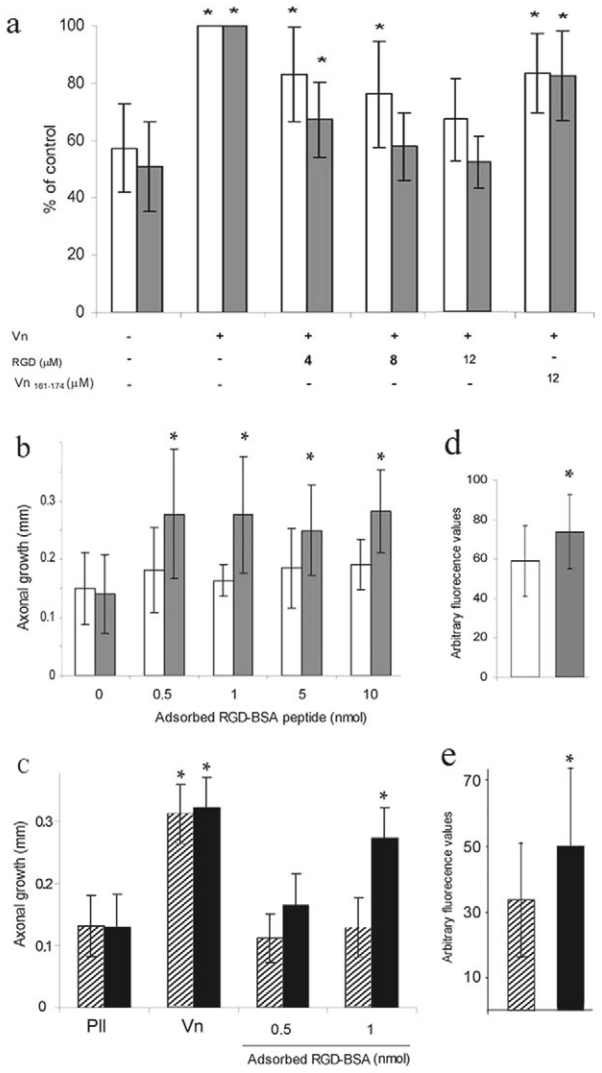

Fig. 7. Integrins compensate for the absence of PrP^C to support Vn-induced axonal growth. (a) Vn_{RGD} peptide abrogates Vn-induced axonal growth in cultured ZrchI *Prnp*$^{0/0}$ (grey bars) DRGs at lower concentrations (8 μM) than that (12 μM) necessary for the same effect in *Prnp*$^{+/+}$ (white bars) DRGs. Treatment with the irrelevant peptide $Vn_{161\text{-}174}$ (12 μM) had no effect. **P*<0.001 vs poly-L-lysine (Pll) Tukey's test. (b) Exposure to adsorbed Vn_{RGD}-BSA peptide (0.5, 5, 1 or 10 nmol) increased axonal growth in DRG cells from ZrchI *Prnp*$^{0/0}$ mice, but not from ZrchI *Prnp*$^{+/+}$ mice. **P*<0.001 vs Pll control, Tukey's test. (c) Adsorbed Vn_{RGD}-BSA peptide (1 nmol) induced axonal growth in cultured DRG cells from Npu *Prnp*$^{-/-}$ mice (black bars) whereas no axonal growth was present at this concentration of absorbed Vn_{RGD}-BSA peptide in Npu *Prnp*$^{+/+}$ cells (striped bars). **P*<0.001 vs Pll control, Tukey's test. (d) ZrchI *Prnp*$^{0/0}$ dissociated DRG cells exhibited greater WOW-1 immunoreactivity than those from ZrchI *Prnp*$^{+/+}$ mice, indicating that the knockouts had greater levels of activated $\alpha_v\beta_3$ integrin. **P*<0.001 vs *Prnp*$^{+/+}$, Mann-Whitney's test. (e) Npu *Prnp*$^{-/-}$ dissociated DRG cells exhibited greater AP5 immunoreactivity than Npu *Prnp*$^{+/+}$, indicating that the knockouts had greater levels of activated β_3 integrin. **P*<0.001 vs Npu *Prnp*$^{+/+}$, Mann-Whitney's test.

PrP^C-binding site in Ln) does not disrupt the PrP^C-Vn complex (Fig. 1d). Thus, it is plausible that in vitro, the Ln molecule may interact with PrP^C, and thereby disturb PrP^C-Vn binding by steric hindrance. On the other hand, steric hindrance may not occur in vivo because of the ECM organization or to the presence of biologically active proteolytic fragments from the Ln molecule (Chen, Z. et al., 2003). Indeed, the signals triggered by each of these PrP^C ligands may have cooperative roles in some biological events. In developing cerebellar granule cells, the presence of Ln induces proliferation, whereas during migration these cells find Vn and differentiate (Pons et al., 2001). Therefore, we believe that PrP^C has pleiotropic functions that depend upon its cellular expression as well as the greater contextual cellular milieu.

We exploited the complementary hydropathy principle (Brentani, 1988) to map a.a. 309-322 as the PrP^C-binding site in the human Vn molecule. To date, more than 40 protein-protein interactions have been shown to comply with this principle (Heal et al., 2002), including a Vn and fibrinogen interaction with the integrin αIIbβ3 (Gartner et al., 1991) and the PrP^C-STI1 interaction (Martins et al., 1997; Zanata et al., 2002b). This region (residues 309-322) of human Vn has never been shown to bind other proteins (Schvartz et al., 1999). According to the three-dimensional theoretical model of Vn (Xu et al., 2001), this mainly hydrophobic peptide is partially buried. Conversely, it should be considered that the threading algorithm (Xu and Xu, 2000) used to create this model makes use of an energy function that penalizes the exposure of hydrophobic side chains, whereas it is known that protein-binding sites are generally hydrophobic (Tsai et al., 1997). Since it was not considered that this particular region could be a binding site, protein interactions were not taken into consideration in these calculations (Xu et al., 2001).

Vn is composed of multiple domains known to bind distinct proteins (see supplementary material Fig. S2a). The first 44 amino acids comprise a somatomedin-like domain, which harbors plasminogen activator inhibitor-1. This somatomedin-like domain is followed by the RGD peptide domain (residues 53-64), which is responsible for integrin binding, and an acidic stretch involved in binding of the thrombin-antithrombin III complex. Two binding sites for collagen have been described, one adjacent to the RGD site and other adjacent to the heparin-binding site. The Vn is composed of six hemopexin domains (a.a. 132-459). The C-terminal part of the molecule harbors a plasminogen (a.a. 332-348), a heparin (a.a. 348-346) and a glycosaminoglycan-binding site (a.a. 348-361). A subregion of this domain (a.a. 348-370) has also been implicated in plasminogen activator inhibitor-1 binding (Preissner, 1991; Schvartz et al., 1999). Thus although the PrP^C-binding site in Vn has not been assigned to bind other proteins, it is close to the heparin-binding domain. Heparin is efficient in competing PrP^C-Vn interaction (see supplementary material Fig. S2a), since it is able to bind both PrP^C (Pan et al., 2002) and Vn (Francois et al., 1999). Thus, as proposed above, PrP^C pleiotropic functions are dependent on the greater contextual cellular milieu.

There are many Vn receptors found on the cell surface, such as integrins αIIbβ3, αvβ1, αvβ3 and αvβ5 (Felding-Habermann and Cheresh, 1993). Each one of these binds to the Vn RGD domain with a different affinity and induces specific signals within cells (Takagi et al., 2002). Our demonstration herein that RGD peptide did not compete for the PrP^C-Vn

interaction indicates that Vn binds PrP^C at a domain that is distinct from the integrin-binding domain.

Since both PrP^C and integrins participate in axonal growth, it was surprising to observe a complete inhibition of Vn-stimulated axonal growth in the presence of anti-PrP^C antibody. This finding suggests that PrP^C occupies a part of the macromolecular complex such that its inactivation by antibodies may disturb the whole complex. The ability of Vn peptide containing the PrP^C-binding site to reproduce the biological effects of the whole Vn in wild-type but not in PrP^C-null DRG, further suggests that PrP^C is an exclusive ligand for the Vn 307-320 domain. The fact that Vn$_{307\text{-}320Mo}$ (Fig. 7) and Vn$_{RGD}$ (Danilov and Juliano, 1989) are both able to substitute for the whole Vn molecule in the axonal growth phenomenon is consistent with the hypothesis that PrP^C and integrins act through the same signal transduction pathway. Notably, the data showing that Vn$_{RGD}$ is able to inhibit axonal growth in wild-type neurons highlights the importance of the integrins in this process.

In spite of the important functions for PrP^C described over the past few years (Chiarini et al., 2002; Lopes et al., 2005; Mouillet-Richard et al., 2000; Rambold et al., 2006; Steele et al., 2006), PrP^C-null mice have only minor defects (Bueler et al., 1992). One explanation for this near-normal phenotype is that PrP^C ablation may be compensated by proteins with redundant functions (Bueler et al., 1992). This seems to be the case here, because the whole Vn molecule induced DRG axonal growth in both wild-type and PrP^C-null neurons. On the other hand, PrP^C-null (both ZrchI and Npu) DRG axonal growth is more sensitive to RGD than the wild-type, indicating that the cellular signaling involved in this phenomenon is more dependent upon integrins in neurons from the knockout animals. Additionally, we observed 30% more activated αvβ3 in DRG from PrP^C-null mice than in their wild-type counterparts. This increase in activated integrins may represent a compensatory mechanism developed by the PrP^C-null animals, where the use of proteins already involved in this specific phenotype can prevent malformation of the nervous system.

Numerous examples of compensatory mechanisms have been reported (Kitami and Nadeau, 2002; Schwarz et al., 2002) and promiscuous cell signaling transduction pathways are targets for molecular redundancy (Xian et al., 2001). Indeed, PrP^C-null mice have been reported to have hyper-activation of extracellular signal-related kinase (ERK) (Chiarini et al., 2002; Lopes et al., 2005; Brown et al., 2002). PrP^C (Zanata et al., 2002b) and integrins (Roberts et al., 2003) are upstream MAPK effectors, which means that at least in this situation, an integrin could substitute for PrP^C signaling.

GPI-anchored proteins, such as PrP^C, can perform signaling roles, integrating the ECM with the cytoskeleton. For example the GPI-anchored raft-associated protein urokinase type plasminogen activator receptor (uPAR) performs complex signaling involved in cell adhesion, proliferation and migration in response to several ligands including Vn (Blasi and Carmeliet, 2002). To modulate internal cell signaling, GPI-anchored proteins must interact with transmembrane adaptors, such as integrins, G-protein-coupled receptors and caveolins (Blasi and Carmeliet, 2002). Despite the involvement of uPAR in cell signaling and diverse biological functions, uPAR-null mice have an apparently normal phenotype (Bugge et al., 1995). Thus, a GPI-anchored protein can be associated with critical regulatory cell tasks and the lack of a severe phenotype in knockout mice cannot demonstrate that the protein is not normally involved in important phenotypes.

In summary, the characterization of PrP^C as a ligand for Vn and its involvement in axonal growth allowed us to demonstrate the relevance of PrP^C in the development of the peripheral nervous system (PNS). Additionally, compensatory mechanisms occurring during embryogenesis are turned on when PrP^C is ablated. Thus, at least for this event, our findings indicate that redundancy for PrP^C interactions resides within the integrin pathway. The importance of PrP^C in the PNS has been increasingly recognized because PNS is a target for PrP^C conversion to PrP^{Sc}, and thus is critically involved in the prion neuroinvasion (Glatzel et al., 2004). Providing further support for PNS involvement in prion neuroinvasion, are the observations that PrP^C is retrogradely transported in peripheral nerves (Moya et al., 2004) and that prion accumulation occurs in DRG and in autonomic ganglia isolated from patients with Creutzfeldt-Jakob and Gerstmann-Sträussler-Scheinker (Haik et al., 2003; Ishida et al., 2005; Lee et al., 2005). The present findings together with these previous observations indicate that the physiological functions of PrP^C in peripheral nerves warrant further investigation.

Materials and Methods

Proteins

Vn and Fn were purified from human plasma (Engvall and Ruoslahti, 1977; Yatohgo et al., 1988) and mouse His$_6$-PrP^C was cloned (Zahn et al., 1997) and expressed (Zanata et al., 2002b). Type IV collagen and albumin are from Sigma. Four PrP^C deletion mutants were constructed using wild-type cDNA by sequential PCR amplification (Ausubel et al., 1993); cloned into pRSET A vector (Invitrogen) and expressed and purified as the wild-type His$_6$-PrP^C. Mutant His$_6$-PrP^C molecules are soluble, sensitive to proteinase K and posses nearly the same α-helix and β-sheet content as the wild-type protein. The following internal primers were used for sequential PCR amplification: Δ51-900R-TACCCCCTCCTGGGTAACGGTTG-CCTCC; F-GAGGGATCCAAAAAGCGGCCAAAG; Δ105-112R-CCAGCTGC-CGCAGCCCCTGGTTGGCTGG; F-CCCAGCAAACCAGGGGCTGCGGCAGC-TGG; Δ113-119R-CCCCATTACTGCCACATGCTTGAGGTTG; F-AAGCATGT-GGCAGTAGTGGGGGGCCTT; Δ120-125R-CAGCATGTAGCCTGCCCCAGC-TGCCGC; F-GCAGCTGGGGCAGGCTACATGCGGGAGC; Δ105-128F-GGAA-CAAGCCCAGCAAACCACTGGGGAGCGCCATGACGG; R-GTCCATGGCGC-TCCCCAGTGGTTTGCTGGGCTTTGTTCC. The following external primers were used for all mutants: F-AGAGAATTCTCAGCTGGATCTTCTCCCGTC; R-GAG-GGATCCAAAAAGCGGCCAAAG.

Peptides

Twenty peptides covering the whole mouse PrP^C (23-231) (Zanata et al., 2002b) were used. STI1 peptide (230-ELGNDAYKKKDFDKAL-245) (Zanata et al., 2002b), laminin γ-1 peptide (1575-RNIAEIIKDI-1584) (Graner et al., 2000a) and six Vn peptides: Vn$_{RGD}$ KPQVTRGDVFTMPE; Vn$_{161\text{-}174}$ AEEELCSGKPFDAF; Vn$_{262\text{-}275}$ AHSYSGRERVYFFK; Vn$_{289\text{-}302}$ SQEECEGSSLSAVF; Vn$_{309\text{-}322Hu}$ QRDSWEDIFELLFW and Vn$_{307\text{-}320Mo}$ QRDSWENIFELLFW were synthesized by Neosystem (Strasbourg, France). The subscript numbers indicate amino acid position in the Vn molecule; the first five peptides follow the human (Hu) Vn sequence and the last one follows the mouse (Mo) Vn sequence.

Antibodies

Anti-PrP^C used for western blotting, immunohistochemistry and immunofluorescence reactions is a polyclonal antibody obtained by His$_6$-PrP^C immunization in PrP^C-null mice. Rabbit polyclonal antibodies obtained by His$_6$-PrP^C (Bethyl) or PrP^C peptide 106-126 (Neosystem) immunization were used in DRG axon growth assays (Chiarini et al., 2002; Zanata et al., 2002b).

The WOW-1 antibody, kindly provided by Prof. Sanford Shattil (University of California), recognizes the active form of αvβ3; the heavy chain hypervariable region of an antibody against activated αIIbβ3 was replaced with a single αv integrin-binding domain (from an adenovirus RGD-rich protein involved in its internalization mediated by αv) (Felding-Habermann et al., 2001; Pampori et al., 1999). The AP5 antibody (GTI Diagnostics) is an anti-LIBS antibody that recognizes the β3 N-terminus and is regulated by cation binding at a site distinct from the LIBS (Honda et al., 1995). At normal extracellular Ca^{2+} levels, AP5 binds

to β3 only when the integrin is in the 'activated' conformation (Faccio et al., 2002). Anti-GFP was from Becton Dickinson and anti-Vn was obtained by rabbit immunization with purified Vn.

Overlay assay

The indicated amounts of Ln, Fn, Vn, type IV collagen and BSA were adsorbed onto nitrocellulose membranes. Blocking was performed in 5% milk in TBST (TBS 0.05% pH 7.4 Tween-20) for 2 hours at room temperature and membranes were then washed. His_6-PrP^C (7 μg) was labeled with 0.5 mCi $Na^{125}I$ (Amersham Biosciences) using one iodobead (Pierce). The labeled protein was incubated with the membrane for 16 hours at 4°C. After washing, an X-ray film (Hyperfilm, Amersham Biosciences) was exposed to the membrane.

3 μg His_6-PrP^C or PrP^C peptides 43-62 or 103-122 was adsorbed onto nitrocellulose membranes. After blocking, $Vn_{307\text{-}320Mo}$ was labeled with biotin using an EZ-Link Sulfo-NHS-LC-Biotinylation Kit (Pierce) and incubated with the membrane for 16 hours at 4°C, followed by Streptavidin-HRP (Sigma) for 1 hour at room temperature.

Binding assays

Binding experiments were conducted as previously described (Graner et al., 2000a; Martins et al., 1997). Briefly, His_6-PrP^C or His_6-PrP^C deletion mutants (2 μg) were adsorbed in polystyrene wells and blocked with 2% BSA. Wells were incubated for 3 hours at 37°C with $Na^{125}I$-labeled Vn or $Vn_{307\text{-}320Mo}$ coupled to BSA. The wells were washed, and radioactivity was measured in a gamma counter (Mini gamma counter, LKB-Wallac). Data were analyzed using the Scatchard Method (Scatchard, 1949).

Competition assays

Unlabeled PrP^C peptides (32 μM) were pre-incubated with 38 nM of ^{125}I-Vn for 2 hours at room temperature. Peptides and ^{125}I-Vn were added to the His_6-PrP^C coated wells and incubated for 3 hours at 37°C. The wells were washed and the radioactivity was measured. Vn, STI1, Ln whole proteins or STI1 and Ln peptides were pre-incubated with coated His_6-PrP^C for 2 hours at room temperature followed by 3 hours at 37°C with ^{125}I-Vn. After washing, the radioactivity was measured.

Cell transfection and pull-down assay

HEK293 cells were transfected with pEGFP-C1 (Clontech) or pEGFP-STI1 (Zanata et al., 2002b) by calcium phosphate co-precipitation as previously described (Puchel et al., 1995). After 48 hours in culture, transfected cells were lysed in NP40 (0.5% in PBS). Cell extracts were pre-cleared by treatment with 30 μl of inactive CNBr-Sepharose (reactive groups previously blocked) for 1 hour at 4°C.

Vn was covalently coupled to CNBr-Sepharose 4B (Amersham) according to the manufacturer's instructions, and 30 μl Vn-CNBr-Sepharose was incubated in pre-cleared cell extracts for 16 hours at 4°C. After washing with 0.5% NP-40 in PBS, bound proteins were eluted with Laemmli buffer and analyzed by western blotting using mouse anti-PrP^C (1:1000) or anti-GFP (1:3000) followed by anti-mouse HRP.

Alexa Fluor 568 Vn labeling and co-localization assay

Vn labeling was performed using an Alexa Fluor 568 labeling kit (Molecular Probes). SN-56 cells, a mouse cholinergic septal neuronal cell line (Blusztajn et al., 1992; Hammond et al., 1990), were transfected with GFP-PrP^C using lipofectamine (Invitrogen) as described previously (Lee et al., 2001). Transfected and differentiated (1 mM cAMP for 1 day) SN-56 cells, were treated with 4 μg Alexa 568-Vn for 1 hour at 4°C. After several washes with PBS, images of live cells were acquired using a Bio-Rad Radiance 2100 laser-scanning confocal system coupled to a Nikon microscope (TE2000-U). Dissociated DRG cells were incubated with 4 μg labelled Vn for 1 hour at 4°C, fixed, submitted to immunofluorescence using mouse anti-PrP^C followed by anti-mouse Alexa Fluor 488, and images were acquired as for SN-56 cells.

Animals

The 'Principles of laboratory animal care' (NIH publication 85-23, 1996) were strictly followed in all experiments. ZrchI $Prnp^{0/0}$ were provided by Dr Charles Weissmann (Scripps Florida, FL) (Bueler et al., 1992). ZrchI $Prnp^{+/+}$ mice were generated by crossing F1 descendants from 129/SV and C57BL/6J matings. Npu $Prnp^{-/-}$ (Manson et al., 1994) were provided by Bruce Chesebro and Richard Race (Rocky Mountain Laboratories, National Institute of Allergy and Infectious Diseases, MT). These animals were backcrossed to C57BL/10 mice for at least eight generations. Heterozygous animals were mated and homozygous F1 descendants from the same litter were crossed to generate Npu $Prnp^{-/-}$ or Npu $Prnp^{+/+}$ embryos. All of the adult animals used to generate Npu $Prnp^{-/-}$ and Npu $Prnp^{+/+}$ embryos were genotyped by PCR (Manson et al., 1994).

DRG explants

DRG from E12.5 mice (Bueler et al., 1992) were dissected and cultured in poly-L-lysine coated glass coverslip in neurobasal medium (Invitrogen) with 2 mM glutamine, 100 IU penicillin, 100 μg/ml streptomicyn, B-27 (Invitrogen) and 50 ng/ml nerve growth factor (Sigma). In Fig. 7b,d, DRGs were plated in Vn_{RGD}-BSA adsorbed coverslips. Treatments were performed immediately after plating and ganglia were cultured for 24 (Fig. 6i,j, Fig. 7a-c) or 36 hours (Fig. 6a-h), fixed in 4% paraformaldehyde/0.12 M sucrose and stained with haematoxylin. The neurite length was measured as the distance from the edge of the DRG to the tip of the three longest neurites, and the mean value was used as the neurite length for each DRG (Zanata et al., 2002a). At least 12 ganglia from three independent experiments were considered for each individual data point. Cultures were dissociated by enzymatic digestion of the dissected ganglia for 30 minutes with 1% trypsin in neurobasal medium. After mechanical dissociation, 5×10^4 cells per 13 mm^2 well were plated in the presence of Vn for 6 hours. Cells were fixed and stained as described above and the percentage of cells presenting a neurite longer than one cell body was calculated.

Immunohistochemistry

DRG explants grown in the presence of Vn were fixed and incubated for 4 hours at 4°C with a mouse polyclonal antibody anti-PrP^C, 1:250 (Chiarini et al., 2002) followed by Alexa Fluor 568 anti-mouse IgG (Molecular Probes, Eugene, OR), for 40 minutes at room temperature. Ganglia were viewed with an Olympus IX70 microscope equipped with epifluorescence.

Formalin-fixed E12.5 mice embryos were embedded in paraffin and sections submitted to immunohistochemistry as previously described (Lopes et al., 2005) with mouse polyclonal anti-PrP^C antibody (1:1000) (Chiarini et al., 2002) or with rabbit polyclonal anti-Vn antibody (1:250).

Confocal immunofluorescence

E12.5 mouse embryos were immediately frozen and 3-μm-thick cryostat sections submitted to immunofluorescence as previously described (Lopes et al., 2005) with a mouse polyclonal anti-PrP^C antibody (1:250) (Chiarini et al., 2002) and rabbit anti-Vn serum (1:100).

αvβ3 activity assays

Dissociated DRG cells were plated on poly-L-lysine-coated coverslips and incubated for 24 hours, fixed, and blocked as described above. Immunofluorescence reaction with WOW-1 antibody (1:4) (Pampori et al., 1999) was undertaken for 16 hours at room temperature followed by Alexa Fluor 568 anti-mouse IgG (1:3000) (Molecular Probes). Immunofluorescence with AP5 antibody (50 μg/ml) was performed in PBS with 3 mM Ca^{2+} for 16 hours at room temperature followed by Alexa Fluor 568 anti-mouse IgG (1:3000). Images were acquired with an Olympus IX70 microscope equipped with epifluorescence. To acquire the images, the digital camera (Olympus DP70) exposure was set so that no fluorescence could be observed in cells incubated with only secondary antibody. At least five fields of each coverslip were imaged and the fluorescence of each cell was measured with the Image-Pro Plus 4.1 (Media Cybernetics). At least 100 cells per coverslip were considered.

Statistical analysis

The mean values of at least three independent datasets are shown in the figures; the error bars represent s.d. Fit to a normal distribution was evaluated with the Kolmogorov-Smirnov test. The homogeneity of variances was assessed using Levene's test. The comparison of means for two independent samples was performed using Student's *t*-test or Mann-Whitney's test. When comparing more than two groups, an ANOVA or Kruskal Wallis test was used and a Tukey-HSD test was used for multiple comparisons.

This work was supported by FAPESP (Fundação de Amparo a Pesquisa do Estado de São Paulo) (99/07124-8 and 03-13189-2) and V.R.M. is supported by the Howard Hughes Medical Institute. G.N.M.H., M.H.L. and T.G.S. are fellows from FAPESP. We are grateful to Ricardo Brentani for helpful discussions. We acknowledge Sanford Shattil for providing WOW antibody and Bruce Chesebro, Richard Race and Charles Weissmann for providing the PrP^C-null mice. We dedicate this work to the memory of Saul Jacchieri, an extraordinarily bright example of a life dedicated to science.

References

Ausubel, F. M., Brent, R., Kingston, R. E., Moore, D. D., Seidman, J. D., Smith, J. A. and Struhl, K. (1993). Constructing recombinant DNA molecules by the polymerase chain reaction. In *Current Protocols in Molecular Biology* (1st edn), p. 3.17.1. New York: Wiley Interscience.

Blasi, F. and Carmeliet, P. (2002). uPAR: a versatile signalling orchestrator. *Nat. Rev. Mol. Cell Biol.* **3**, 932-943.

Blusztajn, J. K., Venturini, A., Jackson, D. A., Lee, H. J. and Wainer, B. H. (1992). Acetylcholine synthesis and release is enhanced by dibutyryl cyclic AMP in a neuronal cell line derived from mouse septum. *J. Neurosci.* **12**, 793-799.

Brentani, R. R. (1988). Biological implications of complementary hydropathy of amino acids. *J. Theor. Biol.* **135**, 495-499.

Brown, D. R. and Besinger, A. (1998). Prion protein expression and superoxide dismutase activity. *Biochem. J.* **334**, 423-429.

Brown, D. R., Qin, K., Herms, J. W., Madlung, A., Manson, J., Strome, R., Fraser, P. E., Kruck, T., von Bohlen, A., Schulz-Schaeffer, W. et al. (1997). The cellular prion protein binds copper in vivo. *Nature* **390**, 684-687.

Brown, D. R., Nicholas, R. S. and Canevari, L. (2002). Lack of prion protein expression results in a neuronal phenotype sensitive to stress. *J. Neurosci. Res.* **67**, 211-224.

Bueler, H., Fischer, M., Lang, Y., Bluethmann, H., Lipp, H. P., DeArmond, S. J., Prusiner, S. B., Aguet, M. and Weissmann, C. (1992). Normal development and behaviour of mice lacking the neuronal cell-surface PrP protein. *Nature* **356**, 577-582.

Bugge, T. H., Suh, T. T., Flick, M. J., Daugherty, C. C., Romer, J., Solberg, H., Ellis, V., Dano, K. and Degen, J. L. (1995). The receptor for urokinase-type plasminogen activator is not essential for mouse development or fertility. *J. Biol. Chem.* **270**, 16886-16894.

Chen, S., Mange, A., Dong, L., Lehmann, S. and Schachner, M. (2003). Prion protein as trans-interacting partner for neurons is involved in neurite outgrowth and neuronal survival. *Mol. Cell. Neurosci.* **22**, 227-233.

Chen, Z. L., Indyk, J. A. and Strickland, S. (2003). The hippocampal laminin matrix is dynamic and critical for neuronal survival. *Mol. Biol. Cell* **14**, 2665-2676.

Chiarini, L. B., Freitas, A. R., Zanata, S. M., Brentani, R. R., Martins, V. R. and Linden, R. (2002). Cellular prion protein transduces neuroprotective signals. *EMBO J.* **21**, 3317-3326.

Coitinho, A. S., Freitas, A. R., Lopes, M. H., Hajj, G. N., Roesler, R., Walz, R., Rossato, J. I., Cammarota, M., Izquierdo, I., Martins, V. R. et al. (2006). The interaction between prion protein and laminin modulates memory consolidation. *Eur. J. Neurosci.* **24**, 3255-3264.

Cordeiro, Y., Kraineva, J., Ravindra, R., Lima, L. M., Gomes, M. P., Foguel, D., Winter, R. and Silva, J. L. (2004a). Hydration and packing effects on prion folding and beta-sheet conversion. High pressure spectroscopy and pressure perturbation calorimetry studies. *J. Biol. Chem.* **279**, 32354-32359.

Cordeiro, Y., Lima, L. M., Gomes, M. P., Foguel, D. and Silva, J. L. (2004b). Modulation of prion protein oligomerization, aggregation, and beta-sheet conversion by 4,4′-dianilino-1,1′-binaphthyl-5,5′-sulfonate (bis-ANS). *J. Biol. Chem.* **279**, 5346-5352.

Danilov, Y. N. and Juliano, R. L. (1989). (Arg-Gly-Asp)n-albumin conjugates as a model substratum for integrin-mediated cell adhesion. *Exp. Cell Res.* **182**, 186-196.

Easley, C. A., Faison, M. O., Kirsch, T. L., Lee, J. A., Seward, M. E. and Tombes, R. M. (2006). Laminin activates CaMK-II to stabilize nascent embryonic axons. *Brain Res.* **1092**, 59-68.

Engvall, E. and Ruoslahti, E. (1977). Binding of soluble form of fibroblast surface protein, fibronectin, to collagen. *Int. J. Cancer* **20**, 1-5.

Ettaiche, M., Pichot, R., Vincent, J. P. and Chabry, J. (2000). In vivo cytotoxicity of the prion protein fragment 106-126. *J. Biol. Chem.* **275**, 36487-36490.

Faccio, R., Grano, M., Colucci, S., Villa, A., Giannelli, G., Quaranta, V. and Zallone, A. (2002). Localization and possible role of two different alpha v beta 3 integrin conformations in resting and resorbing osteoclasts. *J. Cell Sci.* **115**, 2919-2929.

Felding-Habermann, B. and Cheresh, D. A. (1993). Vitronectin and its receptors. *Curr. Opin. Cell Biol.* **5**, 864-868.

Felding-Habermann, B., O'Toole, T. E., Smith, J. W., Fransvea, E., Ruggeri, Z. M., Ginsberg, M. H., Hughes, P. E., Pampori, N., Shattil, S. J., Saven, A. et al. (2001). Integrin activation controls metastasis in human breast cancer. *Proc. Natl. Acad. Sci. USA* **98**, 1853-1858.

Francois, P. P., Preissner, K. T., Herrmann, M., Haugland, R. P., Vaudaux, P., Lew, D. P. and Krause, K. H. (1999). Vitronectin interaction with glycosaminoglycans. Kinetics, structural determinants, and role in binding to endothelial cells. *J. Biol. Chem.* **274**, 37611-37619.

Gabriel, J. M., Oesch, B., Kretzschmar, H., Scott, M. and Prusiner, S. B. (1992). Molecular cloning of a candidate chicken prion protein. *Proc. Natl. Acad. Sci. USA* **89**, 9097-9101.

Gartner, T. K., Loudon, R. and Taylor, D. B. (1991). The peptides APLHK, EHIPA and GAPL are hydropathically equivalent peptide mimics of a fibrinogen binding domain of glycoprotein IIb/IIIa. *Biochem. Biophys. Res. Commun.* **180**, 1446-1452.

Gauczynski, S., Peyrin, J. M., Haik, S., Leucht, C., Hundt, C., Rieger, R., Krasemann, S., Deslys, J. P., Dormont, D., Lasmezas, C. I. et al. (2001). The 37-kDa/67-kDa laminin receptor acts as the cell-surface receptor for the cellular prion protein. *EMBO J.* **20**, 5863-5875.

Glatzel, M., Giger, O., Braun, N. and Aguzzi, A. (2004). The peripheral nervous system and the pathogenesis of prion diseases. *Curr. Mol. Med.* **4**, 355-359.

Gonzalez-Iglesias, R., Pajares, M. A., Ocal, C., Espinosa, J. C., Oesch, B. and Gasset, M. (2002). Prion protein interaction with glycosaminoglycan occurs with the formation of oligomeric complexes stabilized by Cu(II) bridges. *J. Mol. Biol.* **319**, 527-540.

Graner, E., Mercadante, A. F., Zanata, S. M., Forlenza, O. V., Cabral, A. L., Veiga, S. S., Juliano, M. A., Roesler, R., Walz, R., Minetti, A. et al. (2000a). Cellular prion protein binds laminin and mediates neuritogenesis. *Brain Res. Mol. Brain Res.* **76**, 85-92.

Graner, E., Mercadante, A. F., Zanata, S. M., Martins, V. R., Jay, D. G. and Brentani, R. R. (2000b). Laminin-induced PC-12 cell differentiation is inhibited following laser inactivation of cellular prion protein. *FEBS Lett.* **482**, 257-260.

Haik, S., Faucheux, B. A., Sazdovitch, V., Privat, N., Kemeny, J. L., Perret-Liaudet, A. and Hauw, J. J. (2003). The sympathetic nervous system is involved in variant Creutzfeldt-Jakob disease. *Nat. Med.* **9**, 1121-1123.

Hammond, D. N., Lee, H. J., Tonsgard, J. H. and Wainer, B. H. (1990). Development and characterization of clonal cell lines derived from septal cholinergic neurons. *Brain Res.* **512**, 190-200.

Heal, J. R., Roberts, G. W., Raynes, J. G., Bhakoo, A. and Miller, A. D. (2002). Specific interactions between sense and complementary peptides: the basis for the proteomic code. *Chembiochem.* **3**, 136-151.

Honda, S., Tomiyama, Y., Pelletier, A. J., Annis, D., Honda, Y., Orchekowski, R., Ruggeri, Z. and Kunicki, T. J. (1995). Topography of ligand-induced binding sites, including a novel cation-sensitive epitope (AP5) at the amino terminus, of the human integrin beta 3 subunit. *J. Biol. Chem.* **270**, 11947-11954.

Hundt, C., Peyrin, J. M., Haik, S., Gauczynski, S., Leucht, C., Rieger, R., Riley, M. L., Deslys, J. P., Dormont, D., Lasmezas, C. I. et al. (2001). Identification of interaction domains of the prion protein with its 37-kDa/67-kDa laminin receptor. *EMBO J.* **20**, 5876-5886.

Hynes, R. O. (2002). Integrins: bidirectional, allosteric signaling machines. *Cell* **110**, 673-687.

Isahara, K. and Yamamoto, M. (1995). The interaction of vascular endothelial cells and dorsal root ganglion neurites is mediated by vitronectin and heparan sulfate proteoglycans. *Brain Res. Dev. Brain Res.* **84**, 164-178.

Ishida, C., Okino, S., Kitamoto, T. and Yamada, M. (2005). Involvement of the peripheral nervous system in human prion diseases including dural graft associated Creutzfeldt-Jakob disease. *J. Neurol. Neurosurg. Psychiatr.* **76**, 325-329.

Jimenez-Huete, A., Lievens, P. M., Vidal, R., Piccardo, P., Ghetti, B., Tagliavini, F., Frangione, B. and Prelli, F. (1998). Endogenous proteolytic cleavage of normal and disease-associated isoforms of the human prion protein in neural and non-neural tissues. *Am. J. Pathol.* **153**, 1561-1572.

Kitami, T. and Nadeau, J. H. (2002). Biochemical networking contributes more to genetic buffering in human and mouse metabolic pathways than does gene duplication. *Nat. Genet.* **32**, 191-194.

Lee, C. C., Kuo, L. T., Wang, C. H., Scaravilli, F. and An, S. F. (2005). Accumulation of prion protein in the peripheral nervous system in human prion diseases. *J. Neuropathol. Exp. Neurol.* **64**, 716-721.

Lee, K. S., Magalhaes, A. C., Zanata, S. M., Brentani, R. R., Martins, V. R. and Prado, M. A. (2001). Internalization of mammalian fluorescent cellular prion protein and N-terminal deletion mutants in living cells. *J. Neurochem.* **79**, 79-87.

Lee, K. S., Linden, R., Prado, M. A., Brentani, R. R. and Martins, V. R. (2003). Towards cellular receptors for prions. *Rev. Med. Virol.* **13**, 399-408.

Lopes, M. H., Hajj, G. N., Muras, A. G., Mancini, G. L., Castro, R. M., Ribeiro, K. C., Brentani, R. R., Linden, R. and Martins, V. R. (2005). Interaction of cellular prion and stress-inducible protein 1 promotes neuritogenesis and neuroprotection by distinct signaling pathways. *J. Neurosci.* **25**, 11330-11339.

Manson, J. C., Clarke, A. R., Hooper, M. L., Aitchison, L., McConnell, I. and Hope, J. (1994). 129/Ola mice carrying a null mutation in PrP that abolishes mRNA production are developmentally normal. *Mol. Neurobiol.* **8**, 121-127.

Martinez-Morales, J. R., Marti, E., Frade, J. M. and Rodriguez-Tebar, A. (1995). Developmentally regulated vitronectin influences cell differentiation, neuron survival and process outgrowth in the developing chicken retina. *Neuroscience* **68**, 245-253.

Martinez-Morales, J. R., Barbas, J. A., Marti, E., Bovolenta, P., Edgar, D. and Rodriguez-Tebar, A. (1997). Vitronectin is expressed in the ventral region of the neural tube and promotes the differentiation of motor neurons. *Development* **124**, 5139-5147.

Martins, V. R. and Brentani, R. R. (2002). The biology of the cellular prion protein. *Neurochem. Int.* **41**, 353-355.

Martins, V. R., Graner, E., Garcia-Abreu, J., de Souza, S. J., Mercadante, A. F., Veiga, S. S., Zanata, S. M., Neto, V. M. and Brentani, R. R. (1997). Complementary hydropathy identifies a cellular prion protein receptor. *Nat. Med.* **3**, 1376-1382.

Mastrianni, J. A. and Roos, R. P. (2000). The prion diseases. *Semin. Neurol.* **20**, 337-352.

Miele, G., Alejo Blanco, A. R., Baybutt, H., Horvat, S., Manson, J. and Clinton, M. (2003). Embryonic activation and developmental expression of the murine prion protein gene. *Gene Expr.* **11**, 1-12.

Monier-Gavelle, F. and Duband, J. L. (1997). Cross talk between adhesion molecules: control of N-cadherin activity by intracellular signals elicited by beta1 and beta3 integrins in migrating neural crest cells. *J. Cell Biol.* **137**, 1663-1681.

Mouillet-Richard, S., Ermonval, M., Chebassier, C., Laplanche, J. L., Lehmann, S., Launay, J. M. and Kellermann, O. (2000). Signal transduction through prion protein. *Science* **289**, 1925-1928.

Moya, K. L., Hassig, R., Creminon, C., Laffont, I. and Di Giamberardino, L. (2004). Enhanced detection and retrograde axonal transport of PrPc in peripheral nerve. *J. Neurochem.* **88**, 155-160.

Oesch, B., Westaway, D., Walchli, M., McKinley, M. P., Kent, S. B., Aebersold, R., Barry, R. A., Tempst, P., Teplow, D. B., Hood, L. E. et al. (1985). A cellular gene encodes scrapie PrP 27-30 protein. *Cell* **40**, 735-746.

Pampori, N., Hato, T., Stupack, D. G., Aidoudi, S., Cheresh, D. A., Nemerow, G. R. and Shattil, S. J. (1999). Mechanisms and consequences of affinity modulation of integrin alpha(V)beta(3) detected with a novel patch-engineered monovalent ligand. *J. Biol. Chem.* **274**, 21609-21616.

Pan, T., Wong, B. S., Liu, T., Li, R., Petersen, R. B. and Sy, M. S. (2002). Cell-surface prion protein interacts with glycosaminoglycans. *Biochem. J.* **368**, 81-90.

Pierschbacher, M. D. and Ruoslahti, E. (1984). Cell attachment activity of fibronectin can be duplicated by small synthetic fragments of the molecule. *Nature* **309**, 30-33.

Pierschbacher, M. D. and Ruoslahti, E. (1987). Influence of stereochemistry of the sequence Arg-Gly-Asp-Xaa on binding specificity in cell adhesion. *J. Biol. Chem.* **262**, 17294-17298.

Pons, S. and Marti, E. (2000). Sonic hedgehog synergizes with the extracellular matrix protein vitronectin to induce spinal motor neuron differentiation. *Development* **127**, 333-342.

Pons, S., Trejo, J. L., Martinez-Morales, J. R. and Marti, E. (2001). Vitronectin regulates Sonic hedgehog activity during cerebellum development through CREB phosphorylation. *Development* **128**, 1481-1492.

Preissner, K. T. (1991). Structure and biological role of vitronectin. *Annu. Rev. Cell Biol.* **7**, 275-310.

Puschel, A. W., Adams R. H. and Betz, H. (1995). Murine semaphoring D/collapsing is a member of a diverse gene family and creates domains inhibitory for axonal growth. *Neuron* **14**, 941-948.

Rambold, A. S., Miesbauer, M., Rapaport, D., Bartke, T., Baier, M., Winklhofer, K. F. and Tatzelt, J. (2006). Association of Bcl-2 with misfolded prion protein is linked to the toxic potential of cytosolic PrP. *Mol. Biol. Cell* **17**, 3356-3368.

Riek, R., Hornemann, S., Wider, G., Billeter, M., Glockshuber, R. and Wuthrich, K. (1996). NMR structure of the mouse prion protein domain PrP(121-321). *Nature* **382**, 180-182.

Roberts, M. S., Woods, A. J., Shaw, P. E. and Norman, J. C. (2003). ERK1 associates with alpha(v)beta 3 integrin and regulates cell spreading on vitronectin. *J. Biol. Chem.* **278**, 1975-1985.

Ruoslahti, E. and Pierschbacher, M. D. (1987). New perspectives in cell adhesion: RGD and integrins. *Science* **238**, 491-497.

Sales, N., Hassig, R., Rodolfo, K., Di Giamberardino, L., Traiffort, E., Ruat, M., Fretier, P. and Moya, K. L. (2002). Developmental expression of the cellular prion protein in elongating axons. *Eur. J. Neurosci.* **15**, 1163-1177.

Santuccione, A., Sytnyk, V., Leshchyns'ka, I. and Schachner, M. (2005). Prion protein recruits its neuronal receptor NCAM to lipid rafts to activate p59fyn and to enhance neurite outgrowth. *J. Cell Biol.* **169**, 341-354.

Scatchard, G. (1949). The attractions of proteins for small molecules and ions. *Ann. N. Y. Acad. Sci.* **51**, 666-672.

Schmitt-Ulms, G., Legname, G., Baldwin, M. A., Ball, H. L., Bradon, N., Bosque, P. J., Crossin, K. L., Edelman, G. M., DeArmond, S. J., Cohen, F. E. et al. (2001). Binding of neural cell adhesion molecules (N-CAMs) to the cellular prion protein. *J. Mol. Biol.* **314**, 1209-1225.

Schvartz, I., Seger, D. and Shaltiel, S. (1999). Vitronectin. *Int. J. Biochem. Cell Biol.* **31**, 539-544.

Schwarz, D. G., Griffin, C. T., Schneider, E. A., Yee, D. and Magnuson, T. (2002). Genetic analysis of sorting nexins 1 and 2 reveals a redundant and essential function in mice. *Mol. Biol. Cell* **13**, 3588-3600.

Seiffert, D., Iruela-Arispe, M. L., Sage, E. H. and Loskutoff, D. J. (1995). Distribution of vitronectin mRNA during murine development. *Dev. Dyn.* **203**, 71-79.

Steele, A. D., Emsley, J. G., Ozdinler, P. H., Lindquist, S. and Macklis, J. D. (2006). Prion protein (PrPc) positively regulates neural precursor proliferation during developmental and adult mammalian neurogenesis. *Proc. Natl. Acad. Sci. USA* **103**, 3416-3421.

Takagi, J., Petre, B. M., Walz, T. and Springer, T. A. (2002). Global conformational rearrangements in integrin extracellular domains in outside-in and inside-out signaling. *Cell* **110**, 599-511.

Tom, V. J., Doller, C. M., Malouf, A. T. and Silver, J. (2004). Astrocyte-associated fibronectin is critical for axonal regeneration in adult white matter. *J. Neurosci.* **24**, 9282-9290.

Tsai, C. J., Lin, S. L., Wolfson, H. J. and Nussinov, R. (1997). Studies of protein-protein interfaces: a statistical analysis of the hydrophobic effect. *Protein Sci.* **6**, 53-64.

Turney, S. G. and Bridgman, P. C. (2005). Laminin stimulates and guides axonal outgrowth via growth cone myosin II activity. *Nat. Neurosci.* **8**, 717-719.

Xian, C. J., Li, L., Deng, Y. S., Zhao, S. P. and Zhou, X. F. (2001). Lack of effects of transforming growth factor-alpha gene knockout on peripheral nerve regeneration may result from compensatory mechanisms. *Exp. Neurol.* **172**, 182-188.

Xu, D., Baburaj, K., Peterson, C. B. and Xu, Y. (2001). Model for the three-dimensional structure of vitronectin: predictions for the multi-domain protein from threading and docking. *Proteins* **44**, 312-320.

Xu, Y. and Xu, D. (2000). Protein threading using PROSPECT: design and evaluation. *Proteins* **40**, 343-354.

Yatohgo, T., Izumi, M., Kashiwagi, H. and Hayashi, M. (1988). Novel purification of vitronectin from human plasma by heparin affinity chromatography. *Cell Struct. Funct.* **13**, 281-292.

Zahn, R., von Schroetter, C. and Wuthrich, K. (1997). Human prion proteins expressed in Escherichia coli and purified by high- affinity column refolding. *FEBS Lett.* **417**, 400-404.

Zanata, S. M., Hovatta, I., Rohm, B. and Puschel, A. W. (2002a). Antagonistic effects of Rnd1 and RhoD GTPases regulate receptor activity in Semaphorin 3A-induced cytoskeletal collapse. *J. Neurosci.* **22**, 471-477.

Zanata, S. M., Lopes, M. H., Mercadante, A. F., Hajj, G. N., Chiarini, L. B., Nomizo, R., Freitas, A. R., Cabral, A. L., Lee, K. S., Juliano, M. A. et al. (2002b). Stress-inducible protein 1 is a cell surface ligand for cellular prion that triggers neuroprotection. *EMBO J.* **21**, 3307-3316.

Anexo 2 - Interação entre a proteína prion celular e o peptídeo da cadeia γ1 de laminina ativa receptores metabotrópicos de glutamato do tipo 1.

Neste trabalho foi demonstrado que receptores metabotrópicos de glutamato tipo I (mGluR1 e mGluR5) são responsáveis pela sinalização intracelular envolvida com a interação entre PrP^C e o peptídeo da cadeia γ1 de laminina.

Dados anteriores do grupo demonstraram que a ligação PrP^C-LNn-γ1 modula plasticidade neuronal e formação de memória. Entretanto, os mecanismos pelos quais PrP^C transduz seus sinais permaneciam obscuros, uma vez que PrP^C não apresenta um domínio transmembrana. No presente manuscrito demonstramos que o peptídeo Ln-γ1, através de seu domínio KDI, estimula a neuritogênese e aumenta a concentração intracelular de Ca^{2+} em neurônios tipo-selvagem. Por outro lado, nenhum efeito foi observado em neurônios deficientes de PrP^C após tratamento com o peptídeo da cadeia γ1 de Ln.

Os efeitos induzidos pela interação PrP^C-Lnγ1 são bloqueados por inibidores específicos das vias de fosfolipase C (PLC) e inositol-trifosfato ($InsP_3$) que estão envolvidas na mobilização de Ca^{2+} de retículo endoplasmático. Estes resultados sugerem que um receptor acoplado a proteína G poderia estar envolvido no processo, e diante de dados prévios da literatura, os receptores de metabotrópicos de glutamato tipo I (mGluR1 e mGluR5) apresentam-se como potenciais candidatos. De fato, a inibição de mGluR1 e mGluR5 bloqueou os efeitos da interação PrP^C-laminina-γ1 sobre o aumento intracelular de cálcio, ativação de proteína quinase C (PKC) e neuritogênese.

Adicionalmente, a expressão conjunta de mGluR1 ou mGluR5 e PrP^C em células HEK293 reconstituiu a sinalização mediada por PrP^C-Lnγ1. Estes dados indicam que receptores metabotrópicos tipo I estão envolvidos na sinalização celular e na neuritogênese mediada pela interação PrP^C-lamininaγ1.

Minha contribuição neste trabalho foi a realização dos ensaios com o agonista e antagonistas de mGluR1 e mGluR5 sobre os níveis intracelulares de Ca^{2+} (Figs 4c-f) e na inibição da neuritogênese promovida pelo peptídeo da cadeia γ1 de laminina (Fig. 7).

Prion protein transduces signals after binding to laminin γ-1 chain via metabotropic receptors

Flavio H. Beraldo[1,4#], Camila P. Arantes[1,2#], Tiago G. Santos[1,3], Cleiton F. Machado[1,3], Kill S. Lee[1], Ana C. Magalhães[4], Fabiana A. Caetano[4,5], Gabriel L. Mancini[1], Gláucia N. Hajj[1], Margareth Magdesian[6], Tatiana Américo[6], Stephen S.G. Ferguson[4]; Rafael Linden[6], Marco A. M. Prado[4,7*], Vilma R. Martins[1*]

# These authors contributed equally for this work

1 – Ludwig Institute for Cancer Research, Hospital Alemão Oswaldo Cruz – São Paulo, SP - Brazil

2 – Departamento de Bioquímica, Instituto de Química, Universidade de São Paulo – São Paulo, SP - Brazil

3 – Centro de Tratamento e Pesquisa do Hospital AC Camargo, São Paulo, SP – Brazil

4 - Robarts Research Institute, Department of Physiology and Pharmacology – University Western Ontario– London – ON – Canada

5 - Program in Molecular Pharmacology, Universidade Federal de Minas Gerais, Belo Horizonte, MG – Brazil

6 - Instituto de Biofísica Carlos Chagas Filho, Universidade Federal do Rio de Janeiro, Rio de Janeiro, RJ, Brazil

7 - Department of Anatomy and Cell Biology, University Western Ontario – London – ON – Canada

*To whom correspondence should be addressed:
Vilma Regina Martins, Ludwig Institute for Cancer Research, Rua Joao Julião 245 1A, São Paulo, SP 01323-903, Brazil, Tel: 55-11-33883239; e-mail vmartins@ludwig.org.br or Marco Antonio Maximo Prado, Robarts Research Institute, University Western Ontario, P.O. Box 5015, 100 Perth Drive London, ON N6A 5K8, Canada, Tel: 519-663-5777 Ext. 24888; e-mail mprado@robarts.ca.

Abstract

The prion protein (PrP^C) is a cell surface glycoprotein highly expressed in the nervous system, a conformationally modified isoform of which is associated with prion diseases. PrP^C interacts with various proteins thus modulating neuronal survival, plasticity and memory. Conversely binding of Aβ oligomers to PrP^C promotes neuronal dysfunction. Transmembrane proteins are likely required for PrP^C-mediated intracellular signaling with consequences for neuronal function/dysfunction. We show here that a laminin γ1 chain peptide (RNIAEIIKDI) induces PrP^C-dependent neuritogenesis thought an increase in intracellular Ca^{2+} and activation of PKC. Inhibition of phospholipase C, inositol 3-phosphate receptor and group I metabotrobic glutamate receptors (mGluR1/5) abrogates both PrP^C dependent Ca^{2+} signaling and neuritogenesis. In addition, the expression of mGluR1 or mGluR5 receptors in HEK 293 cells reconstitutes the signaling pathways mediated by PrP^C-laminin γ1chain peptide interaction. These data show that group I mGluRs are involved in neurotrophic properties of PrP^C-laminin interaction.

Introduction

The cellular prion protein (PrP^C) is a copper-binding glycoprotein highly expressed in nervous tissue, and attaches to the cell surface by a glycosylphosphatidylinositol (GPI) anchor. A conformationally modified isoform of PrP^C (PrP^{Sc}) is the major component of prions, infectious agents that cause neurodegenerative diseases known as transmissible spongiform encephalopathies (TSEs). These illnesses affect humans and other mammals and present as either sporadic, genetic or infectious forms of the disease (Weissmann, 2004).

A number of potential physiological functions of PrP^C have been described in the last several years, which are likely to be of importance for both neuronal function and neurodegenerative diseases (Linden et al., 2008). PrP^C has neuroprotective properties against oxidative insults and injury and is associated with neuronal differentiaion.

PrP^C has been shown to regulate the production of amyloid β-peptide (Aβ) peptide, a major culprit in Alzheimer`s disease, by controlling BACE activity (Parkin et al., 2007). Recently, PrP^C was also found to be the major receptor for amyloid-β (Aβ) oligomers in neurons and their interaction is important for the effects of Aβ on synaptic plasticity (Lauren et al., 2009). These data indicate that PrP^C may be a key player in Alzheimer's disease, in addition to its known roles in prion diseases.

Some PrP^C functions have been associated with its binding to specific cellular proteins. Previously, we have demonstrated that PrP^C binds to stress inducible protein 1 (STI1) to mediate neuronal survival and differentiation via the activation of cAMP-dependent protein kinase (PKA) and extracellular regulated kinase (ERK1/2) signaling pathways (Chiarini et al., 2002;Zanata et al., 2002;Lopes et al., 2005).

Neurite outgrowth is also induced by PrP^C interaction with neuronal cell adhesion molecule (NCAM), in a mechanism triggered by recruitment of NCAM to lipid rafts and thereby regulating the activation of Fyn kinase (Santuccione et al., 2005). PrP^C has also been shown to bind to extracellular matrix proteins with high affinity, in particular laminin (Kd= 2 X 10^{-8} M) (Graner et al., 2000). By using competition binding assays with synthetic laminin peptides, the binding site for laminin was mapped to amino acids 1575 to 1584 (RNIAEIIKDI) of the laminin γ1 chain (Graner et al., 2000) and to amino acids 170 to 178 in PrP^C (Coitinho et al., 2006). The laminin peptide representing the PrP^C binding site, named here Ln γ1 peptide, reproduces the effect of laminin and promotes neuritogenesis in primary cultures of hippocampal neurons, but has no activity in neuronal cultures from PrP^C-null mice (Graner et al., 2000). In agreement with a role of PrP^C- Ln γ1 peptide interaction as a potential signal in the nervous system, it has been demonstrated that this interaction increases memory consolidation (Coitinho et al., 2006). The Ln γ1 peptide is able to modulate neuronal excitability and is highly expressed in neocortical and hippocampal rat neurons (Hager et al., 1998; Liesi et al., 1989). The KDI sequence at the C-terminus of the Ln γ1 peptide represents the functional domain of the laminin γ-1 chain and is responsible for promoting neuronal differentiation (Liesi et al., 2001).

Although PrP^C-Ln γ1 peptide engagement may modulate a number of physiological activities, the mechanisms by which extracellular PrP^C activates intracellular signaling pathways is unknown. The fact that PrP^C is GPI-anchored suggests the need for a transmembrane protein to form a functional complex with PrP^C for extracellular signals to be transduced. In the present work we use primary

hippocampal neurons from wild-type and PrP^C-null mice to evaluate the early and sequential signaling events associated with PrP^C-Ln γ1 interaction. We find that signaling through PrP^C results in activation of phospholipase C (PLC), increases inintracellular calcium concentrations and the activation of protein kinase C (PKC), suggesting that a Gq-coupled G-protein coupled receptor (GPCR) connects PrP^C to intracellular signaling pathways. We provide evidence that type I metabotropic glutamate receptors (mGluR1 or mGluR5) mediate both signaling and the neuritogenic effects in response to activation of PrP^C with Ln γ1 peptide. Our data reveal a new signaling pathway involving metabotropic glutamate receptors in PrPC-dependent activation of neuronal differentiation.

Material and Methods

Peptides and Chemicals (signaling pathway inhibitors and activators): Ln γ-1 peptide (RNIAEIIKDI) coupled to BSA, Ln γ-1 peptide where KDI domain was changed to GGG (RNIAEIIGGG), Ln γ-1 scrambled peptide (IRADIEIKID) and caldendrin (RDIRRIIRDV) peptide were synthesized by GenScript Corp. (NJ, USA) and NeoMPS SA (Strasbourg, France). MAP/extracellular signal-regulated kinase (ERK) kinase (MEK) inhibitor 1,4-diamino-2,3-dicyano-1,4-bis (2-aminophenyltio) butadiene (U0126) was purchased from Promega (Madison, WI), PKA inhibitor KT5720, PKC inhibitor chelerethrin chloride (Chel), PLC inhibitor U73122, phorbol 12-myristate 13-acetate (PMA) and phosphodiesterase inhibitor 3-isobutyl-1-methylxantine (IBMX) were purchased from Calbiochem (La Jolla, CA). The PKA activator (forskolin) and the PKC activator (PMA) were purchased from LC Laboratories (Woburn, MA). The L-type calcium channel blocker (Nifedipine),

$InsP_3$ receptor blocker (2APB), Ca^{2+} ATPase inhibitor (thapsigargin) and Bradykinin B2 receptor antagonist (HOE 140) were purchased from Sigma-Aldrich (St Louis, MO). The Q-type Ca^{2+} channel blocker ω-conotoxin MCVII was from Latoxan (Valence, France). SOC inhibitor (SKF 96365), the group I metabotropic agonist (DHPG), mGluR1 inhibitor (LY367385) and mGluR5 blocker (MPEP) were from Tocris Biociences (Ellisvile, MO). Bradikynin (BK) (H-Arg-Pro-Pro-Gly-Phe-Ser-Pro-Phe-Arg-OH) were from Bachem (Torrance, CA).

Animals: PrP^C-null mice (*Prnp*$^{0/0}$) were provided by Dr. Charles Weissmann (Scripps Florida, FL, USA). The animals are descendants from the *ZrchI* line (Bueler et al., 1992) and their respective wild-type animals were generated by crossing F1 descendants from 129/SV and C57BL/6J mating. The second PrP^C-null mice (*Prnp*$^{-/-}$) are descendants from the *Npu* line (Manson et al., 1994) and were provided by Drs. Bruce Chesebro and Richard Race (Rocky Mountain Laboratories, National Institute of Allergy and Infectious Diseases, MT, USA). These animals were backcrossed to C57Bl/10 mice for at least 10 generations. Heterozygous animals were mated and homozygous F1 descendents from the same littermate crossed to generate PrP^C-null (*Prnp*$^{-/-}$) embryos and their respective wild-type controls, herein nominated *Prnp*$^{wt/wt}$. All of the adult animals used to generate *Prnp*$^{-/-}$ and *Prnp*$^{wt/wt}$ embryos were genotyped by PCR as previously described (Lima et al., 2007).

Neuritogenesis assays: primary hippocampal neuronal cultures from E17 wild-type (*Prnp*$^{+/+}$ or *Prnp*$^{wt/wt}$) or PrP^C-null mice (*Prnp*$^{0/0}$ or *Prnp*$^{-/-}$) were obtained as described in Lopes et al (2005). The cells ($4x10^4$) were plated onto coverslips (13 mm^2) coated with 5μg/ml of poly-L-lysine (Sigma) or 37 μM of BSA Ln γ-1 peptide, Ln γ-1 peptide GGG, Ln γ-1 scrambled peptide or Caldendrin peptide and

incubated by 24 hours at 37º C and 5% CO_2 atmosphere. Neuritogenesis mediated by Ln γ-1 peptide was also evaluated upon cell treatment with specific signaling pathway inhibitors: U0126 (10 μM), KT5720 (60nM), BIM (0.5 μM) or U73122 (1 μM). The participation of metabotropic receptors in the neuritogenesis mediated by Ln γ-1 peptide was dissected in cells treated with the mGluR1/R5 agonist DHPG (100μM) and/or antagonists of mGluR1, LY367385 (100 μM) and mGluR5, MPEP (10 μM). Cells were pre-incubated with signaling pathway inhibitors or mGluR1/2 antagonists for 30 min before Ln γ-1 peptide treatment. The cells were them fixed with 4% p-paraformaldhyde in 0.12 M sucrose in PBS for 20 minutes at room temperature, washed 3 times with PBS and stained with hematoxylin.

Analyze of morphometry was done using ImageJ software (National Institute of Health) and NeuronJ plug in. The analyzed parameters were: percentage or cells with neurites, number of neurites/cell (total number of neurites/number of cells with neurites), mean length of neurites and percentage of with neurites longer than 30 μm (represents 3 or more times the average cell body). A total of about 200 cells were analyzed per sample.

Immunofluorescence: *Prnp*$^{+/+}$ neurons were plated on glass coverslips, fixed with 4% paraformaldehyde and 0.12M sucrose in PBS and permeabilized with 0.2% Triton X-100 in PBS for 5 min at room temperature (RT). After rinsing with PBS, cells were blocked with PBS plus 5% BSA and labeling with βIII-tubulin (Tuj, Chemicon) or anti-Tuj (1:100) antibodies for one hour. The reaction proceeded by incubation of secondary antibody, anti-mouse Alexa Fluor® 546 (1:1000, Molecular Probes) followed by nuclei staining with 4′,6-diamino-2-phenylindole (1:1000, DAPI). Coverslips were mounted on slides using Fluorsave Reagent (Calbiochem).

Immunolabeled cells were imaged with Bio-Rad (Hercules, CA) Radiance 2100 laser scanning confocal system running the software Laser Sharp 3.0, coupled to a Nikon (Melville, NY) Microscope (TE2000-U). Green HeNe (543 nm) and Blue Diode (405 nm) lasers were used to excite the fluorophores.

PKC activity: primary hippacampal ($1x10^6$ cells) neurons cultured onto poly-L-lysine were incubated with Ln γ-1 peptide (37 μM), at different time points (0.5s to 30 min). Control treatment with PMA (50 nM) was procedure for 20 min at room temperature (RT). Cells were also pre-incubated with or without U0126 (10 μM), KT5720 (60nM), BIM (0.5 μM), U73122 (1 μM) for 30 min at 37º C followed by Ln γ-1 peptide (37 μM), Ln γ-1 peptide GGG or Ln γ-1 scrambled peptide for 1 min at RT. PKC activity triggerd by PrPC-Ln γ-1 peptide was also evaluated in cells incubated with antagonists of mGluR1, LY367385 (100 μM) and mGluR5, MPEP (10μM). Control treatment was procedure in cells treated the mGluR1/R5 agonist DHPG (100 μM.). Cells were washed with PBS and homogenized in ice-cold extraction buffer (150 mM NaCl, 20mM MgCl2, 1% Triton X-100, and 25 mM Tris-HCl, pH 7.4) plus Complete Protease Inhibitor Cocktail (Roche). Cellular debris was removed by centrifugation at 6000 x *g* for 10 min. The PKC activity was determined by γ-ATP incorporation to a PKC-specific substrate provided by the PKC assay system kit (Upstate Biotechnology, Lake Placid, NY). The reaction was performed according to the manufacturer's instructions.

PKA activity: primary hippacampal ($1x10^6$ cells) neurons cultured onto poly-L-lysine were pre-incubated with 100 μM IBMX for 1h at 37° C and incubated with Ln γ-1 peptide (37 μM), at different time points (0.5 to 10 min) or with Forskolin (10 μM) for 20 min at 37° C as positive control. Cells were them washed with cold PBS

and homogenized in ice-cold extraction buffer (150 mM NaCl, 20mM $MgCl_2$, 1% Triton X-100, and 25 mM Tris-HCl, pH 7.4) plus Complete Protease Inhibitor Cocktail (Roche). Cellular debris was removed by centrifugation at 6000 x *g* for 10 min. The PKA activity was determined by [^{32}P]γ-ATP incorporation to a PKA-specific substrate provided by the PKA assay system kit (Upstate Biotechnology, Lake Placid, NY). The reaction was performed according to the manufacturer's instructions.

Erk1/2 activity: Primary hippacampal (1x10^6 cells) neurons from *Prnp*$^{+/+}$ or *Prnp*$^{0/0}$ were plated on dishes pre-treated with poly-L-lysine and stimulated with Ln γ-1 chain peptide (37 μM) at different time points (0.5 to 30 min). Cells were also treated for 0.5 min with Ln γ-1 chain peptide (37 μM) after a pre-incubation with or without U0126 (10 μM), KT5720 (60nM), BIM (0.5 μM), U73122 (1 μM) for 30min. Cells were rinsed with ice-cold PBS and lysed in Laemmli buffer. Cell extracts were subject to SDS-PAGE (10%) and proteins were transferred onto polyvinylidene difluoride membranes. The membranes were immersed in blocking solution (5% milk, 0.1 % Tween 20 in TBS) for 1 hour at RT and incubated with anti-Phospho ERK1/2 (p44-p42) and anti total-ERK1/2 antibodies (Cell Signaling Tecnology Beverly, MA) at 1:2000 dilution over night at 4ºC). Membranes were them incubated with a peroxidase-coupled, goat anti-rabbit secondarary antibody 1:2000 (GE Healthcare Life in Sciences, Buckinghamshire-UK) in 5% milk/TBST for 1 hour at RT, immersed in enhanced chemiluminescence (ECL) solution (GE Healthcare Life in Sciences, Buckinghamshire-UK) and exposed to ECL-Hyperfilm (Amersham).

The bands obtained after X-ray film exposure to the membranes, were analyzed by densitometric scanning and quantified using the Scion image Software (Frederick,

MD). Values represent the ratio between phospho- ERK1/2 and total- ERK1/2 for each sample.

Ca^{2+} signaling and data analysis: hippocampal cell cultures ($5x10^5$ cells) from *Prnp*$^{+/+}$ or *Prnp*$^{0/0}$ were plated onto coverslips (35 mm) coated with 5µg/ml of poly-L-lysine (Sigma) for 3 days. CF10, a PrP^C-null immortalized cell line and its counterpart expressing 3F4-tagged mouse PrPC were obtained as previously described (Caetano et al., 2008). CF10 cells ($1x10^4$) were plated onto coverslips as hippocampal neurons and serum-starved for 48h before the experiments. Hippocampal neurons and CF10 were loaded with 10 µM of the intracellular Ca^{2+} indicator Fluo 3 AM (Invitrogen, Carlsbad-CA) for 30 min at 37oC in each culture Neurobasal medium (Invitrogen Carlsbad-CA) for neurons or Optimen (Invitrogen, Carlsbad-CA) supplemented with 2mM $CaCl_2$ for CF10. Cells were washed three times with HBSS (Invitrogen, Carlsbad-CA) and ressuspended in Krebs buffer (124 mM NaCl, 4 mM KCl, 25 mM Hepes, 1.2 mM $MgSO_4$, 10 mM glucose) supplemented with 2 M $CaCl_2$. Calcium-free experiments were performed in Krebs buffer without $CaCl_2$ plus 1mM EGTA. Cells were per-incubated in presence or absence of SKF-96365 (25µM), VGCC inhibitors (ω-conotoxin MCVII 1µM plus Nifedipine 50 µM), 2APB (50µM), U73122 (1µM), Bradykinin (1µM), HOE140 (1µM), DHPG (100µM), LY367385 (100 µM) or MPEP (10µM) for 30 min. Hippocampal neurons were them treated with Ln γ-1 peptide, Ln γ-1 peptide GGG or Ln γ-1 scramble peptide at the concentration of 37 µM while CF10 and CF10-PrP^C cells received 120µM of these peptides. In control experiments cells were also treated with THG (1µM). All experiments were done at 37° C. Data acquisition was performed in confocal microscope Bio-Rad Radiance 2100/Nikon (TE2000U) –

excitation 488 nm (argon laser) and emission colleted with band pass filter 522-535 nm. The fluorescence was normalized as F1/F0 (F1, maximal fluorescence after drug addition and F0, basal fluorescence before drug addition). Software-based analysis (WCIF ImageJ – NIH) allowed fluorescence imaging in the selected cell as function of time. Experiments were carried out with at least 3 different cell cultures, and 40-50 cells were monitored in each experiment. Traces represent typical single cell response.

HEK cells transfection with mGLUR1 and mGLUR5 and reconstitution of the PrP^C-Ln γ-1 peptide signaling: Human Embryonic Kidney cells (HEK 293) were maintained in minimal essential medium MEM (Invitrogen) supplemented with 10% fetal bovine serum and 100 IU penicillin, 100 μg/ml streptomicyn at 37oC in a humidified atmosphere containing 5% CO2. Cells were transfected using a modified calcium phosphate method (Cullen, 1987) with a plasmid expressing a mouse PrP^C (Sunyach et al., 2003) plus Flag-mGluR1a or Flag-mGluR5a cDNAs (Anborgh et al., 2005;Dale et al., 2001). For Ca^{2+} experiments, HEK 293 cells expressing PrPC plus mGluR1 or mGluR5a were loaded with Fluo-3 AM (10 μM) for 30 min at 37oC in MEM supplemented with 2 mM $CaCl_2$. Cells were then washed three times with HBSS and resuspended in Krebs buffer supplemented with 2 mM $CaCl_2$. Intracellular Ca^{2+} increases were analyzed using Zeiss LSM-510 confocal microscope and defined as the relative change in cytoplasmic fluorescence intensity ratio (F1/F0) as described above. For PKC translocation experiments, HEK 293 cells were transfected with PrPC and GFP-PKCβII49 alone or along with either mGluR1 or mGluR5 expression vectors and incubated in Krebs buffer supplemented with 2 mM $CaCl_2$. Cells were analysed using Zeiss LSM 510 software as previously

described (Policha et al., 2006). Briefly, a region of interest was delimited at the cell cytosol and fluorescence intensity was evaluated over time. Translocation to the membrane was considered when there was a decrease in cytosolic fluorescence accompanied by an accumulation of fluorescence at the cell surface. As a positive control for PKC translocation49, 50, in the end of each experiment we used THG (1 μM) for transfected cells with PrP^C alone and DHPG (100 μM) or Quisqualate (100 μM) for mGluR1 and mGluR5 respectively (data not shown). From four independent transfections a total of 36 cells were analyzed for PrP^C, 33 cells for PrP^C and mGluR1 and 18 cells for PrP^C and mGluR5.

Statistical analysis: The statistical analyses were done using Graph Pad Prism Prism 4. Results are represented as mean ± standard error from at least three independent experiments. Data were compared by one-way ANOVA and Newman-Keuls test.

Results

Signaling pathways involved with the neuritogenesis induced by γ1 peptide interaction with PrP^C

We previously described that PrP^C-laminin interactions induced neuritogenesis and that the Ln γ1 peptide reproduced this effect (Graner et al., 2000). However, the signaling pathways activated by PrP^C remained elusive. Neuritogenesis assays were initially done to test if the KDI domain of the Ln γ1 peptide (RNIAEIIKDI) was the primary domain for PrP^C interactions required for the promotion of neuritogenesis. This region of the peptide has been previously described to induce neuronal differentiation (Liesi et al., 2001). Primary hippocampal cultures from either $Prnp^{+/+}$ or $Prnp^{0/0}$ mice embryos (E17) were treated with Ln γ1

peptide, an Ln γ1 peptide where the tri-peptide (KDI) was changed for GGG (GGG) and a scrambled Ln γ1 peptide (SCR). Treatment of *Prnp*$^{+/+}$ neurons with Ln γ1 peptide induced a 99 ± 15 % increase in the number of cells with neurites, herein defined as a growing process in the neurons, when compared to poly-Lysine (Figs. 1a ,b see also Fig. 7 for examples of neurons undergoing neuritogenesis), whereas no effect of the peptide was observed in *Prnp*$^{0/0}$ neurons (Fig. 1a) The Ln γ1 peptide with the KDI sequence replaced by GGG did not induce neuritogenesis, thus confirming the importance of this domain for PrP^{C}-dependent differentiation. Blast searches indicated that the Ln γ1 peptide presents high homology to a domain found in caldendrin (CAL), a cytoplasmatic calcium sensor protein highly expressed in neurons (Laube et al., 2002). However, the caldendrin homologue peptide had no effect on neuritogenesis (Fig. 1a). The scrambled peptide (SCR), used as control, was inactive upon neuritogenesis (Fig. 1a). Thus, the effect of Ln γ1 peptide was mediated by PrP^{C} and was dependent on the KDI domain of Ln γ1 peptide. We evaluated also other measures of neuritogenesis and found that PrP^{C}- Ln γ1 peptide also promotes an increase in the number of neurites/cell (total number of neurites/number of cells with neurites) (Supplementary Fig. 1a) However, the peptide did not affect the mean length of neurites (Supplementary Fig. 1b) or percentage of neurites longer than 30 μm (Supplementary Fig. 1c).

It is likely that interaction between the Ln γ1 peptide and PrP^{C} triggered intracellular signal transduction cascades that promoted an increase in the number of cells with neurites. Therefore, an initial screen for the signaling pathway involved was conducted using a pharmacological approach. Figure 1b shows that inhibition of PLC with U73122, PKC with BIM and ERK1/2 with U0126 impaired neuritogenesis

evoked by Ln γ1 peptide. In contrast, the PKA inhibitor KT5720 was inactive with respect to inhibiting neuritogenesis.

We next measured the activity of ERK1/2, PKC and PKA to confirm that these pathways were activated in response to PrP^{C}-Ln γ1 interaction. *Prnp*$^{+/+}$ hippocampal neurons, treated with Ln γ1 peptide, presented a rapid increase in ERK1/2 phosphorylation of both p42 and p44 forms (Fig. 1c). In contrast, Ln γ1 peptide treatment had no effect on *Prnp*$^{0/0}$ neurons (Fig. 1d). Similarly, Ln γ1 peptide promoted PKC activation only in neurons from *Prnp*$^{+/+}$ mice, an effect that was blocked by bisindolylmaleimide (BIM, Fig. 1e). Phorbol 12-miristate 13- acetate (PMA), a PKC activator, induced enzyme activity in both *Prnp*$^{+/+}$ and *Prnp*$^{0/0}$ neurons. In contrast the PKA pathway was not activated by Ln γ1 peptide in neurons, while the PKA activator Forskolin promoted an increase on the enzyme activity in both cell types (Fig. 1f)

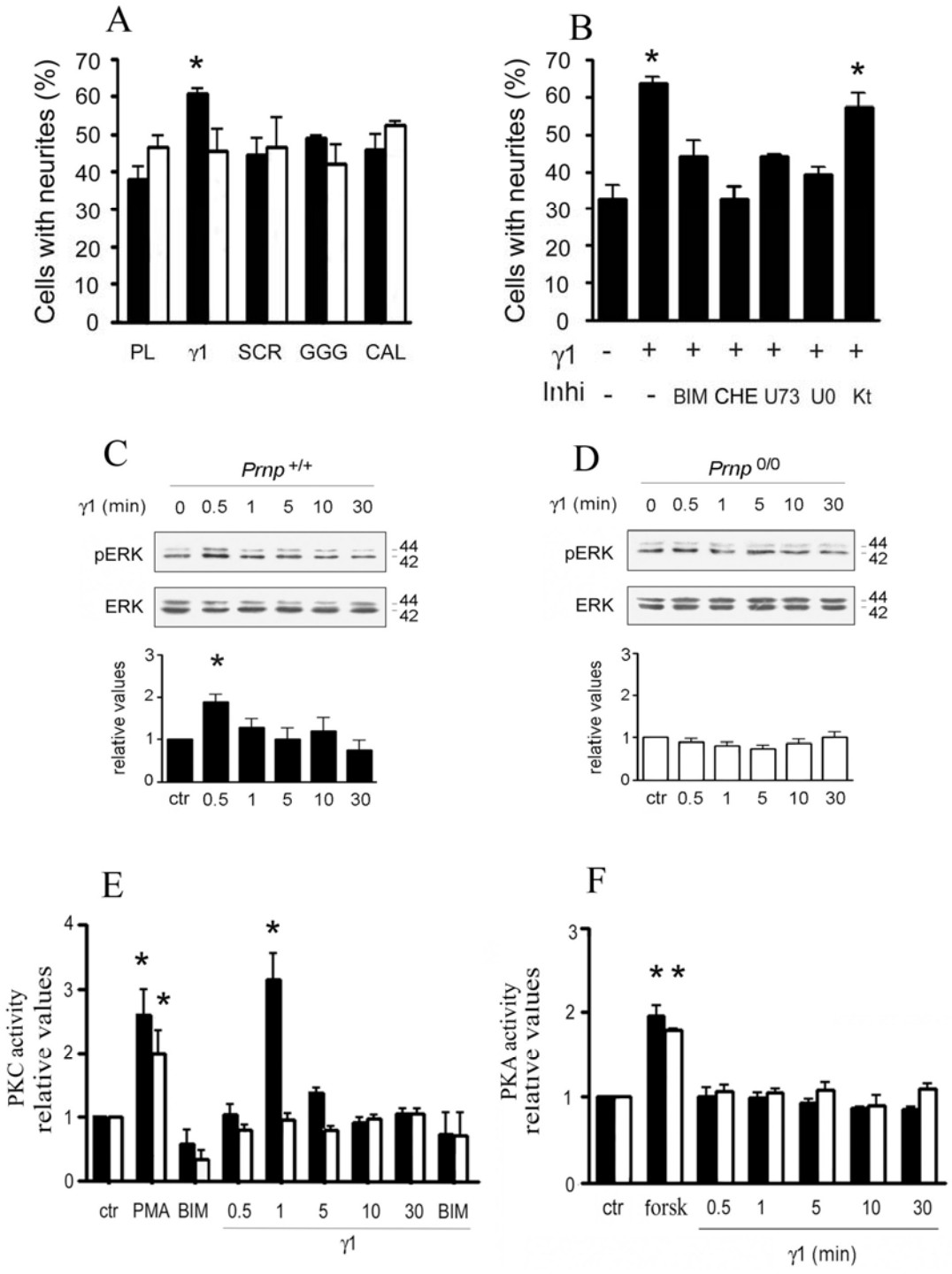

Figure 1 – Ln γ-1 peptide interaction to PrP^{C} induces PLC, PKA and ERk1/2-dependent neuritogenesis. (A) Primary hippocampal neuron cultures from *Prnp*$^{+/+}$ (filled bars) or *Prnp*$^{0/0}$ (open bars) mice were incubated with 37 μM of Ln γ-1 peptide (γ1), scrambled peptide (SCR), Ln γ-1 peptide where the KDI domain was modified (GGG) or a peptide from the caldendrin molecule (CAL). (B) *Prnp*$^{+/+}$ neurons were treated with Ln γ-1 peptide plus specific signaling inhibitors for PLC (U73122), PKC (BIM), ERK1/2 (UO) or PKA (Kt). (A, B) The percentage of cells with neurites was quantified in each condition. ERK1/2 phosphorylation in (C) *Prnp*$^{+/+}$ or in (D) *Prnp*$^{0/0}$ neurons treated with Ln γ-1 peptide (37 μM) at different time points (0.5 to 30 min) by immunobloting assays using antibodies

against ERK1/2 (ERK) or against the phosphorilated form of the enzyme (pERK). Relative levels of enzyme activity represent the ratio between phosphorilated ERK1/2 and total ERK, normalized to the untreated group (ctr). (E) PKC activity in cultured hippocampal neurons from *Prnp*$^{+/+}$ (filled bars) or *Prnp*$^{0/0}$ mice (open bars) treated or not (ctr) with Ln g-1 peptide (37 μM) at different time points (0.5 to 30 min). Phorbol 12-myristate 13-acetate (PMA) was used as internal control for PKC activation and BIM is a specific PKC inhibitor. (F) PKA activity in cultured hippocampal neurons from *Prnp*$^{+/+}$ (filled bars) or *Prnp*$^{0/0}$ mice (open bars) treated with Ln γ-1 peptide at different time points (0.5 to 30 min). Forskolin (Forsk) was used as internal control for PKA activation. The results represent media and standard error of at least three independent experiments analyzed and compared by one-way ANOVA and Newman-Keuls post test. * Denotes statistical significance when compared to control cells without treatment, $p < 0.05$.

In order to define the upstream signal for these pathways in response to PrP^{C}-Ln γ1 peptide binding, we evaluated ERK1/2 and PKC activation in the presence of specific inhibitors. The treatment of neurons with the PLC inhibitor U73122 blocked Ln γ1 peptide-mediated ERK1/2 phosphorylation (Fig. 2a) and PKC activity (Fig. 2b). In the presence of BIM, ERK1/2 phosphorylation was inhibited in *Prnp*$^{+/+}$ neurons treated with Ln γ1 peptide (Fig. 2a). However, PKC activity in response to Ln γ1 peptide treatment was unaffected when neurons were treated with an ERK1/2 inhibitor U0126 (Fig. 2b). Similar to the results obtained for the neuritogenesis studies (Fig. 1a), the SCR or GGG peptides did not affect the activity of either ERK1/2 or PKC in neurons (Fig. 2a,b). Taken together these results indicated that neuritogenesis induced by PrP^{C} interaction to Ln γ1 peptide required an initial activation of PLC which was followed by PKC and ERK1/2 activation.

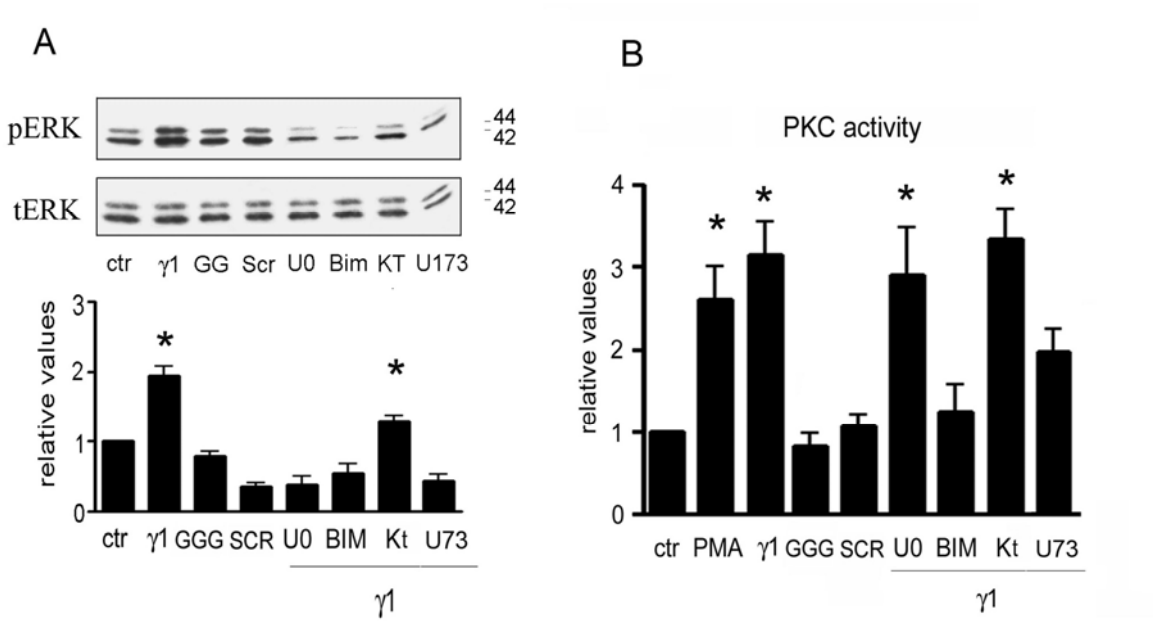

Figure 2 – Ln γ-1 peptide binding to PrP^C induces a sequential activation of PLC, PKC and ERK1/2. Hippocampal neuronal cultures from *Prnp*$^{+/+}$ mice were treated with γ-1 peptide (37 μM) with or without (ctr) PKC (BIM), PKA (Kt) or ERK1/2 (U0) inhibitors. Cultures were also treated with a peptide where the KDI domain of the Ln γ-1 peptide was substituted by three glycines (GGG) (37 μM) or a scrambled Ln γ-1 peptide (SCR) (37 μM). (A) ERK1/2 or (B) PKC activation was evaluated. (A) Relative levels of ERK1/2 activity represent the ratio between phosphorylated ERK1/2 and total ERK, normalized to the untreated group (ctr). (B) Relative levels of PKC represent the normalization of the phosphorylation in each condition and the phosphorylation in the untreated group (ctr). The results show the media and standard error of three independent experiments analyzed and compared by one-way ANOVA and Newman-Keuls test. * Denotes statistical significance when compared to control cells without treatment, $p < 0.01$.

Interaction of laminin γ-1 peptide with PrP^C increases intracellular Ca^{2+}

The experiments outlined above indicated that PrP^C-Ln γ1 peptide interaction resulted in the activation of PLC, which is coupled to the release of intracellular Ca^{2+} stores. Therefore, we first examined whether PrP^C-Ln γ1 peptide triggered the release of intracellular calcium in cultured neurons. Primary neuronal cultures from *Prnp*$^{+/+}$ and *Prnp*$^{0/0}$ mice were loaded with the intracellular Ca^{2+} dye- Fluo 3 AM. The addition of Ln γ1 peptide to *Prnp*$^{+/+}$ neurons cultured in the presence of extracellular Ca^{2+} resulted in a transient increase in fluorescence (Fig. 3a, solid line and 3f). When Ca^{2+} was removed from culture medium a significant calcium response to Ln γ1 peptide was still detected, but in lower levels than that evoked in the presence of extracellular Ca^{2+} (Fig. 3a, dashed line and 3a). In contrast, no alterations in intracellular Ca^{2+} concentrations were observed in *Prnp*$^{0/0}$ hippocampal neurons treated with Ln γ1 peptide (Figs. 3b,f). However, the treatment of these cells with thapsigargin (THG), a blocker of the Ca^{2+}-ATPase from endoplasmic reticulum, mobilized the release of intracellular Ca^{2+} stores (Fig. 3b), suggesting that these stores were available in *Prnp*$^{0/0}$ neurons. These results were reproduced in a second PrP^C-null mouse strain (Manson et al., 1994) with a different genetic background and its respective wild-type control, indicating that these observations are specifically associated to PrP^C-Ln γ1 peptide interaction (Supplementary Fig. 2).

The effect of Ln γ1 peptide on intracellular Ca^{2+} increase was completely blocked by PLC and $InsP_3$ receptor inhibitors (Fig. 3c), whereas the inactive analogue of U73122 (U73343) had no effect on intracellular Ca^{2+} release (data not shown). These results indicated that $InsP_3$ receptor-mediated release of endoplasmic

reticulum Ca^{2+} stores was required for the observed extracellular Ca^{2+} influx in response to Ln γ1 peptide treatment (Fig. 3a,f).

It is well known that, once mobilized from intracellular stores, calcium can activate channels in the plasma membrane (SOCs – store operated channels) and the opening of these channels promotes a Ca^{2+} influx from extracellular medium by a mechanism called Capacitative Calcium Entry, (CCE) (Putney, Jr. et al., 2001). In order to identify the type of plasma membrane channel involved in the PrP^C-Ln γ1 peptide evoked calcium influx, we incubated hippocampal neurons with SKF-96365 (dashed lines), a specific inhibitor of store operated channels (SOCs) or a mix of voltage-gated calcium channel (VGCC) inhibitors (Omega-conotoxin MVIIC – 1 μM plus Nifedipine – 50 μM, solid lines). The increase in intracellular Ca^{2+} evoked by Ln γ1 peptide diminished 58 ± 5% by SKF-96365 (Fig. 3d, dashed line and 3f), whereas no inhibition was detected in the presence of VGCC inhibitors (Fig. 3d, solid line and 3f). Control experiments demonstrated that KCl induced an increase of intracellular Ca^{2+} by VGCC activation which was totally blocked by the VGCC inhibitors cocktail (data not show). In order to test the specificity of Ln γ1 peptide-PrP^C interactions in the release of intracellular Ca^{2+} stores, *Prnp*$^{+/+}$ neurons were treated with either a Ln γ1 peptide lacking the KDI domain (Fig. 3e, solid line) or a scrambled Ln γ1 peptide (Fig. 3e, dashed line). There was no effect of these control peptides on Ca^{2+} increase. A summary of the relative levels of intracellular Ca^{2+} in hippocampal neurons following the different treatments with inhibitors is presented in Fig. 3f.

To further confirm the role of PrP^C in the response to Ln γ1 peptide we used CF10 cells, an immortalized neuronal cell line derived from a PrP^C-null mice

(Caetano et al., 2008). As expected CF10 cells did not present an intracellular Ca^{2+} response upon Ln γ1 peptide treatment (Fig. 3g). However, the re-expression of PrP^C (CF10-PrP^C) rescued signaling in these cells (Fig. 3g,h). Similar to what was observed in primary neuronal cultures (Fig. 3a-f), in CF10 cells re-expressing PrP^C, Ln γ1 peptide treatment resulted in increased intracellular Ca^{2+} concentrations that were mobilized from intracellular stores and by extracellular Ca^{2+} influx (Figs. 3g,h). Control experiments demonstrated that the inactive peptides, GGG and SCR, did not increase Ca^{2+} in CF10 cells reconstituted with PrP^C (supplementary Fig. 3). Together, these data indicated that Ln γ1 peptide engagement of PrP^C activated the PLC-dependent mobilization of Ca^{2+} from the endoplasmic reticulum followed by the subsequent activation of SOCs on the plasma membrane.

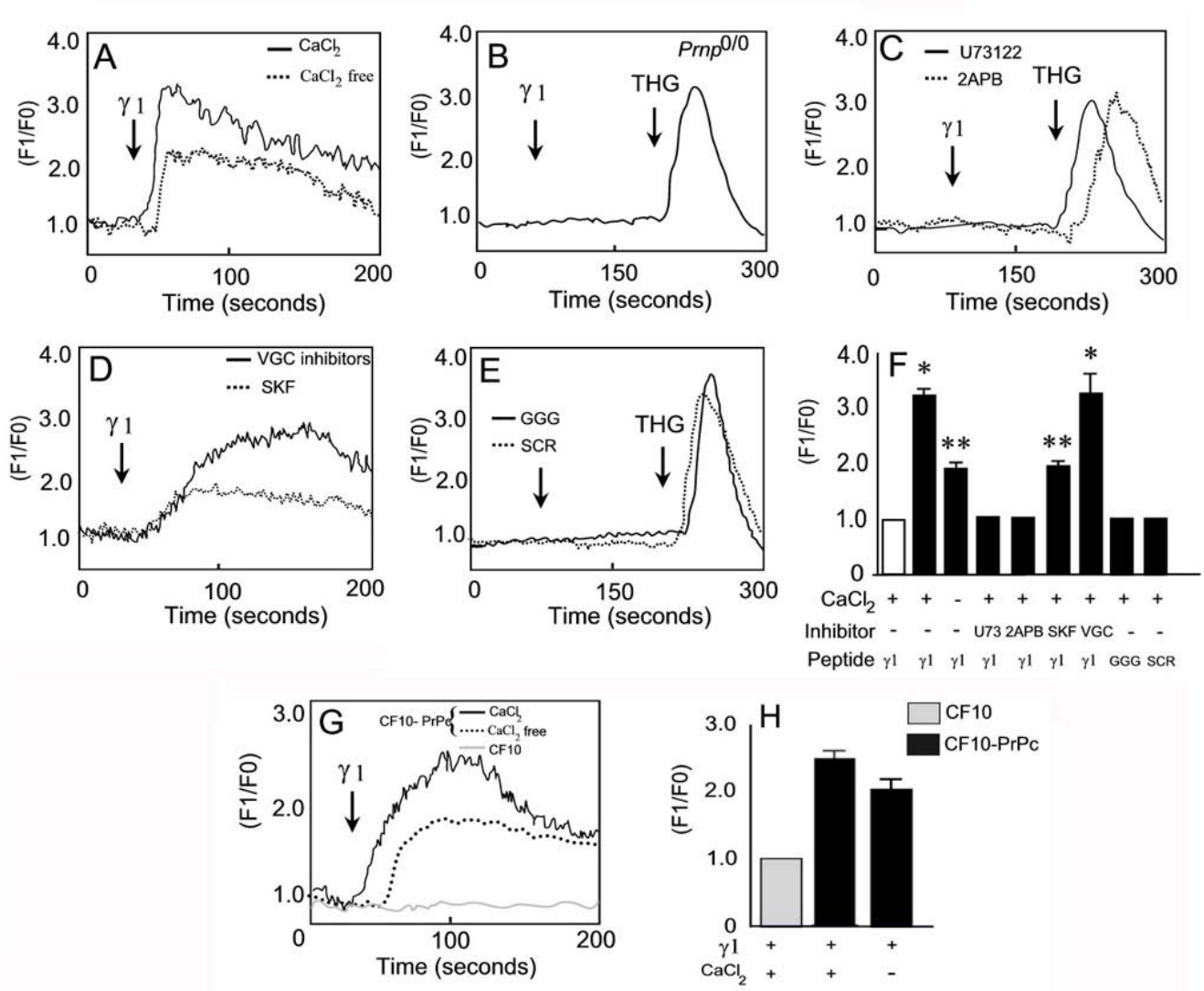

Figure 3 - Ln γ-1 peptide interaction with PrP^C increases $[Ca^{2+}]_i$. (A) *Prnp*$^{+/+}$ or (B) *Prnp*$^{0/0}$ hippocampal neurons loaded with Fluo 3 AM were treated with Ln γ-1 peptide (37 μM) in the presence (solid line) or absence (dashed line) of Ca^{2+} at the extracellular medium. *Prnp*$^{0/0}$ cell cultures were also treated with thapsigargin (THG) and show intracellular Ca^{2+} stocks. (C) *Prnp*$^{+/+}$ neurons were pre-incubated with PLC inhibitor (U73122), $InsP_3$ receptor blocker (2APB) or (D) voltage gated Ca^{2+} channel or Store Operated channel inhibitors before Ln γ-1 peptide treatment. (E) *Prnp*$^{+/+}$ neurons were treated with a Ln γ-1 peptide where the KDI domain was changed by three glycines (GGG) or SCR peptide. (F) Relative intracellular Ca^{2+} levels in neurons treated with Ln γ-1 peptide and/or signaling pathway inhibitors. (G) CF10 PrP^C-null immortalized neuronal cell line or a CF10 where the PrP^C was re-expressed (CF10-PrP^C) treated with Ln γ-1 peptide (120μM) in medium supplemented (solid lines) or not with (dashed line) $CaCl_2$. (H) Relative intracellular Ca^{+2} levels in CF10 and CF10-PrP^C cells treated with Ln γ-1 peptide in the presence or absence of extracellular $CaCl_2$. (F, H) The results represent the media and standard error of three independent experiments analyzed and compared by one-way ANOVA and Newman-Keuls test. * Denotes statistical significance when compared to control cells without treatment and ** denotes statistical significance when compared to control cells without treatment and to cells treated with Ln γ-1 peptide in the presence of extracellular Ca^{2+}, $p < 0.01$.

*GPCR receptors mediate PrP^C-Ln γ-1 peptide signaling and neuritogenes*is

The signaling pathways activated by PrP^C-Ln γ1 peptide resembled those commonly activated by Gq/11-coupled GPCRs such as bradykinin (BK) and metabotropic glutamate receptors. BK receptor activation was previously demonstrated to stimulate intracellular Ca^{2+} release in N2a cells infected with prions (Kristensson et al., 1993). Thus, we examined whether the BK receptor might be a candidate GPCR linking PrP^C-Ln γ1 peptide engagement to the activation of PLC-mediated Ca^{2+} release. However, the treatment of hippocampal neurons from wild-type mice with a BK receptor type 2 antagonist (HOE-140) failed to block Ln γ1 peptide-mediated increases of intracellular Ca^{2+} (Fig. 4a dashed line). In contrast, HOE-140 completely blocked BK-stimulated increases in intracellular Ca^{2+} concentrations (Fig. 4b, dashed line). Thus, these data indicated that type 2 BK receptors were not involved in the signaling promoted by PrP^C-Ln γ1 peptide interaction.

Group I metabotrophic receptors (mGluR1 and mGluR5) signaling was previously found to be altered in cerebral cortex of Creutzfeldt-Jakob disease patients (Rodriguez et al., 2005). Thus, we tested whether either mGluR1 (LY367385) or mGluR5 (MPEP) antagonists, which effectively blocked increases in intracellular Ca^{2+} concentrations mediated by the non-selective Group I mGluR agonist (Fig 4d), would prevent Ln γ1 peptide-stimulated increases in intracellular Ca^{2+} concentrations. When hippocampal neurons were treated with LY367385 or MPEP at concentrations that specifically block mGluR1 or mGluR5 (Kingston et al., 2002;Gasparini et al., 1999), a reduction of 72 ± 4 or 77 ± 5 % was respectively observed in the intracellular Ca^{2+} increase promoted by the γ1 peptide (Fig. 4c,e).

mGluR1 or mGluR5 antagonists effectively attenuated Ln γ1 peptidemediated PKC activation (Fig. 4f). In addition, the combination of these inhi itors did not present addictive blocking effect upon Ln γ1 peptide-mediated increase in Ca^{2+} levels and PKC activity (Figs. 4e,f).

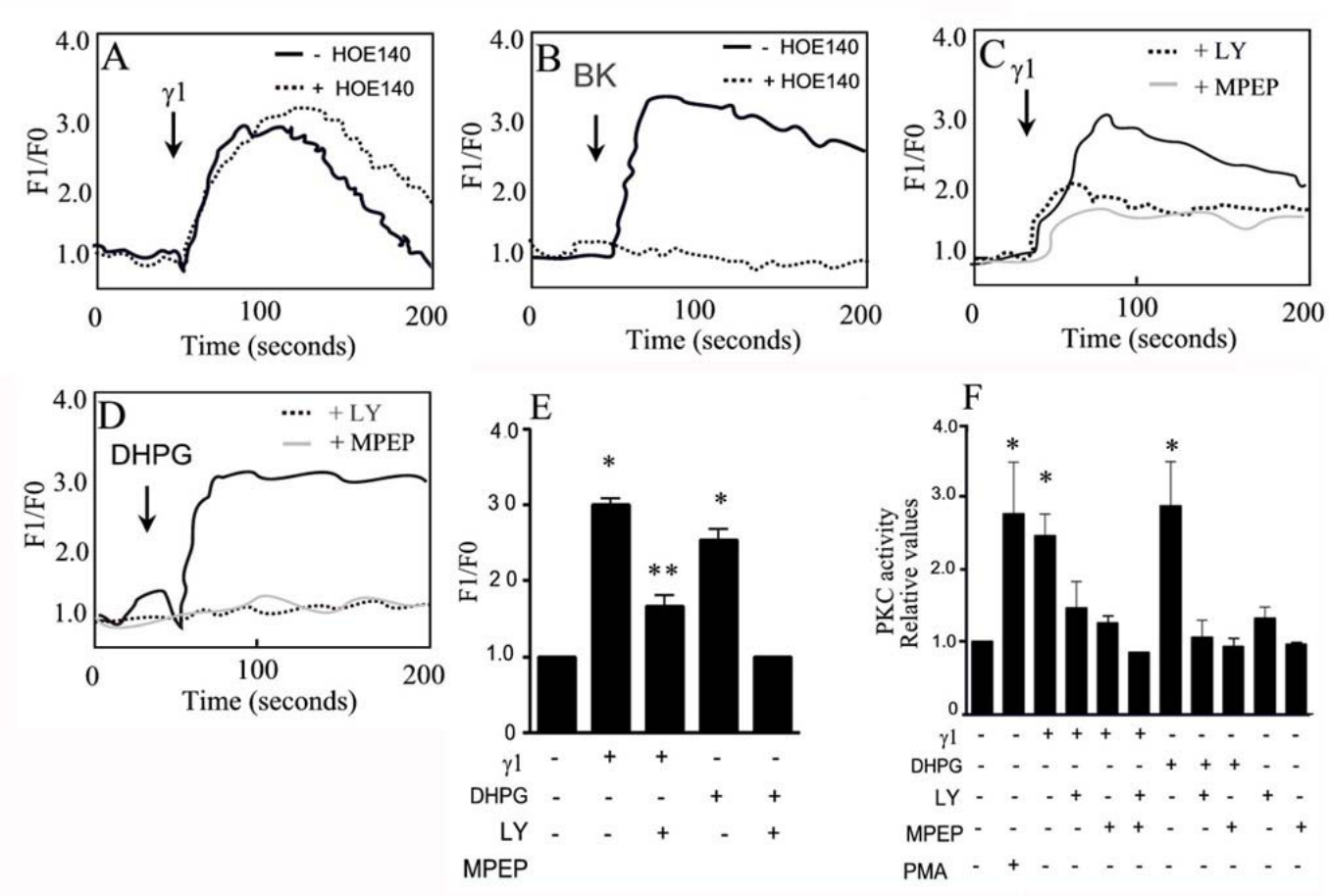

Figure 4 –Group I mGluRs mediate intracellular Ca^{2+} increase and PKC activation promoted by PrP^{C}-Ln γ-1 peptide interaction. (A) *Prnp*$^{+/+}$ hippocampal neurons loaded with Fluo 3 AM were treated with Ln γ-1 peptide (37 μM) or (B) bradikinin in the absence (solid lines) or presence (dashed lines) of the bradykinin receptor inhibitor HOE 140. (C) *Prnp*$^{+/+}$ neurons were also treated with Ln γ-1 peptide (37 μM) or (D) the metabotrophic glutamate receptor agonist DHPG in the absence (solid black line) or presence or of mGluR1 (LY367385, dashed lines) or mGluR5 (MPEP solid gray line) antagonists. (E) Intracellular Ca^{2+} levels for all treatments are shown as relative values to that in control conditions (without treatment). (F) PKC activity was measured in primary neuronal cultures treated with Ln γ-1 peptide (37 μM) or DHPG in the presence or absence of LY367385 or MPEP. Values as relative to the control condition without treatment. (E, F) The results represent the media and standard error of three independent experiments analyzed and compared by one-way ANOVA and Newman-Keuls test. * Denotes statistical significance when compared to control cells without treatment and ** denotes statistical significance when compared to control cells without treatment or to cells treated with Ln γ-1 peptide, $p < 0.01$.

To confirm the role of Group I mGluRs in PrP^C-Ln γ1 peptide-mediated signaling we transfected human embryonic kidney (HEK 293) cells with PrP^C and either mGluR1 or mGluR5. When HEK 293 cells were transfected with PrP^C alone and treated with Ln γ1 peptide no increase in intracellular Ca^{2+} concentration was observed (Fig. 5a,c). However, the expression of PrP^C along with either mGluR1 or mGluR5 resulted in an increase in intracellular Ca^{2+} in response to Ln γ1 peptide treatment (Fig. 5a,c). No Ca^{2+} response was observed when cells were treated with Ln γ1 scrambled peptide (Fig. 5a,c). Cells expressing PrP^C failed to respond to DHPG, but when they expressed either mGluR1 or mGluR5, increased Ca^{2+} release was observed following agonist treatment (Fig. 5b).

The PrP^C-Ln γ1 peptide-dependent activation of GFP-PKCβII plasma membrane translocation was also analyzed in HEK 293 cells transiently transfected to express PrP^C alone or along with either mGluR1 or mGluR5 (Fig. 6). Under resting conditions GFP-PKCβII was diffusely localized within the cytoplasm of cells and the treatment of cells with Ln γ1 peptide (Fig. 6b,d,f), but not the SCR peptide (Fig. 6a,c,e), resulted in the redistribution of GFP-PKCβII to plasma membrane in 54% of the cells expressing PrP^C along with mGluR1a (Fig. 6d, n=33 cells) and in 33% of the cells expressing PrP^C along with mGluR5 (Fig. 6f, n=18). There was no GFP-PKCβII translocation in response to Ln γ1 peptide in cells expressing PrP^C alone (Fig. 6b, n = 36 cells).

Finally, the role of group I mGluRs in regulating the neuritogenesis mediated by PrP^C interaction with Ln γ1 peptide was evaluated in primary neuronal cultures. We found that the treatment of cells with mGluR1- and mGluR5-specific antagonists (LY367385 and MPEP, respectively) abrogated neuritogenesis mediated by PrP^C- Ln

γ1 peptide engagement (Fig. 7a-c and h). Moreover, the activation of endogenous mGluRs with the group I metabotropic receptor agonist DHPG promoted neuritogenesis, which could also be blocked by the antagonists LY367385 and MPEP (Fig. 7d-f and i). Thus, group I mGluRs were involved in the neuritogenic actions of Ln γ1 peptide and remarkable, group I mGluRs activation can by itself induce neuritogenesis. Together, these data indicated that neuritogenesis mediated by PrP^{C}- Ln γ1 peptide interaction was triggered by the activation of mGluR1 and/or mGlurR5 metabotropic receptor-mediated signal transduction.

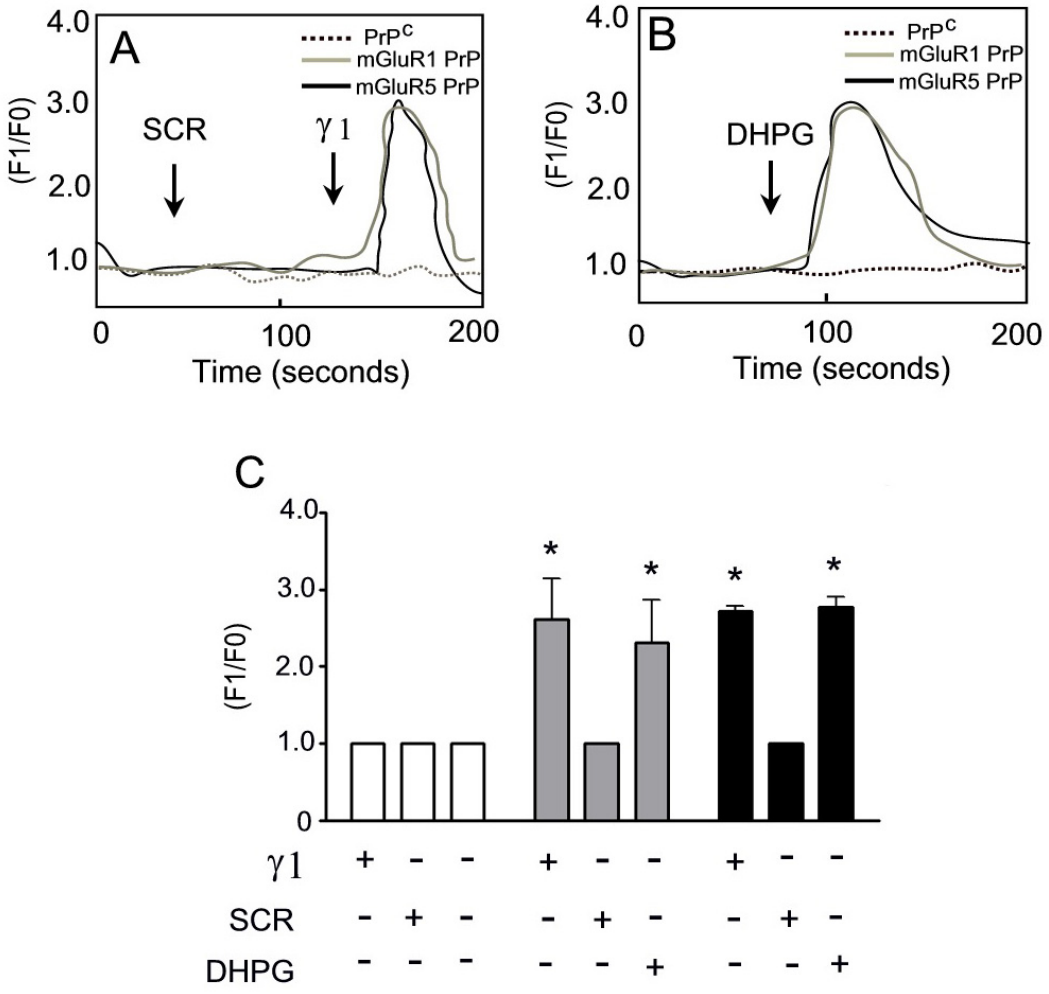

Figure 5 – Expression of mGluR1 and mGluR5 receptors rescues intracellular Ca^{2+} increase promoted by Ln γ-1 peptide in HEK293 cells. (A) HEK293 cells were transfected with PrP^C (dashed lines) or PrP^C plus mGluR1 (solid gray lines) or PrP^C plus mGluR5 expression (solid black lines) vectors and treated with scrambled Ln γ-1 peptide (SCR) followed by Ln γ-1 peptide (g1) both at 75 μM. (B) Cells transfected as in (A) were treated with the metabotrophic glutamate receptor agonist, DHPG (100 μM). (C) Intracellular Ca^{2+} levels for all treatments are shown as relative values to that in control conditions (without treatment). Open bars represent cells transfected with the PrP^C expression vector, gray bars represent cells transfected with PrP^C plus mGluR1 expression vectors and black bars represent cells transfected with PrP^C plus mGluR5 expression vectors. The results represent the media and standard error of three independent experiments analyzed and compared by one-way ANOVA and Newman-Keuls test. * Denotes statistical significance when compared to control cells without treatment, $p < 0.01$.

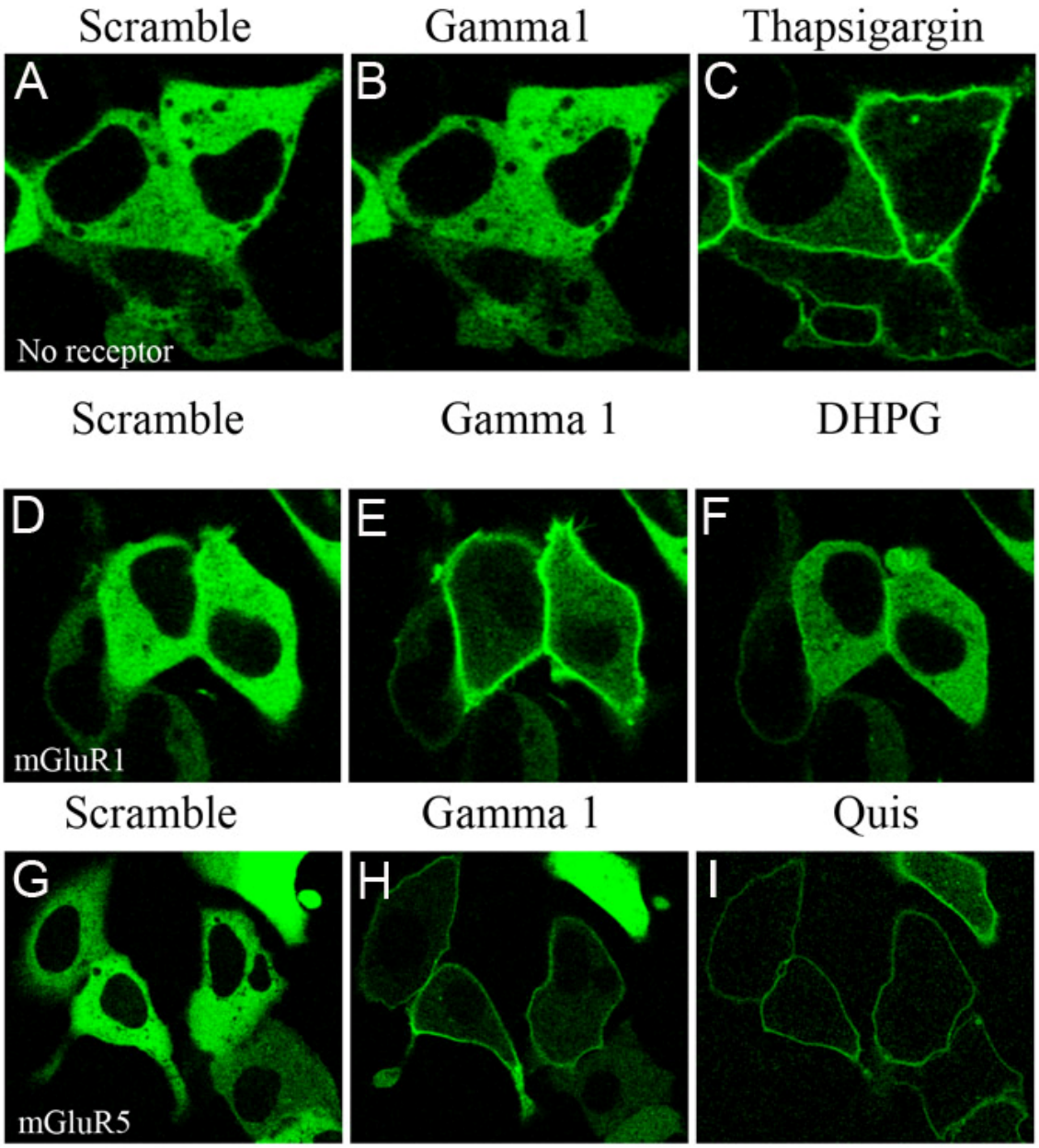

Figure 6 - Expression of mGluR1 and mGluR5 receptors rescues PKC activation induced by PrP^{C}-Ln γ-1 peptide in HEK 293 cells. Live HEK 293 cells expressing PrP-3F4 alone (A-C) or with either mGluR1a (D-F) or mGluR5 (G-I) receptors were treated sequentially with scramble peptide (A, D and G), γ1 peptide (B, E and H), DHPG for mGluR1a (G) and quisqualate for mGluR5 (I). Cells expressing PrP-3F4 were treated with thapsigargin as a positive control (C). There was no GFP-PKC$^{\beta}$II translocation in response to γ1 peptide in cells expressing PrP alone (top panel, n = 36 cells) whereas 54% of the cells expressing mGluR1a (middle panel, n = 33 cells) and 33% of the cells expressing mGluR5 (lower panel, n = 18 cells) responded to γ1 peptide. None of the cells responded to the scramble peptide. These results were obtained in 4 separate transfections.

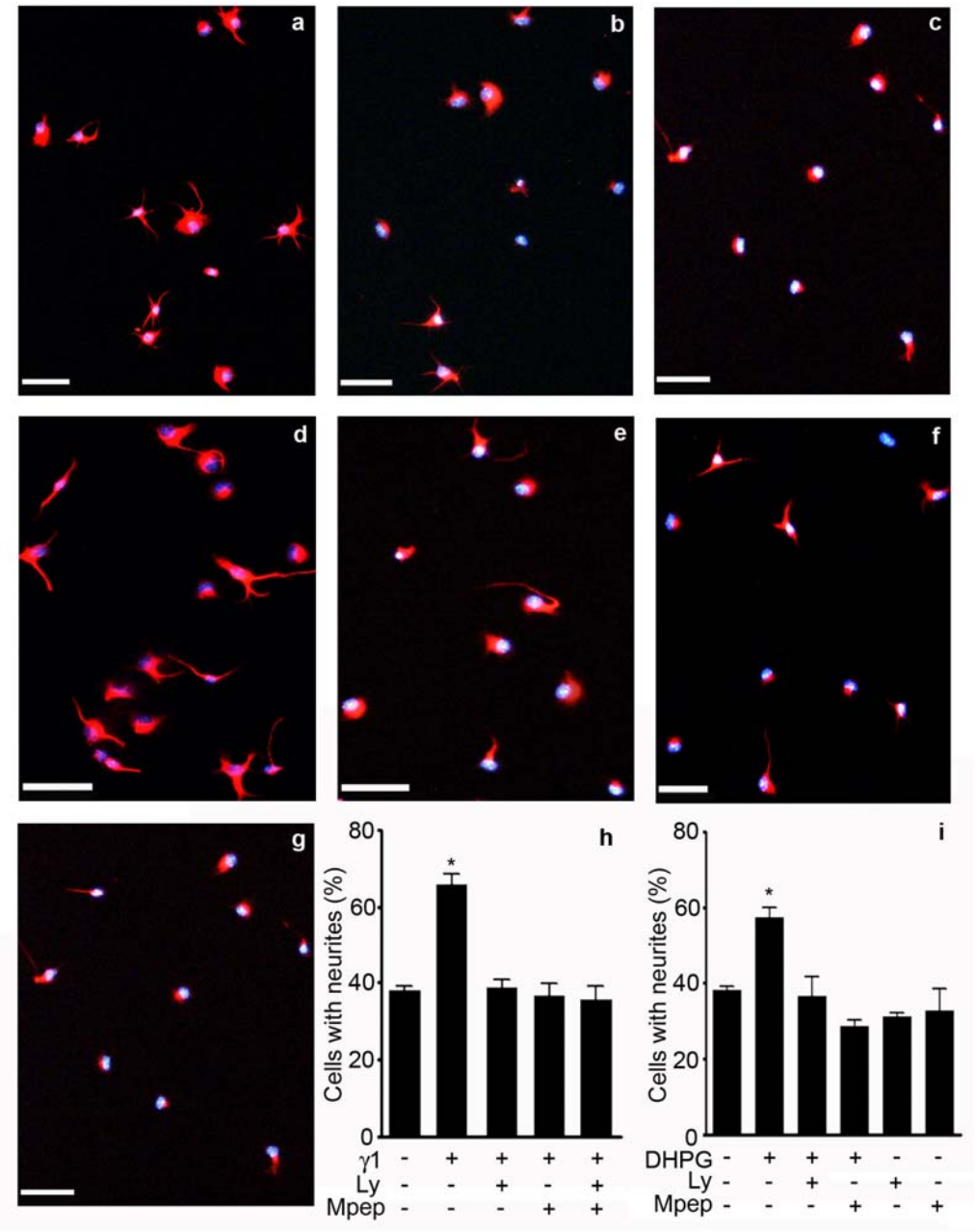

Figure 7- Neuritogenesis induced by PrP^{C}-Ln γ-1 peptide interaction is abolished by group I metabotropic glutamate receptor inhibitors. (A) Representative images of *Prnp*$^{+/+}$ primary hippocampus neurons treated with with Ln γ-1 peptide (upper panel) or with the metabotrophic glutamate agonist DHPG (botton panel) in the presence of mGluR1 (LY367385) or mGluR5 (MPEP) inhibitors. Inset represents cell plated over polilysine). (B) cells treated with Ln γ-1 peptide or with (C) the metabotrophic glutamate agonist DHPG in the presence of mGluR1 (LY367385) or mGluR5 (MPEP) inhibitors. The percentage of cells with neurites was quantified in each condition. Values represent the media and standard error of three independent experiments analyzed and compared by one-way ANOVA and Newman-Keuls test. *Denotes statistical significance when compared to control cells without treatment, $p < 0.01$.

Discussion

The present study elucidates a novel mechanism by which PrP^C transduces extracellular signals to evoke neuronal differentiation. Here we show that upon interaction with Ln γ1 peptide, PrP^C is able to modulate Group I metabotropic glutamate receptors (mGluR1 and mGluR5) causing PLC activation, increasing Ca^{2+} mobilization from intracellular stores followed by Ca^{2+} influx, PKC and ERK1/2 activation that leads to an increase in neuronal differentiation (Fig. 8). These data provide evidence on a pathway through which a multiprotein complex organized by PrP^C (Linden et al., 2008; Martins et al., 2002) leads to intracellular signaling that promotes neuritogenesis.

Extracellular matrix (ECM) components, in particular laminin, are fundamental for survival and differentiation of neurons in the developing nervous system and in remodeling of both normal and diseased adult brain (Rauch, 2004). Laminin is a heterotrimeric molecule that is composed of a diverse variety of α, β and γ chains from which α-2, β-1 and γ-1 are highly expressed in hippocampal structures (Hagg et al., 1997). Remarkably, the carboxy-terminal peptide from Ln γ1 chain (RNIAEIIKDI) has been associated with neurite outgrowth (Liesi et al., 1989; Liesi et al., 2001), neuronal migration (Liesi, 1985) and axonal guidance (Wiksten et al., 2003), which is consistent with the localization of the Ln γ-1 chain to cellular bodies and proximal processes (Hagg et al., 1997). Interestingly, the tri-peptide KDI from Ln γ1 chain peptide specifically modulates neurite outgrowth (Liesi et al., 2001), neuronal protection against glutamate excitotoxicity mediated by glutamate receptors (Wiksten et al., 2004) and defense against 6-hydroxydopamine (6-OHDA)-induced neurotoxicity, a rat experimental model for Parkinson's disease (Vaananen et

al., 2006). Herein, we confirmed previous data showing that PrP^C is the cellular receptor for Ln γ1 peptide whose binding promotes neuritogenesis (Graner et al., 2000) and mapped the KDI domain within the Lnγ1 peptide as the functional binding site for PrP^C. These findings have major implications since they suggest that the PrP^C-LN γ1 peptide complex can be targeted for therapeutic interventions in neuronal injury.

The present experiments also maps the signaling pathways triggered by PrP^C-Ln γ1 peptide interaction which involves PLC activation, generation of $InsP_3$ and Ca^{2+} mobilization from ER. Interesting, prion infection modifies Ca^{2+} responses by altering plasma membrane composition and by a decrease of $InsP_3$ production, consequently reducing Ca^{2+} mobilization from intracellular stores (Kristensson et al., 1993). Under oxidative stress, PrP^C induces intracellular Ca^{2+} increases that modulate neuroprotective functions (Krebs et al., 2007). PrP^C expression in non neuronal cells also induces Ca^{2+} influx, limits Ca^{2+} release from the ER as well as uptake by mitochondria; these events may prevent the activation of cell death pathways (Brini et al., 2005). In contrast, calcium influx is reduced in neurons derived from PrP^C-null mice when compared to wild-type mice (Fuhrmann et al., 2006). Therefore, PrP^C is able to organize different cellular signals that control Ca^{2+} homeostasis, which may be corrupted in cells derived from PrP^C-null animals, during prion infection, or in any other neurodegenerative condition where PrP^C plays a role, such as in Alzheimer's disease in which PrP^C can specifically bind to the Aβ oligomers (Lauren et al., 2009).The participation of PrP^C in diverse signaling pathways has been described.

Some of these pathways were defined when the signaling between PrP^C-null and wild-type cells was compared under different conditions. A few were dependent also upon the crosslinking of PrP^C with antibodies, and others were dependent on PrP^C engagement by specific ligands. However, only a limited number of transmembrane proteins that interact with PrP^C have been identified (Linden et al., 2008). Thus, little is known about the mechanisms by which the activation of the extracellular GPIanchored PrP^C is transduced to intracellular signals. The identification of transmembrane proteins involved with this mechanism is of major interest, as they permit the connection of proposed PrP^C-organized cell surface multiprotein complexes to signaling pathways responsible for the specificity and diversity of PrP^C cellular functions.

Our data indicate that PrP^C signaling in response to the Ln γ1 peptide binding uses a Gq/11-coupled receptor. One of the most widely expressed GPCRs in the brain coupled to Gq/11 are the group I metabotropic glutamate receptors, mGluR1 and mGluR5. These receptors are coupled to the release of intracellular Ca^{2+} and the activation of PKC (Bruno et al., 2001). Previous studies have demonstrated reduced group I mGluR signaling (PLC and PKC activity) in CJD (Rodriguez et al., 2005). Our data reveal that pharmacological blockade of either mGluR1 or mGluR5 attenuates PrP^C-Ln γ1 peptide-mediated increases in intracellular Ca^{2+} and PKC activity, while inhibition of both receptors abolished intracellular signaling evoked by Ln γ1 peptide. Thus, the PrP^C-Ln γ1 peptide complex induces cellular signaling using both mGluR1 and mGluR5. This was further confirmed by experiments in which we functionally reconstituted PrP^C-Ln γ-1 mediated signaling in HEK 293 cells, by expressing either mGluR1 or mGluR5. Specificity of this signaling pathway

was demonstrated by the fact that the antagonist of the type II BK receptor, which is also a Gq/11- coupled GPCR, did not block Ca^{2+} release following PrP^C-Ln γ-1 engagement.

Group I mGluRs have been implicated in the targeting of thalamic axons to somatosensory cortical barrels (Hannan et al., 2001) and were found to promote dendritic protein synthesis. The activation of mGluR1 decreases the proliferation and increases differentiation of early neuronal progenitors, whereas mGluR5 promotes the survival of neuronal-restricted precursors (Castiglione et al., 2008), indicating that group I mGluRs control neuronal differentiation. In fact, our data support these observations, in that we demonstrate that the blockade of either mGluR1 or mGluR5 inhibits PrP^C-Ln γ1 peptide-induced neuritogenesis and pharmacological activation of group I mGluRs induces neuritogenesis in hippocampal neurons. Together these data point to an important role for the functional interaction between PrP^C-laminin, mGluR1 and mGluR5 in neuronal differentiation.

The pharmacological blockade of either mGluR1 or mGluR5 has been implicated in long-term memory and spatial memory impairment respectively (Baker et al., 2008;Bikbaev et al., 2008). Interestingly, in mice lacking mGluR5 the acquisition of fear conditioning is partially impaired, whereas extinction of both contextual and auditory fear is completely abolished (Xu et al., 2009). It has been previously demonstrated that PrP^C-null mice exhibit eficits in hippocampal-dependent spatial learning which are rescued in transgenic mice expressing PrP^C only in neurons (Criado et al., 2005). We also demonstrated that PrP^C-Ln γ1peptide interaction mediates long-term memory (Coitinho et al., 2006). Thus, these data is

consistent with a role of Group I mGluRs in PrP^C–Ln γ1 peptide signaling associated with memory consolidation.

Signaling by PrP^C may have wider consequences than just providing a mechanism(s) that becomes disrupted in prion diseases. Recent work has shown that PrP^C is also a receptor for Aβ oligomers (Lauren et al., 2009). PrP^C- Aβ engagement interferes with synaptic plasticity, as long-term potentiation (LTP) is disrupted in wild-type mice following Aβ treatment but it is unaffected in hippocampal slices from PrP^C-null mice (Lauren et al., 2009). In addition, it has been recently demonstrated that Aβ oligomers enhance long-term depression (LTD), reduce dendritic spine density and disrupt memory41. Remarkable, the increase in LTD is mediated by the activation of either Group I/II mGluRs or NMDA receptors due to a decrease in glutamate uptake (Li et al., 2009). In addition to promoting signaling through group I mGluRs, PrP^C also interacts with NMDA receptors resulting in the inhibition of excitatory responses in neurons (Khosravani et al. 2008).

Amyloid precursor protein (APP) is also a highly specific ligand for the IKVAV peptide found within the α-chain of laminin and their interaction also mediates neuritogenesis (Kibbey et al., 1993). Therefore, as PrP^C and APP interact with different laminin domains, a more extensive protein complex may be organized at the cell surface comprising laminin, APP, PrP^C and mGluR1/5. This functional organization might be disrupted by altered APP cleavage and release of Aβ oligomers. Hence, the association of Aβ oligomers with PrP^C may result in the activation and/or disruption of signaling pathways engaged by physiological PrP^C ligands, leading to impaired neuronal plasticity and neuronal death. If this is the case, the functional interaction of PrP^C with mGluRs activated by the LN γ1 peptide may

also be implicated in Alzheimer's disease. Engagement of receptors of the GPCR family by PrP^C may provide unique opportunities to modulate PrP^C-dependent signaling in neurodegenerative disorders.

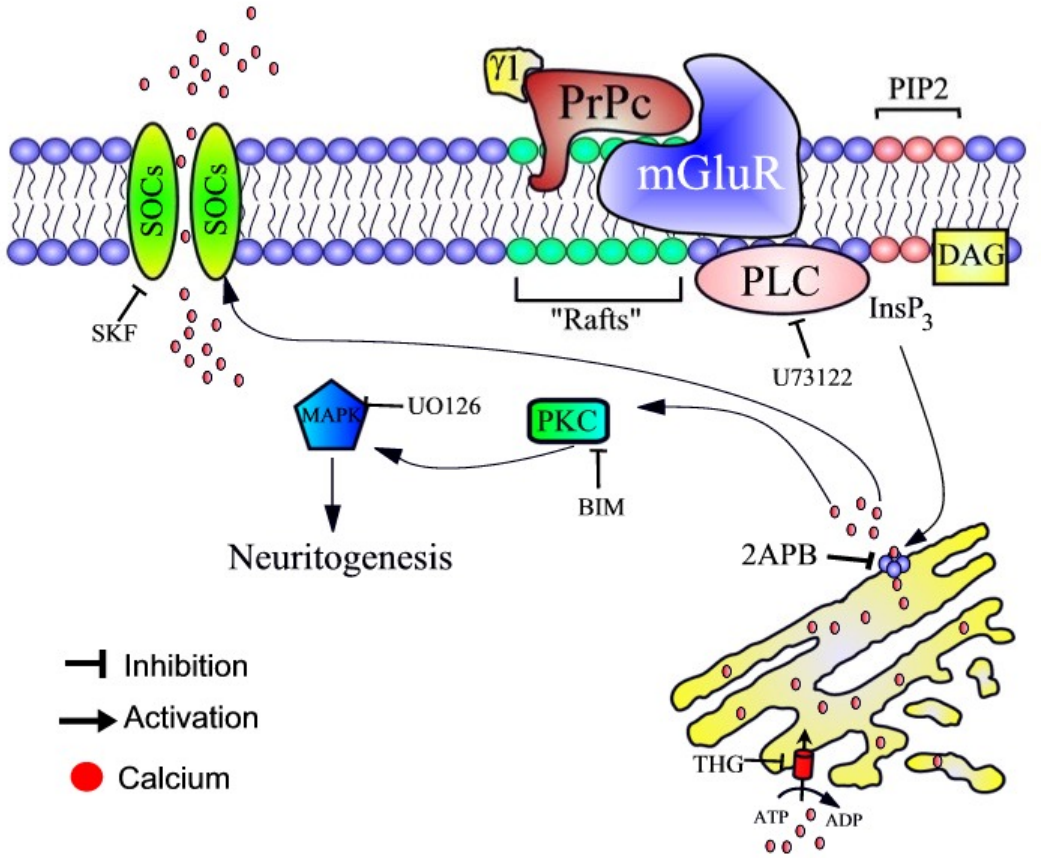

Figure 8 – Schematic model of signaling events mediated by PrP^C-Ln γ-1 peptide interaction. PrP^C-Ln γ-1 peptide interaction recruits mGluR1 and/or mGluR5 receptors, promoting activation of PLC which generates $InsP_3$ that binds to specific receptors in endoplasmatic reticulum (ER). The activation of these last receptors cause Ca^{2+} mobilization from ER and promotes PKC followed ERK1/2 which mediate neuritogenesis. Ca^{2+} mobilization from ER also activates Ca^{2+} influx from extracellular space by SOCs.

Supplementary Figures

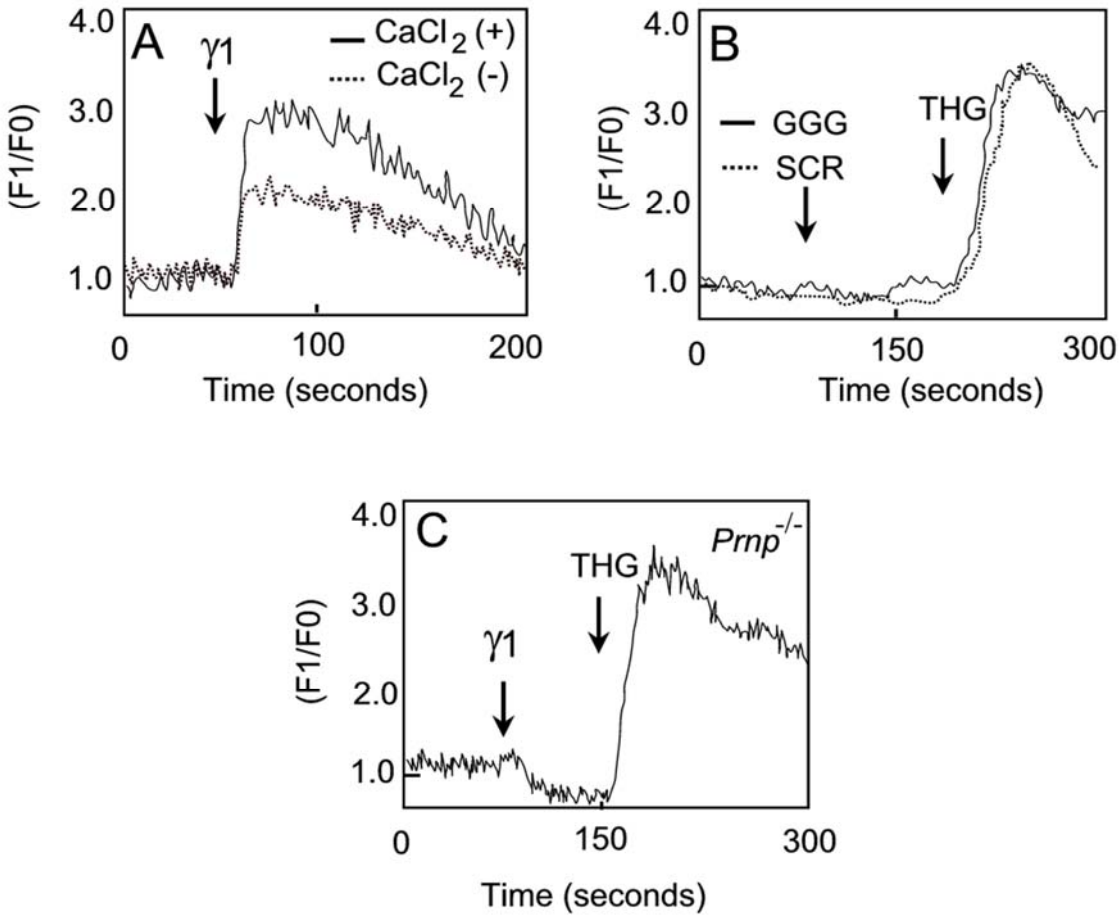

S1 - Ln γ-1 peptide interaction with PrP^C Increases $[Ca^{2+}]_i$. Cultured hippocampal neurons from *Prnp*$^{wt/wt}$ or *Prnp*$^{-/-}$ (Manson et al., 1994) were loaded with intracellular calcium probe Fluo3 AM. (A) *Prnp*$^{wt/wt}$ or (B) *Prnp*$^{-/-}$ neurons were treated with Ln γ-1 peptide (37 μM) in the absence (dashed line) or presence (solid line) of Ca^{2+} at the extracellular medium. *Prnp*$^{-/-}$ were treated with Thapsigargin (THG) to demonstrate the presence of normal intracellular stocks of Ca^{2+}. (C) *Prnp*$^{wt/wt}$ neurons were treated with an Ln γ-1 peptide where the KDI domain was substituted by glycines (GGG) (solid line) or with a scrambled Ln γ-1 peptide (dashed line).

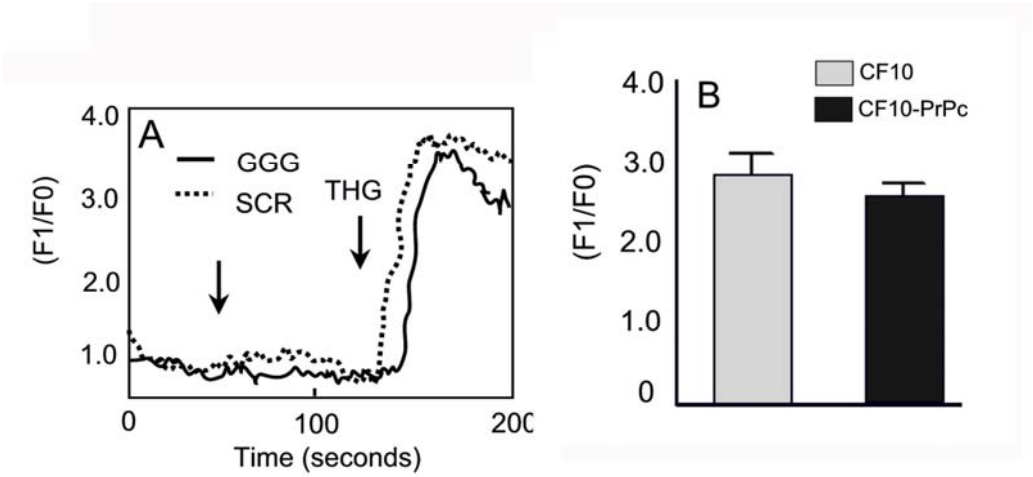

S2 - Ln γ-1 peptide interaction with PrP^C increases $[Ca^{2+}]_i$. (A) CF10 PrP^C-null immortalized neuronal cell line or a CF10 where the PrP^C was re-expressed (CF10-PrP^C) were loaded with the intracellular calcium probe Fluo3 AM and treated with a Ln γ-1 peptide where the KDI domain was substituted by (GGG) (solid lines) or with scrambled peptide (open line). After that, cells were treated with THG to demonstrate that Ca^{2+} can be mobilized from ER in these cells. (B) Intracellular Ca^{2+} levels after THG treatment in CF10 (gray bar) or CF10 PrP^C (black bar) cells are relative to the untreated condition (open bar).

References

Anborgh PH, Godin C, Pampillo M, Dhami GK, Dale LB, Cregan SP, Truant R, Ferguson SS (2005) Inhibition of metabotropic glutamate receptor signaling by the huntingtin-binding protein optineurin. J Biol Chem 280:34840-34848.

Baker KD, Edwards TM, Rickard NS (2008) Inhibition of mGluR1 and IP3Rs impairs long-term memory formation in young chicks. Neurobiol Learn Mem 90:269-274.

Bikbaev A, Neyman S, Ngomba RT, Conn J, Nicoletti F, Manahan-Vaughan D (2008) MGluR5 mediates the interaction between late-LTP, network activity, and learning. PLoS One 3:e2155.

Brini M, Miuzzo M, Pierobon N, Negro A, Sorgato MC (2005) The prion protein and its paralogue Doppel affect calcium signaling in Chinese hamster ovary cells. Mol Biol Cell 16:2799-2808.

Bruno V, Battaglia G, Copani A, D'Onofrio M, Di IP, De BA, Melchiorri D, Flor PJ, Nicoletti F (2001) Metabotropic glutamate receptor subtypes as targets for neuroprotective drugs. J Cereb Blood Flow Metab 21:1013-1033.

Bueler H, Fischer M, Lang Y, Bluethmann H, Lipp HP, DeArmond SJ, Prusiner SB, Aguet M, Weissmann C (1992) Normal development and behaviour of mice lacking the neuronal cell-surface PrP protein. Nature 356:577-582.

Caetano FA, Lopes MH, Hajj GN, Machado CF, Pinto AC, Magalhaes AC, Vieira MP, Americo TA, Massensini AR, Priola SA, Vorberg I, Gomez MV, Linden R, Prado VF, Martins VR, Prado MA (2008) Endocytosis of prion protein is

required for ERK1/2 signaling induced by stress-inducible protein 1. J Neurosci 28:6691-6702.

Castiglione M, Calafiore M, Costa L, Sortino MA, Nicoletti F, Copani A (2008) Group I metabotropic glutamate receptors control proliferation, survival and differentiation of cultured neural progenitor cells isolated from the subventricular zone of adult mice. Neuropharmacology 55:560-567.

Chiarini LB, Freitas AR, Zanata SM, Brentani RR, Martins VR, Linden R (2002) Cellular prion protein transduces neuroprotective signals. EMBO J 21:3317-3326.

Coitinho AS, Freitas AR, Lopes MH, Hajj GN, Roesler R, Walz R, Rossato JI, Cammarota M, Izquierdo I, Martins VR, Brentani RR (2006) The interaction between prion protein and laminin modulates memory consolidation. Eur J Neurosci 24:3255-3264.

Criado JR, Sanchez-Alavez M, Conti B, Giacchino JL, Wills DN, Henriksen SJ, Race R, Manson JC, Chesebro B, Oldstone MB (2005) Mice devoid of prion protein have cognitive deficits that are rescued by reconstitution of PrP in neurons. Neurobiol Dis 19:255-265.

Dale LB, Babwah AV, Bhattacharya M, Kelvin DJ, Ferguson SS (2001) Spatial-temporal patterning of metabotropic glutamate receptor-mediated inositol 1,4,5-triphosphate, calcium, and protein kinase C oscillations: protein kinase C-dependent receptor phosphorylation is not required. J Biol Chem 276:35900-35908.

Fuhrmann M, Bittner T, Mitteregger G, Haider N, Moosmang S, Kretzschmar H, Herms J (2006) Loss of the cellular prion protein affects the Ca2+ homeostasis in hippocampal CA1 neurons. J Neurochem 98:1876-1885.

Gasparini F, Lingenhohl K, Stoehr N, Flor PJ, Heinrich M, Vranesic I, Biollaz M, Allgeier H, Heckendorn R, Urwyler S, Varney MA, Johnson EC, Hess SD, Rao SP, Sacaan AI, Santori EM, Velicelebi G, Kuhn R (1999) 2-Methyl-6-(phenylethynyl)-pyridine (MPEP), a potent, selective and systemically active mGlu5 receptor antagonist. Neuropharmacology 38:1493-1503.

Graner E, Mercadante AF, Zanata SM, Forlenza OV, Cabral AL, Veiga SS, Juliano MA, Roesler R, Walz R, Minetti A, Izquierdo I, Martins VR, Brentani RR (2000) Cellular prion protein binds laminin and mediates neuritogenesis. Brain Res Mol Brain Res 76:85-92.

Hager G, Pawelzik H, Kreutzberg GW, Zieglgansberger W (1998) A peptide derived from a neurite outgrowth-promoting domain on the gamma 1 chain of laminin modulates the electrical properties of neocortical neurons. Neuroscience 86:1145-1154.

Hagg T, Portera-Cailliau C, Jucker M, Engvall E (1997) Laminins of the adult mammalian CNS; laminin-alpha2 (merosin M-) chain immunoreactivity is associated with neuronal processes. Brain Res 764:17-27.

Hannan AJ, Blakemore C, Katsnelson A, Vitalis T, Huber KM, Bear M, Roder J, Kim D, Shin HS, Kind PC (2001) PLC-beta1, activated via mGluRs, mediates activity-dependent differentiation in cerebral cortex. Nat Neurosci 4:282-288.

Kibbey MC, Jucker M, Weeks BS, Neve RL, Van Nostrand WE, Kleinman HK (1993) beta-Amyloid precursor protein binds to the neurite-promoting IKVAV site of laminin. Proc Natl Acad Sci U S A 90:10150-10153.

Kingston AE, Griffey K, Johnson MP, Chamberlain MJ, Kelly G, Tomlinson R, Wright RA, Johnson BG, Schoepp DD, Harris JR, Clark BP, Baker RS, Tizzano JT (2002) Inhibition of group I metabotropic glutamate receptor responses in vivo in rats by a new generation of carboxyphenylglycine-like amino acid antagonists. Neurosci Lett 330:127-130.

Krebs B, Wiebelitz A, Balitzki-Korte B, Vassallo N, Paluch S, Mitteregger G, Onodera T, Kretzschmar HA, Herms J (2007) Cellular prion protein modulates the intracellular calcium response to hydrogen peroxide. J Neurochem 100:358-367.

Kristensson K, Feuerstein B, Taraboulos A, Hyun WC, Prusiner SB, DeArmond SJ (1993) Scrapie prions alter receptor-mediated calcium responses in cultured cells. Neurology 43:2335-2341.

Laube G, Seidenbecher CI, Richter K, Dieterich DC, Hoffmann B, Landwehr M, Smalla KH, Winter C, Bockers TM, Wolf G, Gundelfinger ED, Kreutz MR (2002) The neuron-specific Ca2+-binding protein caldendrin: gene structure, splice isoforms, and expression in the rat central nervous system. Mol Cell Neurosci 19:459-475.

Lauren J, Gimbel DA, Nygaard HB, Gilbert JW, Strittmatter SM (2009) Cellular prion protein mediates impairment of synaptic plasticity by amyloid-beta oligomers. Nature 457:1128-1132.

Li S, Hong S, Shepardson NE, Walsh DM, Shankar GM, Selkoe D (2009) Soluble oligomers of amyloid Beta protein facilitate hippocampal long-term depression by disrupting neuronal glutamate uptake. Neuron 62:788-801.

Liesi P (1985) Do neurons in the vertebrate CNS migrate on laminin? EMBO J 4:1163-1170.

Liesi P, Laatikainen T, Wright JM (2001) Biologically active sequence (KDI) mediates the neurite outgrowth function of the gamma-1 chain of laminin-1. J Neurosci Res 66:1047-1053.

Liesi P, Narvanen A, Soos J, Sariola H, Snounou G (1989) Identification of a neurite outgrowth-promoting domain of laminin using synthetic peptides. FEBS Lett 244:141-148.

Lima FR, Arantes CP, Muras AG, Nomizo R, Brentani RR, Martins VR (2007) Cellular prion protein expression in astrocytes modulates neuronal survival and differentiation. J Neurochem 103:2164-2176.

Linden R, Martins VR, Prado MA, Cammarota M, Izquierdo I, Brentani RR (2008) Physiology of the prion protein. Physiol Rev 88:673-728.

Lopes MH, Hajj GN, Muras AG, Mancini GL, Castro RM, Ribeiro KC, Brentani RR, Linden R, Martins VR (2005) Interaction of cellular prion and stress-inducible protein 1 promotes neuritogenesis and neuroprotection by distinct signaling pathways. J Neurosci 25:11330-11339.

Manson JC, Clarke AR, Hooper ML, Aitchison L, McConnell I, Hope J (1994) 129/Ola mice carrying a null mutation in PrP that abolishes mRNA production are developmentally normal. Mol Neurobiol 8:121-127.

Martins VR, Linden R, Prado MA, Walz R, Sakamoto AC, Izquierdo I, Brentani RR (2002) Cellular prion protein: on the road for functions. FEBS Lett 512:25-28.

Parkin ET, Watt NT, Hussain I, Eckman EA, Eckman CB, Manson JC, Baybutt HN, Turner AJ, Hooper NM (2007) Cellular prion protein regulates beta-secretase

cleavage of the Alzheimer's amyloid precursor protein. Proc Natl Acad Sci U S A 104:11062-11067.

Policha A, Daneshtalab N, Chen L, Dale LB, Altier C, Khosravani H, Thomas WG, Zamponi GW, Ferguson SS (2006) Role of angiotensin II type 1A receptor phosphorylation, phospholipase D, and extracellular calcium in isoform-specific protein kinase C membrane translocation responses. J Biol Chem 281:26340-26349.

Putney JW, Jr., Broad LM, Braun FJ, Lievremont JP, Bird GS (2001) Mechanisms of capacitative calcium entry. J Cell Sci 114:2223-2229.

Rauch U (2004) Extracellular matrix components associated with remodeling processes in brain. Cell Mol Life Sci 61:2031-2045.

Rodriguez A, Freixes M, Dalfo E, Martin M, Puig B, Ferrer I (2005) Metabotropic glutamate receptor/phospholipase C pathway: a vulnerable target to Creutzfeldt-Jakob disease in the cerebral cortex. Neuroscience 131:825-832.

Santuccione A, Sytnyk V, Leshchyns'ka I, Schachner M (2005) Prion protein recruits its neuronal receptor NCAM to lipid rafts to activate p59fyn and to enhance neurite outgrowth. J Cell Biol 169:341-354.

Sunyach C, Jen A, Deng J, Fitzgerald KT, Frobert Y, Grassi J, McCaffrey MW, Morris R (2003) The mechanism of internalization of glycosylphosphatidylinositol-anchored prion protein. EMBO J 22:3591-3601.

Vaananen AJ, Rauhala P, Tuominen RK, Liesi P (2006) KDI tripeptide of gamma1 laminin protects rat dopaminergic neurons from 6-OHDA induced toxicity. J Neurosci Res 84:655-665.

Weissmann C (2004) The state of the prion. Nat Rev Microbiol 2:861-871.

Wiksten M, Liebkind R, Laatikainen T, Liesi P (2003) Gamma 1 laminin and its biologically active KDI-domain may guide axons in the floor plate of human embryonic spinal cord. J Neurosci Res 71:338-352.

Wiksten M, Vaananen A, Liebkind R, Rauhala P, Liesi P (2004) Soluble KDI domain of gamma1 laminin protects adult hippocampus from excitotoxicity of kainic acid. J Neurosci Res 78:411-419.

Xu J, Zhu Y, Contractor A, Heinemann SF (2009) mGluR5 has a critical role in inhibitory learning. J Neurosci 29:3676-3684.

Zanata SM, Lopes MH, Mercadante AF, Hajj GN, Chiarini LB, Nomizo R, Freitas AR, Cabral AL, Lee KS, Juliano MA, de OE, Jachieri SG, Burlingame A, Huang L, Linden R, Brentani RR, Martins VR (2002) Stress-inducible protein 1 is a cell surface ligand for cellular prion that triggers neuroprotection. EMBO J 21:3307-3316.